

SOME IMPROVED APPROACHES TO MINERAL INVENTORY
ESTIMATION OF PORPHYRY-TYPE MINERAL DEPOSITS

by

TOMASZ APOLINARY POSTOLSKI

M.Sc.Eng., The University of Mining and Metallurgy,
Krakow, Poland, 1989

A THESIS SUBMITTED IN PARTIAL FULFILLMENT OF
THE REQUIREMENTS FOR THE DEGREE OF
MASTER OF APPLIED SCIENCE

in

THE FACULTY OF GRADUATE STUDIES
(Geological Engineering Programme)

We accept this thesis as conforming
to the required standard

THE UNIVERSITY OF BRITISH COLUMBIA

October 1998

© Tomasz Apolinary Postolski, 1998

In presenting this thesis in partial fulfilment of the requirements for an advanced degree at the University of British Columbia, I agree that the Library shall make it freely available for reference and study. I further agree that permission for extensive copying of this thesis for scholarly purposes may be granted by the head of my department or by his or her representatives. It is understood that copying or publication of this thesis for financial gain shall not be allowed without my written permission.

Department of Earth and Ocean Sciences

The University of British Columbia
Vancouver, Canada

Date October 14 / 1998

ABSTRACT

Geological information utilized at early stages of resource/reserve calculation highly improves mineral inventory estimation in porphyry-type deposits. It is useful to review this topic in the context of modern approaches to geological data accumulation and interpretation as well as methodologies of mineral inventory estimation. Detailed geology provides information for a geometric model of a deposit. Substantial effort is required to characterize the geometric margins of a deposit and the relation of these margins to simplistic geometric forms that normally emerge as an interpretation. Several widely accepted models are discussed to illustrate the range of geological features that require special attention in establishing mineral inventory in porphyry-type deposits. Recognition of the different styles of mineralization allow division of the deposit into different mineralization domains having different continuities, which has a profound impact on the development of semivariogram models that are used for geostatistical resource/reserve estimation. Mineralogical studies are also emphasized, because they relate to many aspects of deposit evaluation including abundances of ore, spatial distribution of ore and finally liberation properties of ores.

Three separate mineralized zones (Main and East zones of Huckleberry deposit and the Virginia zone of the Copper Mountain porphyry system) are used to illustrate the impact of close geological control on semivariogram modeling and, consequently, the economic impact on geostatistical resource/reserve estimation. Analyses are done using both geostatistical and metal accounting procedures. In the Main zone of the Huckleberry

deposit copper grade contour maps show significant variations in trend directions, that coincide with dominant direction of stockwork development. These directions of dominant mineralization control, effectively separate the Main zone into three domains, each domain having a substantially different semivariogram model. Metal accounting calculations showed that the application of deposit-general (less accurate) semivariogram model produces an annual loss of 300 tonnes of metal in operating profit. Similar procedures applied to the East zone of Huckleberry deposit reveal the possibility of an annual loss of 700 tonnes of metal in operating profit. In the case of Virginia zone the principal control on mineralization is a set of easterly striking, vertically dipping veins. Contour maps of Cu and Au grades for all levels showed remarkable similarity and reflected the direction of strongest geological continuity (east striking vertical plane). The widely spaced exploration data are barely adequate to demonstrate the existing anisotropy. The geology thus provided insight into principal directions controlling the semivariogram model for the deposit.

The effect of average errors of block grade estimates can be evaluated quantitatively using computer program GAINLOSS that has been developed for this purpose by the author. For a given estimation error and cutoff grade, GAINLOSS calculates both the quantity of metal that is lost as a result of misclassifying ore blocks as waste and the dilution that results from misclassifying waste blocks as ore. Calculations are presented using realistic block grade distribution parameters for both porphyry-type and gold deposits. In addition, the effect of dilution and ore loss on grade of production is calculated. As a result the following fundamental relations were revealed:

1. Where the cutoff grade is on the lower tail of the grade distribution, dilution and ore loss can lead to higher than expected grade of production.
2. Where the cutoff grade is on the higher tail of the grade distribution, dilution and ore loss can lead to lower than expected grade of production.

Calculations were done for variety of levels of block estimation errors. Thus, GAINLOSS program provides a basis for determining the worth of improving block estimation errors.

TABLE OF CONTENTS

ABSTARCT.....	ii
TABLE OF CONTENTS.....	v
LIST OF TABLES.....	ix
LIST OF FIGURES.....	xi
ACKNOWLEDGEMENT.....	xix
CHAPTER 1: INTRODUCTION.....	1
CHAPTER 2: GEOLOGIC FEATURES OF PORPHYRY-TYPE DEPOSITS:	
AN AID TO RESOURCE/RESERVE ESTIMATION.....	4
Abstract.....	4
2.1 Introduction.....	5
2.2 Geological mapping.....	6
2.3 Three-dimensional (geometric) modeling and ore-waste boundaries.....	7
2.4 Ore deposit models.....	12
2.4.1 Lowell-Guilbert model (Quartz Monzonite model).....	13
2.4.1.1 Mineral zoning.....	15
2.4.1.2 Style of mineralization.....	16
2.4.1.3 Alteration zoning.....	18
2.4.1.4 Leached caps, oxide and supergene zones.....	23
2.4.1.5 Domains and domain boundaries.....	23
2.4.2 Diorite model.....	24
2.4.3 Porphyry molybdenum deposit models.....	27

2.4.3.1 Climax-type molybdenum deposit model.....	28
2.4.3.2 Quartz monzonite-type molybdenum deposit model.....	33
2.5 Concepts of geologic and value continuity.....	34
2.6 Models of geological domains and their relation to continuity.....	38
2.6.1 The Boss Mountain example.....	40
2.6.2 The Endako example.....	46
2.6.3 The Bougainville example.....	46
2.7 Metal zoning and definition of domains.....	49
2.8 A critical relationship between geological features and semivariogram models.....	51
2.8.1 Relationship between geology of porphyry-type deposits and variography.....	52
2.9 Problems of mineral beneficiation in porphyry-type deposits.....	63
2.9.1 Mineral identification and mineral assemblages.....	65
2.9.2 Quantified mineral abundances.....	66
2.9.3 Textural analysis.....	68
2.9.3.1 Grain size and spatial variations of grain size.....	68
2.9.3.2 Classification of intergrowths.....	68
2.9.3.3 Liberation properties of ores.....	69
2.10 Conclusions.....	72
Acknowledgements.....	73
References.....	74
CHAPTER 3: GEOLOGY AS A BASIS FOR REFINING SEMIVARIOGRAM	
MODELS FOR PORPHYRY-TYPE DEPOSITS.....	80
Abstract.....	80

3.1 Introduction.....	81
3.2 Main zone (Huckleberry).....	83
3.2.1 Semivariogram analysis.....	85
3.2.2 Cross-validation of estimates.....	88
3.2.3 Comparative kriging results.....	91
3.3 East zone (Huckleberry).....	94
3.3.1 Semivariogram analysis.....	94
3.3.2 Cross-validation of estimates.....	99
3.3.3 Comparative kriging results.....	99
3.4 Virginia zone (Copper Mountain).....	103
3.4.1 Semivariogram analysis.....	103
3.4.2 Cross-validation of estimates.....	108
3.4.3 Block estimation results.....	108
3.5 Conclusions.....	113
Acknowledgements.....	113
References.....	114
 CHAPTER 4: QUANTITATIVE ESTIMATION OF DILUTION AND ORE LOSS	
RESULTING FROM BLOCK ESTIMATION ERRORS AND	
A SPECIFIED CUTOFF GRADE.....	116
Abstract.....	116
4.1 Introduction.....	117
4.1.1 Biased block estimates by the application of a cutoff grade.....	117
4.2 Effect of error of block estimates on tonnage, grade, and metal recovery.....	121

4.3 Application of GAINLOSS to the Huckleberry deposit.....	134
4.4 Application of GAINLOSS to the Oritz gold deposit, New Mexico.....	143
4.5 Conclusions.....	149
Acknowledgements.....	150
References.....	150
CHAPTER 5: CONCLUSIONS.....	152
REFERENCES.....	156
APPENDIX 1: HUCKLEBERRY MAIN ZONE, GENERAL SEMIVARIOGRAM	
MODEL.....	163
APPENDIX 2: HUCKLEBERRY, MAIN ZONE, DOMAIN SEMIVARIOGRAM	
MODELS.....	170
APPENDIX 3: HUCKLEBERRY EAST ZONE, GENERAL SEMIVARIOGRAM	
MODEL.....	184
APPENDIX 4: HUCKLEBERRY EAST ZONE, DOMAIN SEMIVARIOGRAM	
MODELS.....	191
APPENDIX 5: VIRGINIA ZONE, SEMIVARIOGRAM MODELS.....	205
APPENDIX 6: EQUATIONS USED IN THE GAINLOSS PROGRAM.....	218
APPENDIX 7: ALGORITHM OF THE GAINLOSS PROGRAM AND	
THE PROGRAM PRINTOUT.....	222

LIST OF TABLES

TABLE 3-1: Huckleberry, Main zone, spherical semivariogram models for copper.....	89
TABLE 3-2: Huckleberry, Main zone, SW domain, summary of metal accounting.....	93
TABLE 3-3: Huckleberry, East zone, spherical semivariogram models for copper.....	98
TABLE 3-4: Huckleberry, East zone, East domain, summary of metal accounting.....	102
TABLE 3-5: Virginia zone, spherical semivariogram models for copper and gold.....	109
TABLE 4-1: Number of waste blocks mistakenly included in ore due to various levels of error, Bougainville porphyry deposit, copper grade distribution.....	125
TABLE 4-2: Number of ore blocks mistakenly included in waste due to various levels of error, Bougainville porphyry deposit, copper grade distribution.....	126
TABLE 4-3: Metal accounting summary of operating loss (metal) for block misclassification due to various levels of error, Bougainville porphyry deposit, copper grade distribution.....	132
TABLE 4-4: Number of waste blocks mistakenly included in ore due to various levels of error, Huckleberry porphyry deposit, East zone, W domain, copper grade distribution.....	139
TABLE 4-5: Number of ore blocks mistakenly included in waste due to various levels of error, Huckleberry porphyry deposit, East zone, W domain, copper grade distribution.....	140
TABLE 4-6: Metal accounting summary of operating loss (metal) for block misclassification due to various levels of error, Huckleberry porphyry deposit, East zone, W domain, copper grade distribution.....	141

TABLE 4-7: Number of waste blocks mistakenly included in ore due to various levels of error, Oritz gold deposit, New Mexico, gold grade distribution.....	145
TABLE 4-8: Number of ore blocks mistakenly included in waste due to various levels of error, Oritz gold deposit, New Mexico, gold grade distribution.....	146
TABLE 4-9: Metal accounting summary of operating loss (metal) for block misclassification due to various levels of error, Oritz gold deposit, Oritz gold deposit,gold grade distribution.....	147

LIST OF FIGURES

FIGURE 2-1: Schematic representation of contact dilution.....	9
FIGURE 2-2: Schematic representation of gradation and sinuosity of ore/waste boundary.....	11
FIGURE 2-3: Lowell-Guilbert model of copper and copper molybdenum porphyry deposits. Schematic representation of concentric (a) alteration zones, (b) mineralization zones, and (c) occurrence of sulphides.....	14
FIGURE 2-4: Vertical cross section of fluid circulation around a shallow intrusion in homogenously permeable wall rocks.....	19
FIGURE 2-5: Graphic representation of the manner in which fracturing and alteration evolve with time in intrusions and adjacent wall rocks.....	20
FIGURE 2-6: Diorite model of copper porphyry deposits.....	26
FIGURE 2-7: Conceptual geologic models of porphyry molybdenum deposits.....	29
FIGURE 2-8: Schematic sections showing multiple phases of intrusion, mineralization, and progressive tilting at Climax mine.....	30
FIGURE 2-9: Plan view of the Climax orebody showing concentric shells surrounding and extending outwards from the core of the multiple intrusion.....	32
FIGURE 2-10: Example of an estimation problem. The grade at "x" is to be estimated using information from the eight surrounding holes.....	39
FIGURE 2-11: Example from figure 2-10 conditioned by adding additional geologic information.....	39
FIGURE 2-12: Surface geology of the Boss Mountain deposit showing distinct mineralization domains.....	41

FIGURE 2-13: Longitudinal section (A) and cross section (B) of Main Breccia Zone and Stringer Zone of Boss Mountain deposit.....	43
FIGURE 2-14: Two significantly different orientations of major veins in East and West parts of Endako open pit.....	47
FIGURE 2-15: Idealized model of directional structures.....	48
FIGURE 2-16: Spatial superposition of gold and copper grades on upper level of the Dizon deposit, Philippines.....	50
FIGURE 2-17: Schematic representation of a typical deep seated porphyry deposit having shape of an inverted cup and near vertical axis; (a) section A-A' along axis of porphyry, (b) section B-B' normal to the axis of porphyry.....	54
FIGURE 2-18: Bar graph showing sample values across the mineralization (along line C C') from figure 2-17.....	55
FIGURE 2-19: Directional semivariograms in porphyry deposit as shown on figure 2-17, in 3 different directions.....	55
FIGURE 2-20: Schematic representation of a typical porphyry copper deposit with supergene enrichment; five different domains defined.....	59
FIGURE 2-21: Bar graphs showing sample values in two rock types - andesite (upper), and diorite (lower) for supergene and hypogene sulphide mineralization zones of porphyry copper deposit from figure 2-20.....	60
FIGURE 2-22: Down hole semivariograms in porphyry copper deposit as shown on figure 2-20 developed for four different domains.....	61
FIGURE 2-23: Huckleberry, East zone, Mo grade contour map for 8 m bench, level 940 m.....	67

FIGURE 3-1: Geological map of the Huckleberry deposit showing Main zone and East zone.....	84
FIGURE 3-2: Huckleberry, Main zone, Cu grade contour map for 24 m interval.....	86
FIGURE 3-3: Geological map of the Huckleberry deposit Main zone showing three different domains with dominant directions of stockwork development.....	87
FIGURE 3-4: Quantile - Quantile plot of Cu cross-validation results for Huckleberry Main zone SW domain, using general semivariogram model (a), and domain specific semivariogram model (b).....	90
FIGURE 3-5: Huckleberry Main zone, SW domain, Cu ordinary kriging results for 100 blocks using domain specific and general semivariogram models.....	92
FIGURE 3-6: Huckleberry, East zone, Cu grade contour map for 8 m bench, level 940 m.....	96
FIGURE 3-7: Geological map of the Huckleberry deposit East zone showing two different domains with dominant directions of stockwork development.....	97
FIGURE 3-8: Quantile - Quantile plot of Cu cross-validation results for Huckleberry East zone East domain, using general semivariogram model (a), and domain specific semivariogram model (b).....	100
FIGURE 3-9: Huckleberry East zone, East domain, Cu ordinary kriging results for 100 blocks using domain specific and general semivariogram models.....	101
FIGURE 3-10: Geological pit map of Virginia zone with dominant direction of stockwork development.....	104
FIGURE 3-11: Virginia zone, Cu grade contour map for 100 ft interval above level 3400 ft.....	106

FIGURE 3-12: Virginia zone, Au grade contour map for 100 ft interval above level 3400 ft.....	107
FIGURE 3-13: Virginia zone, scatter diagram of Au vs. Cu for assay data.....	111
FIGURE 3-14: Virginia zone, scatterplot of 100 Au regression results versus Au kriging results.....	112
FIGURE 4-1: Normal estimated grade distribution with mean of 0.05 oz/t and standard deviation of 0.01 oz/t.....	119
FIGURE 4-2: Estimated and true grades of production versus cutoff grade for the normal distribution of figure 4-1.....	120
FIGURE 4-3: (Upper) Two examples of error curves superimposed on a blasthole grade 0.225% Cu. (Lower) An error curve centered on a true blasthole grade of 0.25% Cu.....	122
FIGURE 4-4: Four examples of various error curves centered on various true grades, illustrating that a significant proportion of estimates will be below the Bougainville cutoff grade of 0.215% Cu.....	123
FIGURE 4-5: Huckleberry, East zone, West domain. Naive histogram of Cu 8 m composites.....	135
FIGURE 4-6: Huckleberry, East zone, West domain. (Upper) declustered histogram of Cu 8 m composites; (Lower) binary diagram of declustered mean Cu value versus block dimensions used for declustering.....	137
FIGURE A1-1: Cu semivariogram model in vertical direction.....	164
FIGURE A1-2: Cu semivariogram models in horizontal directions; azimuth 0 (top) and 22 (bottom).....	165

FIGURE A1-3: Cu semivariogram models in horizontal directions; azimuth 45 (top) and 67 (bottom).....	166
FIGURE A1-4: Cu semivariogram models in horizontal directions; azimuth 90 (top) and 112 (bottom).....	167
FIGURE A1-5: Cu semivariogram models in horizontal directions; azimuth 135 (top) and 157 (bottom).....	168
FIGURE A1-6: Structural ellipse of ranges in the eight directions showing directions of maximum (azimuth 22) and minimum (azimuth 112) continuity of Cu semivariogram model.....	169
FIGURE A2-1: Cu semivariogram model in vertical direction, NE domain.....	172
FIGURE A2-2: Cu semivariogram models in horizontal directions, NE domain; azimuth 0 (top) and 55 (bottom).....	173
FIGURE A2-3: Cu semivariogram models in horizontal directions, NE domain; azimuth 90 (top) and 145 (bottom).....	174
FIGURE A2-4: Structural ellipse of ranges in the four directions showing directions of maximum (azimuth 145) and minimum (azimuth 55) continuity of Cu semivariogram model, NE domain.....	175
FIGURE A2-5: Cu semivariogram model in vertical direction, SE domain.....	176
FIGURE A2-6: Cu semivariogram models in horizontal directions, SE domain; azimuth 0 (top) and 30 (bottom).....	177
FIGURE A2-7: Cu semivariogram models in horizontal directions, SE domain; azimuth 90 (top) and 120 (bottom).....	178
FIGURE A2-8: Structural ellipse of ranges in the four directions showing	

an isotropic Cu semivariogram model, SE domain.....	179
FIGURE A2-9: Cu semivariogram model in vertical direction, SW domain.....	180
FIGURE A2-10: Cu semivariogram models in horizontal directions, SW domain; azimuth 0 (top) and 80 (bottom).....	181
FIGURE A2-11: Cu semivariogram models in horizontal directions, SW domain; azimuth 90 (top) and 170 (bottom).....	182
FIGURE A2-12: Structural ellipse of ranges in the four directions showing directions of maximum (azimuth 80) and minimum (azimuth 170) continuity of Cu semivariogram model, SW domain.....	183
FIGURE A3-1: Cu semivariogram model in vertical direction.....	185
FIGURE A3-2: Cu semivariogram models in horizontal directions; azimuth 0 (top) and 22 (bottom).....	186
FIGURE A3-3: Cu semivariogram models in horizontal directions; azimuth 45 (top) and 67 (bottom).....	187
FIGURE A3-4: Cu semivariogram models in horizontal directions; azimuth 90 (top) and 112 (bottom).....	188
FIGURE A3-5: Cu semivariogram models in horizontal directions; azimuth 135 (top) and 157 (bottom).....	189
FIGURE A3-6: Structural ellipse of ranges in the eight directions showing directions of maximum (azimuth 67) and minimum (azimuth 157) continuity of Cu semivariogram model.....	190
FIGURE A4-1: Cu semivariogram model in vertical direction, E domain.....	193
FIGURE A4-2: Cu semivariogram models in horizontal directions, E domain;	

azimuth 0 (top) and 22 (bottom).....	194
FIGURE A4-3: Cu semivariogram models in horizontal directions, E domain;	
azimuth 45 (top) and 67 (bottom).....	195
FIGURE A4-4: Cu semivariogram models in horizontal directions, E domain;	
azimuth 90 (top) and 112 (bottom).....	196
FIGURE A4-5: Cu semivariogram models in horizontal directions, E domain;	
azimuth 135 (top) and 157 (bottom).....	197
FIGURE A4-6: Structural ellipse of ranges in the eight directions showing directions	
of maximum (azimuth 112) and minimum (azimuth 22) continuity	
of Cu semivariogram model, E domain.....	198
FIGURE A4-7: Cu semivariogram model in vertical direction, W domain.....	199
FIGURE A4-8: Cu semivariogram models in horizontal directions, W domain;	
azimuth 0 (top) and 22 (bottom).....	200
FIGURE A4-9: Cu semivariogram models in horizontal directions, W domain;	
azimuth 45 (top) and 67 (bottom).....	201
FIGURE A4-10: Cu semivariogram models in horizontal directions, W domain;	
azimuth 90 (top) and 112 (bottom).....	202
FIGURE A4-11: Cu semivariogram models in horizontal directions, W domain;	
azimuth 135 (top) and 157 (bottom).....	203
FIGURE A4-12: Structural ellipse of ranges in the eight directions showing directions	
of maximum (azimuth 67) and minimum (azimuth 157) continuity	
of Cu semivariogram model, W domain.....	204
FIGURE A5-1: Cu experimental semivariograms in vertical direction, East part (top),	

middle part (bottom), with superimposed model for the entire zone.....	207
FIGURE A5-2: Cu experimental semivariograms in vertical direction, West part (top), entire zone (bottom), with superimposed model for the entire zone.....	208
FIGURE A5-3: Cu semivariogram models in horizontal directions, azimuth 90; dip 0 (top) and dip -10 (bottom).....	209
FIGURE A5-4: Cu semivariogram models in horizontal directions, azimuth 90; dip -20 (top) and dip -30 (bottom).....	210
FIGURE A5-5: Cu semivariogram model in horizontal direction, azimuth 0, dip 0.....	211
FIGURE A5-6: Au experimental semivariograms in vertical direction, East part (top), middle part (bottom), with superimposed model for the entire zone.....	212
FIGURE A5-7: Au experimental semivariograms in vertical direction, West part (top), entire zone (bottom), with superimposed model for the entire zone.....	213
FIGURE A5-8: Au semivariogram models in horizontal directions, azimuth 90; dip 0 (top) and dip -10 (bottom).....	214
FIGURE A5-9: Au semivariogram models in horizontal directions, azimuth 90; dip -20 (top) and dip -30 (bottom).....	215
FIGURE A5-10: Au semivariogram model in horizontal direction, azimuth 0, dip 0.....	216
FIGURE A5-11: Structural ellipses of ranges in the two directions showing directions of maximum (azimuth 90) and minimum (azimuth 0) continuity of Cu semivariogram model (top) and Au semivariogram model (bottom).....	217

ACKNOWLEDGMENTS

Special thanks and gratitude are extended to Dr. A.J. Sinclair for supervising the research work on the entire thesis, assisting with problems, providing very constructive criticism, and offering an unlimited help as well as financial support throughout the study.

The author is indebted to Dr. Richard Poulin for providing practical insight into the problems of ore reserve estimation and their impact on economic analysis in the mineral industry.

Special thanks are given to Asger Bentzen and Arne Toma for help and discussion of some problems with computer applications during various stages of this work. The author is also indebted to D.A. Sketchley for cheerfully lending from his great reservoir of geological experience.

At various times this study benefited from advice of G.R. Raymond, C.R. Stanley, and K. Illerbrun. Mr. G.A. Whiton and Mr. G.R. Raymond were instrumental in making Huckleberry data available; Mr. P.M. Holbek kindly provided Virginia data. The generosity of these people and their organizations in releasing data for this study is greatly appreciated.

Finally thanks go to Teresa, Ewelina and Adrian for their patience and personal support.

CHAPTER 1

INTRODUCTION

Geological information is an important early guide in the development of resource/reserve models for porphyry-type deposits. Geological control is particularly important in the case of such deposits because individual block estimates involve very large tonnages of ore or waste. Thus very small improvements in grade control can have a significant impact on operating profit.

This study is organized as a series of three independent papers, each forming a chapter and each dealing with a different set of problems related to improvement of quality in resource/reserve estimation in porphyry-type deposits.

Chapter 2 emphasizes importance of geological information toward producing high quality resource/reserve estimates. Detailed geology provides information for a geometric model of a deposit. Characterization of the geometric margins of a deposit is emphasized and the relation of these margins to simplistic geometric form that normally emerges as an interpretation. Several widely accepted models serve to illustrate the range of geological features that require special attention in establishing mineral inventory of porphyry-type deposits. A very important problem of different mineralization domains having different continuity, which impacts on the development of semivariogram models that are used for geostatistical resource/reserve estimation is also addressed here. Finally mineralogical studies are emphasized, because they relate to many aspects of deposit evaluation

including abundances of ore and deleterious materials, spatial distribution of ore, and liberation properties of ores.

Chapter 3 emphasizes the importance of geology for improving semivariogram models for porphyry-type deposits. Three separate mineralized zones from two large porphyry-type systems are used to illustrate the impact of close geological control on semivariogram modeling and thus, the economic impact on geostatistical resource/reserve estimation; these are the Main and East zones of Huckleberry deposit and Virginia zone of the Copper Mountain porphyry system.

During the course of the analysis a variety of procedures are used. First the general (less accurate) semivariogram model is developed for an entire mineralized zone in each case. Then, geological information and contour maps are examined in order to divide the entire mineralized zone into different domains. Consequently, semivariogram models are developed independently for each domain. Cross-validation is followed by ordinary kriging, which is used to estimate a 3-dimensional block array. Finally the metal accounting procedures are employed.

Chapter 4 demonstrates a novel approach to errors of block grade estimates. Where block (selective mining unit) grade distribution can be approximated by a normal or lognormal distribution, the effect of average errors of block grades can be evaluated quantitatively using a computer program GAINLOSS that has been developed for this purpose by the author. For a given estimation error and a cutoff grade, the GAINLOSS program calculates both the quantity of metal that is lost as a result of misclassifying ore blocks as waste and the dilution that results from misclassifying waste blocks as ore.

Chapter 4 includes example calculations using computer program GAINLOSS and realistic block grade distribution parameters.

CHAPTER 2

GEOLOGIC FEATURES OF PORPHYRY-TYPE DEPOSITS: AN AID TO RESOURCE/RESERVE ESTIMATION

ABSTRACT

Geology contributes important information toward producing high quality resource/reserve estimates. It is useful to review this topic in the context of modern approaches to geological data accumulation and interpretation as well as methodologies of mineral inventory estimation. For discussion purposes in this context geology can be considered under the following overlapping topics: detailed (deposit) geology, ore deposit models, continuity and mineralogy. Each of these topics will be considered here in terms of their potential contributions to "*improved*" mineral inventory estimation.

Important results of this evaluation are:

1. Detailed geology provides information for a geometric model of a deposit, a model that serves as a basis for mine planning. It is important to distinguish fact from interpretation in such models. Substantial effort is required to characterize the geometric margins of a deposit and the relation of these margin to the simplistic geometric form that normally emerges as an interpretation.
2. Ore deposit models contribute substantially to confidence in developing a 3-dimensional geometric model of a deposit for mine planning. Specifically, they

contribute to recognition of domains, each with its own characteristic continuity and margin character.

3. Continuity is dependent on mineralization style and may be controlled structurally and/or lithologically. It is important to distinguish geological continuity and value continuity. A wide range of classical geological methods are useful in examining geological continuity; value continuity is best viewed as a statistical characteristic that is quantified by any of several measures of autocorrelation.
4. Mineralogical studies relate to many aspects of deposit evaluation including abundances of ore and deleterious minerals, spatial distribution of ore and deleterious minerals, grain size characteristics of important minerals, liberation properties of ores, etc.

2.1: Introduction

Geological information traditionally has been the basis for resource/reserve estimation. Particular aspects of geology that are of concern include (Sinclair, 1995; 1998):

- (i) general geological mapping
- (ii) 3-dimensional modeling,
- (iii) ore deposit model
- (iv) nature of ore/waste margins,
- (v) domains, and
- (vi) mineralogical/textural attributes, and
- (vii) continuity.

Each of these overlapping topics will enter the discussion below.

2.2: Geological mapping

Detailed geological mapping is used to establish geological controls of mineralization as well as the general character and spatial extent of these controls. Geological history is important because it is essential to distinguish pre-, syn-, and post-ore processes, since they certainly will affect ore continuity. Geological mapping will reveal secondary aspects of geological continuity (folding, faulting, metamorphism) that commonly disrupt primary mineralized zones.

Detailed geological mapping with representations on cross sections and plans forms the classical approach to documenting geology for mineral inventory estimation. These 2-dimensional graphical schemes are an easy form of representation on which to distinguish factual information from interpretive aspects of geometric models and they have been used for these purposes for many years.

Thus while preparing plans and sections that depict an interpretation, it is important to indicate the locations of data on which the interpretation is based. Knowledge of the locations of underground workings and drill holes that provide the data used for interpretations provides a factual basis for evaluating an interpretation and indicating where it is most suspect.

For most mineral deposits much of the detailed geological information is obtained from logging (i.e. "mapping") drill core. As geological information is accumulated, the interpretations might change. In such a case a new geological interpretation can be considered most effectively only if half the drill core was retained.

2.3: Three-dimensional (geometric) modeling and ore-waste boundaries

Ore/waste boundaries traditionally are interpolated as smooth, perhaps curved, surfaces. Interpolations are first done on cross sections and/or plans and these 2-dimensional interpolations are then projected between sections to produce geometric forms that are sensible from a mining perspective with relatively smooth margins. In reality, these margins are only approximations and they have errors associated with them (e.g. Sides, 1994). The magnitude of these interpolation errors are generally unknown; they are generally small in large deposits with gradational ore/waste margins. Where margins are sharp (faults, post-mineral intrusive margins) the errors can be larger and can result in significant dilution as well as loss of ore to waste.

Sides (1994) describes a case history for the Garca orebody in southern Portugal in which he demonstrates that the smaller error of ore/waste contact location is near control points (close to the plane of drill hole sections) in contrast to interpolations for zones removed from control points (falling between sections). His work was confined to massive sulphide lenses, but the generality of his conclusions is widely accepted.

Interpolation is commonly a subjective undertaking and David (1988, p. 172) has proposed a geostatistical procedure, indicator kriging, as a more objective approach. The method requires that a threshold be defined (e.g. cutoff grade) to transform grade data to indicator values, that is, zeros (less than threshold) and ones (equal to or greater than threshold). A semivariogram model of the indicator values must be obtained and the transformed data can then be used to krig the probability at any point, that the point is in ore or waste. If such kriging is done for a very closely spaced grid of points it is possible

to construct an objective vision of the most likely place for the ore/waste boundary. Of course, such procedures are highly labour intensive and assume perfect stationarity, both undesirable features. An additional problem is that kriging, though very sophisticated, like any other estimation procedure, will always smooth the ore/waste contact.

It is possible to develop an appreciation of the magnitude of interpolation errors in some cases where the nature of the ore/waste margin can be mapped in detail (Sinclair, 1995) and a series of smooth interpolations between two pseudo-sections can be determined. The procedure as described by Sinclair (*ibid.*) involves detailed mapping of the ore/waste boundary both geologically and with assayed samples, over lengths somewhat greater than the spacing of cross sections. Then, a series of smooth 2-dimensional interpolations of the ore/waste boundary can be superimposed on the mapped zone, each interpolation removed from the previous interpolation by a few metres. For each interpolation it is possible to measure the ore lost to waste and the waste lost to ore as described below.

Vertical lines along the upper margin of the orebody (Figure 2-1) are sites used to measure distances from the interpreted "average contact" or mining margin (dashed line) to the true ore/waste contact. Negative values (above the dashed line) are ore lost to wallrock, while positive values (below the dashed line) represent dilution of wallrock extending across the mining margin into ore. A histogram of these distances can be prepared and can be used for estimating the proportion of length between control points (e.g. two drill holes on adjacent sections) where waste penetrates across the mining margin into ore. The "average thickness" of such waste extending into ore can be determined as a weighted average using frequencies as weights for the mid values of

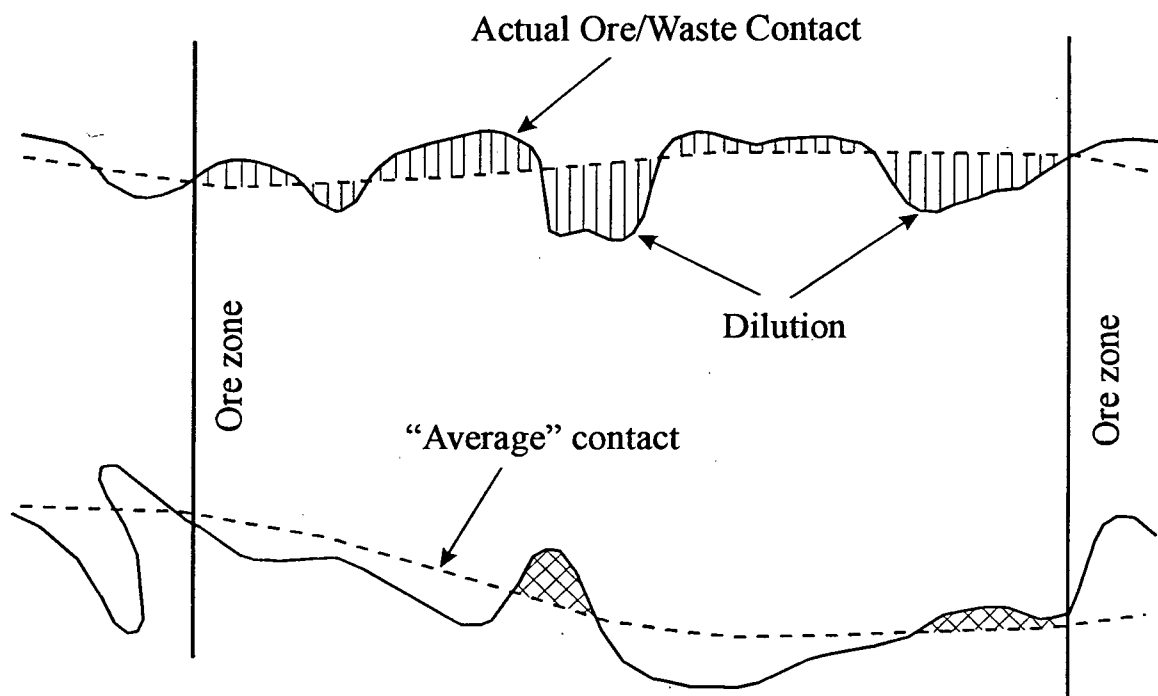


Figure 2-1: Schematic representation of contact dilution. Vertical lines in the upper margin of the hypothetical deposit can be measured to characterize the dilution population relative to the interpreted smooth contact. Modified from Stone (1986).

corresponding class intervals. Of course, the length over which positive values occur can be measured directly from the figure. The product of this length and the “average thickness” of waste protrusions is a 2-dimensional estimate of the quantity of contact dilution along one mining margin. An identical estimate can be made along the opposite margin and the total area of contact dilution can be calculated. Several such estimates, averaged, provide a ‘global’ estimate. A comparable estimate can be made for negative values (above the dashed line) to calculate the total area of ore lost to waste.

A conceptual model for ore-waste margin with application to porphyry-type deposits (Figure 2-2) includes the combined effects of variations of gradation of ore/waste boundary versus complexity of geometry (roughness or sinuosity) of ore/waste margins. Irregularity of contact of ore and waste increases in the vertical direction, from relatively simple and straight contact, through increased degree of sinuosity to quite an irregular contact zone, which becomes a zone of mixing of ore and waste (d – distance of mixing of ore and waste). In the horizontal direction Figure 2-2 represents changes from sharp ore/waste contact to gradational contact.

Computer based graphical display systems are widely used to model ore/waste boundary. Some caution should be applied in using such graphic displays, mainly because of the highly regular interpolation routines that are a part of the software and which may lead to smooth interpolations that depart substantially from reality. These highly sophisticated software packages now available for 3-dimensional modeling are an important component of modern capabilities in data handling. However, their built-in interpolation routines might produce smooth ore/waste contacts that can oversimplify real geological contacts. Insight into how these interpolations are done is very important for

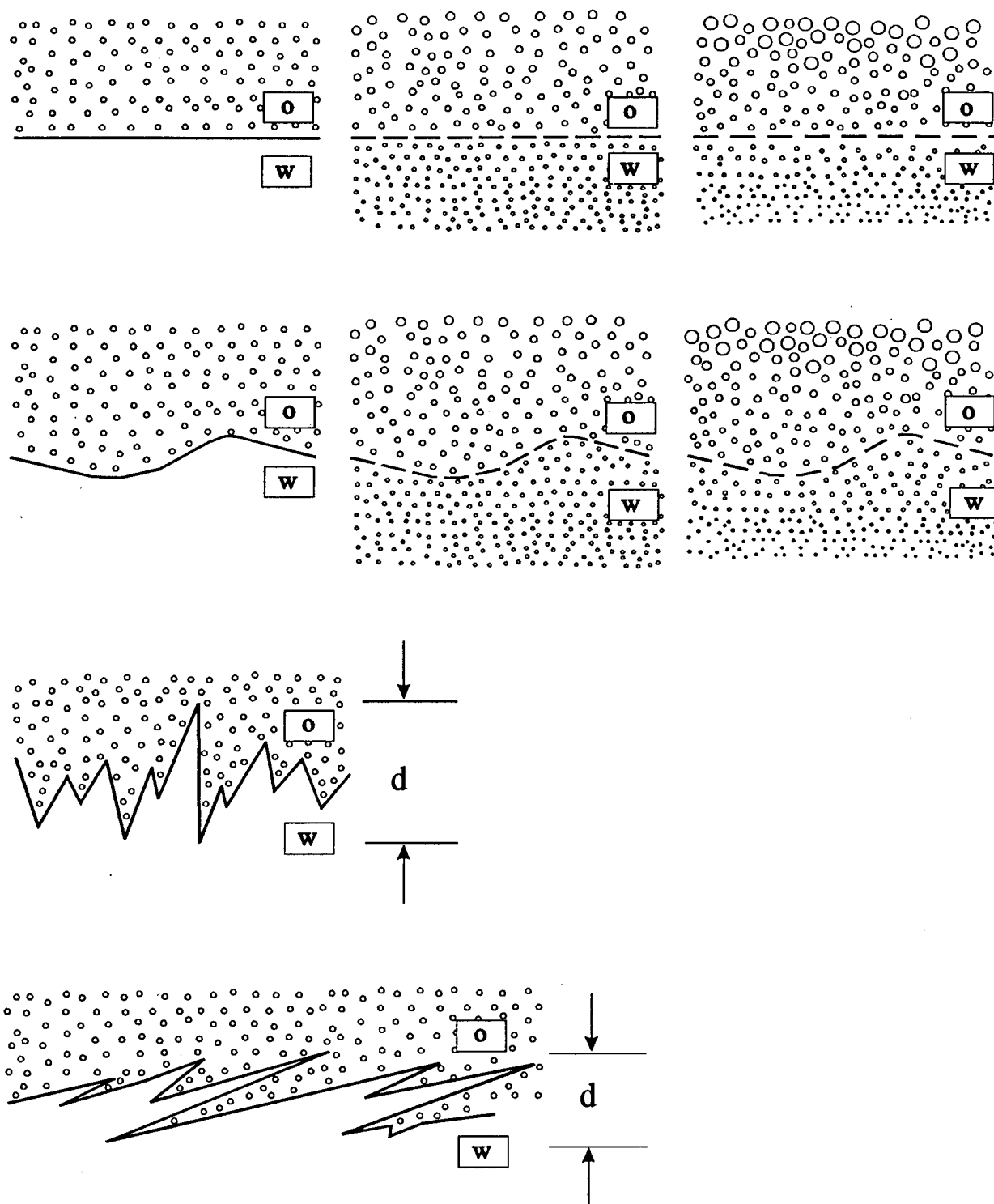


Figure 2-2: Schematic representation of gradation and sinuosity of ore/waste boundary. Irregularity of ore/waste contact increases vertically, gradational changes occur horizontally; o- ore, w- waste, d- distance of mixing of ore and waste.

the user. Nevertheless, such a 3-dimensional view is a powerful aid to conceptualizing a mineral deposit for the purpose of mineral inventory estimation and mine design, providing that limitations of the software are kept in mind.

2.4: Ore deposit models

Ore deposit models are useful in organizing ideas and information about a deposit, because they represent a “standard” of comparison for a particular class of deposit. Deposit models generally are developed from an especially important deposit or from the combined information of numerous similar deposits. Deposit models are important because they give confidence in defining geological continuity and different geological domains.

Porphyry copper and related systems are so variable in character that a variety of models have been formulated to describe the spatial patterns of their various geological features. For example, the class includes porphyry copper-gold deposits (Sillitoe, 1979), porphyry molybdenum deposits (White et al, 1981), porphyry copper-molybdenum deposits (Drummond and Godwin, 1976; Kirkham and Sinclair, 1995) and so on. Consequently, from the perspective of mineral inventory estimation it is not possible to consider only a single model that generally describes all porphyry deposits and the characteristics that are important for resource/reserve estimation. Several widely accepted models will serve to illustrate the range of geological features that require special attention in establishing the mineral inventory of a porphyry-type deposit. In particular, three well established deposit categories will be considered: Lowell-Guilbert model, the Diorite model and Porphyry molybdenum deposit models.

2.4.1: Lowell-Guilbert Model (Quartz Monzonite Model)

Lowell and Guilbert (1970) were the first to describe a 3-dimensional model of the geological attributes of a porphyry system. Their model relates to copper and copper molybdenum porphyry deposits that are concentrically zoned about a core of igneous rock that is related genetically to an igneous system that involves at least some porphyritic units (Figure 2-3). These mineralizing systems are 100's of metres to several kilometres in diameter and generally are of economic importance for their content of copper and byproduct molybdenum. Copper sulphides are commonly controlled in a stockwork or in disseminated form in altered wallrock and less commonly as breccia pipes. Mineralization may be predominantly in the core intrusion or in adjoining wallrock or may straddle the contact zone (James, 1971). Hydrothermal alteration can be either extensive, to the point that original rock material is totally replaced, or relatively much less intense. Both ore minerals and alteration minerals are zoned concentrically about the core intrusion.

The ideal deposit described by the model is generally large in 3 dimensions, up to a few thousand meters in diameter in plan and is either circular or elliptical in outline (Guilbert and Lowell, 1974). The central stock is generally complex, of intermediate composition (granodiorite - quartz monzonite) and includes units having porphyritic texture. There are commonly dykes of various ages related to the central intrusion and these can be pre-, syn- and post-mineralization. Consequently, dykes can be either mineralized and contribute to ore, or they can be barren and contribute to potential dilution.

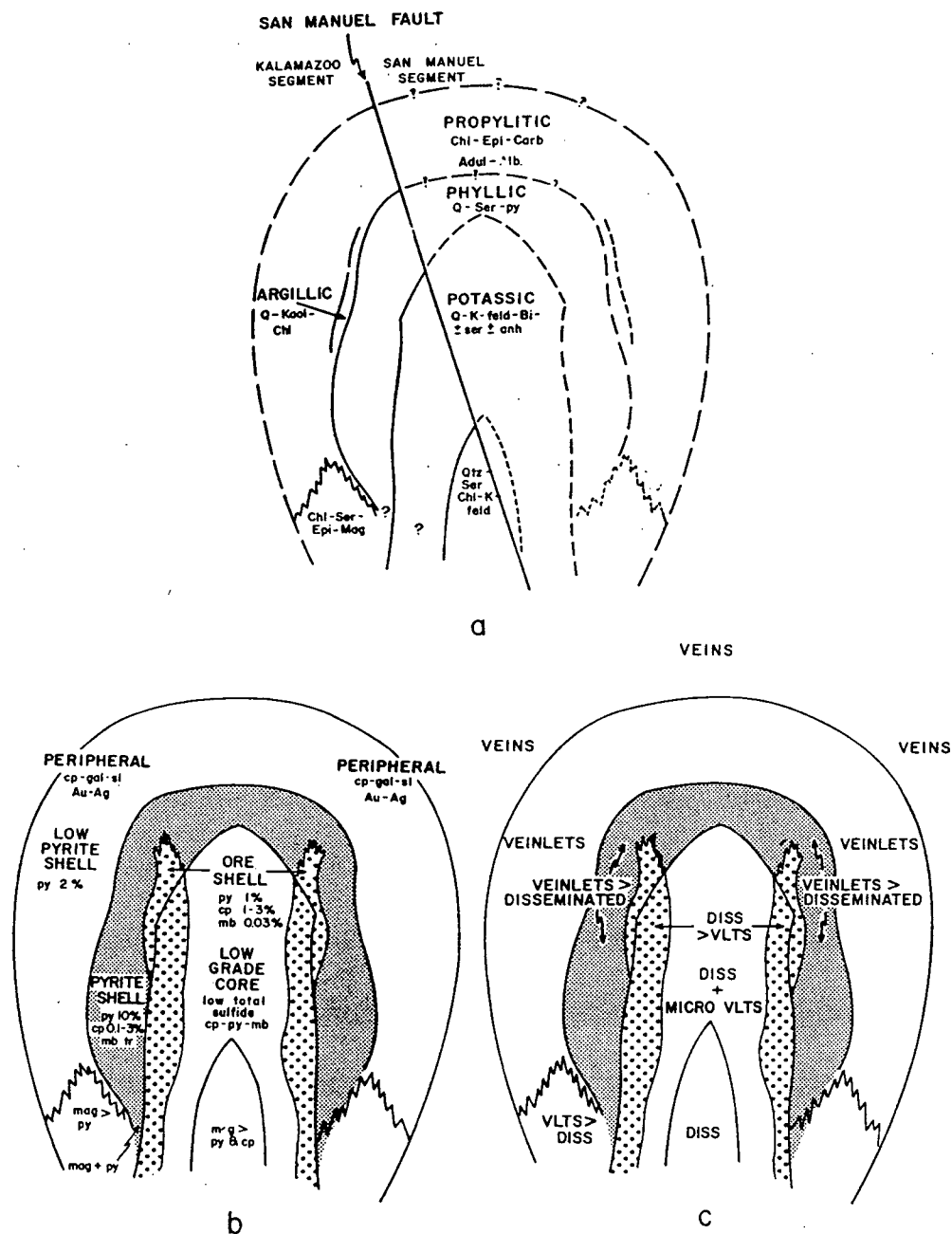


Figure 2-3: Lowell - Guilbert model of copper and copper molybdenum porphyry deposits. Schematic representation of concentric (a) alteration zones, (b) mineralization zones, and (c) occurrence of sulphides. After Lowell and Guilbert (1970).

Porphyry deposits contain significant amounts of pyrite, chalcopyrite and molybdenite and in some cases minor amounts of other ore minerals and metals including galena, sphalerite, gold and silver. The grade of hypogene mineralization commonly is in the range 0.25 to 1.0% Cu and about 0.02% Mo. All porphyry copper deposits contain at least traces of molybdenite, gold and silver.

2.4.1.1: Mineral Zoning

Pyrite is the most common sulphide, followed in order of decreasing abundance by chalcopyrite, bornite, and molybdenite. Zoning of the sulphide mineralization is highly characteristic. The ore minerals occur in mineralogical zones that are arranged concentrically about the centre of the igneous core complex outward from the center of the deposit, as follows (Guilbert and Lowell, 1974; Nielsen, 1984):

1. chalcopyrite, pyrite, bornite, molybdenite (inner)
2. pyrite, chalcopyrite, molybdenite, bornite
3. pyrite, chalcopyrite
4. sphalerite, galena, silver, gold (outer)

A typical upward sequence is pyrite-chalcopyrite-molybdenite assemblage grading upward into pyrite.

Ore textures can impinge seriously on metal recovery in a mill (Craig and Vaughan, 1981). Thus, assays alone are not sufficient with which to evaluate a porphyry copper deposit. The proportion of molybdenite that can be recovered will be a function of grain size and the proportion that occurs as free grains in contrast to that which is

intergrown with various other minerals. Chalcopyrite usually occurs as anhedral interstitial grains and fracture fillings in pyrite. Bornite, if present, occurs as discrete anhedral grains with the pyrite and chalcopyrite and as exsolution lamellae within chalcopyrite.

2.4.1.2: Style of Mineralization

Hypogene sulphides in porphyry deposits typically form veinlets or disseminated grains (McMillan, 1991; Gustafson, 1978). A progressive change in mineralization style is very typical in the Lowell-Guilbert model (cf. Figure 2-3). This sequence progresses from veins (outermost) in the periphery of the mineralized system, to veinlets in the outer (propylitic) zone, veinlets and minor disseminated grains in the intermediate (argillic) zone, veinlets approximately equal to disseminations in the inner (phyllic) zone, and dominant disseminations in the innermost (potassic) zone (Guilbert and Lowell, 1974). This progressive change in the nature of the continuity of mineralization can lead to systematic differences in continuity from place to place within a deposit and will clearly impact on resource/reserve estimation methodology. In fact, ideally, the direction of greatest geological continuity is cylindrical about the igneous core. In reality, it is common for one vein direction of a stockwork to be better developed than the others, a feature that can lead to dramatic changes in the nature of continuity from place to place in a deposit (Bysouth and Wong, 1995).

Four or five stages of vein formation in a well defined paragenetic sequence are commonly recorded in porphyry deposits, not all of which need contain ore minerals; two or three stages of veins containing significant amounts of ore minerals are common. Because these individual stages form at different times in the tectonic history they are not

necessarily coincident in space and resulting grade distribution may in part reflect vein paragenesis. Heberlein and Godwin (1984) describe 4 generations of veins defined by megascopic cross-cutting relationship at the Berg porphyry Cu-Mo property in North Central British Columbia. Veins of type 1, distributed through the quartz monzonite porphyry stock and the surrounding hornfelsed volcanic rocks, were responsible for deposition of all the copper and part of the molybdenum. Veins of type 2 contain more significant quantities of molybdenum and generally do not contain copper. The highest density of this vein type occurs near the intrusive contact. Veins of type 3 are more abundant outward from the intrusive contact in the propylitic zone. They are mainly filled with quartz and pyrite, with sphalerite as an accessory. The youngest (type 4) vein generation is represented by gypsum-filled postore fractures.

Breccias of various origins are a component of many porphyry copper deposits (Gustafson, 1978), and in some cases they may represent a very significant proportion of ore. Stoiser (1986) describes the Los Bronces breccia pipe system, that contains commercial grades of both copper and molybdenum. The volume of this hydrothermal breccia system puts it among the largest in the world. The Los Bronces breccia system is about 2 km in length and about 800 m wide near the surface. Outer contact limits of the breccia system are generally sharp and dip inward at steep angles. These breccia bodies are commonly isotropic in terms of ore continuity and hence, may differ substantially in this respect from adjoining vein or disseminated styles of mineralization.

2.4.1.3: Alteration Zoning

Four alteration assemblages normally are distinguishable (Figure 2-3). The earliest and most centrally located is a zone of alkali metasomatism within and around the central intrusive porphyry body, a core of potassic alteration. Next in time sequence is a more diffuse zone of propylitic alteration. At a later time and as a result of access by meteoric waters, phyllic and argillic alteration stages overprint the early alkali-metasomatic effects.

According to Beane and Titley (1981) alteration patterns in porphyry deposits are probably connected with the presence of two separate fluid systems (Figure 2-4). One system consisted of magmatic waters that concentrated in the apical portion of the crystallizing porphyry intrusion. The other aqueous component was meteoric or formation waters that underwent convective circulation in the country rocks of the intrusion. Meteoric fluids continued to circulate after the interior magmatic fluids stopped being generated, and eventually the exogenous meteoric system collapsed on the consolidated and fractured porphyry stock. Magmatic fluids produced the potassic zone minerals as an alteration assemblage. Propylitic zone alteration was caused by meteoric waters at the same time as potassic zone was formed by magmatic fluids. A later, collapsing meteoric system formed phyllic alteration that overprinted the existing potassic-altered rocks. Fluid flow was enhanced by the intermittent development of fractures in the porphyry system. Figure 2-5 shows a representation of the manner in which fracturing and alteration evolved. Fracturing begins as a widespread event which is followed by successively younger periods of fracturing, retreating progressively to smaller rock volumes.

Spatially the hydrothermal alteration zones form roughly concentric shells with the

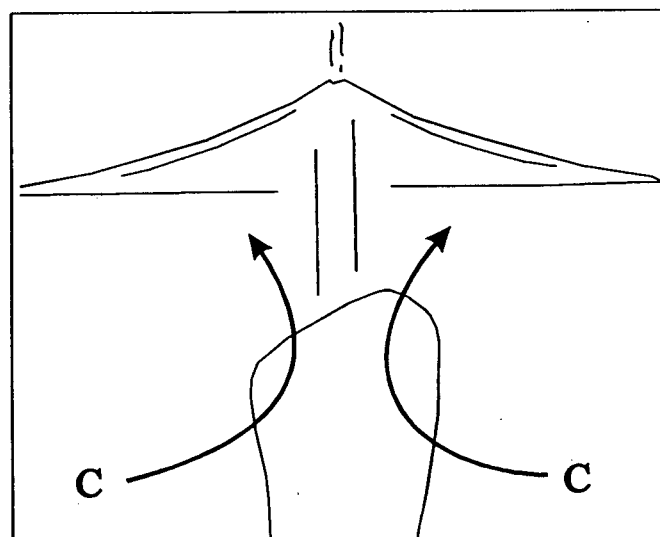
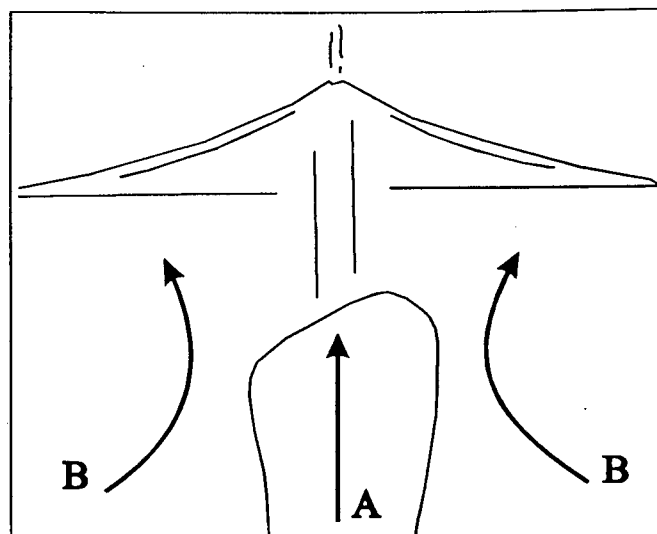


Figure 2-4: Vertical cross section of fluid circulation around a shallow intrusion in homogenously permeable wall rocks. (Upper) circulation at early stage with magmatic (line A) and meteoric (line B) cells. (Lower) circulation at later stages after meteoric cells collapse. After Beane and Titley (1981).

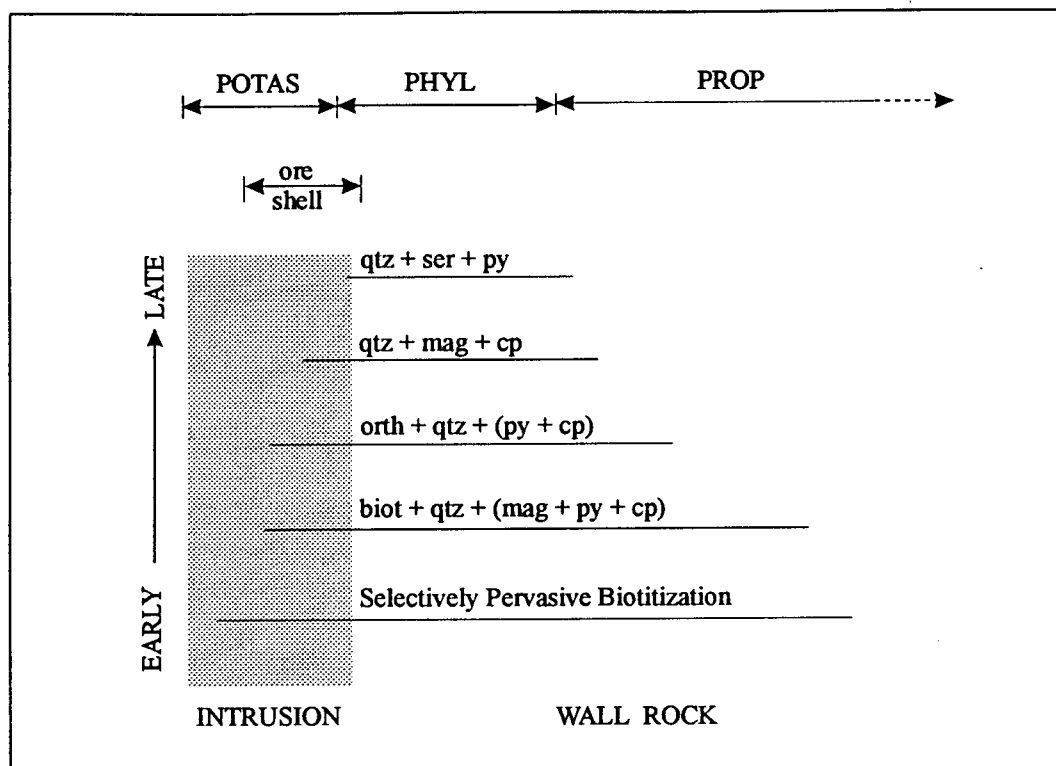


Figure 2-5: Graphic representation of the manner in which fracturing and alteration evolve with time in intrusions and adjacent wall rocks. The horizontal scale shows the lateral extent of fracturing and the various alteration assemblages. The end result of the individual event is overprinting of alteration types: POTAS(SIC), PHYL(LIC), PROP(YLITIC). Modified from Beane and Titley (1981).

innermost potassic zone, followed by a phyllic zone, then an intermediate argillic zone and finally by the outer propylitic zone (Beane and Titley, 1981). The innermost, potassic alteration zone is due to the effects of alkali metasomatism (generally potassic, but can also be sodic) within and around the productive intrusive body. This alteration involves pervasive and veinlet replacement of primary minerals by secondary biotite, K-feldspar, quartz, and to a lesser degree sericite and anhydrite. Common opaque minerals include pyrite, chalcopyrite, bornite and magnetite. The outer part of potassic alteration contains the so called "ore shell". Total sulphide content here is about 3 to 5 percent with an average pyrite content of about 1 percent and a pyrite to chalcopyrite ratio of 1:3. Sulphides in the potassic zone occur as disseminations and microveinlets.

Surrounding and to some extent overlapping the potassic zone is the phyllic or sericitic alteration zone, which forms by leaching of sodium, calcium and magnesium from alumino-silicate bearing rocks, while potassium can be provided largely from feldspar of the parent rock. Alteration minerals include quartz, sericite, pyrite and minor chlorite. The most distinct is usually almost complete replacement of plagioclases and orthoclase by sericite, giving pervasive sericitization. This zone generally contains abundant pyrite, which can be about 10% by volume or higher. Other opaque minerals are chalcopyrite, molybdenite and generally small amounts of bornite, chalcocite, sphalerite and magnetite. Pyrite to chalcopyrite ratio averages 12:1. Total sulphide content is high - about 10 to 12 percent. Sulphides in the phyllic zone occur mainly as veinlets but to some degree also as disseminations. This zone commonly constitutes the ore zone, especially in deposits with chalcocite enrichment.

The argillic zone is commonly the least well developed of the alteration zones and in some deposits it is absent. This zone is characterized by destruction of plagioclase with contemporaneous formation of either kaolinite or montmorillonite. The dominant minerals of argillic assemblage are quartz, kaolinite, montmorillonite and some sericite. Silification is the second most important process in this alteration zone. Pyrite is common, but much less abundant than in the phyllic zone. Other opaque minerals in this zone are chalcopyrite, and sometimes bornite. Pyrite to chalcopyrite ratio is about 20:1. Total sulphide content is moderate - about 6%. Mineralization is distinctly veinlet controlled rather than disseminated.

The outer alteration zone is the propylitic zone. It is the largest of the alteration shells forming a wide halo in the country rock. The main minerals of this assemblage are chlorite, epidote and calcite. This assemblage is invariably outside the ore zone and beyond the phyllic and argillic zones. Opaque minerals are represented by pyrite which is the dominant opaque mineral, though pyrite averages only about 2%. Chalcopyrite is rare. Even smaller amounts of bornite, molybdenite, magnetite, sphalerite and galena might be present. Sparse mineralization is controlled clearly by small veinlets.

Summarizing, figure 2-3 shows, that the best mineralization concentrates in the so called "ore shell". It might contain up to 1 to 3 percent of chalcopyrite and up to 1 percent of pyrite with smaller amounts of molybdenite. Mineralization occurs as dissemination and also in veinlets. The ore shell occurs on the boundary between potassic and phyllic alteration zones. As depth increases a progressively greater portion of the ore shell occurs in the potassic alteration zone. In the upper part of a deposit the ore shell is mainly concentrated in the phyllic zone.

The emplacement of the stocks, various associated dykes and the porphyry-type mineralization are controlled by regional tectonism and commonly directions of fracturing can be related to the regional stress pattern. The shape and size of porphyry host intrusions is related to contemporaneous and younger fault structures. Most of the host intrusions are elongated and districts with strong structural control have very elongated stocks (e.g. Red-Chris; cf. Seraphim and Hollister, 1976; Newell and Peatfield, 1995). The porphyry copper deposits themselves are generally circular to oval in plan view.

2.4.1.4: Leached Caps, Oxide and Supergene Zones

In much of the world weathering processes have resulted in extensive oxidation of the upper reaches of porphyry systems. Even in northern climates the small amount of post-glacial weathering that has taken place can seriously affect the geological character of the near surface portion of deposits. Where well developed the leached caps and related supergene zones are easily recognized and are evaluated separately because of their widely varying milling characteristics (e.g. Gibraltar and Afton deposits; cf. Ney et al., 1976; Drummond et al., 1976; Carr and Reed, 1976).

2.4.1.5: Domains and Domain Boundaries

The remarkably systematic spatial variations of ore mineralogy, style of mineralization and alteration minerals leads to a strong likelihood that more than one domain will be required as a basis for resource/reserve estimation. In general, somewhat different procedures are to be expected where the nature of geological continuity changes so pronouncedly as is inherent in the Lowell-Guilbert model.

One of the most important features of porphyry type deposits from the evaluation point of view are ore boundaries. Ore boundaries are at least in part gradational leading to so called "assay wall" boundaries between ore and waste. Sharp boundaries do occur, as in the case of superimposed faults that cross mineralized zones or the presence of large post-ore dykes.

On average about 30 percent of all ore mineralization associated with porphyries is in surrounding stock wall rocks and about 70 percent of mineralization is concentrated in the intrusive stock; in some cases this ratio can be reversed. Still other deposits contain all mineralization in an intrusive stock (Lowell and Guilbert, 1970).

Zoning sequences can be very uniform for porphyry-type deposits. Most of the deposits show alteration assemblages in the same outward sequence: potassic, phyllic, argillic, and propylitic. Even where certain zonation assemblages are not present, the remaining assemblages occur in the same order. Vertical sequences of zonation are in agreement with lateral zoning. Both outward and upward zoning of most deposits is consistent with the sequence of potassic, phyllic, argillic, and propylitic assemblages. Alteration minerals can have an impact on ease of milling of the ores. In particular, an abundance of argillic alteration and/or fine grained sericite can result in increased mill costs for a variety of reasons such as adsorption of flotation chemicals and clogging of filters.

2.4.2: Diorite Model

Porphyry systems of the diorite type are associated with intrusive rocks deficient in silica, most commonly diorite and syenite (Hollister, 1978; Hollister, 1991). Most diorite-

type porphyry copper deposits are zoned diorite-syenite plutons, and they may contain other phases with compositions intermediate between diorite and syenite. Syenite is commonly the latest intrusion and is closest spatially and in age to copper mineralization.

Diorite type deposits have different alteration-mineralization patterns, than deposits of the Lowell-Guilbert type. The mafic character of the intrusive rocks and surrounding comagmatic volcanics in the diorite type deposits has a very important role. Sulphur in hydrothermal fluids invading dioritic rocks may encounter more iron in the original mafic silicates than can be consumed as pyrite. Excess iron not consumed as pyrite or a silicate tends to form magnetite. The sericite expected in the quartz monzonite model in the phyllic zone, in the diorite model is poorly developed or missing and is replaced by a chlorite rich hydrothermal mineral assemblage due to incomplete removal of iron as pyrite. Also the amount of pyrite in diorite type deposits is much lower than in quartz monzonite type deposits. As a result the phyllic and also argillic zones of Lowell and Guilbert model could not developed and are not present in diorite type model. The alteration zonal sequence of the diorite model commonly is inner potassic shell surrounded by outer, wide propylitic zone (Figure 2-6).

The potassic zone forms the inner core of the deposits. Due to excess iron the addition of potash promotes the occurrence of secondary biotite. Orthoclase on the other hand may be entirely absent. So the potassic zone alteration is characterized by dominance of biotite and chlorite with little or no K-feldspar. Hypogene copper mineralization mainly as chalcopyrite and bornite is concentrated mainly in the potassic zone. Sulphides occur as disseminations and fracture filling.

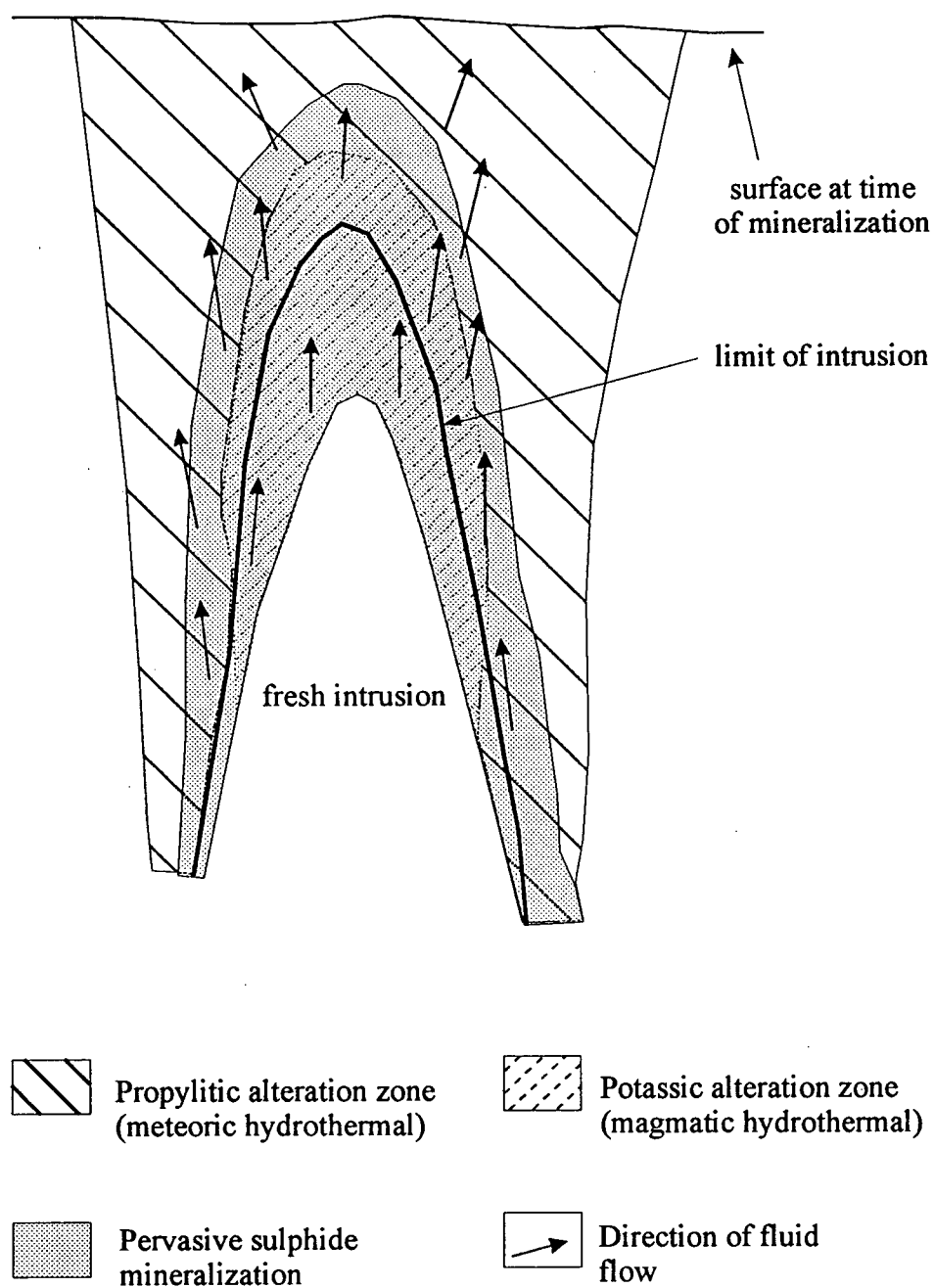


Figure 2-6: Diorite model of copper porphyry deposits. Phyllic alteration zone is absent. Flow direction during simultaneous action by the magmatic - hydrothermal and meteoric - hydrothermal systems is indicated by arrows. After Hollister (1978).

The propylitic zone is the outer alteration zone, that directly surrounds potassic zone, because chlorite dominant mineral assemblages are present instead of quartz, sericite, pyrite mixtures of phyllic zone. As a result the propylitic zone of the diorite model deposits is usually laterally very wide. Chlorite, epidote and calcite constitute a typical mineral assemblage of this zone. In some deposits chalcopryite mineralization, mainly in fractures, can be present in this zone.

Diorite type porphyry deposits are richer in gold and silver and have smaller Mo:Cu ratio, than deposits associated with quartz monzonites. The veins containing the ore minerals commonly contain calcite, zeolite or chlorite, but quartz is either absent or present in minor amounts. In diorite type porphyries the chalcopryite to pyrite ratio is close to 1.0.

2.4.3 : Porphyry Molybdenum Deposit Models

Porphyry molybdenum deposits are spatially, genetically and temporally associated with porphyritic intrusions that range in composition from quartz monzonite to granite. The most important types of porphyry molybdenum deposits from the perspective of economic value are:

1. Climax-type or granite-type deposits, and
2. Quartz-monzonite type deposits.

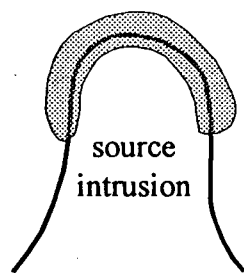
The following descriptions of these deposit types are summaries based on Ranta et al., 1984; White et al., 1981; Wallace et al., 1968; Wallace, 1974; and Wallace, 1991.

Most molybdenum in porphyry molybdenum deposits occurs as molybdenite in quartz stockworks developed in hydrothermally altered rocks adjacent to stocks and within the intrusions themselves. Molybdenite in disseminated form is not common. Porphyry molybdenum deposits are large, commonly in excess of 100 million tons of ore and have complex three-dimensional shapes. Granite-type deposits can be high grade (ca. 0.3-0.4% MoS₂). Quartz-monzonite-type deposits generally have a somewhat lower grade (ca. 0.1-0.2% MoS₂).

2.4.3.1: Climax - type molybdenum deposit model

Climax-type of deposits also known as granite type deposits are associated with small stocks of high silica and alkali-rich granite. These deposits commonly have the shape of an inverted cup or a hollow cylinder (Figure 2-7) with the molybdenite zone occurring near the apex of the related intrusion and having the general shape of the contact between the source intrusion and the country rocks. In an "inverted cup" orebody the ore zone is continuous over the apex. The strongest mineralization is centered on the apex of the source intrusion and generally overlaps the igneous contact. The higher grade molybdenite is continuous within the ore shell from the limbs upward through the apex.

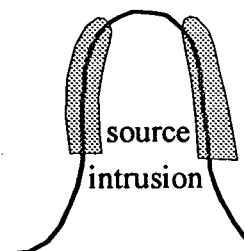
In the "cylindrical" deposits the ore zone is not continuous over the apex, that is, higher grade material is absent from the apical region of the intrusion. Climax-type deposits are characterized by multiple phases of intrusion and mineralization. Figure 2-8 shows a graphic summary of the main igneous, hydrothermal and structural events at the Climax mine. Each of the first three major intrusive phases was accompanied and followed by the development of the molybdenite ore body. The last intrusive phase produced almost no



**INVERTED CUP
(TYPE I)**

1. Ore is in both source and host rocks.
2. Ore zone is continuous over apex in the shape of an inverted cup.

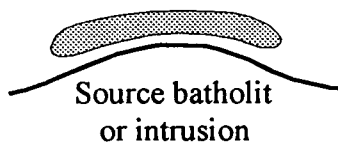
Examples: Climax
Henderson



**HOLLOW CYLINDER
(TYPE II)**

1. Ore is in both source and host rocks.
2. Ore zone is not continuous over the apex and has a hollow cylindrical shape.

Examples: Pine Grove
Mount Emmons



**TABULAR, OR INVERTED BOWL
(TYPE III)**

1. Ore is generally in host rock only.
2. Ore zone is tabular to gently arching.

Examples: Mt. Tolman
Endako



Hypothetical orebody

Figure 2-7: Conceptual geologic models of porphyry molybdenum deposits.
After Ranta et al. (1984).

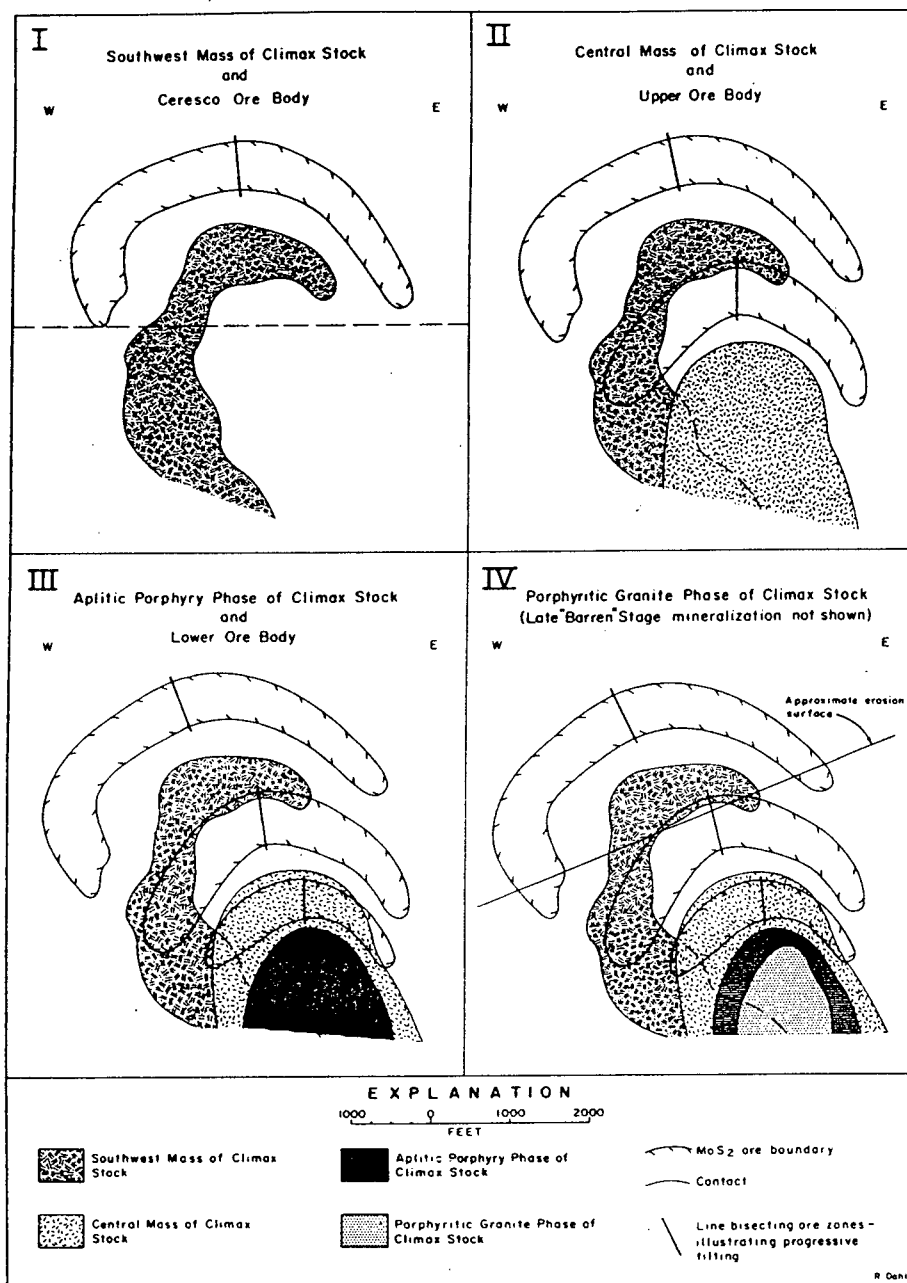


Figure 2-8: Schematic sections showing multiple phases of intrusion, mineralization, and progressive tilting at Climax mine. After Wallace et al. (1968).

commercial mineralization. Uplift and doming accompanied introduction of most of the intrusive phases. Each successive ore body is smaller and formed closer to the upper contact of the intrusion, with which it is genetically associated. Similarly, in the plan view (Figure 2-9), the ore zones form concentric shells, usually seen on different levels, surrounding and extending outwards from the core of the multiphase intrusion. Closest to the core is the youngest ore zone (the lower ore body), whereas the oldest ore zone (Cresco ore body), now mainly eroded and, as such, only projected, forms the outermost shell, which is the furthest from the intrusive core. Thus, Climax-type ore bodies are elliptical in plan and bow-like, concave downward in section. The geometry of the various ore zones becomes important in interpreting geological continuity between drill holes and in this way impacts on resource/reserve estimation.

In Climax-type deposits the intensity and zoning of alteration and ore mineral formation associated with each ore body are systematically distributed in space. Usually over 90% of molybdenite is in thin (less than 3mm thick), quartz-molybdenite veinlets that form the stockwork. At Climax, the veinlet density (number of veinlets per given volume), is greater in the core of an ore body and decreases progressively toward the margins. The molybdenite content of individual veinlets, however, seems to increase outward from the core. This means that grade is a function of both veinlet density and molybdenite content, but the effect of vein density generally dominates.

Alteration zones around each ore body follow a general sequence from a central silicic and potassic zone to peripheral phyllic, argillic, and propylitic zones. The potassic zone is characterized usually by total replacement of plagioclase by potassium feldspar. Secondary biotite is sparsely disseminated and forms less than 1% of the rock volume.

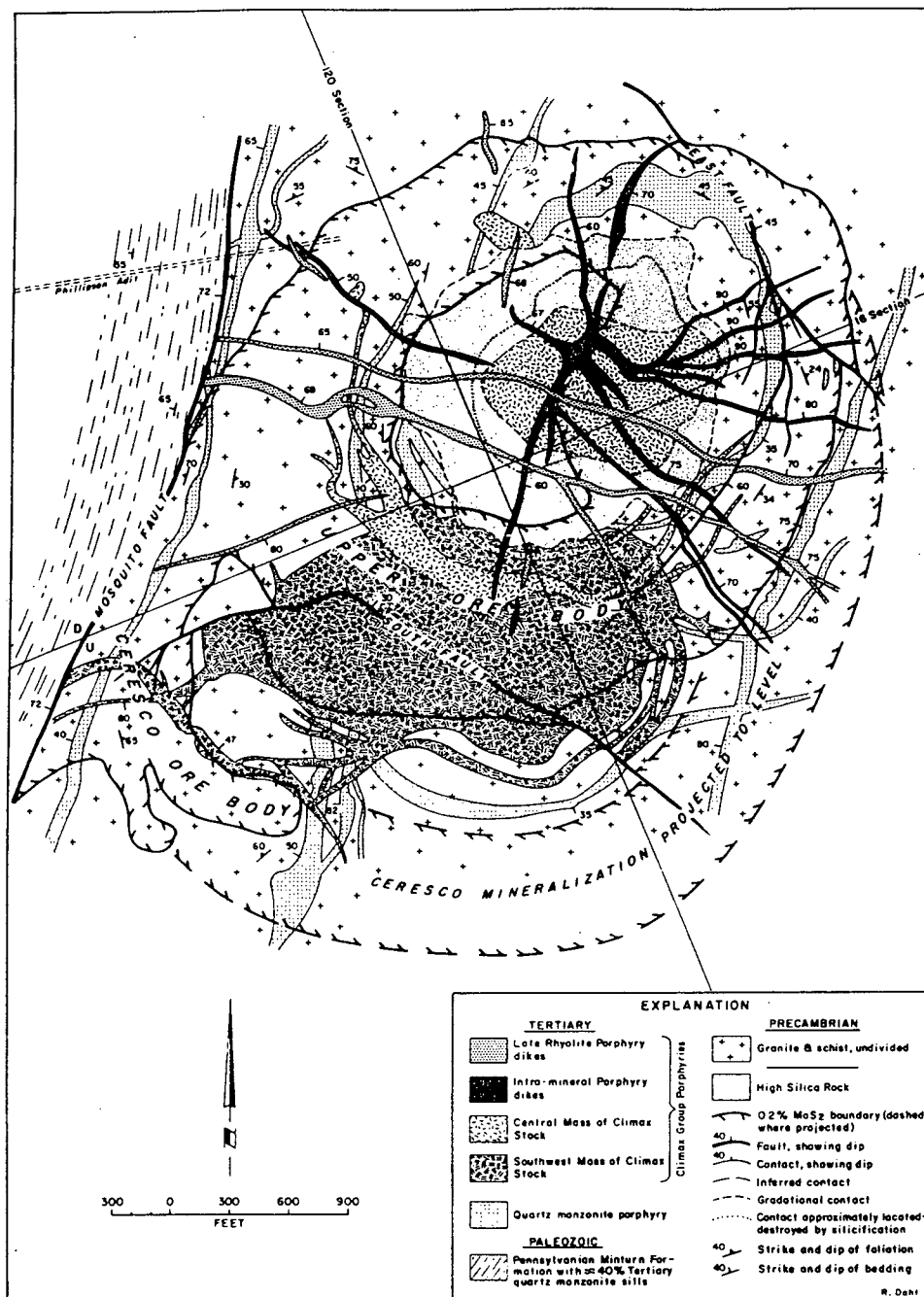


Figure 2-9: Plan view of the Climax orebody showing concentric shells surrounding and extending outwards from the core of the multiple intrusion. After Wallace et al. (1968).

Within the potassic zone there can be development of smaller vein silica zones and/or pervasive silica zones. The former case raises the quartz content of an average K-feldspathized rock from 40% to 70%, whereas, the latter contains pervasive quartz in amount greater than 90% by volume.

The phyllic zone is characterized by a quartz-sericite-pyrite alteration assemblage formed in response to sericitization of potassium feldspar and plagioclase, and by the introduction of sulphur to form pyrite. The argillic zone is characterized by montmorillinitization and kaolinization of plagioclase. The propylitic zone is defined by the presence of chlorite, epidote, calcite, clay and sericite.

Comparing Climax-type deposits alteration to that of porphyry copper deposits, it can be said that Climax-type deposits have intense silicification, relative abundance of fluorine, and small amount of biotite.

2.4.3.2: Quartz monzonite - type molybdenum deposit model

Deposits of the quartz-monzonite type are associated with small composite stocks or late phases of batholiths. Intrusive phases form by magmatic differentiation trends that evolve from a parent of dioritic or quartz dioritic composition and progress through granodiorite to quartz monzonite.

Quartz monzonite molybdenum deposits occur in three common morphologies (Figure 2-7), mainly as inverted cup (type 1) and a hollow cylinder (type 2) or to a large, gently arching, inverted bowl (type 3). Type 1 and type 2 morphological shapes were described in the section on Climax-type deposits. The third type of orebody geometry is associated with source rocks contained within quartz monzonite batholiths. The ore zone

generally lies entirely within the host rocks and does not overlap the batholithic source rock contact; the ore zone is generally tabular to gently arching.

Alteration and mineralization in quartz-monzonite-type deposits are mostly fracture controlled and do not involve as intense wallrock reaction and replacement as do more pervasive Climax-type alteration sequences. Generally, alteration and mineralization zoning are not as well developed. In quartz-monzonite-type molybdenum deposits structural ore controls are more important than chemical controls (chemistry of wall rocks).

From an economic evaluation point of view it is important to notice that molybdenum porphyry deposits, like copper porphyry deposits, have gradational boundaries between ore and waste. A second important feature is that the ore grades of quartz-monzonite-type molybdenum deposits are commonly less than half those of the Climax-type deposits, but their tonnage may be equal or greater.

2.5: Concepts of geologic and value continuity

Reliable estimates and profitable mining operations require good understanding of continuity in mineral deposit evaluation. Sinclair and Vallee (1994 b), and Sinclair (1995) define two types of continuity: geological continuity and value (quality) continuity. Geological continuity is the physical or geometric occurrence of geological features that control localization of mineralization. These controlling features can be either primary lithological (intrusions, volcanic or sedimentary rocks) or secondary lithological (postmineralization dykes) or structural, primary (mineralization controls such as veins, shears, stockwork, stringer, breccia) or secondary (superimposed effect such as faults,

shears, folds, metamorphism). Generally, geological continuity relates to larger volumes than does value continuity. Also alteration zones, which are primary features associated with the deposit (potassic, phyllic, argillic, and propylitic) can have different value (grade) continuity.

Value continuity is described as a statistical continuity of measured values (e.g. grade), that exists within a zone of geological continuity. Within the structural and lithological zones that control mineralization the continuity of metal grades can be highly variable. It is one thing to have identified the structures controlling mineralization (geological continuity), but another to have reasonable expectations that a particular part of the structure is continuously mineralized and of ore grade (value continuity) between control points (e.g. adjacent drill holes).

Grade continuity can be studied by the use of autocorrelation functions such as semivariograms and correlograms (cf. Journel and Huijbregts, 1978; Isaaks and Srivastava, 1989), that quantify a statistical or 'average' continuity in various directions through the deposit.

Statistical continuity described by an autocorrelation function (e.g. the semivariogram) is determined with greatest confidence along the main axis of sampling, which is usually along drill hole axes. Sampling in the other two directions is commonly effected by more widely-spaced drill hole intercepts. In such cases physical and value discontinuities that are shorter than the drill hole grid can be missed, especially where the actual rock exposures are absent. For these less well sampled directions understanding of continuity is very dependent on geological interpretation and clearly would be aided by the careful location of additional sampling sites (drill holes) during exploration.

An example of the above problem is illustrated in Figure A5-7 (bottom), Figure A5-8 (top), and Figure A5-10, which show semivariograms for gold from exploration drill hole samples in Virginia zone. Only vertical semivariogram (cf. Figure A5-7 bottom) can be defined with reasonable confidence, while the absence of close-spaced data horizontally limits the ability to define short range value continuity in the other two directions (cf. Figure A5-8 top, and Figure A5-10).

The above example shows that when the semivariogram is required for an exploration or feasibility mineral inventory estimation it is important, that some of the early exploration work on the deposit is directed to provide sufficient close-spaced data with which to define quantitative 3-dimensional models of both geological and value continuity. Early sampling patterns and continuity estimated from them must be revised and new sampling designed to meet deficiencies in the data base. The objectives are to confirm the geological assumptions, confirm long-range continuity assumptions and quantify the short-range continuity. Rendu (1986) states that a good understanding of factors which control the direction and extent of continuity of the mineralization is needed for development of meaningful semivariogram models.

Information along directions that were less densely sampled at earlier work stages needs to be improved. This usually involves halving the spacing of a drill hole grid in an area of interest. Close-spaced samples should be taken along lines in various orientations to evaluate local (short-range) continuity and to integrate it into geological information. Journel and Huijbregts (1978) recommend that within a large sampling field, locally crosses of closely spaced data should be collected to provide some information on local (short-range) value continuity in different horizontal directions. Closely spaced

information can be obtained from sampling rock exposures, trenches or exploratory underground workings.

To ease the difficulty with semivariogram modelling and to quantify short-range continuity Raymond and Armstrong (1988) say that during exploration of the property at Valley Copper a decline was driven in the orebody "*for the purpose of bulk sampling the upper portion of the deposit*". Valley Copper did not have natural rock exposures, so building a decline and bulk sampling were used to attempt to verify grades estimated from drill hole data and to obtain information in the horizontal direction to model the horizontal semivariogram.

The situation was different in the case of two other porphyry deposits: Virginia zone (Princeton, B. C.) and Huckleberry deposit (central B. C.). Virginia zone has rock exposures, but close-spaced surface information in horizontal directions was not collected to model short-range continuity. In the case of Huckleberry there were no rock exposures on the surface and no underground workings were driven to obtain such information.

Either additional close-spaced drilling or following the strategy of Valley Copper (driving a decline) would reduce one of the common problems encountered in applying geostatistics at a pre-feasibility stage of exploration, that is, the common scarcity of closely spaced data with which to define both the nugget effect and short range grade continuity.

If more than one domain were recognized (see next section), control of short range continuity would be required for each separate domain. Sampling should be closely tied to geology and coded systematically so that data can be easily categorized in domains if the need arises. For example, samples should not cross major lithological boundaries. In many

practical cases the deposit can be divided into several domains, each of which is characterized by its own distinctive semivariogram model. This is because the differences in lithology or structure have produced differences in the local character of mineralization. Sinclair and Vallee (1994 a) emphasize that lithologies can have a marked correlation with continuity, so that it is important to define separate lithological domains and test them for the possibility that they are characterized by different continuity models.

2:6 Models of geological domains and their relation to continuity

In the foregoing discussion it has been suggested that different parts of a single deposit can differ geologically and such differences can be reflected in different value continuity characteristics. As a result, for deposit evaluation purposes it may be necessary to divide a deposit into separate domains using as a basis the structural/lithological features that control mineralization (cf. Krige and Dunn, 1995; Tobar et al., 1997). The concept of domains is emphasized by Srivastava (1987); Figures 2-10 and 2-11 illustrate this concept. Figure 2-10 shows a typical estimation situation. The grade at "x" is to be estimated using grade information from eight surrounding holes. In considering the significance of nearby values the probability of certain outcomes is conditioned with the existing knowledge. Referring to figure 2-10 this conditioning information includes not only the actual grades, but also their locations. Given a few nearby data, certain ore grades at "x" are more likely than others. As Srivastava (1987) emphasizes one of the most overlooked sources of conditioning information is the geology. Looking at Figure 2-10 one could ask 'what would happen to uncertainty about the grade at "x" if some geological information was added to this map'?

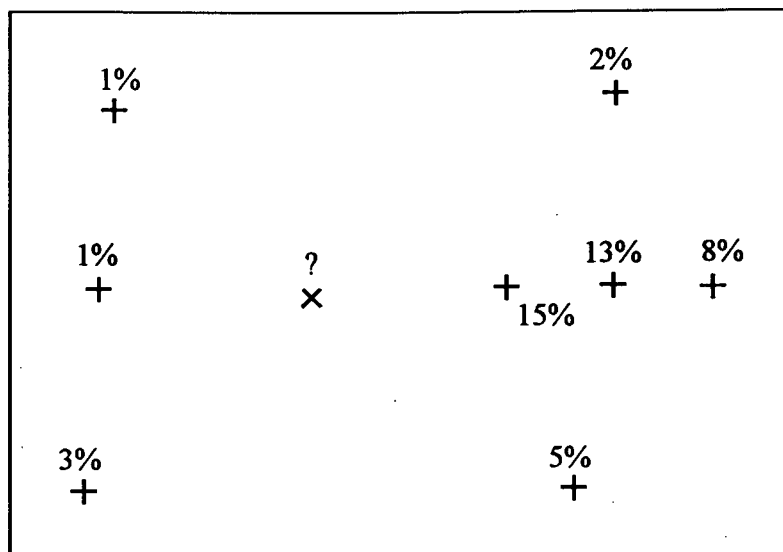


Figure 2-10: Example of an estimation problem. The grade at "x" is to be estimated using information from the eight surrounding holes. After Srivastava (1987).

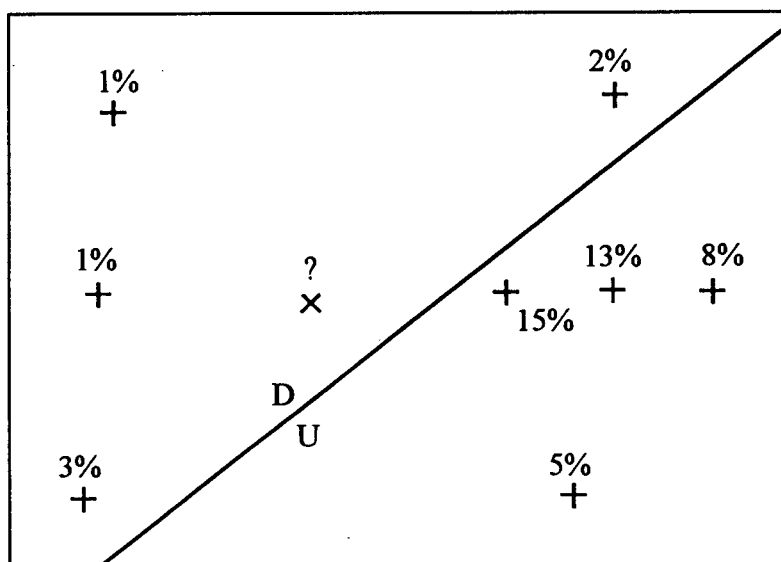


Figure 2-11: Example from figure 2-10 conditioned by adding additional geologic information. After Srivastava (1987).

An answer is provided on Figure 2-11; the location of a fault has been added, which clearly separates high grades from low grades, with the highest grades appearing on the upthrown side of the fault. In such a situation the grade in "x" is expected to be quite low.

A good example of the domain concept is the Boss Mountain porphyry molybdenum deposit (Soregaroli and Nelson, 1976), where economic concentrations of molybdenum occur in domains controlled by structures including collapse breccias, single vein systems and multiple vein systems (stringer zones) containing vein stages of different age and mineralogies.

To identify different structural domains within a deposit it is important to start first with identification of various stages of vein formation. Often each vein stage not only contains different mineralogies (for example molybdenite in one stage and chalcopyrite in another vein stage), but also may be developed in different parts of deposit, having different vein orientations, though often different vein stages at least partly overlap.

2.6.1: The Boss Mountain Example

In the case of Boss Mountain Soregaroli and Nelson (1976) described six vein stages based on cross-cutting relations, attitudes and the mineralogy, only three of which contain ore minerals of economic interest (stages 3 to 5 inclusive). Stage 1 veins contain quartz and minor amounts of pyrite and have attitude N50E, with almost vertical dip. They are widespread through the whole deposit area, but are nowhere abundant. Stage 2 veins are distributed north of Quartz Breccia (Figure 2-12) and extend into matrix of Quartz Breccia. They are filled with quartz and minor pyrite. Stage 3 veins are located roughly north, south and west of the Main Breccia zone (Figure 2-12) and contain quartz,

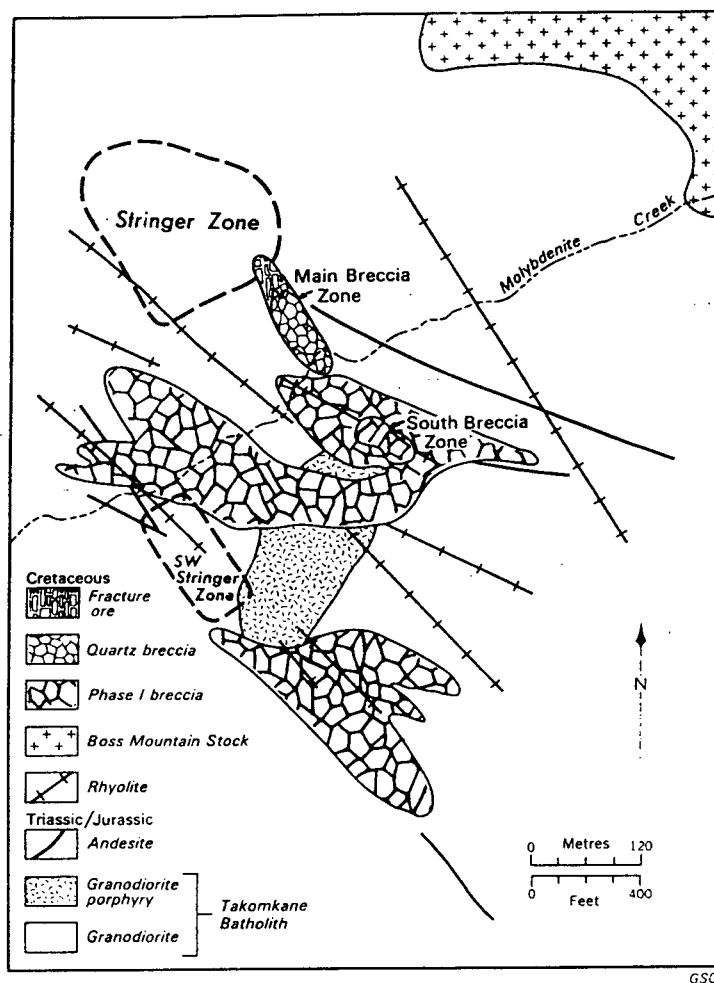


Figure 2-12: Surface geology of the Boss Mountain deposit showing distinct mineralization domains (see text for details). After Soregaroli and Nelson (1976).

molybdenite and minor pyrite. These veins are not abundant enough to form separate ore zones or ore domains, but they add a minor amount of molybdenum to part of the ore mined in Quartz Breccia and in the Stringer Zone. Stage 4 veins contain mainly quartz with molybdenite plus pyrite and orthoclase. They are the stage that is richest in molybdenite and form an important part of several ore bodies, especially the Stringer Zones. Stage 5 veins contain quartz and molybdenite and are the second-most important vein stage economically. They form the High-Grade Vein orebody (Figure 2-13). Stage 6 veins are fractures containing mainly chlorite and represent the final stage in mineralizing event. They do not contain economic mineralization. Stage 6 veins are widespread within the deposit.

As Sinclair and Vallee, (1994 b) emphasize different parts of a single deposit can be distinctive geologically and, thus, can be characterized by different models of physical or statistical continuity. As a result, for mineral inventory purposes it may be necessary to divide deposits into separate domains using as a basis geological features controlling mineralization as well as individual styles of mineralization that usually may characterize different domains.

Based on the presence or absence of vein stages described combined with structural features like collapse breccias and subparallel swarms of fractures the Boss Mountain deposit can be divided into distinct domains as described below.

Main Breccia Zone

This domain is composed mainly of Quartz Breccia (Figure 2-12), with molybdenite occurring along fragment boundaries, and within Stage 3 veins that cut the breccias.

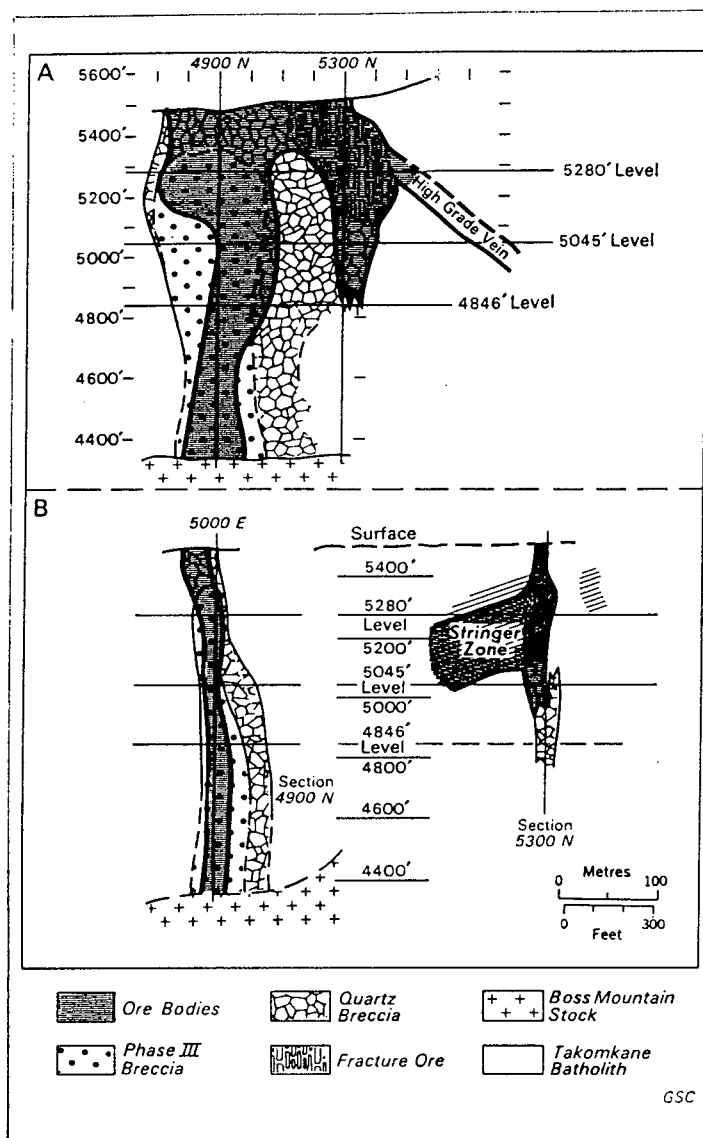


Figure 2-13: Longitudinal section (A) and cross section (B) of Main Breccia Zone and Stringer Zone of Boss Mountain deposit (see text for details). After Soregaroli and Nelson (1976).

Fracture Ore Zone (Figures 2-12 and 2-13).

The term "fracture ore" is used for the re-brecciated upper part of the Quartz Breccia. Molybdenite in this zone was introduced mainly during the emplacement of Stages 4 and 5 veins.

South Breccia Zone (Figure 2-12)

Economic mineralization is erratic, concentrates in the fractures and in the matrix of the breccia. There are Stage 2 veins in some parts of this zone, however Stage 4 veins are widespread in this zone and cut the whole zone.

Stringer Zone and Southwest Stringer Zone (Figures 2-12 and 2-13)

Most veins within the mine area are narrow and individually do not constitute ore. However, where they occur in subparallel swarms (stringers) they form low-grade orebodies. Both stringer zones contain both Stage 4 and Stage 5 quartz-molybdenite veins. Ore boundaries correspond to rapid decreases in the distribution density of veins.

High-Grade Vein (Figure 2-13)

This mineralization domain is characterized by veins of Stage 5. These quartz-molybdenite veins are localized in a sheared and intensely altered andesite dyke north of the Main Breccia Zone.

Recognition and coding of different styles of mineralization allows the organization of assay information into different domains. Main Breccia Zone and South Breccia Zone are two Boss Mountain domains that are characterized by similar continuity. In both of them molybdenite occurs mainly in breccia matrix or along fragment boundaries. This type of mineralization has a strong likelihood of isotropic continuity, which means that there is

no preferred orientation in the measure of value continuity. Some breccias are overprinted by one or more vein stages which can contribute to an anisotropy of value continuity.

Fracture Ore Zone contains economic mineralization in the matrix of the breccia and partly in the stockwork type fractures on the contact of this domain with granodiorite. This type of mineralization also indicates isotropic continuity. Where stockwork type mineralization occurs the situation can be significantly different. Where the planar orientations forming stockworks are more-or-less equally developed the continuity will be isotropic or nearly so. Where one planar direction is much more strongly developed than others, value continuity can be strongly anisotropic with the long axis of anisotropy lying somewhere within the strongly developed planar direction. Stringer Zone and South Stringer Zone are two Boss Mountain domains with one, strongly preferred direction of continuity. High-Grade Vein domain, like the stringer zones, is characterized by one strongly preferred continuity direction (Figure 2-13).

One of the important aspects of the study of different vein stages, from the point of view of resource/reserve estimation is that it allows a comparison (correlation) of the results of a variety of data analysis techniques with geological reality. Good examples are the Stringer Zones in case of Boss Mountain, where two different vein stages constitute a zone of economic mineralization: Stage 4 and Stage 5 veins. They not only have slightly different mineralogies, but also were formed in different periods of time. It is possible that when analyzing assay data from Stringer Zones one would obtain a cumulative distribution curve indicating two molybdenum populations, not just one.

2.6.2: The Endako Example

A second example of the relation of structural (geological) domains to ore continuity is the Endako porphyry molybdenum deposit in central British Columbia. Figure 2-14 shows the orientations of major veins over one level of the Endako open pit (Kimura et al., 1976). Here the east dyke swarm trending roughly 45° forms a divisional boundary that defines two significantly different structural domains: Endako East and Endako West. Individual veins have limited projection, but the vein systems can be traced throughout the deposits and have clearly defined trends. This detailed geological information was generated during production but it illustrates the need to define geological trends during exploration, so that resource/reserve estimates can be optimized.

Figure 2-15 shows an idealized model of directional structures. This simplified model relates 2 characteristics important in resource/reserve estimation. In the vertical direction there is a change in direction of continuity from major direction of continuity trending 0° (at the top), through more or less isotropic model of continuity (middle), to major direction of continuity trending 90° (bottom). In the horizontal direction there is a change in vein density.

2.6.3: The Bougainville Example

The Panguna mine is a large porphyry copper and gold open pit mine on Bougainville Island in Papua New Guinea (King et al., 1985). The ore deposit consists of steeply to moderately dipping quartz-sulphide veins, sulphide veins and joint-controlled mineralization with minor disseminations in rock matrix occurring in diorite, granodiorite, and porphyry intrusive into flat-lying andesite. The deposit contains minor, but high grade

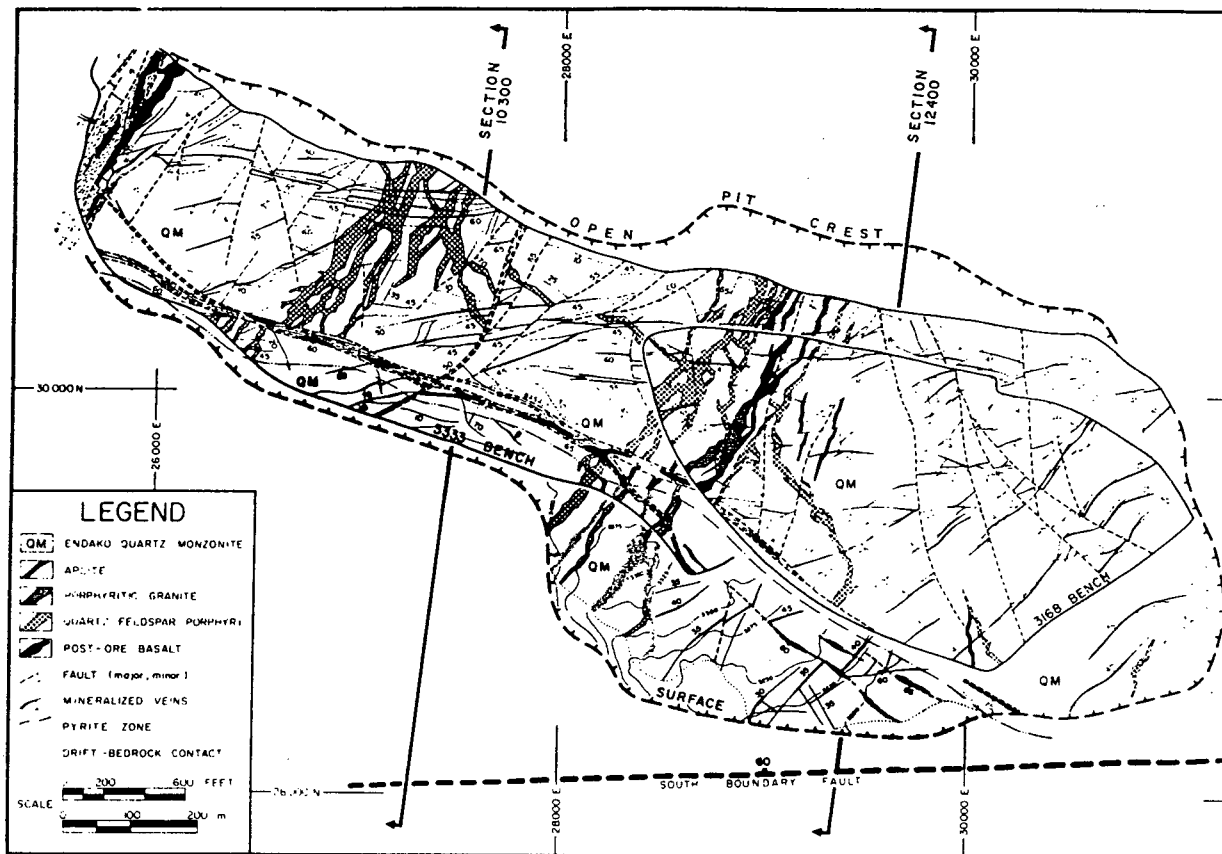


Figure 2-14: Two significantly different orientations of major veins in East and West parts of Endako open pit. After Kimura et al. (1976).

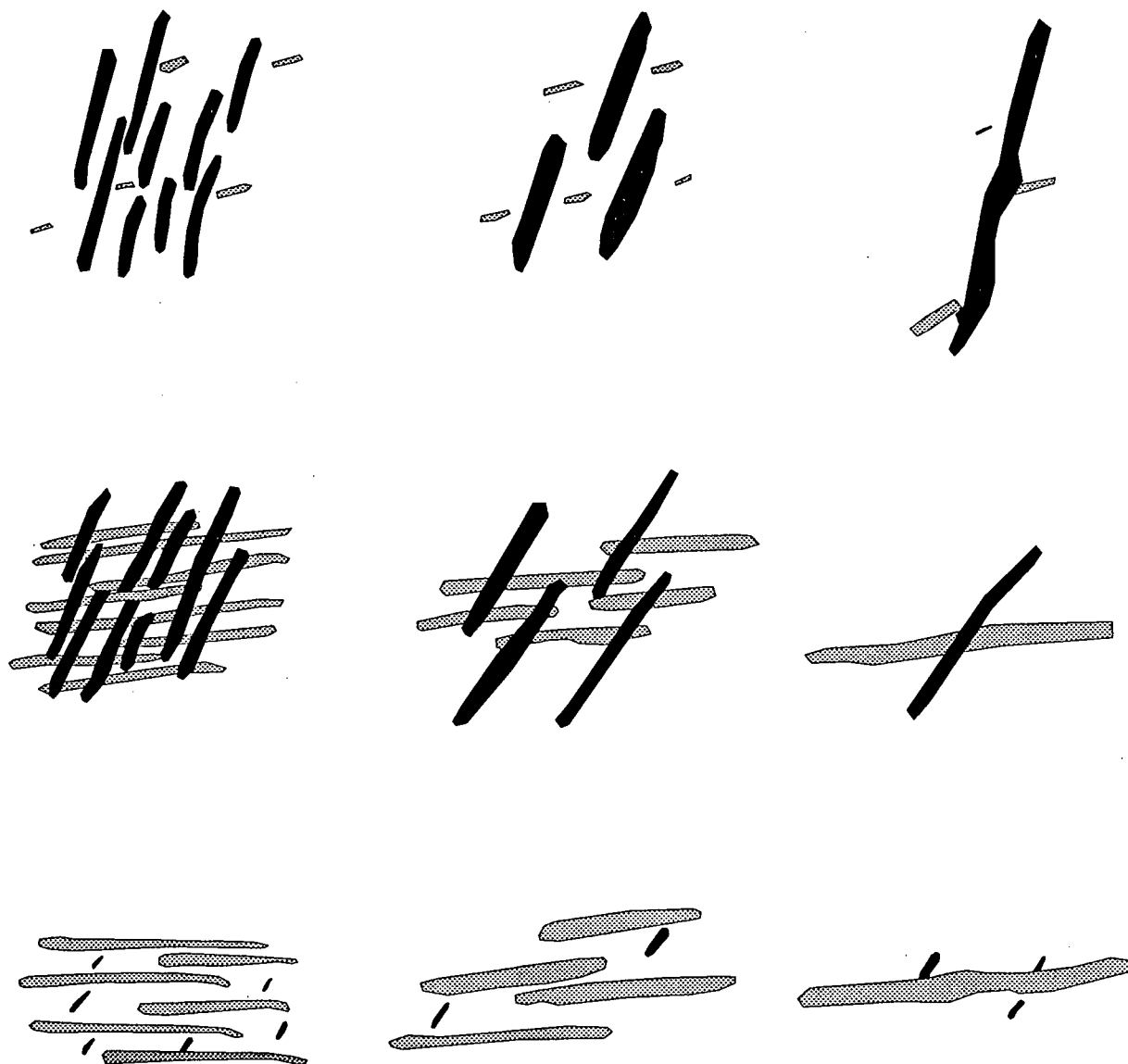


Figure 2-15: Idealized model of directional structures; direction of major continuity changes vertically, while change in vein density occurs horizontally.

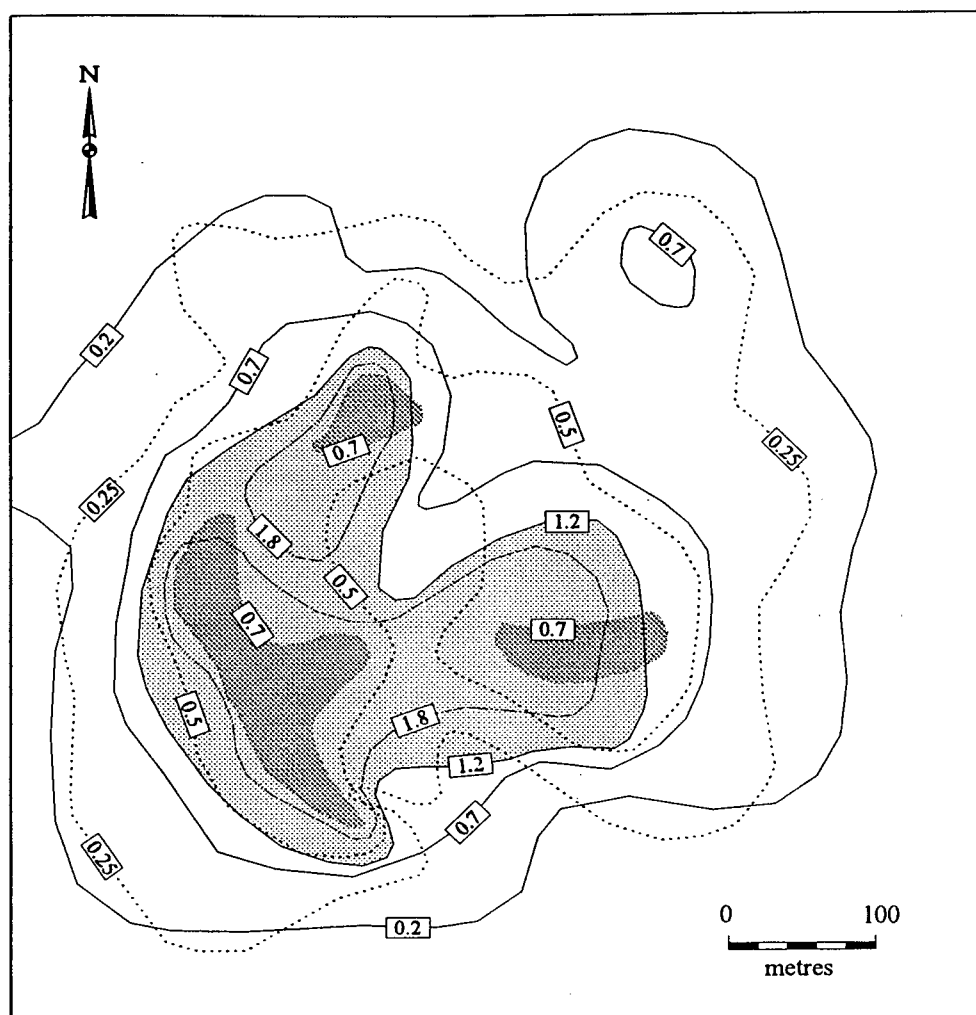
breccia. There are grade variations between the various rock types. King et al. (1985) state that the appreciation of the deposit geology is very important to mineral inventory estimation. They emphasize that each lithological ore-type should be treated as a separate orebody (domain) for purposes of resource/reserve estimation.

2.7: Metal zoning and definition of domains

In addition to styles of mineralization (section 2.6), a pronounced mineral zoning may also lead to a locally distinctive character of continuity. For example, particularly high grade zones may have a significantly different pattern of continuity than a lower grade zone. The matter can be important where multiple metals contribute to the value of a deposit, for example, Cu-Mo deposits or Cu-Au deposits. Consider Cu-Au porphyry deposits as an example of mineral zoning and its impact on domain definition.

According to Lowell (1989) the gold content of porphyry copper deposits ranges from less than 0.05 g/t to more than 1 g/t. Sillitoe (1993) defines gold-rich porphyry deposits as those containing more than 0.4 g/t Au, to as high as 2 g/t Au.

Sillitoe (1993) as well as Vila and Sillitoe (1991) state, that the bulk of gold in gold-rich porphyry deposits is introduced with copper during K-silicate alteration, and as a general rule, gold and copper grades vary sympathetically. The Virginia deposit (Postolski and Sinclair, 1998) illustrates this relationship particularly well. Gold is generally associated with chalcopyrite (Van Nort et al., 1991; Cuddy and Kesler, 1982) or bornite (Cuddy and Kesler, 1982) in gold-rich porphyry deposits in quantities proportional to the copper grade (Reed, 1983; Sillitoe, 1979).



— Gold isopleth (ppm)

● > 1.2 ppm Au

- - - Copper isopleth (%)

● > 0.7% Cu

Figure 2-16: Spatial superposition of gold and copper grades on upper level of the Dizon deposit, Philippines. After Sillitoe and Gappe (1984).

Figure 2-16 shows the spatial superposition of gold and copper grades in Dizon deposit in Philippines. Lowell (1989), describes this deposit as roughly circular in plan with a 500 m diameter. It has the form of 300 m high cylinder. The deposit contains about 100 Mt of 0.5% copper, and 1 g/t gold.

2.8: A critical relationship between geological features and semivariogram models

The semivariogram, the fundamental tool for geostatistics (e.g. Matheron, 1971), is an autocorrelation measure between values at any two sample sites. These autocorrelation values can vary with both distance and direction and, hence, can be isotropic or anisotropic in character. Similarly, geological features can be isotropic or anisotropic in character and various authors have shown the control that geology commonly exerts on the details of a semivariogram model for a deposit or domain (Sinclair and Giroux, 1984; Rendu, 1984). Sinclair and Giroux (1984) state *“semivariogram models clearly reflect geological character of mineral deposits”* and illustrate the close relation between autocorrelation function (semivariogram) and geological features. Their work was confined to precious metal deposits but the generality of their conclusion is widely accepted. In fact, the evidence for geological control of preferred directions of value continuity is so strong that where limited data are available models can be estimated with confidence by restricting variography to principal geological directions (e.g. bedding and perpendicular to bedding; within a preferred vein orientation and perpendicular to the vein orientation; etc.). The importance of quantifying this relationship for the purpose of resource/reserve estimation is apparent qualitatively; in block estimation nearby samples should carry more weight than more distant samples.

Moreover, the complications of anisotropy of a continuity model must be quantified because, for example, a sample in direction x that is a distance h from a block to be estimated might carry the same weight as a sample a distance $3h$ in direction y .

Generally speaking the semivariogram $\gamma(h)$ is a function of both the points x_i and x_{i+h} and the vector h . However, in order to make estimation of the semivariogram function from the available data possible, the so called intrinsic hypothesis is introduced (Journel and Huijbregts, 1978) which states that the semivariogram function $\gamma(x,h)$ depends only on the separation vector h (both its modulus and direction) and not on the location x_i of the point in question. It is then possible to estimate the experimental semivariogram from the available data according to the following relationship:

$$\gamma^*(h) = \{1 / [2 \cdot N(h)]\} \cdot \sum_{i=1}^{N(h)} \{[z(x_i) - z(x_{i+h})]^2\}$$

where $N(h)$ is the number of experimental pairs $[z(x_i) - z(x_{i+h})]$ of data separated by the vector h , and $z(x_i)$ is a sampled data value at location x_i .

2.8.1: Relationship between geology of porphyry-type deposits and variography

Rendu and Readdy (1982) also discuss the relationship of autocorrelation character to geologic domains, the semivariogram, mathematical modeling, and geologic interpretation and include two practical examples involving porphyry-type environments. The first one describes a deep porphyry molybdenum or porphyry copper deposit for

which oxidation, leaching and supergene enrichment have not significantly modified the pattern of hypogene mineralization. In this case the grade distribution throughout the deposit reflects the primary ore controls, mineralization sequence and form. Figure 2-17 shows a typical porphyry deposit having shape of an inverted cup and near vertical axis, representing a single mineralization event (one shell of mineralization). The bottom part of the figure 2-17 shows a horizontal section through such a deposit. In this case the mineralization commonly approximates the shape of a "doughnut" (cf. Noble and Ranta, 1984). In porphyry systems the ore shell is not always continuous with regard to ore grade mineralization. At various depths within the deposit, horizontal sections may show gaps in the economic grade within the mineralization "doughnut".

Figure 2-18 is a bar graph showing the distribution of sample values which can be observed when drilling a hole through the mineralization (line CC' on fig. 2-17). Below the hanging wall of the mineralization the sample values increase rapidly. A maximum is reached at a point which approximately corresponds to the centre of mineralization (point S2 on figures 2-17 and 2-18). Beyond this point, the values decrease, until the footwall of mineralization is reached. Understanding the geometry of the mineralization shell and relationship between sample location and sample value as indicated by figures 2-17 and 2-18 may be helpful to improve the semivariogram study.

Semivariogram measures the dissimilarity between sample values as a function of the distance between the samples. In general applications a straight line distance can be used for this purpose. However when looking at figure 2-17 it seems logical that more complex and geologically meaningful definition of distance is required (Noble and Ranta, 1984). The important remark here is that when calculating semivariogram the very

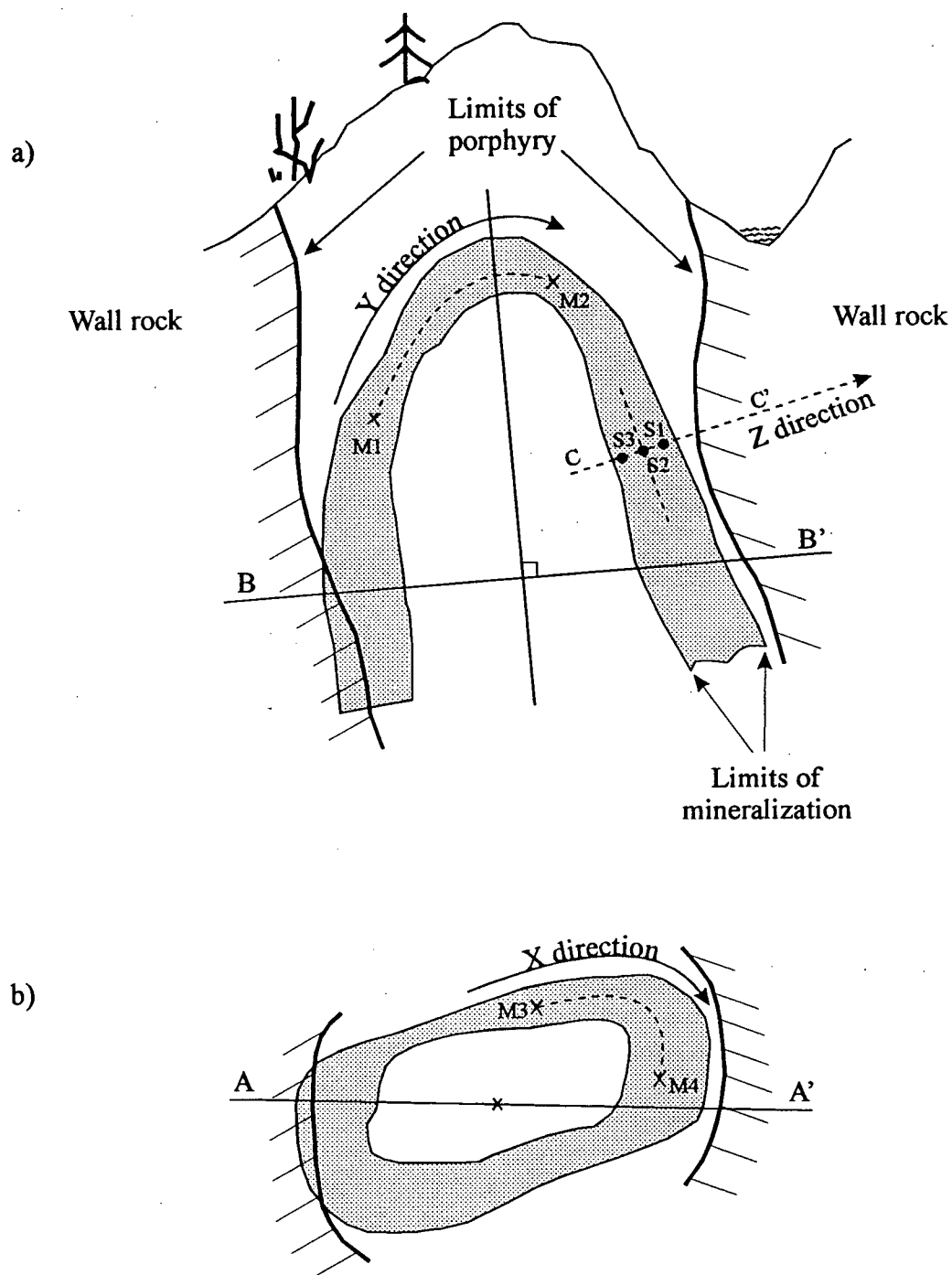


Figure 2-17: Schematic representation of a typical deep seated porphyry deposit having shape of an inverted cup and near vertical axis; (a) section A-A' along axis of porphyry, (b) section B-B' normal to the axis of porphyry. After Rendu and Readdy (1982)

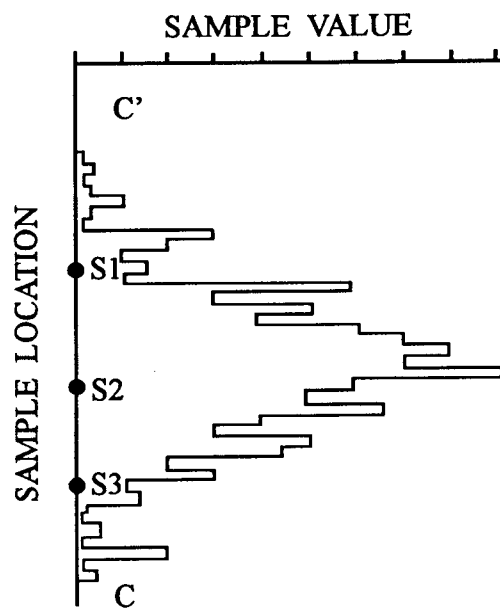


Figure 2-18: Bar graph showing sample values across the mineralization (along line C C') from Figure 2-17. After Rendu and Readdy (1982).

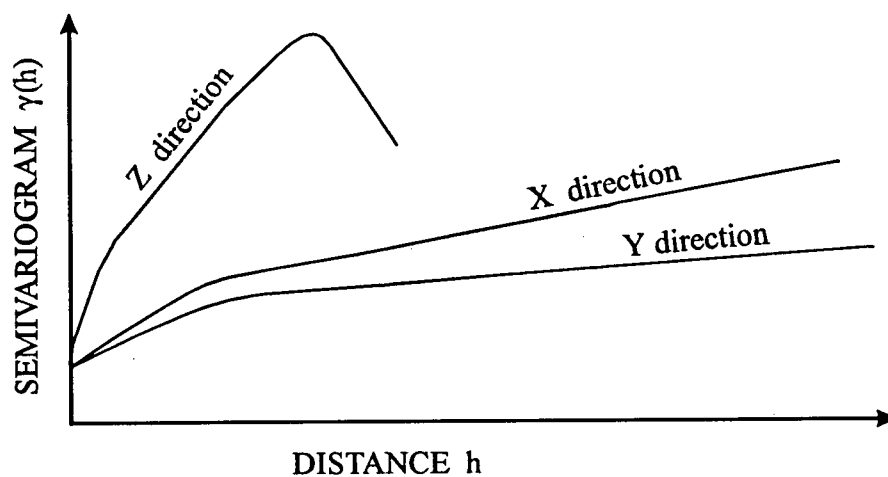


Figure 2-19: Directional semivariograms in porphyry deposit as shown on Figure 2-17, in 3 different directions (discussion in text). After Rendu and Readdy (1982).

important feature that has to be taken into account is the geometry of the mineralization.

The variability in sample values along the line CC' normal to the mineralization (figure 2-17) may be very high over short distances. This is confirmed by figure 2-18, which shows that sample S2 near the centre of the mineralized zone has a high value, while samples S1 and S3, near the hanging wall and footwall of the mineralization respectively, have much lower values.

A semivariogram calculated along the line CC' is shown on Figure 2-19 as "Z direction" semivariogram. It shows a rapidly increasing variability when the distance between samples increases, followed by a rapidly decreasing variability. This behavior of the semivariogram reflects the symmetry of the grade distribution across the mineralized zone, as indicated by figure 2-18. On the other hand the changes in grade values, either within a vertical section plane passing through the axis of the porphyry (Figure 2-17a), or within a plane normal to this axis (Figure 2-17b), may be relatively slow over large distances. However the distances between samples cannot be measured along the straight line, since the straight line distance between two points M1 and M2 (cf. Figure 2-17a) is geologically meaningless. This distance should be measured along the curve parallel to the general shape of the mineralization (cf. Noble and Ranta, 1984). The same situation applies to points M3 and M4 as shown on Figure 2-17b.

The straight line distance between two points is geologically meaningful only if this distance is small with respect to the dimensions of the mineralization.

Semivariogram analysis of a porphyry deposit, as shown above, will often require the definition of a non-cartesian system of coordinates, defined as follows:

1. the X coordinate is measured along the dashed line joining the points M3 and M4 in the section plane as shown in Figure 2-17b
2. the Y coordinate is measured along the dashed line joining the points M1 and M2 in vertical section plane as shown in Figure 2-17a
3. the Z coordinate is measured along normal to the mineralized shell (direction CC' as shown on Figure 2-17a and Figure 2-18)

Examining once again figure 2-19 it can be seen that in the X and Y directions the semivariogram shows much slower increase in variability than semivariogram in the Z direction. Also, in the X and Y directions the semivariograms show continuous increase in variability over rather large distances, but the sill of semivariogram in directions X and Y is definitely much lower than in the Z direction. Also semivariogram ranges in X and Y directions are much longer than in the direction Z, indicating that the continuity of mineralization in directions X and Y is much better than in the Z direction.

However comparing the semivariogram in the X direction with the semivariogram in the Y direction it is clear that the semivariogram calculated in the Y direction shows the best continuity of mineralization.

Thus, all three semivariogram models in X, Y, and Z directions give a geological interpretation, that is in agreement with the geological model from figure 2-17.

The second practical example showing a critical relationship between geology and the semivariogram that corresponds to porphyry environments discussed in paper by Rendu and Readdy (1982) describes a supergene enriched porphyry copper deposit. In this example the effect of past erosion and supergene processes is such that significant oxidation, leaching, and enrichment took place.

A typical porphyry copper deposit with supergene enrichment is shown on figure 2-20. In this situation, each one of the different geological zones of the mineralization (domains) should be analyzed separately. Rendu (1984), defined five such zones (domains) as follows:

domain 1 - a leached zone (both in andesite and in diorite)

domain 2 - an enriched zone in andesite

domain 3 - an enriched zone in diorite

domain 4 - primary mineralization in andesite

domain 5 - primary mineralization in diorite

Semivariogram model should be constructed for each of the five domains separately.

From the above description it can be seen that the mineralization is contained in andesite (host rock type 1), and in diorite (host rock type 2). These host rocks have similar chemical composition but different physical properties. The fracture density is higher in the diorite, what results in easier circulation of the supergene fluids and more surface area in contact with them. On the other hand the acidity of supergene fluids is more rapidly neutralized in andesite, what inhibits the development of supergene enrichment.

This geological interpretation is illustrated by figure 2-21, which compares graphs of sample values vs. depth (so called "histograms"), down the drill hole, in the supergene and hypogene sulfide mineralization for both andesite and diorite.

Figure 2-22 shows semivariograms calculated for four domains, namely: supergene sulfide enrichment in andesite (rock type 1), supergene sulfide enrichment in diorite (rock

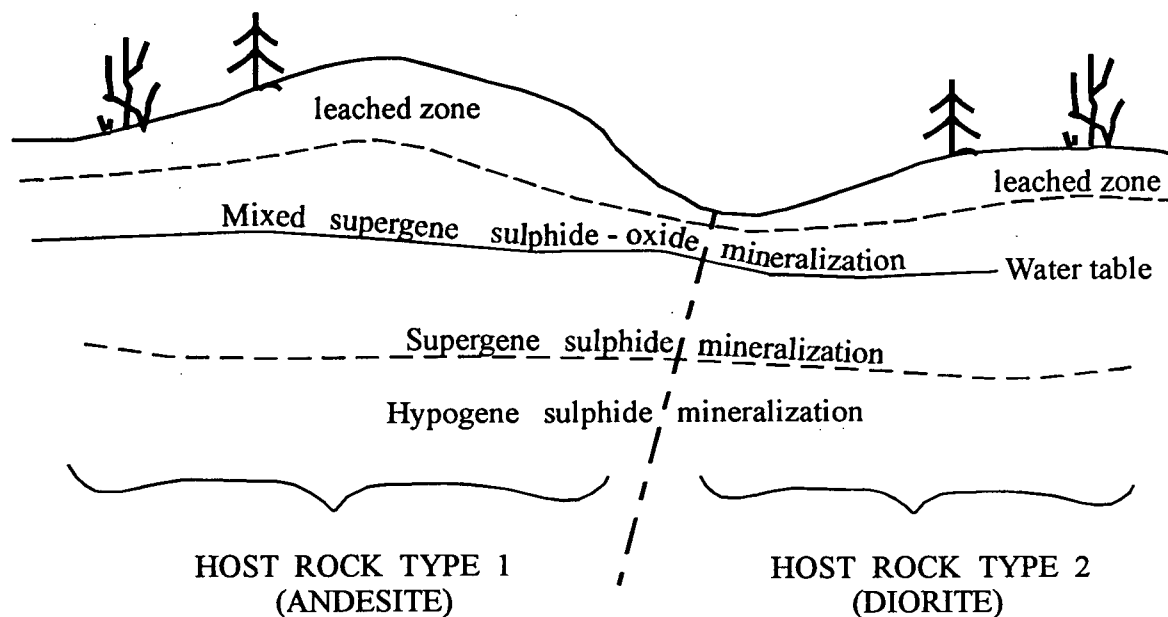


Figure 2-20: Schematic representation of a typical porphyry copper deposit with supergene enrichment; five different domains defined (for details see text). Modified from Rendu and Readdy (1982).

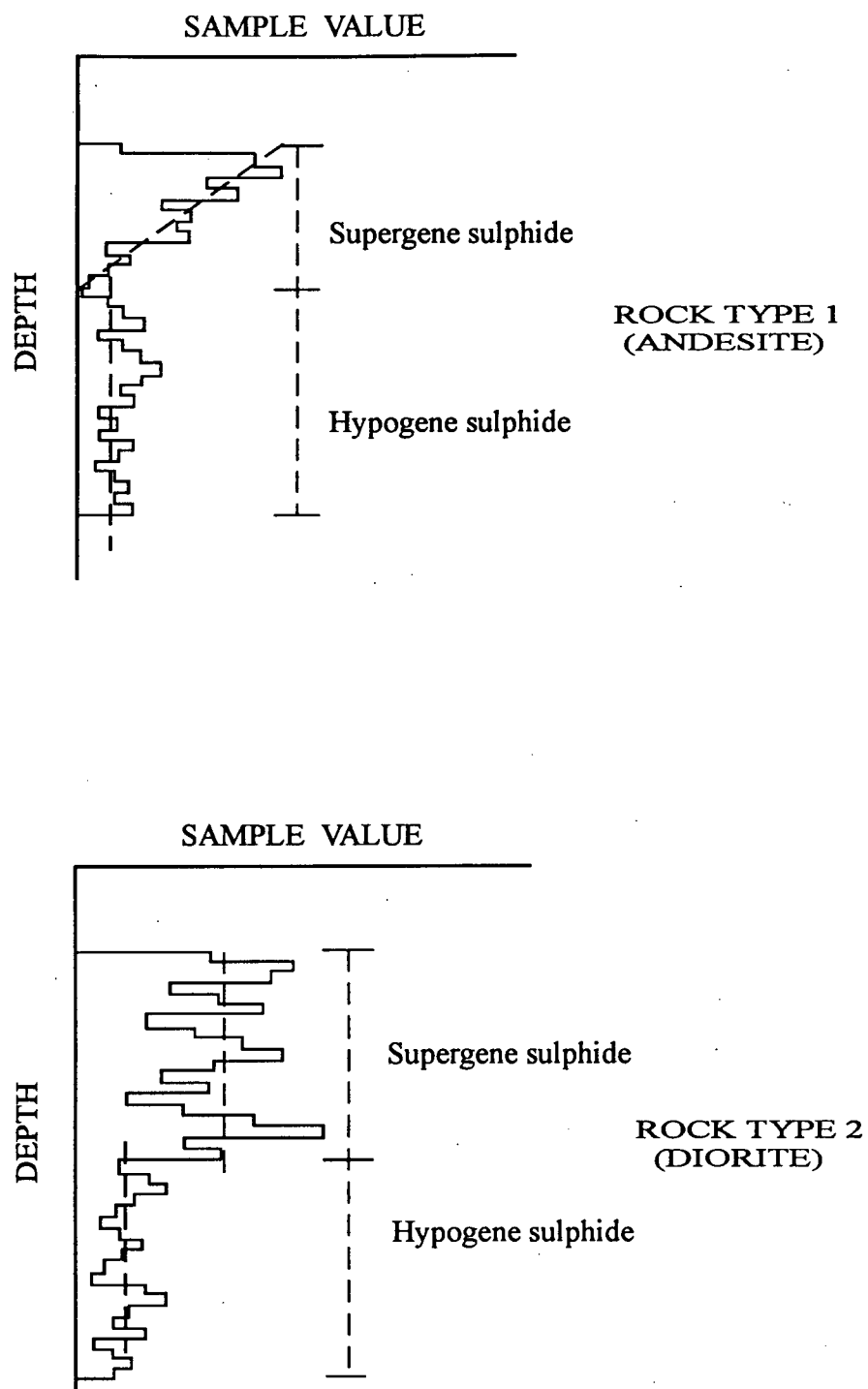


Figure 2-21: Bar graphs showing sample values in two rock types - andesite (upper), and diorite (lower) for supergene and hypogene sulphide mineralization zones of porphyry copper deposit from Figure 2-20. After Rendu and Readdy (1982).

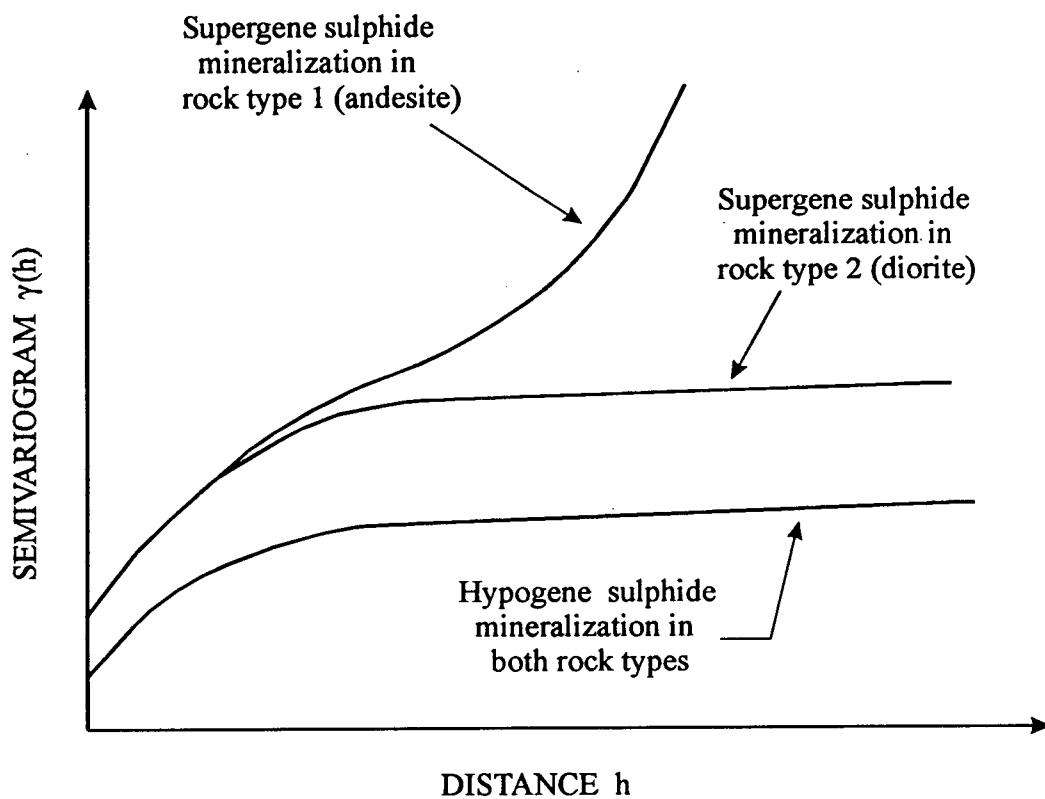


Figure 2-22: Down hole semivariograms in porphyry copper deposit as shown on Figure 2-20 developed for four different domains (discussion in text). After Rendu and Readdy (1982).

type 2), primary (hypogene) sulfide mineralization in andesite, and finally primary sulfide mineralization in diorite.

In the case of the primary sulfide mineralization semivariogram for andesite is identical to the semivariogram for diorite, which means that semivariograms are independent of rock type. The reason for this might be that the difference in fracture density within the two rock types was insignificant at the time of deposition of the hypogene mineralization.

The next conclusion is that the variability of sample values is much higher in the enriched zone, than in the primary zone. The geological interpretation may be that factors, which controlled enrichment, like fracture density and permeability of the supergene mineralized zone must have had much higher spatial variability, than the fractures and permeability that controlled deposition of the primary mineralization.

The semivariogram of the enriched mineralization in andesite (rock type 1) shows a very rapid parabolic increase in variability over large distances. This behaviour of the semivariogram reflects a systematic linear decrease in grade with increasing depth. As illustrated by figure 2-21 the enrichment in andesite is concentrated near the reduction - oxidation surface (the water table) and then rapidly and systematically decreases with depth.

On the other hand the supergene sulfide mineralization in diorite extends to a greater depth and does not show any systematic variation, what is confirmed by the semivariogram model, which is a transition model with sill of moderate level.

The geologic interpretation of this situation may be the presence of higher fracture density within diorite. The meteoric waters could follow the mineralized fractures, which resulted in enrichment at significant depths. On the other hand in andesite, because of the fewer open significant fractures, the movement and penetration of the supergene fluids were limited.

2.9: Problems of mineral beneficiation in porphyry-type deposits

As described above, mineralogical and textural variations of porphyry-type deposits have a significant impact on economics because they affect continuity models and thus impact on estimation. Equally importantly, mineralogy relates directly to metal recoveries in the mill, hence impacting on cutoff grade. The following example illustrates the kind of unpleasant surprises that can arise where detailed mineralogical studies have not been conducted.

“Recoveries averaged 67.68% for gold and 45.13% for copper....Given that the targeted recovery for gold was 82%, the lower-than-projected recoveries have been cause for concern.....Recoveries are complicated by the fact that there are many different styles of mineralization with individual metallurgical properties. (Robertson, 1998)”

The forgoing statement relates to recent problems at the Mount Polley porphyry Cu-Au mine in northern British Columbia in connection with 1.2 million tonnes grading 0.69 g/t Au and 0.353% Cu, production for the first 3 months of 1998. From these figures one can

calculate the average Au 'loss' per tonne relative to expectations, to be $(0.820 - 0.6768) \cdot 0.69 = 0.0987$ g Au (0.00289 ounces), that is, roughly US\$1.00/tonne assuming a gold price of US\$300.00 per ounce. Considering a daily production in excess of 13000 tonnes, such an unexpected loss mounts rapidly and the importance of recognizing metallurgical character early in the definition of ore is apparent.

The application of mineralogical techniques to mineral resource evaluation is commonly known as 'process mineralogy' (Kingston, 1992). One of the most useful aspects of process mineralogy is the 'mapping' of mineralogical and textural variations throughout a mineral deposit; most deposits are mineralogically heterogeneous so that significant variations from one part of a deposit to another are to be expected. These variations may be closely tied to the geological history of a deposit and include overlapping events such as several stages of mineralization, tectonism and metamorphism, all of which can have impact on ore mineralogy and texture. An extensive literature exists regarding these aspects of applied mineralogy, but such accounts involving porphyry-type deposits are limited, apparently because of a presumption of 'mineralogical simplicity'. One such example (Mueller, 1981) for the San Manuel mine, Arizona suggests that the resident mineralogist spends much more time dealing with metallurgical products rather than ore or concentrates.

Some of the specific attributes studied by process mineralogy include:

1. Identification, compositions and physical characteristics of individual minerals and mineral assemblages and their spatial array.
2. Quantified mineral abundances.

3. Textural analysis and spatial variations of important textural characteristics.
4. Classification and quantification of mineral intergrowths.
5. Liberation properties of important minerals.

In the early stages of property evaluation mineralogical studies are an integral part of practical procedures such as bulk sampling and the conceptual development of an ore deposit model. The same procedures can be extended if necessary to provide more comprehensive mineralogical data pertaining to resource/reserve estimation.

2.9.1: Mineral identification and mineral assemblages

Simple mineral identification is the basic information for many practical mineralogical applications including recognition of mineral zoning, localization of precious metals, paragenesis and vein stages, and so on. Generally, the mineralogy of porphyry-type deposits is simple but complexities can arise, particularly with gangue and supergene minerals.

Gangue minerals, which may include worthless opaque phases, are also very important. Problems with flotation can arise from the presence of fine layered silicates, such as sericite, which is the dominant mineral in phyllic alteration zone of porphyry-type deposits, or kaolinite, which can be found in the argillic zone. These minerals tend to float during flotation and in this way interfere with the efficiency of the flotation process.

Mineralographic studies are important, because the first concern in the untreated ore is to identify the phase or phases that carry the valuable metal or metals, since the initial information is available only as chemical analysis of the drillhole core. This analysis

does not provide either information on mineral phases present nor on their sizes and textural relations.

2.9.2: Quantified mineral abundances.

Mineral recognition is only a first step in a practical mineralogical study. Relative or absolute abundances are also essential. In some cases where a metal is confined to a single mineral of known composition these abundances can be estimated from assay information. Where possible, such estimates are usually much better than those obtained by mineralogical analysis because they are based on more and larger samples. Consider the example of unwanted Pb as galena in the Cu concentrate of the Brenda porphyry Cu-Mo deposit (Oriol, 1972). Contoured blast hole assays showed that galena was concentrated in certain parts of the Cu-Mo deposit and that blending of production from different localities could reduce the Pb concentrate to acceptable levels.

Another example comes from East zone of Huckleberry deposit. Figure 2-23 is a contour map of molybdenum assay values from this deposit. Since molybdenite is the only mineral containing molybdenum in this deposit the assay values can be easily transformed to absolute abundances of molybdenite.

Contour intervals for molybdenite in volume percent can be obtained by multiplying assay contour interval values (cf. Figure 2-23) by 0.95, a factor which was obtained from the following equation using atomic masses of the appropriate elements and specific gravities of molybdenite and the host rock:

$$(\text{MoS}_2 \cdot \text{S.G.}_{\text{rock}}) / (\text{Mo} \cdot \text{S.G.}_{\text{molybdenite}}) = [(96 + 2 \cdot 32) \cdot 2.69] / [96 \cdot 4.7] = 0.95$$

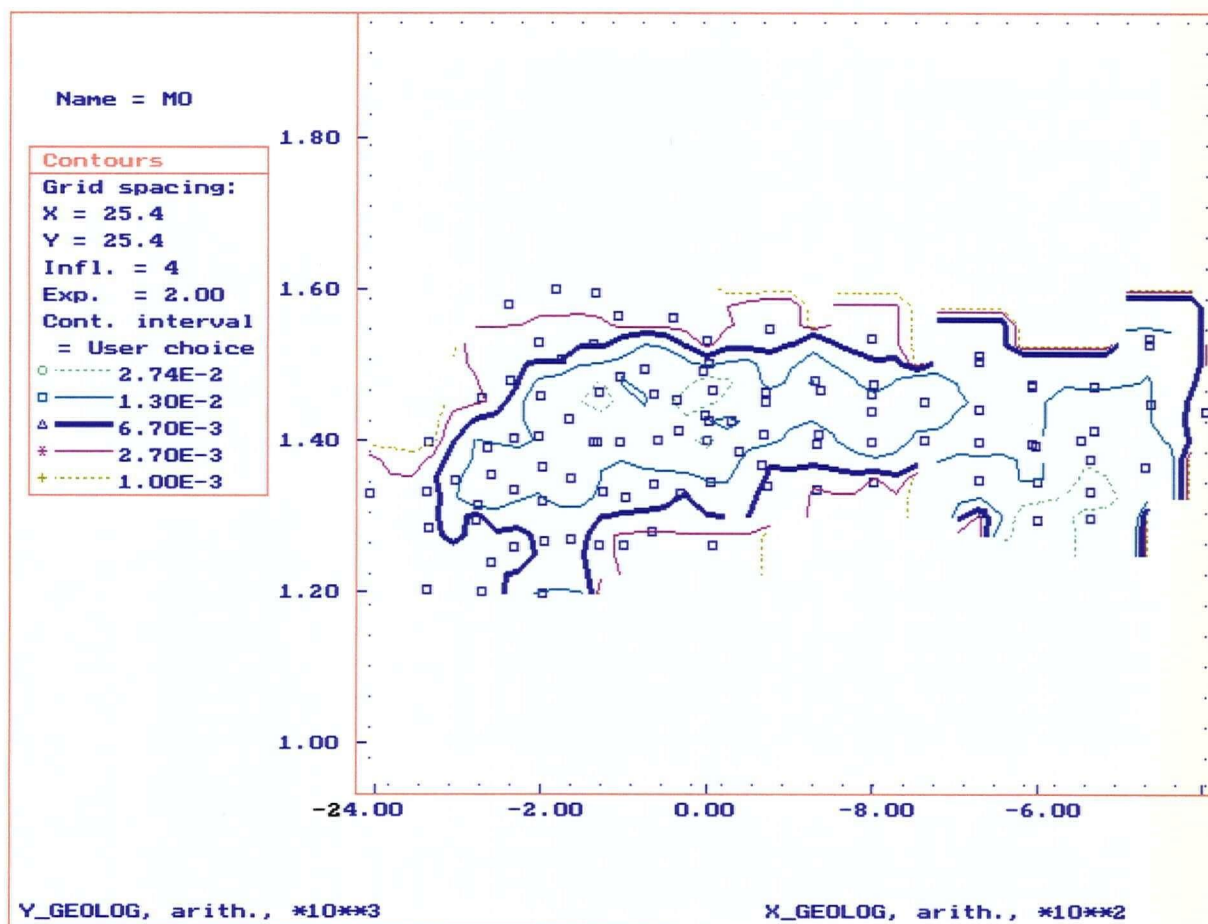


Figure 2-23: Huckleberry, East zone, Mo grade contour map for 8 m bench, level 940 m. Open squares are sample locations from drill holes; Mo values in percent.

Contour maps are very efficient in indicating spatial element (cf. Ranjbar, 1997) and mineral distribution patterns.

Mineralogical studies may be limited to simply recognizing 'major', 'minor' and 'trace' constituents.

2.9.3: Textural analysis

2.9.3.1: Grain size and spatial variations of grain size.

Chalcopyrite is the dominant copper mineral in porphyry type deposits. It usually occurs as anhedral interstitial grains and as fracture fillings in pyrite. Chalcopyrite is commonly moderate to coarse-grained. Bornite, if present, usually forms discrete anhedral grains that are also moderate to coarse-grained. Pyrite, especially in phyllic alteration zone is in the form of coarse (0.5 mm – 2 mm) subhedral vein fillings and disseminated grains. In molybdenum rich deposits such as Climax, the molybdenite is present as random to subparallel tinny (<0.1 mm) hexagonal plates embedded in the vein-filling quartz.

Coarse-grained chalcopyrite is common in potassic alteration zone, while coarse-grained pyrite dominates in phyllic alteration zone of porphyry type deposits.

2.9.3.2: Classification of intergrowths

An understanding of textures and intergrowths is fundamental to optimizing metal recovery in concentrates. Textures of the principal ore minerals in porphyry-type deposits are commonly simple. Copper minerals commonly are moderate to coarse-grained and generally are not intergrown complexly with other opaque minerals that are non-economic, such as pyrite and magnetite. Molybdenite can be finer grained and locked in

other sulphides, especially chalcopyrite, in porphyry copper deposits leading to relatively low recovery, perhaps 50 to 65 percent. In contrast, molybdenite commonly occurs as free grains in porphyry molybdenum deposits and recovery is high. Pyrite ordinarily occurs as anhedral to euhedral grains or blebs. Chalcopyrite as a dominant copper mineral occurs usually as anhedral interstitial grains in veinlets or as disseminated blebs in altered rock. Bornite, if present forms discrete anhedral grains with the pyrite and chalcopyrite and also occurs as exsolution lamellae within chalcopyrite.

2.9.3.3: Liberation properties of ores.

The majority of mineral beneficiation processes consists of two principal stages. The first stage is reduction in size of the particles of mined ore to a size as close as possible to that of individual economic mineral crystals. This process is very often called comminution. Its goal is the liberation of valuable minerals from the gangue and, in the case of complex ore, liberation of different valuable minerals from one another. The size of reduction required to achieve liberation is usually only a few hundreds of microns or even less in diameter, which means that extensive crushing followed by milling (grinding) of the ore is required.

The second stage in beneficiation is mineral separation in which the valuable minerals are removed as a concentrate, and remaining, usually valueless materials are removed as the tailings. The separation is usually achieved by using differences in the physical, chemical, or surface properties between ore and gangue minerals. Sulphide copper ores of porphyry-type deposits are very well suited to separation (recovery) method called froth flotation. In this method the surface chemistry of fine ore particles

suspended in aqueous solution is modified by addition of conditioning and activating reagents to be selectively attracted to fine air bubbles that are passed through this suspension called the pulp. These air bubbles, with the associated mineral particles, are trapped in a froth that forms on the surface of the pulp and can be skimmed off to accomplish the separation.

The simple textural picture of most hypogene ores is complicated somewhat by the presence of secondary minerals. In near surface ores covellite, chalcocite, and digenite commonly occur as replacement rims on pyrite, chalcopyrite and bornite. Commonly these secondary minerals are concentrated along grain boundaries of the host sulphides; in other cases they form along fractures cutting the earlier sulphides. Secondary bornite may also form oxidation lamellae within chalcopyrite (cf. Craig and Vaughan, 1981).

Molybdenite is present in significant amounts in the molybdenum-rich porphyry deposits, but is minor in many copper-rich deposits where it is commonly at least partly intergrown with chalcopyrite. Most molybdenite, however, occurs as subparallel foliae or rosettes in quartz-rich veinlets. Molybdenite in deposits like Climax may form subparallel, very small (< 0.1 mm) hexagonal plates surrounded by vein filling quartz (cf. Craig and Vaughan, 1981).

The precise identification and characterization of the ore minerals can save a great deal of work in the establishing of an efficient beneficiation system. As mentioned above in the first stage of beneficiation, which is comminution, the knowledge of the sizes and intergrowth relationships of ore mineral grains is very important, because the insufficient grinding may result in loss of valuable minerals in the tailings. On the other hand the overgrinding wastes energy and may produce slimes that are difficult to treat later in the

processing. In porphyry-type deposits, where the ore is mainly chalcopyrite and pyrite liberation is usually easy and can be achieved by grinding.

The process of liberation becomes more complex as the complexity of the mineralogy increases because of the increased likelihood of intergrowths. Moreover, the formation of supergene minerals such as chalcocite, covellite and native copper can lead to more complex textural relations. After comminution covellite may form microscopic or submicroscopic rims around pyrite grains. If ore in this condition were treated by froth flotation the pyrite grain coated by a rim of covellite would go to the copper concentrate, thus diluting it. This problem may be solved by dissolving the covellite coating before sending ore to flotation.

Flotation can be negatively affected also by oxide coatings of sulphide grains. Recognition of copper oxides in the sulphide flotation circuit is very important, because such material will not appear in a copper sulphide concentrate, but will go to the tailings.

A small percentage of chalcopyrite in many porphyry-type deposits occurs as small, rounded inclusions in pyrite or as very thin veinlets in pyrite and will be difficult or impossible to recover. The veinlet form may produce 'chalcopyrite surfaces' on what are mainly pyrite fragments and can end up diluting the copper flotation concentrate.

Another problem may arise in recovering the gold or silver from porphyry-type deposits, a matter of increasing importance in these times where gold-rich porphyry deposits represent one of the more important exploration targets internationally. Significant amounts of both elements can follow pyrite to the tailings during flotation. In the evaluation of a deposit it is imperative to recognize the possibility of systematic variations in the occurrence of gold. In some deposits problems may arise in recovering

gold, because it may be closely associated with pyrite and as such it will follow pyrite into the tailings. An example is the association of gold with pyrite in the 66 zone of the Mt. Milligan deposit, where gold occurs as inclusions in pyrite or adheres to imperfections on pyrite grains (cf. Sketchley et al., 1995).

In other porphyry copper deposits gold is closely associated with chalcopyrite, in which case gold should follow chalcopyrite into the copper concentrate. An example might be the association of gold with chalcopyrite in the Huckleberry deposit. Postolski and Sinclair (1994) state that multivariate geochemical data analysis shows a strong correlation of gold with copper in the Huckleberry case.

2.10: Conclusions

Geology contributes important information towards producing high quality resource/reserve estimates. Following is a general summary of types of geological and related information that can be useful in developing a comprehensive knowledge of mineral inventory in porphyry type deposit.

1. Detailed geological mapping is the basis for the integration of geological features into the resource/reserve estimation process.
2. Three dimensional modeling imposes hard ore-waste boundaries where they may or may not exist and can lead to significant dilution that must be estimated.
3. The ability to classify a deposit as representative of a particular, well defined ore deposit model provides a high level of confidence for various decisions relating to geological continuity of mineralization in porphyry-type deposits.

4. Ore deposit models incorporate variations in zoning patterns of mineralization, alteration, and style of sulphide occurrence in porphyry type deposits, all of which can impact on continuity. Hence, geological character helps define domains with different continuity character.
5. Value continuity generally is quantified by semivariogram models fitted to experimental semivariograms. A thorough, systematic approach to semivariogram modeling, incorporating a knowledge of geological features, is an essential step in resource/reserve estimation. Presence of anisotropy implies that the spatial continuity of grade values is different in different directions.
6. Multiple domains, each characterized by its individual continuity model for grade values, are common features that must be taken into account by the resource/reserve estimation process.
7. Domain boundaries may be hard or soft; their character will limit the acceptable methods of resource/reserve estimation.
8. Mineralogical characterization of porphyry-type deposits should be an ongoing undertaking that documents the spatial distribution of mineralogical and textural characteristics and their impact on metal recoveries.

Acknowledgements

Special thanks are extended to Dr. A.J. Sinclair for supervising the research work on which this paper is based, assisting with problems and providing constructive criticism throughout the study.

References

- Beane, R.E. and Titley, S.R., 1981, Porphyry copper deposits, Part II. Hydrothermal alteration and mineralization; *Economic Geology*, 75th Anniversary Volume, p. 235-269
- Bysouth, G.D. and Wong, G.Y., 1995, The Endako molybdenum mine, central British Columbia: An update; in Schroeter, T.G., ed., *Porphyry Deposits of the Northwestern Cordillera of North America*; Canadian Institute of Mining Metallurgy, Special Volume 46, p. 697-703
- Carr, J.M. and Reed, A.J., 1976 Afton: A supergene copper deposit; in Sutherland Brown, A., ed., *Porphyry Deposits of the Canadian Cordillera*; Canadian Institute of Mining and Metallurgy, Special Volume 15, p. 376-387
- Cuddy, A.S. and Kesler, S.E., 1982, Gold in the Gransile and Bell Copper porphyry copper deposits, British Columbia; in Levison, A.A., ed., *Precious Metals in the Northern Cordillera*; The Association of Exploration Geochemists p. 139-155
- Craig, J.R. and Vaughan, D.J., 1981, *Ore microscopy and ore petrography*; John Wiley and Sons, New York, 406 p.
- David M., 1988, *Handbook of applied advanced geostatistical ore reserve estimation*; Developments in geomathematics 6, Elsevier, Amsterdam, 216p.
- Drummond, A.D. and Godwin, C.I., 1976, Hypogene mineralization - an empirical evaluation of alteration zoning; in Sutherland Brown, A., ed., *Porphyry Deposits of the Canadian Cordillera*; Canadian Institute of Mining and Metallurgy, Special Volume 15, p. 52-63
- Drummond, A.D., Sutherland Brown, A., Young, R.J. and Tennant, S.J., 1976, Gibraltar - regional metamorphism, mineralization, hydrothermal alteration and structural development; in Sutherland Brown, A., ed., *Porphyry Deposits of the Canadian Cordillera*; Canadian Institute of Mining and Metallurgy, Special Volume 15, p. 195-205
- Guilbert, J.M. and Lowell, J.D., 1974, Variations in zoning patterns in porphyry ore deposits; *Canadian Institute of Mining and Metallurgy, Bulletin*, v.67, no. 742, p. 99-109
- Gustafson, L.B., 1978 Some major factors of porphyry copper genesis; *Economic Geology*, v.73, p.600-607
- Heberlein, D.R. and Godwin, C.I., 1984, Hypogene alteration at the Berg porphyry copper-molybdenum property, North-Central British Columbia; *Economic Geology*, v. 79, p. 902-918

Hollister, V.F., 1991, Chapter 1: Porphyry copper and related skarn deposits; in Hollister, V.F., ed., Porphyry copper, molybdenum and gold deposits, volcanogenic deposits (massive sulphides), and deposits in layered rocks, AIME, Case histories of mineral discoveries, Volume 3; Society for Mining, Metallurgy and Exploration Inc., p. 1-43

Hollister, V.F., 1978, Geology of the porphyry copper deposits of the western hemisphere; Society of Mining Engineers of AIME, New York, 219 p.

Isaaks, E.H. and Srivastava, R.M., 1989, An introduction to applied geostatistics; Oxford University Press, New York, 561 p.

James, A.H., 1971, Hypothetical diagrams of several porphyry copper deposits; Economic Geology, v. 66, p. 43-47

Journel A.G. and Huijbregts, 1978, Mining geostatistics; Academic Press, New York, 599 p.

Kimura, E.T., Bysouth, G.D. and Drummond, A.D., 1976, Endako; in Sutherland Brown, A., ed., Porphyry Deposits of the Canadian Cordillera; Canadian Institute of Mining and Metallurgy, Special Volume 15, p. 444-454

King, H.F., McMahon, D.W., Bujtor, G.J. and Scott, A.K., 1985, Geology in the understanding of ore reserve estimation: an Australian viewpoint; Society of Mining Engineers of AIME, preprint no. 85-355, 13 p.

Kingston, G. A., 1992, Mineralogy in the evaluation of ore deposits; in Annels, A. E. (ed.), Case Histories and Methods in Mineral Resource Evaluation: Geol. Soc. Spec. Pub. No. 63, p. 47-59.

Kirkham, R.V. and Sinclair, W.D., 1995, Chapter 19: Porphyry copper, gold, molybdenum, tungsten, tin, silver; in Eckstrand, O.R., Sinclair, W.D and Thrope, R.I., eds., Geology of Canadian mineral type deposits, Geology of Canada, no. 8; Geological Survey of Canada, p.420-446

Krige, D.G. and Dunn, P.G., 1995, Some practical aspects of ore reserve estimation at Chuquibambilla Copper Mine, Chile; Proc. APCOM XXV Conference, 9-14 July, 1995, Brisbane, Australia, p. 125-133

Lowell, J.D., 1989, Gold mineralization in porphyry copper deposits discussed; Mining Engineering, v. 41, no. 4, p.227-231

Lowell, J.D. and Guilbert, J.M., 1970, Lateral and vertical alteration-mineralization zoning in porphyry ore deposits; Economic Geology, v. 65, p. 373-408

Matheron, G., 1971, The theory of regionalized variables and its applications; Centre de Morphologie Mathématique de Fontainebleau, France, Cahiers No. 5, 211 p.

McMillan, W.J., 1991, Porphyry deposits in the Canadian Cordillera; in Ore deposits, tectonics and metallogeny in the Canadian Cordillera; British Columbia Ministry of Energy, Mines and Petroleum resources, paper 1991-4, 253-276

Mueller, W., 1981, The role of the process mineralogist in the operation of Magma Copper Company's mine and plant, San Manuel, Arizona; in Hausen, D. M., and W. C. Park (eds.), Process mineralogy, The Metallurgical Soc. Of A.I.M.E., Warrendale, Pa., p. 397-406.

Newell, J.M and Peatfield, G.R., 1995, The Red-Chris porphyry copper-gold deposit, northwestern British Columbia, in Schroeter, T.G., ed., Porphyry Deposits of the Northwestern Cordillera of North America; Canadian Institute of Mining Metallurgy, Special Volume 46, p. 674-688

Ney, C.S., Cathro, R.J., Panteleyev, A. and Rotherham, D.C., 1976, Supergene copper mineralization; in Sutherland Brown, A., ed., Porphyry Deposits of the Canadian Cordillera; Canadian Institute of Mining and Metallurgy, Special Volume 15, p. 72-78

Nielsen, R.L., 1984, Evolution of porphyry copper ore deposit models; Mining Engineering, v. 36, no. 12, p. 1637-1641

Noble, A.C. and Ranta, D.E., 1984, Zoned kriging - a successful union of geology and geostatistics; in Erickson, A.J., Jr., ed., Applied mining geology; Society of Mining Engineers of AIME, p. 115-128

Oriel, W.M., 1972, Detailed bedrock geology of the Brenda copper-molybdenum mine, Peachland, British Columbia; unpublished MSc thesis, UBC

Postolski, T.A., and Sinclair, A.J., 1998, Geology as a basis for refining semivariogram models for porphyry-type deposits; In Press (Paper presented at CIM 100th Annual General Meeting, Quality Control of Resource Estimation: An ISO Perspective Session, Montreal, Quebec, 03 - 07 May, 1998)

Postolski, T. A., and Sinclair, A. J., 1994, Mineralogy and Paragenesis of nine sulphide-bearing specimens from the Huckleberry deposit; unpublished report submitted to New Canamin resources Ltd., Vancouver, B.C.

Ranjbar, H., 1997, Litogeochemical patterns associated with the Darrehzar porphyry copper deposit, Pariz area, Iran, Canadian Institute of Mining and Metallurgy, Bulletin, v.90, no. 1014, p. 85-90

- Ranta, D.E., Ward, A.D. and Ganster, M.W., 1984, Ore zoning applied to geologic reserve estimation of molybdenum deposits; in Erickson, A.J., Jr., ed., *Applied mining geology*; Society of Mining Engineers of AIME, p. 83-114
- Raymond, G.F. and Armstrong, W.P., 1988, Sample bias and conditional probability ore reserve estimation at Valley; *Canadian Institute of Mining and Metallurgy, Bulletin*, v.81, no. 911, p.128-136
- Reed, A., 1983, Structural geology and geostatistical parameters of the Afton copper-gold mine, Kamloops, B.C.; *Canadian Institute of Mining and Metallurgy, Bulletin*, v.76, no. 856 p. 45-55
- Rendu, J.M., 1986, How the geologist can prevent a geostatistical study from running out of control: some suggestions; in Ranta, D.E., ed., *Applied mining geology: ore reserve estimation*; Society of Mining Engineers of AIME, p. 11-17
- Rendu, J.M., 1984, Geostatistical modelling and geological controls; *Trans. Inst. Min. Metall, Sect. B.*, v. 93, p. B166-B172
- Rendu, J.M. and Readdy L., 1982, Geology and the semivariogram - a critical relationship; 17th APCOM Application of Computers and Operations Research in the Mineral Industry (ed. Readdy, L.), p. 771-783
- Robertson, R., 1998, Imperial hopes to stave off closure of Mount Polley mine; *The Northern Miner*, June 29, p. 1.
- Seraphim, R.H. and Hollister, V.F., 1976, Structural settings; in Sutherland Brown, A., ed., *Porphyry Deposits of the Canadian Cordillera*; Canadian Institute of Mining and Metallurgy, Special Volume 15, p. 30-43
- Sillitoe, R.H., 1993, Gold-rich porphyry copper deposits: Geological model and exploration implications; in Kirkham, R.V., Sinclair, W.D., Thrope, R.I. and Duke, J.M., eds., *Mineral deposit modeling*; Geological Association of Canada, Special Paper 40, p. 465-478
- Sides, E.J., 1994, Quantifying differences between computer models of orebody shapes; in Whateley, M.K.G., and Harvey, P.K. (eds.), *Mineral resource evaluation II: methods and case histories*; Geological Society Spec. Pub. No. 79, p. 109-121
- Sillitoe, R.H., 1979, Some thoughts on gold-rich porphyry copper deposits; *Mineralium Deposita (Berl.)*, v. 14, p. 161-174
- Sillitoe, R.H. and Gappe, I.M., Jr., 1984, Philippine porphyry copper deposits: Geologic setting and characteristics; United Nations ESCAP, CCOP Technical Publication 14, 89 p.

Sinclair, A.J., 1998, A new look at geological controls in resource/reserve estimation; In Press (Paper presented at CIM 100th Annual General Meeting, Quality Control of Resource Estimation: An ISO Perspective Session, Montreal, Quebec, 03 – 07 May, 1998)

Sinclair, A.J., 1995, Selected topics in mineral inventory estimation; short course notes for a lecture series sponsored by the British Columbia and Yukon Chamber of Mines, Vancouver, B.C.

Sinclair, A.J. and Giroux, G.H., 1984, Geological controls of semi-variograms in precious metal deposits; in Verley, G., et al., eds., *Geostatistics for Natural Resources Characterization*, Part 2, p. 965-978, D. Reidel Pub. Co., Dordrecht, Netherlands.

Sinclair, A.J. and Vallee, M., 1994a, Improved sampling control and data gathering for improved mineral inventories and production control; in Dimitrakopoulos, R., ed., *Geostatistics for the next century*; Kulwer Academic publishers, The Netherlands, p.323-329

Sinclair, A.J. and Vallee, M., 1994b, Reviewing continuity: an essential element of quality control for deposit and reserve estimation; *Exploration and Mining Geology*, v. 3, no. 2, p. 95-108

Sketchley, D.A., Rebagliati, C.M. and DeLong, C., 1995, Geology, alteration and zoning patterns of the Mt. Milligan copper-gold deposits; in Schroeter, T.G., ed., *Porphyry Deposits of the Northwestern Cordillera of North America*; Canadian Institute of Mining Metallurgy, Special Volume 46, p. 650-665

Soregaroli, A.E. and Nelson, W.I., 1976, Boss Mountain; in Sutherland Brown, A., ed., *Porphyry Deposits of the Canadian Cordillera*; Canadian Institute of Mining and Metallurgy, Special Volume 15, p. 432-443

Srivastava, R.M., 1987, Minimum variance or maximum profitability; *Canadian Institute of Mining and Metallurgy, bulletin*, v. 80, no. 901, p.63-68

Stoiser, L.R., 1986, Exploration and geologic evaluation of the Los Bronces copper-molybdenum deposit, Chile; *Mining Engineering*, v. 38, no.3, p. 187-194

Tobar, A., Lyall, G. and Betzhold J., 1997, Quellaveco, Peru: Evaluating resources of a porphyry copper; in Baafi, E.Y. and Schofield, N.A., (eds.), *Geostatistics Wollongong'96*, Volume 2, p. 882-894, Kulwer Academic Publishers.

Van Nort, S.D., Atwood, G.W., Collinson, T.B., Flint, D.C. and Potter, D.R., 1991, Geology and mineralization of the Grasberg porphyry copper-gold deposit, Irian Jaya, Indonesia; *Mining Engineering*, v. 43, no. 3, p.300-304

Vila, T. and Sillitoe, R.H., 1991, Gold-rich porphyry systems in the Maricunga Belt, Northern Chile; *Economic Geology*, v. 86, p.1238-1260

Wallace, S.R., 1991, Model development: porphyry molybdenum deposits; in Hutchinson, R.W. and Grauch, R.I eds., *Economic Geology monograph 8 - Historical perspectives of genetic concepts and case histories*, p. 207-224

Wallace, S.R., 1974, The Henderson ore body - elements of discovery, reflections; *Am. Inst. Mining Metall. Petroleum Engineers Transactions*, v.256, p. 216-256

Wallace, S.R., Muncaster, N.K., Jonson, D.C., MacKenzie, W. B., Bookstrom, A.A. and Surface, V.E., 1968, Multiple intrusion and mineralization at Climax, Colorado, in Ridge, J.D., ed., *Ore deposits of the United States, 1933-1967 (Graton-Sales Vol.)*; New York, Am. Inst. Mining Metall. Petroleum Engineers, p.605-640

White, W.H., Bookstrom, A.A., Kamilli, R.J., Ganster, M.W., Smith, R.P., Ranta, D.E. and Steininger, R.C., 1981, Character and origin of Climax-type molybdenum deposits; *Economic Geology*, 75th Anniversary Volume, p.270-316

CHAPTER 3

GEOLOGY AS A BASIS FOR REFINING SEMIVARIOGRAM MODELS FOR PORPHYRY-TYPE DEPOSITS

ABSTRACT

Three examples are used to describe how geological features impact on the development of semivariogram models to be used for geostatistical resource/reserve estimation of porphyry-type deposits. In the Main zone of the Huckleberry porphyry copper deposit mineralization is concentrated in fracture zones localized in volcanic rocks, along the eastern and southern margins of a granitic stock; two geological domains are recognized based on lithology--volcanic and mixed volcanic-plutonic. Each has its characteristic vertical continuity demonstrated by semivariograms. Horizontal continuity for the mixed volcanic-plutonic data is defined by relatively widely spaced exploration drilling. The volcanic domain has insufficient data with which to define horizontal continuity. Nevertheless, calculations show that when blasthole data are available it would be worthwhile to develop independent models for each geological domain because a common model produces large errors.

The East zone at Huckleberry deposit, spatially distinct from the Main zone, is controlled by a fracture zone elongate roughly east-westerly and bounded on the south by a major fault (easterly striking and steeply dipping) across which there is a dramatic drop

in grades. The eastern part of the East zone appears to be coaxial with large intrusive body; the western part contains small, elongate intrusion. Contoured Cu values for many levels suggest that the principal direction of geological elongation of the east and west parts of the East zone differs significantly. Independently derived semivariogram models for each zone are different and reflect this difference in trend. Block estimates using these two models suggest that significantly better selection will be obtained from two models than by using a common model for the entire East zone.

The Virginia zone is a small porphyry copper-gold deposit near Princeton, B. C. The principal control on mineralization is a set of easterly striking, vertically dipping fractures mineralized with chalcopyrite, bornite, biotite and K-feldspar that cut volcanic rocks of the Nicola Fm., which itself is cut here and there by northerly striking, late barren dykes. Contour maps of Cu and Au grades for all levels show remarkable similarity and reflect the direction of strongest geological continuity (east-striking, vertical plane). The widely space exploration data are barely adequate to demonstrate the geological anisotropy. The geology thus provides insight into the principal directions controlling the semivariogram model for the deposit.

3.1: Introduction

Geological information has been shown to be an essential early guide in the development of resource/reserve models for many types of mineral deposits (e.g. Rendu, 1984; Sinclair and Giroux, 1984). Porphyry-type deposits are no exception to the rule (cf. Ranta et al, 1984); in fact, geological control is particularly important in the case of such deposits because individual block estimates involve very large tonnages of ore or waste so

block classification errors affect very large tonnages. Moreover, because such large tonnages of ore are normally treated over periods of months or a year, very small improvements in grade control can have significant impact on operating profit.

Three separate mineralized zones from two large porphyry-type systems are used to illustrate the impact of close geological control on semivariogram modeling and thus, on the economic impact on geostatistical resource/reserve estimation; these are the Main and East zones of the Huckleberry deposit (e.g. Jackson and Illerbrun, 1995) in central British Columbia and the Virginia zone of the Copper Mountain porphyry system (e.g. Stanley et al, 1995) in southern British Columbia.

The general procedure followed here is:

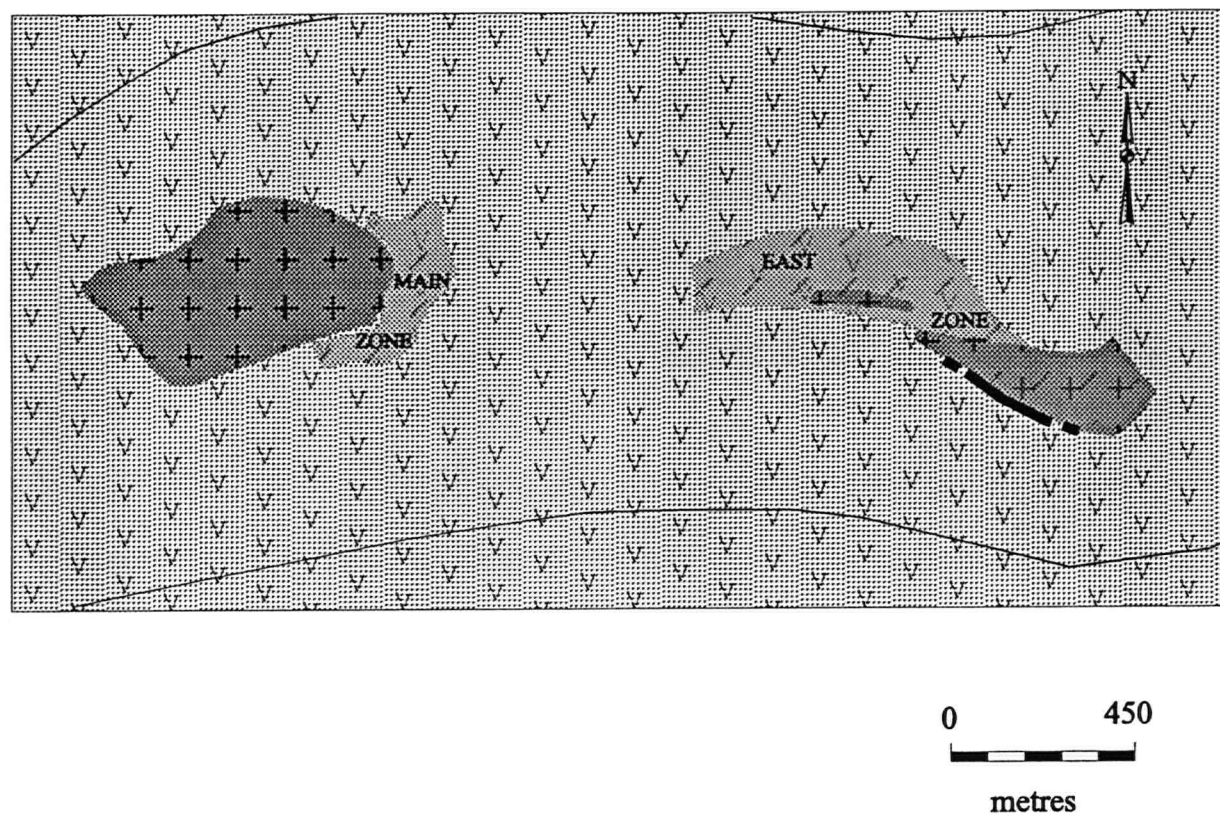
1. Determine a general semivariogram model for an entire mineralized zone (without taking geology into consideration) by evaluating experimental semivariograms in a number of different directions, particularly those directions with the closest 'regular' spacing of data.
2. Examine geological information and contoured maps to assist in defining separate domains for which value continuity (semivariogram model) might be characteristic, that is, different from one domain to another.
3. Develop semivariogram models independently for each domain.
4. For all (selected) domains conduct cross validation by both the general zone semivariogram model and the domain model.

5. For selected domains estimate (using ordinary kriging) a 3-D block array (5x5x4) using both the general semivariogram model and the domain model.
6. Compare the two estimation approaches using metal accounting procedures (cf. Sinclair, 1995)

Semivariogram analysis, cross-validation and kriging were done using 3-dimensional programs available in GSLIB (Deutsch and Journel, 1992). Some of the semivariogram modeling was done using the interactive program GAMMAFIT in GEOSTATISTICAL TOOLBOX. Contour grade maps and binary diagrams were produced using P-RES software (Bentzen and Sinclair, 1994).

3.2: Main zone (Huckleberry)

The Main zone of the Huckleberry deposit is a stockwork of veinlets concentrated in Hazelton Group (Jurassic) volcanic rocks along the eastern and southern margins of a Late Cretaceous (Bulkley Intrusions) stock (Figure 3-1), a porphyritic hornblende-biotite granodiorite (Jackson and Illerbrun, 1995). Veinlets that form the stockwork contain chalcopyrite, quartz, and molybdenite with lesser anhydrite and pyrite (Postolski and Sinclair, 1994). Resources based on a 0.3% Cu cutoff grade are 54 million tonnes grading 0.44% Cu, 0.013% Mo and 0.06 g/tonne Au (Jackson and Illerbrun, 1995).



Legend

	Horblende-biotite-feldspar porphyry		Hazelton volcanics
	Pyrite zone		Fault
	Cu-mineralization zone		

Figure 3-1: Geological map of the Huckleberry deposit showing Main zone and East zone (modified from Jackson and Illerbrun, 1995)

3.2.1: Semivariogram analysis

Data consist of 1267 8m composites generated from shorter sample lengths of core from 106 drill holes with a spatial density of about one hole per 1000 m². Drill sections are oriented easterly and are separated by about 30m or 60m. These sections show a general steep dip to the mineralized zone. In the near surface zone of production concern there is a general control of mineralization in volcanic wallrock at the contact with the porphyry body.

A general semivariogram model for the entire mineralized zone was developed by evaluating experimental semivariograms in the vertical direction as well as in 8 different horizontal directions (Appendix 1). Figure A1-6 shows an ellipse, which is a schematic representation of ranges of the general (incorrect), anisotropic semivariogram model developed for the entire Main zone without taking geology into consideration.

Levels contoured for copper grade show significant variations in trend directions (Figure 3-2), that coincide with dominant directions of stockwork development (Figure 3-3). These preferred directions of mineralization separate the Main zone into three domains: NE domain, SE domain, and SW domain. This geological separation into three separate domains is based on the different directions of preferred continuity (i.e. different models of anisotropy) rather than significant differences in grade abundances.

In each domain, contoured cross sections and longitudinal projections were examined to provide some insight into preferred directions of geological continuity in the vertical and subvertical directions. Then, in each domain, semivariograms were determined horizontally in a number of different directions as well as in the vertical direction.

Appendix 2 contains vertical and horizontal semivariogram models for different directions

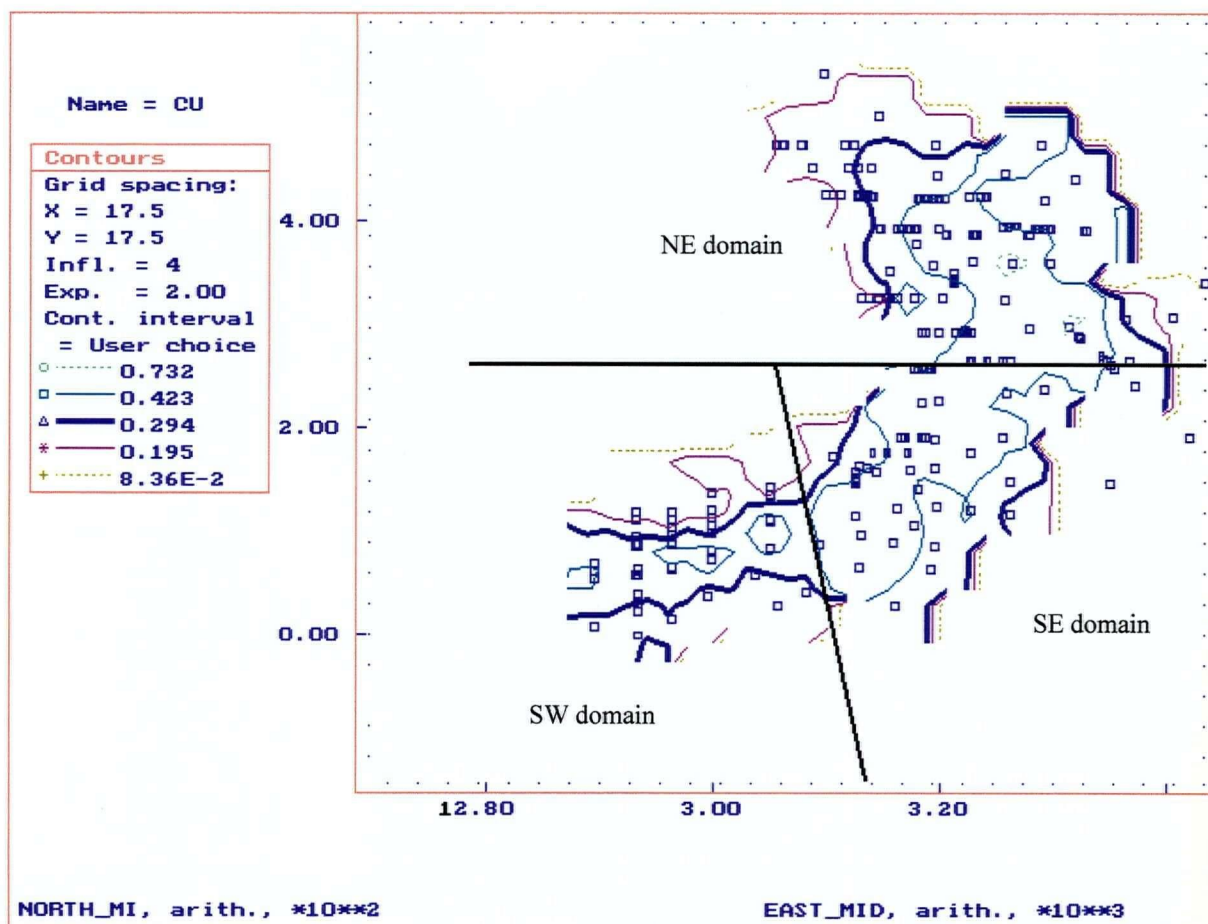
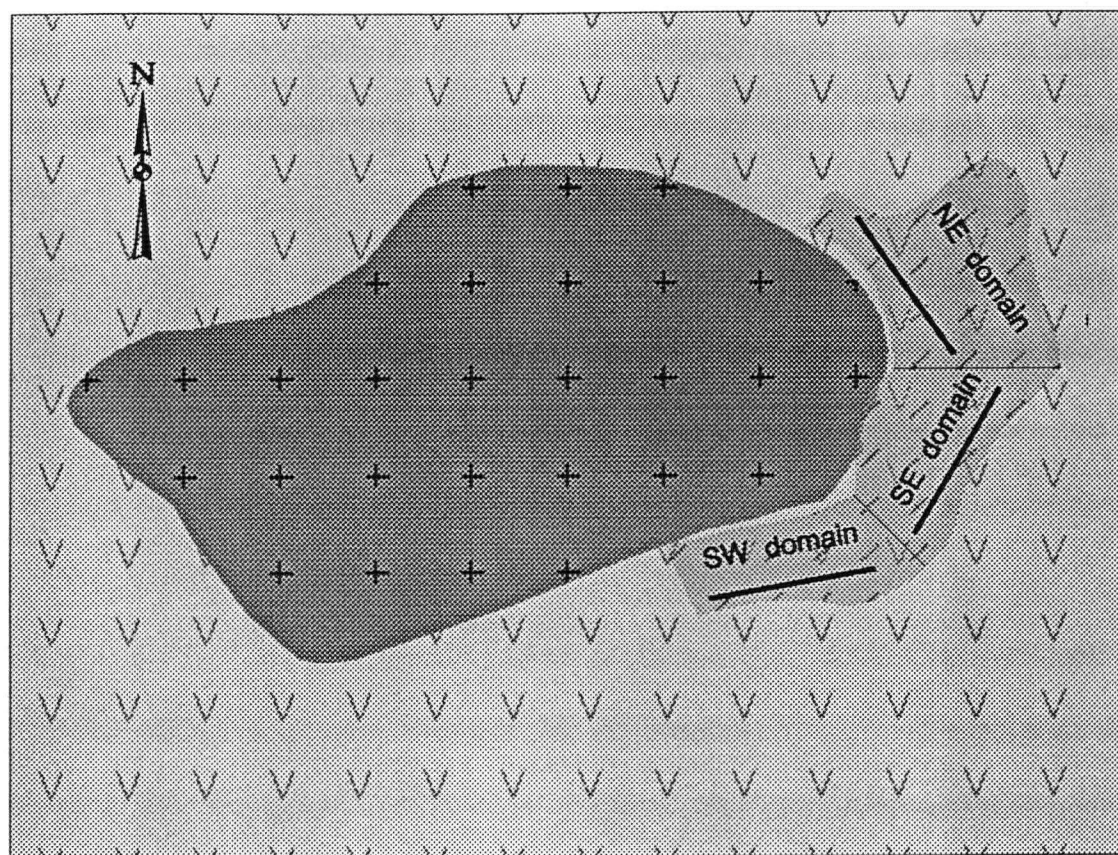


Figure 3-2: Huckleberry, Main zone, Cu grade contour map for 24 m interval.
 Open squares are sample locations from vertical drill holes;
 filled rectangles indicate inclined drill holes. Cu values in percent.



Legend



Horblende-biotite-feldspar
porphyry



Hazelton volcanics



Cu-mineralization
zone



Dominant direction of
stockwork development

0 200
metres

Figure 3-3: Geological map of the Huckleberry deposit Main zone showing 3 different domains with dominant directions of stockwork development (modified from Jackson and Illerbrun, 1995)

for all three domains as well as the three 3-D domain semivariogram models. Figures A2-4, A2-8, and A2-12 show three ellipses that are a schematic representation of ranges of semivariogram models in the three domains. It is evident that each of the three domain models differs significantly from the others.

Parameters of the resulting 3-dimensional models for all three domains, as well as a general (less accurate) semivariogram model for the Main zone are summarized in Table 3-1. The general model, although incorrect, is provided to demonstrate the impact on reserve estimation of using a less detailed model than could be obtained.

3.2.2: Cross-validation of Estimates

General and domain semivariogram models are each validated by re-estimating the known values. During this process actual data points are dropped one at a time and re-estimated from the neighboring data. After estimation of a point, the original datum is placed back in the data set. Figure 3-4a is a quantile - quantile (Q-Q) plot of cross-validation results for the SW domain comparing the general (less accurate) semivariogram model with true values. Large disparities are obvious here. The desirable situation is where the distribution of estimated values is identical to the distribution of true values for which the Q-Q plot will be the straight line $y = x$. Consequently, departures of the Q-Q plot from the line $y = x$ are graphical measures of quality of the model used for estimation (crossvalidation). Figure 3-4b is a Q-Q plot for crossvalidation results based on the domain-specific semivariogram model and shows definite improvement relative to Figure 3-4a.

**TABLE 3-1: HUCKLEBERRY, MAIN ZONE, SPHERICAL SEMIVARIOGRAM
MODELS FOR COPPER**

	C0	C1	a [m]	ang. 1	anis. 1	ang. 2	anis. 2	ang. 3
SW domain	0.03	0.16	110	80	0.373	0	0.373	0
SE domain	0.06	0.15	65	0	1.0	0	1.0	0
NE domain	0.03	0.175	73	145	0.699	0	0.521	0
<i>General</i>	<i>0.045</i>	<i>0.16</i>	<i>75</i>	<i>22</i>	<i>0.627</i>	<i>0</i>	<i>0.627</i>	<i>0</i>

C0 – nugget effect

C1 – contribution of the structure

a - range of the structure

ang 1 – angle of the principal direction in the horizontal plane (clockwise from North)

anis 1 - range in the minor direction within horizontal plane (90° from the principal direction) divided by range in the principal direction

ang 2 - angle that rotates the principal direction down from the horizontal plane

anis 2 – range in the third orthogonal direction divided by range in the principal direction

ang 3 - angle that rotates the two directions orthogonal to the principal direction clockwise relative to the principal direction

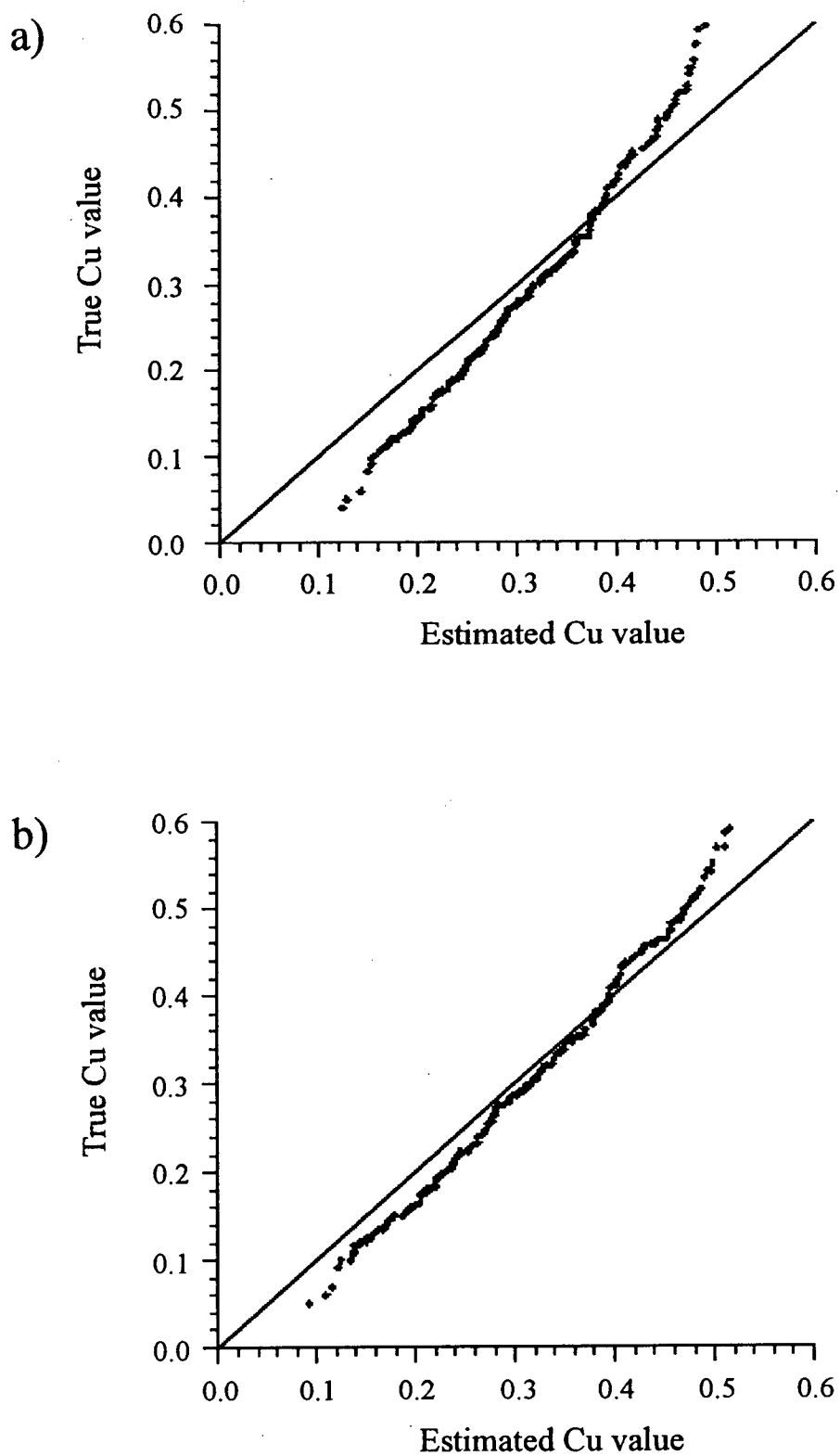


Figure 3-4: Quantile - Quantile plot of Cu cross-validation results for Huckleberry Main zone SW domain, using general semivariogram model (a), and domain specific semivariogram model (b)

3.2.3: Comparative Kriging Results

As an example of the impact of using a less than optimal semivariogram model as a basis for selecting ore and waste, an array of 100 blocks (4 contiguous levels of 25 blocks each) in the centre of the SW domain of the Main zone was estimated using both the general model and the more correct domain-specific model. Block size is $20 \times 20 \times 8 \text{ m}^3$ (i.e. nearly 9000 tonnes per block). Ordinary kriging results for each block by both semivariogram models are plotted on Figure 3-5. A systematic bias is revealed here, which cross-validation indicates arises largely from the incorrect semivariogram-based estimates.

Individual blocks were then categorized as ore or waste relative to a cutoff grade of 0.4% Cu to demonstrate the differences in estimated metal in recovered blocks. For the 100 block array of the SW domain the correct, domain semivariogram model identifies 26 blocks as ore. The less accurate, general semivariogram model identifies only 10 of these blocks as ore, thus the general semivariogram model losses 16 ore blocks to waste, relative to the domain semivariogram model. Table 3-2 summarizes the results in terms of metal accounting (Sinclair, 1995). In metal accounting the block grade minus the cutoff grade can be used to determine the operating profit of a block in terms of amount of metal (i.e. operating profit = $T(g_b - g_c)$ where T is tonnes per block, g_b is block grade and g_c is cutoff grade). Such an analysis reveals that, in terms of recovered metal above cutoff grade, the less accurate, general semivariogram model loses to waste about 55 tonnes or 40% of the metal that is potential profit. Moreover, Table 3-2 indicates that the general or less accurate semivariogram model underestimates Cu content by 8 tonnes relative to the correct semivariogram model, in the 10 blocks that both identify as ore. The same Table shows that if these general condition prevailed for 1 year of production, the annual loss of

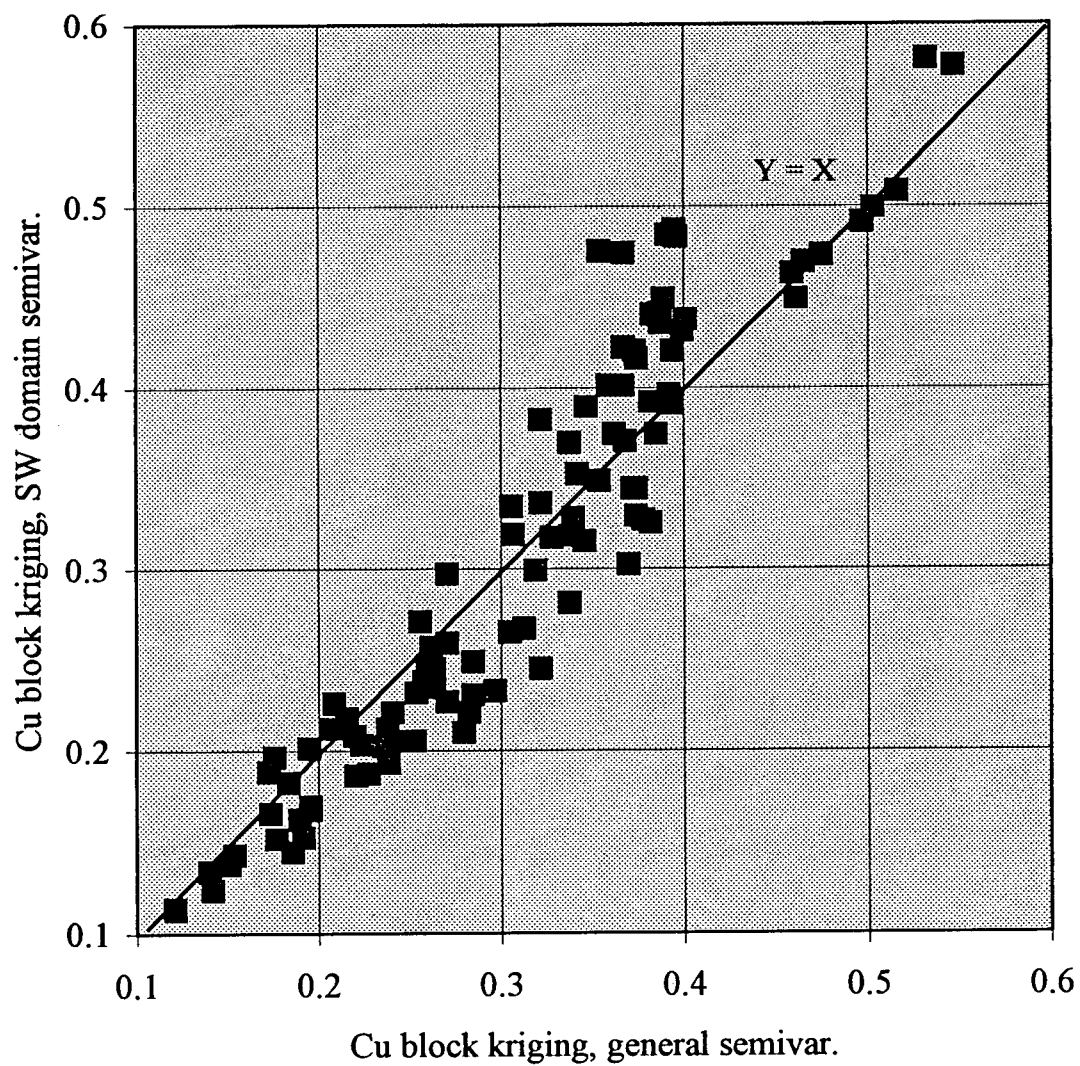


Figure 3-5: Huckleberry, Main zone, SW domain, Cu ordinary kriging results for 100 blocks using domain specific and general semivariogram models

TABLE 3-2: HUCKLEBERRY, MAIN ZONE, SW DOMAIN, SUMMARY OF METAL ACCOUNTING

		domain SV model	general SV model	profit loss	underesti -mation	annual cost of using general SV model	
						in [tonnes]	in [US \$]
profit as metal in tonnes per 100 blocks	16 ore blocks lost to waste by general SV model	132	77	-55		345	610,000
	underest of recovered metal from 10 blocks by general SV model	77	69		8	45	80,000
				TOTAL:		300	530,000

Assume:

8,600 tonne per block
 94% recovery of copper
 18,000 tonnes per day production rate
 300 days per year of production
 US \$ 0.80 per lb. price of copper

operating profit would be the equivalent of 300 tonnes of copper or (at US\$0.80/lb) about US \$530,000.

3.3: East zone (Huckleberry)

The East zone is a stockwork deposit consisting of chalcopyrite-pyrite-quartz veinlets with lesser anhydrite and molybdenite (Postolski and Sinclair, 1994; Jackson and Illerbrun, 1995). The deposit is spatially related to a dyke-like apophysis and a larger Late Cretaceous intrusive body, the East zone stock. The dyke and the associated mineralized zone have an easterly strike/elongation (Figure 3-1). There is the bounding fault present, along the south part of the deposit, across which there is a dramatic drop in grades. The mineralized zone has a general steep to vertical dip. Resources based on a 0.3% Cu cutoff grade are 108 million tonnes grading 0.48% Cu, 0.014% Mo and 0.055 g/tonne Au (Jackson and Illerbrun, *ibid.*).

3.3.1: Semivariogram analysis

Data consist of 2240 8m composites generated from shorter sample lengths of core from 128 drill holes with a spatial density of about one hole per 1400 m². Drill sections are oriented northerly and are separated by about 30m or 60m. A general semivariogram model for the entire mineralized zone was developed by evaluating experimental semivariograms in vertical direction as well as in 8 different horizontal directions (Appendix 3). This general model is shown as an ellipse on Figure A3-6, which is a

schematic representation of the general (incorrect), anisotropic semivariogram model developed for the entire East zone without taking geology into consideration.

Contoured maps for copper grades for all levels show remarkable similarity and indicate the roughly easterly elongation of a high grade core but show a significant difference in trend from East to West (Figure 3-6), that coincide with dominant directions of stockwork development. Note that on Figure 3-6 true north is 25 degrees counterclockwise from a vertical line. These directions of dominant mineralization control (Figure 3-7) separate the East zone into two domains: W and E domains, based on the likelihood of different directions of preferred continuity (anisotropy) rather than significant differences in grade abundance.

In each domain, contoured cross sections and longitudinal projections were examined to provide some insight into preferred directions of geological continuity in vertical and subvertical directions. Then, semivariograms were determined as described above for the Main zone. Appendix 4 contains vertical and horizontal directional semivariogram models for the two domains as well as the two domain 3-D semivariogram models. Figures A4-6 and A4-12 show two ellipses that are a schematic representation of semivariogram models in the two domains; note the substantial difference between the two. Parameters of the resulting 3-dimensional models for the two domains, as well as a general (less accurate) semivariogram model for the East zone are summarized in Table 3-3. The general model, although incorrect, is provided here to demonstrate the impact on reserve estimation by using a less correct model than could be obtained.

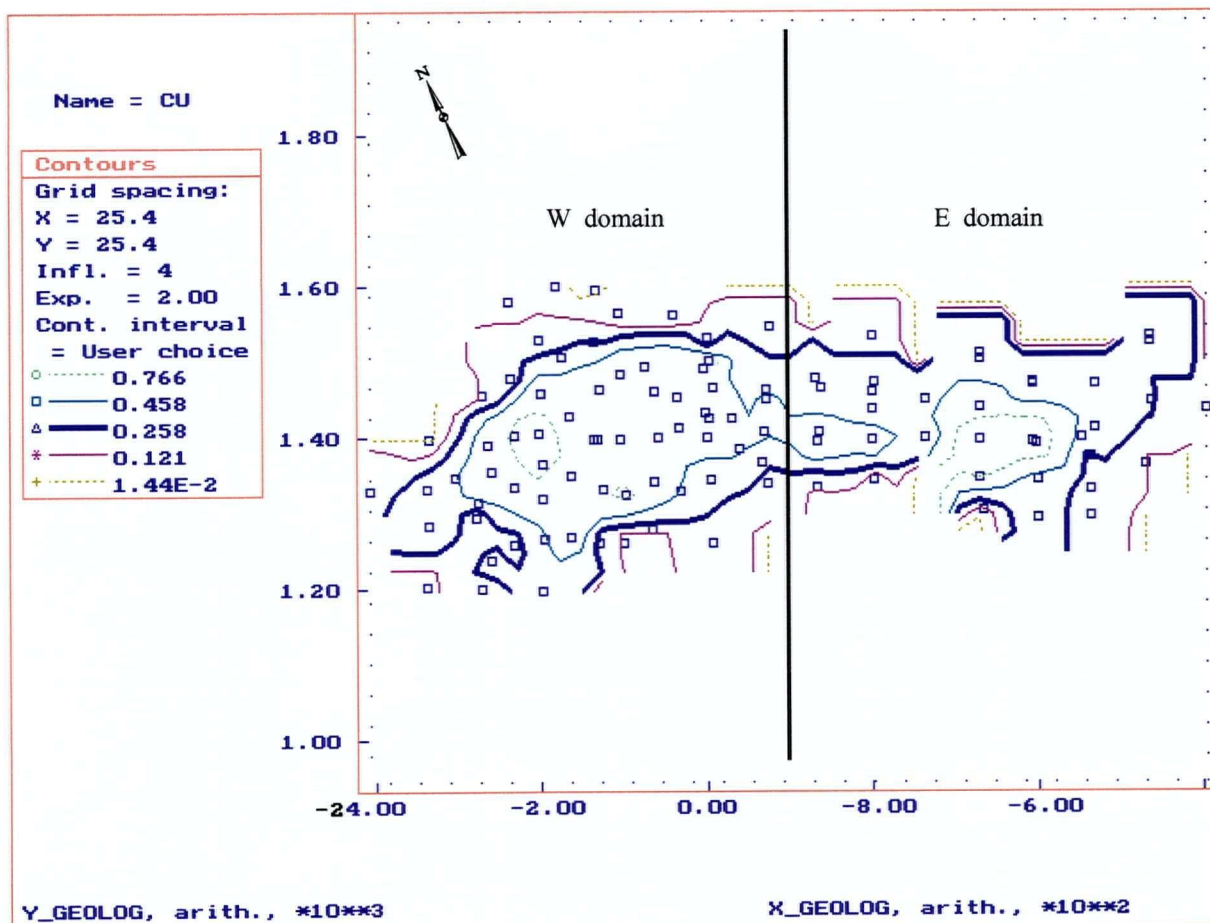
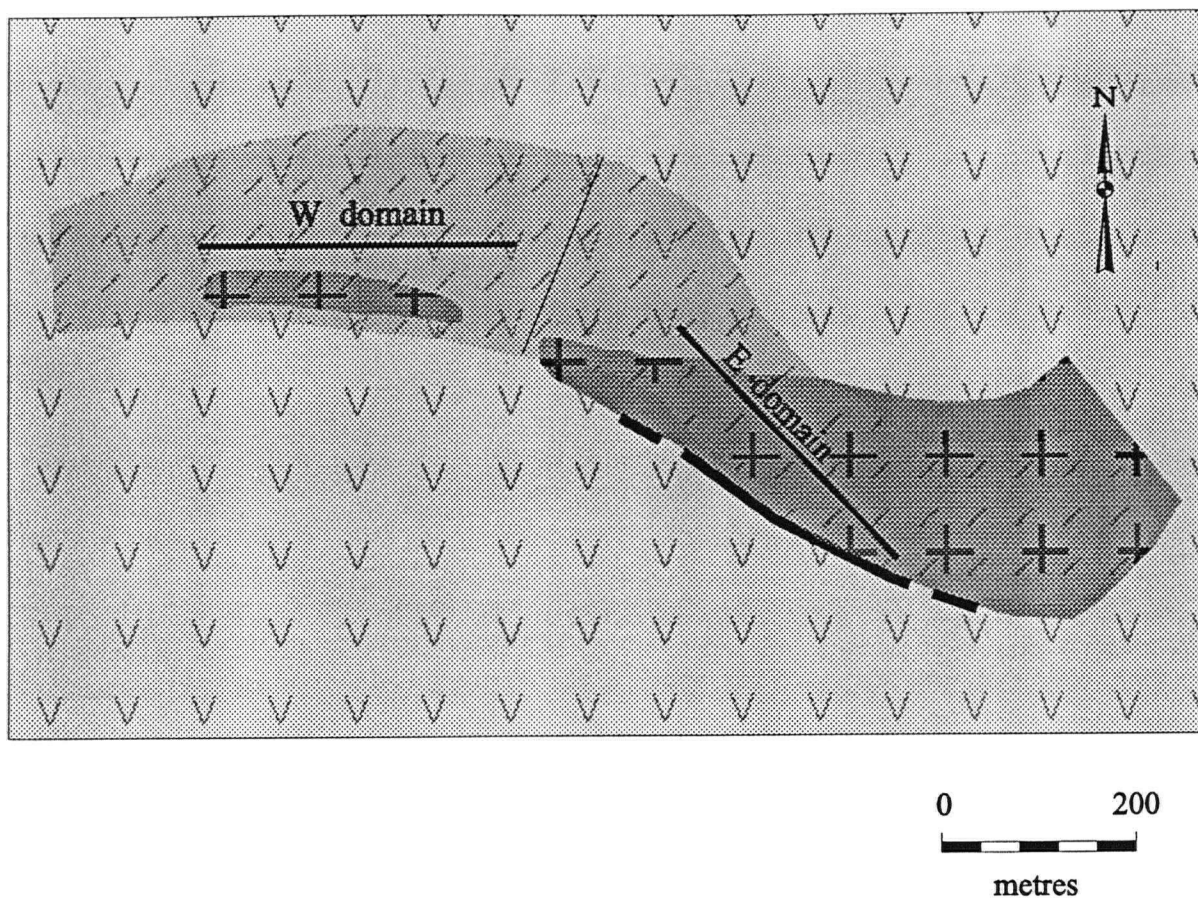


Figure 3-6: Huckleberry, East zone, Cu grade contour map for 8 m bench, level 940 m. Open squares are sample locations from drill holes; Cu values in percent.



Legend

	Horblende-biotite-feldspar porphyry		Dominant direction of stockwork development
	Hazelton volcanics		Fault
	Cu-mineralization zone		

Figure 3-7: Geological map of the Huckleberry deposit East zone showing 2 different domains with dominant directions of stockwork development (modified from Jackson and Illerbrun, 1995)

TABLE 3-3: HUCKLEBERRY, EAST ZONE, SPHERICAL SEMIVARIOGRAM MODELS FOR COPPER

	C0	C1	a1 [m]	C2	a2 [m]	ang 1	anis 1	ang 2	anis 2	ang 3
E domain	0.01	0.048	20	0.412	340	112	0.559	0	1.118	0
W domain	0.055	0.045	32	0.5	670	67	0.358	0	1.269	0
<i>General</i>	<i>0.045</i>	<i>0.05</i>	<i>36</i>	<i>0.5</i>	<i>650</i>	<i>67</i>	<i>0.369</i>	<i>0</i>	<i>1.2</i>	<i>0</i>

C0 – nugget effect

C1 – contribution of the first (isotropic) structure

a1 - range of the first (isotropic) structure

C2 – contribution of the second structure

a2 - range of the second structure

ang 1 – angle of the principal direction in the horizontal plane (clockwise from North)

anis 1 - range in the minor direction within horizontal plane (90° from the principal direction) divided by range in the principal direction

ang 2 - angle that rotates the principal direction down from the horizontal plane

anis 2 – range in the third orthogonal direction divided by range in the principal direction

ang 3 - angle that rotates the two directions orthogonal to the principal direction clockwise relative to the principal direction

3.3.2: Cross-validation of estimates

General and domain semivariogram models were cross-validated. Figure 3-8a is a Q-Q plot of cross-validation results for E domain using the less accurate, general semivariogram model. Figure 3-8b shows improvement in Q-Q plot, when the correct, domain semivariogram model is used for cross-validation.

3.3.3: Comparative kriging results

As an example of the impact of using a less than optimal semivariogram model as a basis for selecting ore and waste, an array of 100 blocks (4 contiguous levels of 25 blocks each) in the centre of the E domain of the East zone were estimated using both the general model and the more correct domain model. Block size is 20x20x8m³ (i.e. nearly 9000 tonnes per block). Ordinary kriging results for both semivariogram models are shown on Figure 3-9. Conditional bias is evident here, and cross-validation shows it to be less with the correct, domain-specific semivariogram model.

Individual blocks were then categorized as ore or waste relative to a cutoff grade of 0.4% Cu to demonstrate the differences in estimated metal in recovered blocks. For the 100 block array of the E domain the correct, domain semivariogram model identifies 91 blocks as ore. The less accurate, general semivariogram model identifies only 81 of these blocks as ore, thus the general semivariogram model losses 10 ore blocks to waste, relative to the domain semivariogram model. Table 3-4 summarizes the results in terms of metal accounting as described above for the Main zone. In terms of recovered metal above cutoff grade, the less accurate, general semivariogram model losses to waste about 34 tonnes of metal that is potential profit. Moreover the general or less accurate

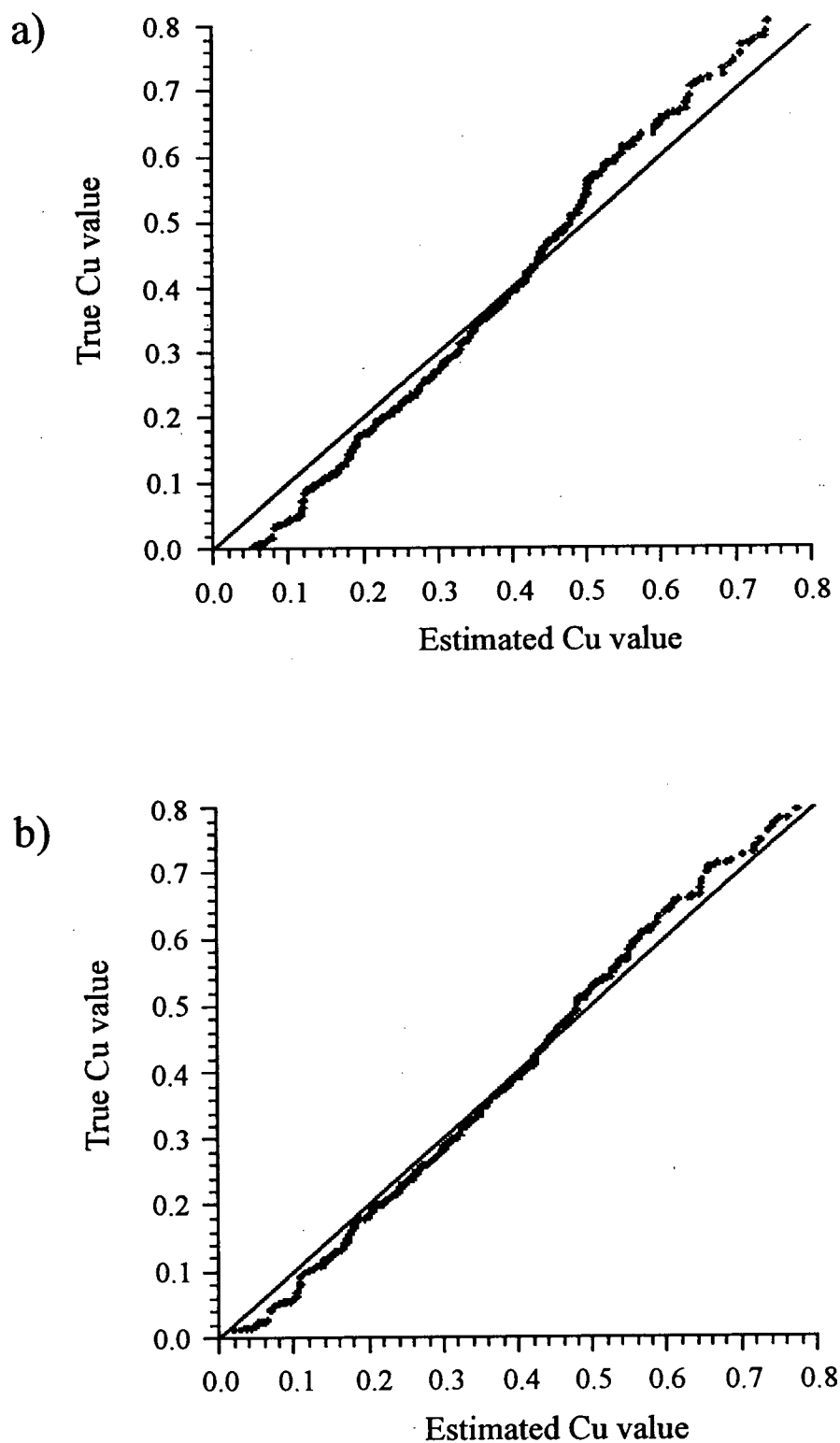


Figure 3-8: Quantile - Quantile plot of Cu cross-validation results for Huckleberry East zone East domain, using general semivariogram model (a), and domain specific semivariogram model (b)

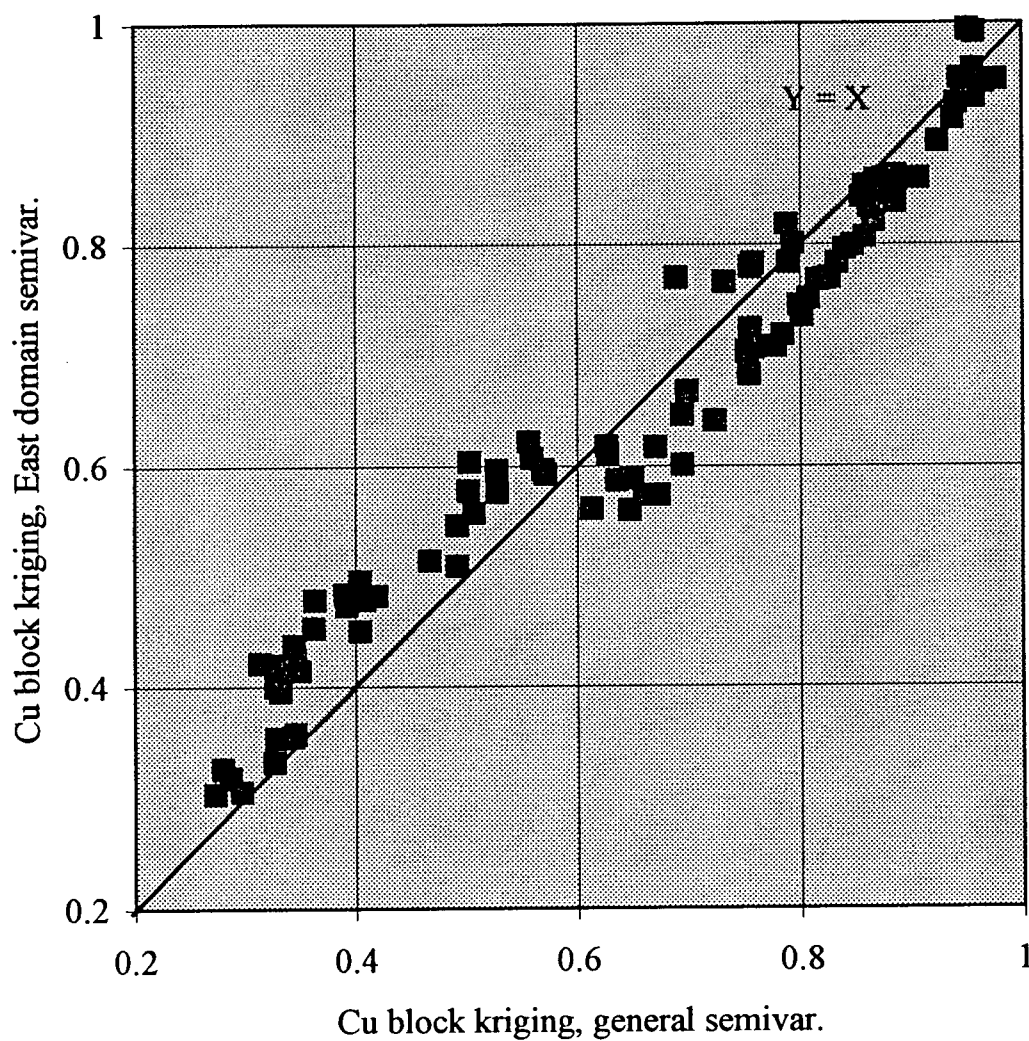


Figure 3-9: Huckleberry, East zone, East domain, Cu ordinary kriging results for 100 blocks using domain specific and general semivariogram models

TABLE 3-4: HUCKLEBERRY, EAST ZONE, EAST DOMAIN, SUMMARY OF METAL ACCOUNTING

		domain SV model	general SV model	profit loss	overesti- mation	annual cost of using general SV model	
						in [tonnes]	in [US \$]
profit as metal in tonnes per 100 blocks	10 ore blocks lost to waste by general SV model	2,267	2,233	34		210	370,000
	overest of recovered metal from 81 blocks by general SV model	2,233	2,312		79	490	870,000
				TOTAL:		700	1,240,000

Assume:

8,600 tonne per block
 94% recovery of copper
 18,000 tonnes per day production rate
 300 days per year of production
 US \$ 0.80 per lb. price of copper

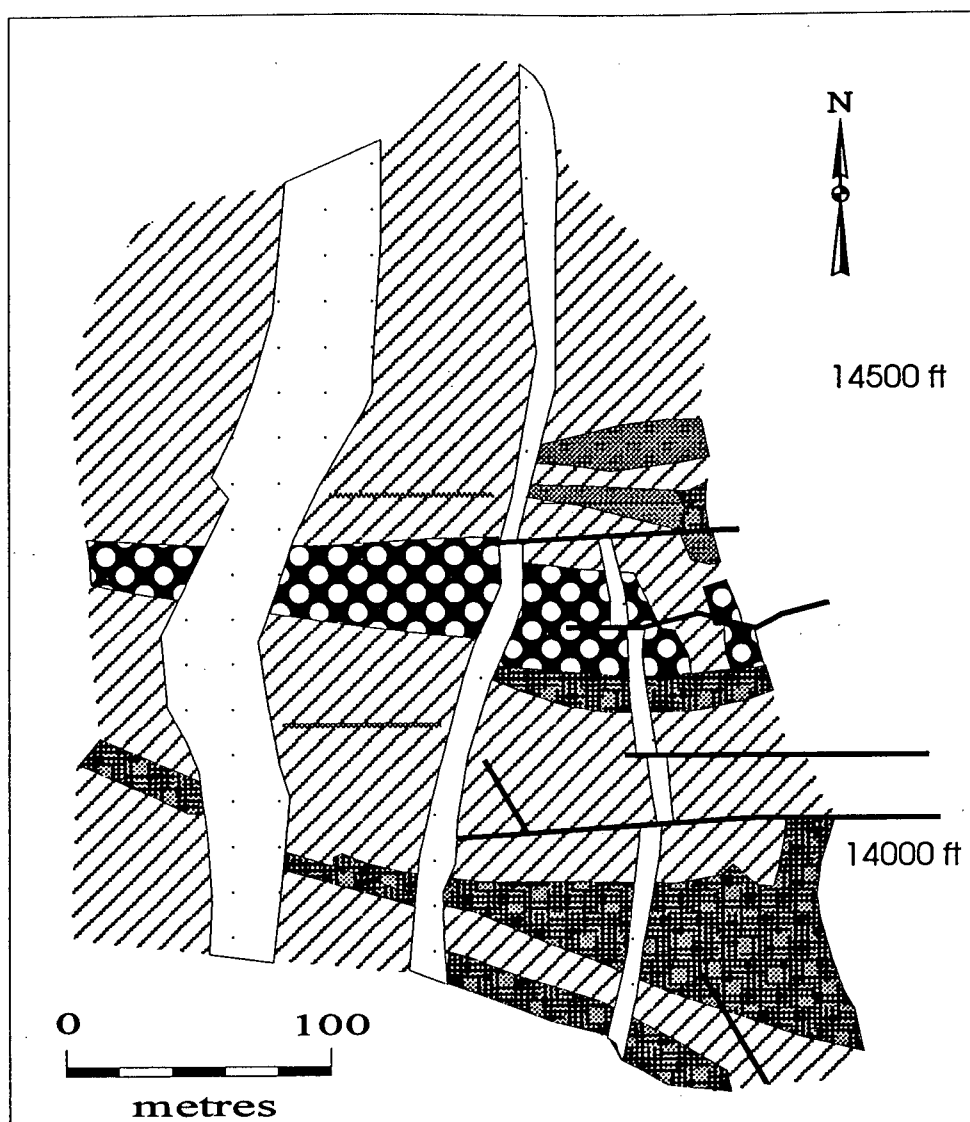
semivariogram model overestimates Cu content by 79 tonnes relative to the correct semivariogram model, in the 81 blocks that both identify as ore. Table 3-4 also reveals that if these differences were projected annually, in terms of recovered metal above cutoff grade, the annual loss would be 700 tonnes of copper in operating profit or, at \$0.80/lb of copper, US \$ 1,240,000 if the incorrect semivariogram model were used instead of the domain-specific semivariogram model for geostatistical block estimates.

3.4: Virginia zone (Copper Mountain)

The Virginia zone is one of several alkalic porphyry-style mineralized zones north of Copper Mountain stock near Princeton, British Columbia. (cf. Stanley et al, 1995). Mineralization occurs in two stages of the Lost Horse Intrusive Complex, a suite of dioritic to monzonitic rocks, which, at the Virginia zone occur as easterly trending dykes. These rocks are cut by a mineralized stockwork with a particularly prominent vein orientation having an easterly strike and a near-vertical dip, generally the same orientation as the host dykes (Figure 3-10). The principal vein type is magnetite-pyrite-chalcopyrite veins with relatively high gold content compared with other zones at Copper Mountain. Pyrite-chalcopyrite veinlets occur locally.

3.4.1: Semivariogram analysis

Data available for this study include more than 5000 samples, 10 feet long, analyzed for more than 20 elements including Cu and Au. Samples are half core taken



Legend

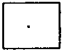





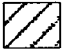
	Felsite dike		Andesite
	Lost Horse LH2 dike		Fault
	BT Lost Horse LH1b dike		Prominent vein orientation
	Lost Horse LH1g dike		

Figure 3-10: Geological pit map of Virginia zone with dominant direction of stockwork development (modified from Stanley et al., 1995)

from diamond drill holes, mostly vertical, with an average spatial density of about 1 drill hole per 15,000 square feet. The widely spaced exploration data are barely adequate to demonstrate the anisotropy. However, geological mapping demonstrated the strong control on mineralization by veins striking 90 degrees with near vertical dip.

Consequently, a cross-vein direction was taken as one of the principal directions of value continuity, expected to be the direction of minor continuity. At the same time the plane of the vein was expected to contain the direction of major continuity; consequently the plane of the vein was investigated for anisotropy by examining contour maps and by developing semivariograms for several directions within the plane. Geology thus provides insight into the principal directions controlling the semivariogram model for the deposit.

However, the stationarity assumption for the entire deposit was checked first. To do this the data were divided into three groups representing the west part (10,700E to 11,500E), the middle part (11,500E to 12,100E) and the east part (12,100E to 12,700E) of Virginia zone. For each part a separate vertical experimental semivariogram was developed and modeled, both for Cu and Au. These semivariogram models are shown in Appendix 5. Experimental vertical semivariograms in each part of the deposit are very similar and thus were estimated by the same model. The small differences between experimental semivariograms from different parts of the Virginia zone do not warrant use of different models and rejection of the stationarity assumption for the entire zone.

Contour maps of Cu and Au grades for all levels show remarkable similarity and reflect the easterly direction of the major direction of grade continuity. Figure 3-11 is a copper contour map and Figure 3-12 is a gold contour map; both contour maps have a strong E - W elongation.

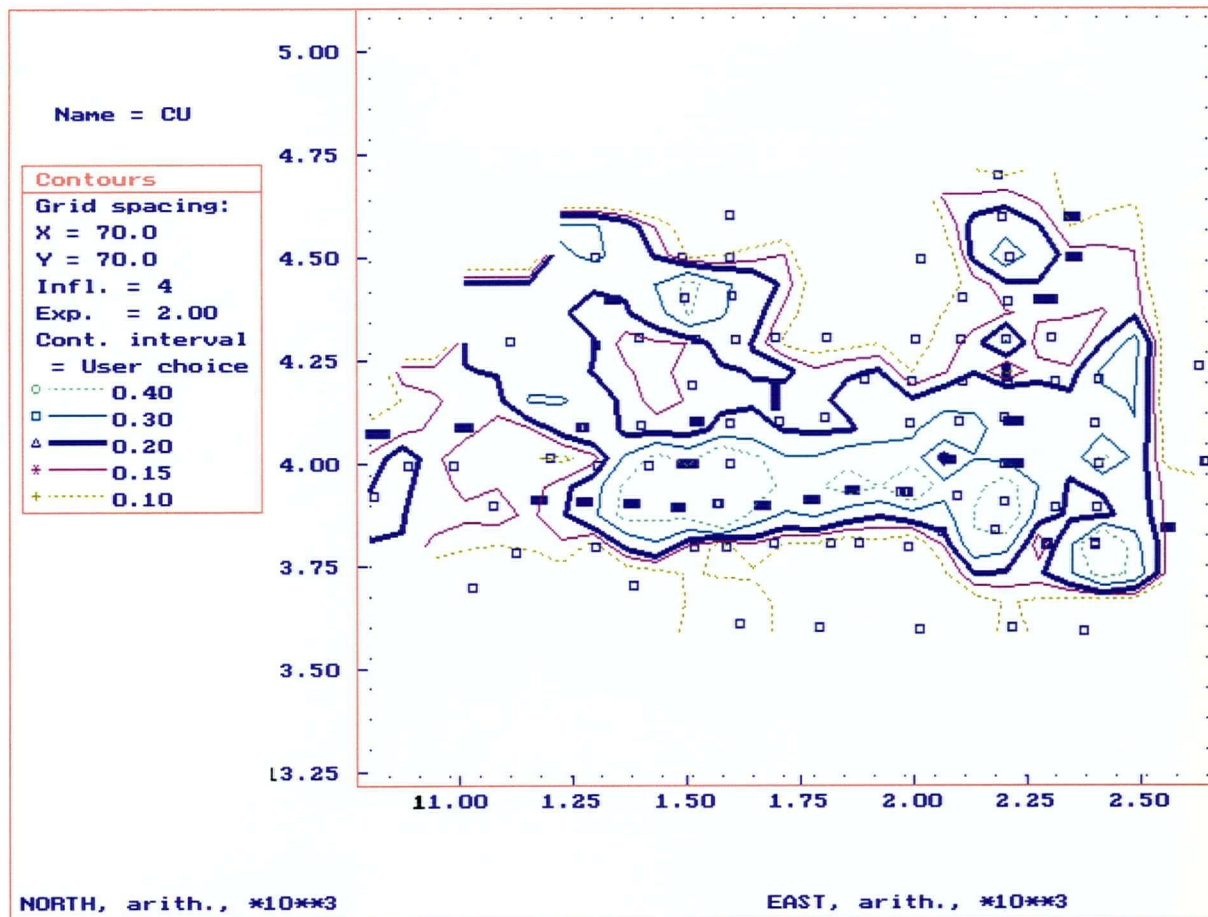


Figure 3-11: Virginia zone, Cu grade contour map for 100 ft interval above level 3400 ft. Open squares are sample locations from vertical drill holes; filled rectangles indicate inclined drill holes. Cu values in percent.

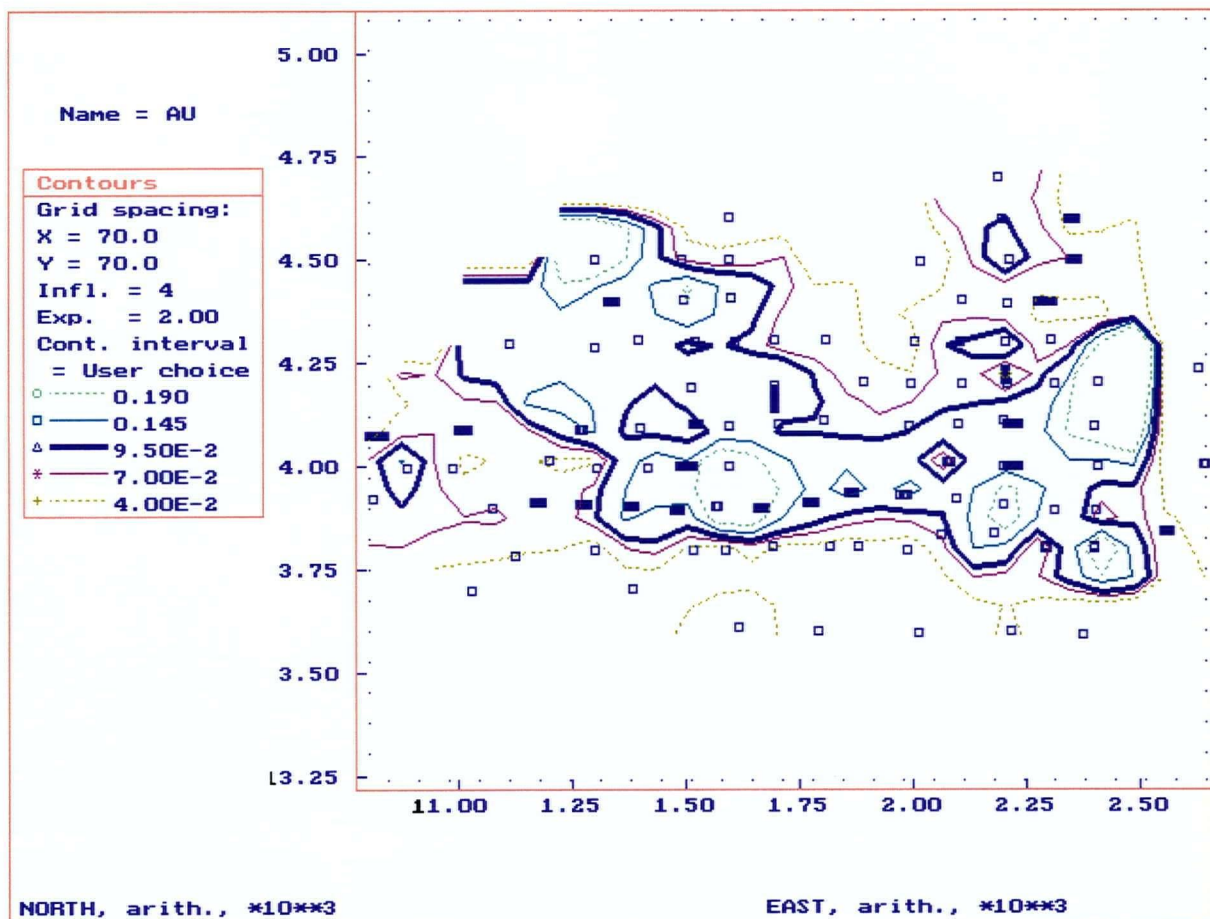


Figure 3-12: Virginia zone, Au grade contour map for 100 ft interval above level 3400 ft. Open squares are sample locations from vertical drill holes; filled rectangles indicate inclined drill holes. Au values in g/t.

Cu and Au semivariogram models for the Virginia zone were developed by evaluating experimental semivariograms for several directions within the vertical East-West trending plane (horizontal direction, -10 degree dip direction, -20 degree dip direction, -30 degree dip direction), as well as in the cross-vein direction (azimuth 0). These semivariogram models are shown in Appendix 5 together with Cu vertical and Au vertical semivariogram models and the Cu 3-D semivariogram model and Au 3-D semivariogram model.

Figure A5-11 (top) shows an ellipse that is a schematic representation of the semivariogram model for Cu, showing strong anisotropism in an east-west direction. The same Figure (bottom) shows an ellipse that is a schematic representation of the semivariogram model for Au, showing even stronger anisotropism in the same direction. The resulting 3-dimensional models for Cu and Au for Virginia zone are summarized in Table 3-5, where symbols are as defined above for the Huckleberry deposit.

3.4.2: Cross-validation of estimates

Cross-validation has been done on Cu and Au variables from Virginia zone. In the case of both metals the results are globally unbiased, though conditional bias is present.

3.4.3: Block estimation results

An array of 100 blocks (4 contiguous levels of 25 blocks each) in the centre of the Virginia zone were estimated for both Cu and Au. Block size is $30 \times 30 \times 30 \text{ft}^3$. Ordinary kriging of 100 blocks for Cu resulted in an average Cu grade of 0.314% and average variance of 0.01855, what gives an average kriging error of about 43%. Ordinary kriging

**TABLE 3-5: VIRGINIA ZONE, SPHERICAL SEMIVARIOGRAM MODELS
FOR COPPER AND GOLD**

	C0	C1	a1 [ft]	C2	a2 [ft]	ang 1	anis 1	ang 2	anis 2	ang 3
Copper	0.22	0.17	50	0.15	220	90	0.591	0	1.409	0
Gold	0.28	0.16	55	0.12	300	90	0.4	0	1.2	0

C0 – nugget effect

C1 – contribution of the first (isotropic) structure

a1 - range of the first (isotropic) structure

C2 – contribution of the second structure

a2 - range of the second structure

ang 1 – angle of the principal direction in the horizontal plane (clockwise from North)

anis 1 - range in the minor direction within horizontal plane (90° from the principal direction) divided by range in the principal direction

ang 2 - angle that rotates the principal direction down from the horizontal plane

anis 2 – range in the third orthogonal direction divided by range in the principal direction

ang 3 - angle that rotates the two directions orthogonal to the principal direction clockwise relative to the principal direction

of 100 blocks for Au resulted in average Au grade of 0.1598g/t and average variance of 0.005839, which gives an average kriging error of almost 48%. Because kriging minimizes the error, these estimates are the best possible with the available data. Clearly, more data are required if estimates of such small blocks are necessary from exploration data. Keep in mind that actual production will be based on much more abundant blast hole assays; hence, better block selectivity will be possible during production than can be done based on exploration data.

As indicated by Figure 3-11 and Figure 3-12 the Cu and Au patterns on contour maps are very comparable. This strong similarity of patterns for Cu and Au values results from a strong correlation between Cu and Au; the correlation coefficient between Cu and Au is high and equals 0.847. This relationship means that simple regression is viable method of estimating Au values based on known Cu values using the following formula (cf. Figure 3-13):

$$Au_g/t = 0.487 \times Cu(\%) - 0.0082$$

This formula was used to estimate Au grades of the same set of 100 blocks that were estimated for Cu and Au using ordinary kriging. Figure 3-14 compares regression results for Au estimates of 100 blocks with respective Au kriging estimates. The correlation between both sets of estimates is extremely high ($r=0.965$). Below roughly 0.26g/t Au simple regression gives generally globally and conditionally unbiased estimates relative to the kriging results for Au. For only few values above roughly 0.26g/t Au the regression method generally underestimates relative to kriging.

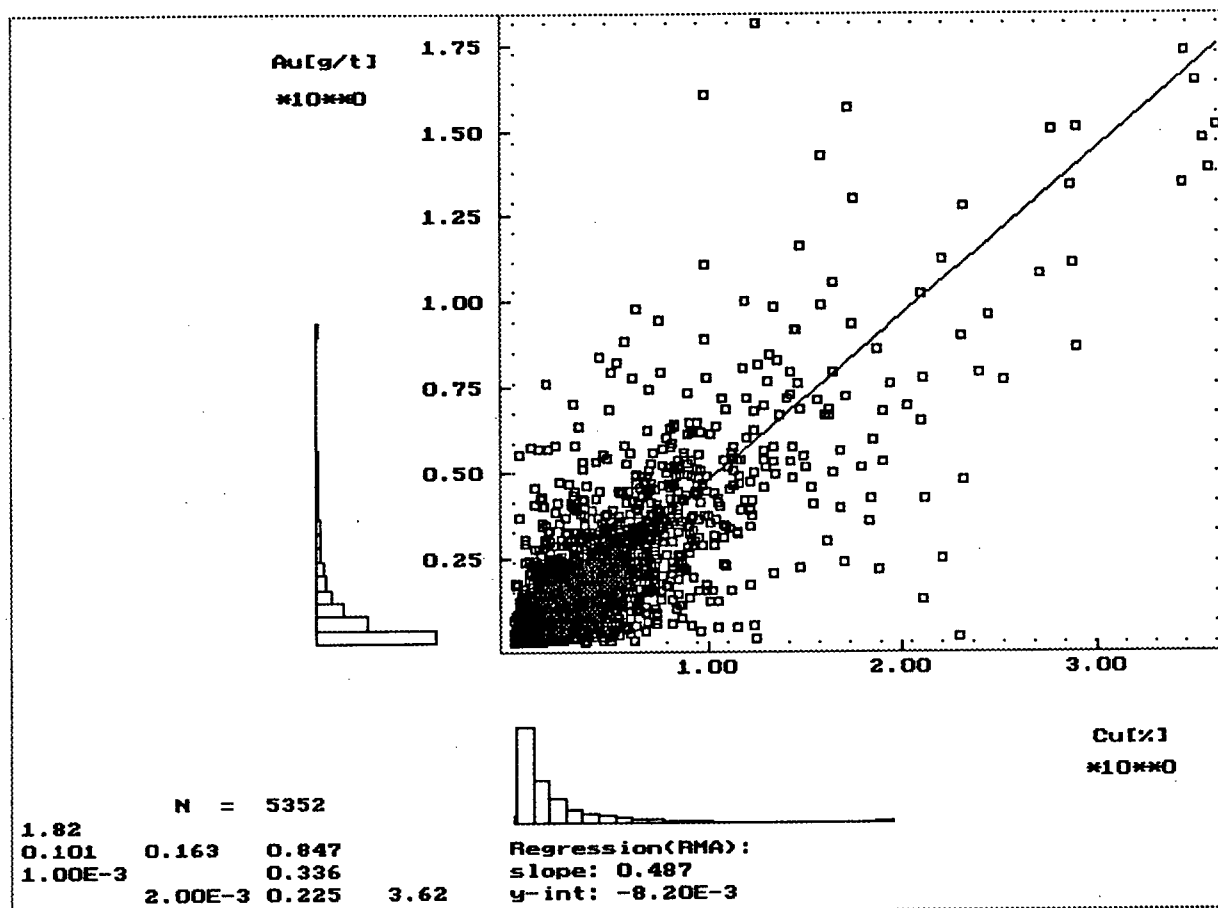


Figure 3-13: Virginia zone, scatter diagram of Au vs. Cu for assay data; the fitted straight line has an equation: $Au = 0.487 * Cu - 0.0082$; Cu assays thus, provide a corresponding estimate for accompanying Au grade.

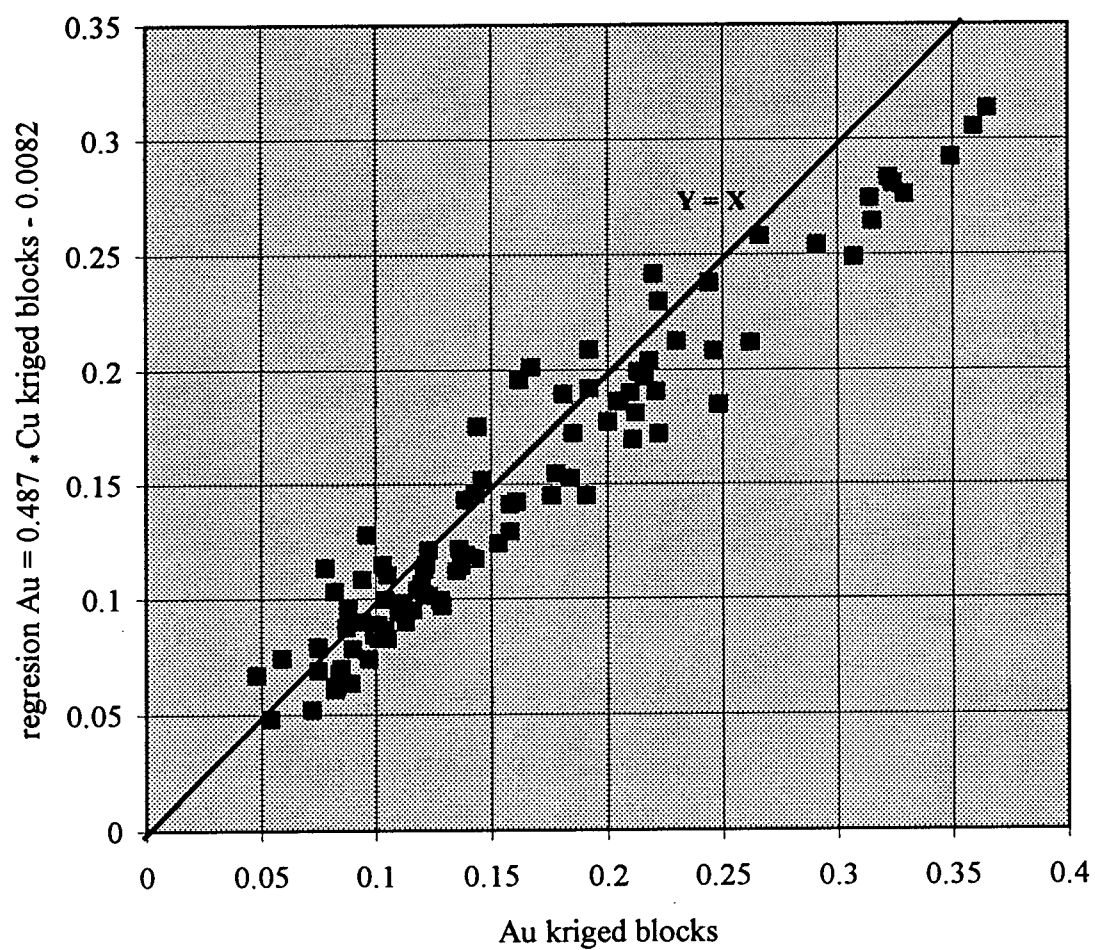


Figure 3-14: Virginia zone, scatterplot of 100 Au regression results versus Au kriging results (in g/t)

Fairweather (1997) suggests use of simple regression analysis to the evaluation of minor elements in both operating mines and new deposits using analytical information readily available. In the case of Virginia example above the use of regression analysis to estimate Au block values from Cu block estimates would decrease the cost of estimation by decreasing the cost of assaying for gold.

3.5: Conclusions

In porphyry-type deposits geology exerts an important control on models of value continuity; experience suggests that anisotropies in value continuity commonly are reflected in both the geology and in elongated grade trends demonstrated by contoured maps of grade. Examination of spatial distribution contour maps of important variables thus is an essential component of a mineral inventory study. All three examples discussed here suffer from a sparsity of closely-spaced samples in all directions except along drill holes resulting in uncertainty in semivariogram modeling. Thus geology provides a basis for confidence in defining domains and preferred directions of value continuity for mineral inventory estimation.

Acknowledgements

Special thanks are extended to Dr. A.J. Sinclair for supervising the research work on which this paper is based, assisting with problems and providing constructive criticism throughout the study. The author is grateful to Asger Bentzen for assistance with computer applications during initial stages of this work. Warm thank you goes to Arne

Toma for help with effective use of CorelDRAW. At various times this study has benefited from the advice of G. R. Raymond, C. R. Stanley, and K. Illerbrun. Mr. G. A. Whiton and Mr. G. R. Raymond were instrumental in making Huckleberry data available; Princeton Mining Company kindly provided the Virginia data. The generosity of these people and their organizations in releasing data for this study is greatly appreciated.

References

- Bentzen A., and Sinclair A. J., 1994, P-RES a computer program to aid in the investigation of polymetallic ore reserves; Tech. Rept. MT-9, Mineral Deposit Research Unit, Dept. of Geological Sciences, Univ. of B.C., Vancouver, Canada, includes diskette
- Deutsch, C. V., Journel, A. G., 1992, GSLIB Geostatistical Software Library and User's Guide; Oxford University Press, New York, 340 p. plus diskette
- Fairweather, M. J., 1997, Values and impurities in base metal concentrates; CIM Bull., v. 90, no. 1014, p.91-94
- Jackson, A., and Illerbrun K., 1995, Huckleberry porphyry copper deposit, Tahtsa Lake district, west-central British Columbia; in Porphyry deposits of the Northwestern Cordillera of North America, Spec. Vol. 46, Can. Inst. Min. Metall., p.313-321
- Postolski, T. A., and Sinclair, A. J., 1994, Mineralogy and Paragenesis of nine sulphide-bearing specimens from the Huckleberry deposit; unpublished report submitted to New Canamin resources Ltd., Vancouver, B.C.
- Ranta, D. E., Ward, A. D., and Ganster M. W., 1984, Ore zoning applied to geologic reserve estimation of molybdenum deposits; in Erickson, A. J., Jr., Metz, R. A. and Ranta, D. E. (eds.), Applied mining geology; Soc. Mining Engineers of A. I. M. E., New York, p.83-114
- Rendu, J-M., 1984, Geostatistical modeling and geological controls; Inst. Min. and Metall. Trans., v. 93B, p. B166-B172
- Sinclair, A. J., 1995, Selected topics in mineral inventory estimation; short course notes for a lecture series sponsored by the British Columbia and Yukon Chamber of Mines, Vancouver, B.C., variable paginations.

Sinclair, A. J., and Giroux, G. H., 1984, Geological controls of semi-variograms in precious metal deposits; in Verley, G., et al. (eds.), *Geostatistics for Natural Resources Characterization, Part 2*, p. 965-978, D. Reidel Pub. Co., Dordrecht, Netherlands.

Stanley, C. R., Holbek, P. M., Huyck, H. L. O., Lang, J. R., Preto, V. A. G., Blower S. J., and Bottaro, J. C., 1995, Geology of the Copper Mountain alcalic copper-gold porphyry deposit, Princeton, British Columbia; in *Porphyry deposits of the Northwestern Cordillera of North America, Spec. Vol. 46, Can. Inst. Min. Metall.*, p. 537-564

CHAPTER 4

QUANTITATIVE ESTIMATION OF DILUTION AND ORE LOSS RESULTING FROM BLOCK ESTIMATION ERRORS AND A SPECIFIED CUTOFF GRADE

ABSTRACT

Where block (selective mining unit) grade distributions can be determined, the effect of average errors of block grade estimates can be evaluated quantitatively. That is, for a given estimation error and cutoff grade, it is possible to calculate the quantity of metal that is lost as a result of misclassifying ore blocks as waste as well as the dilution that ensues from misclassifying waste blocks as ore. Example calculations using a computer program GAINLOSS and realistic block grade distribution parameters for both a porphyry-type deposit and an epithermal gold deposit illustrate some fundamental relations that are important in reconciliations that concern a comparison of estimates with production.

1. Where the cutoff grade is on the lower tail of the grade distribution, metal arising from dilution can be much less than metal lost through misclassifying ore as waste. Hence, average grade of milled material could possibly be higher than expected (estimated) and tonnes milled will be smaller than estimated.

2. Where the cutoff grade is on the higher tail of the grade distribution, tonnes arising from dilution will be greater than tonnes lost by misclassifying ore as waste. Hence, a possibility exists that average grade milled will be less than estimated.
3. The software GAINLOSS permits rapid comparison of the tonnes and average grade for all blocks selected as ore for a variety of levels of block estimation errors. These comparisons can be incorporated in a financial analysis to evaluate whether or not it is worthwhile to improve a high average block estimation error to some lower value.

4.1: Introduction

4.1.1: Biased Block Estimates by the Application of a Cutoff Grade

Truncation of a grade distribution, as in the application of a cutoff grade used to separate ore from waste, necessarily leads to a bias in resulting estimates of recoverable metal even though high quality, unbiased assay data are used to make the estimates. The problem arises because block classification as ore or waste is based on estimates which, no matter what their quality, contain some error. Thus, some values above a cutoff (truncation) grade are estimated as being below cutoff grade and vice versa. A simplistic example after Springett (1989) illustrates the problem:

"...consider the trivial but informative example of a gold deposit with a constant grade of 1.7 g/t (0.05 oz per st) completely homogenously distributed - thus any sample or truck load that is taken from the deposit contains exactly 1.7 g/t (0.05 oz per st) of gold. The operator is unaware of this uniform grade distribution and will carry out

selection by means of blast hole samples. Assume a sampling error that is normally distributed with a mean of zero and standard deviation of 0.34 g/t (0.01 oz per st) that is incurred at both the mill and the mine. Obviously if perfect, error free selection was possible then if the cutoff grade was at any value equal to or below 1.7 g/t (0.05 oz per st) the entire deposit would be delivered to the mill and if the cutoff grade were at any value greater than 1.7 g/t (0.05 oz per st) none of the deposit would be mined. However, given the assumed error distribution described above, the apparent distribution of blast hole sample grades will then be normally distributed with a mean 1.7 g/t (0.05 oz per st) and a standard deviation of 0.34 g/t (0.01 oz per st). If selection is carried out by the polygonal method then two curves can be developed showing for a range of cutoff grades: the average grade reported by the mine (and) the average grade reported by the mill."

In this example a constant grade of 0.05 oz/t with a random estimation error as one standard deviation of 20% (0.01 oz/t) gives the distribution of measured block grades of Figure 4-1. By imposing a cutoff grade, say 0.06 oz/t Au, 16% of the blocks will be selected as ore with an average grade of about 0.065 oz/t Au. In reality the mill will only recover 0.05 oz/t Au. For various cutoff grades the expected average grade of material mined is much higher than is actually reported as recovered at the mill. In general, average grade of blocks classed as ore is always overestimated (Figure 4-2). It is apparent that even in this simplistic case a systematic high bias for estimates of contained metal, is introduced by truncation (selection relative to a cutoff grade) despite the unbiased character of the sampling error.

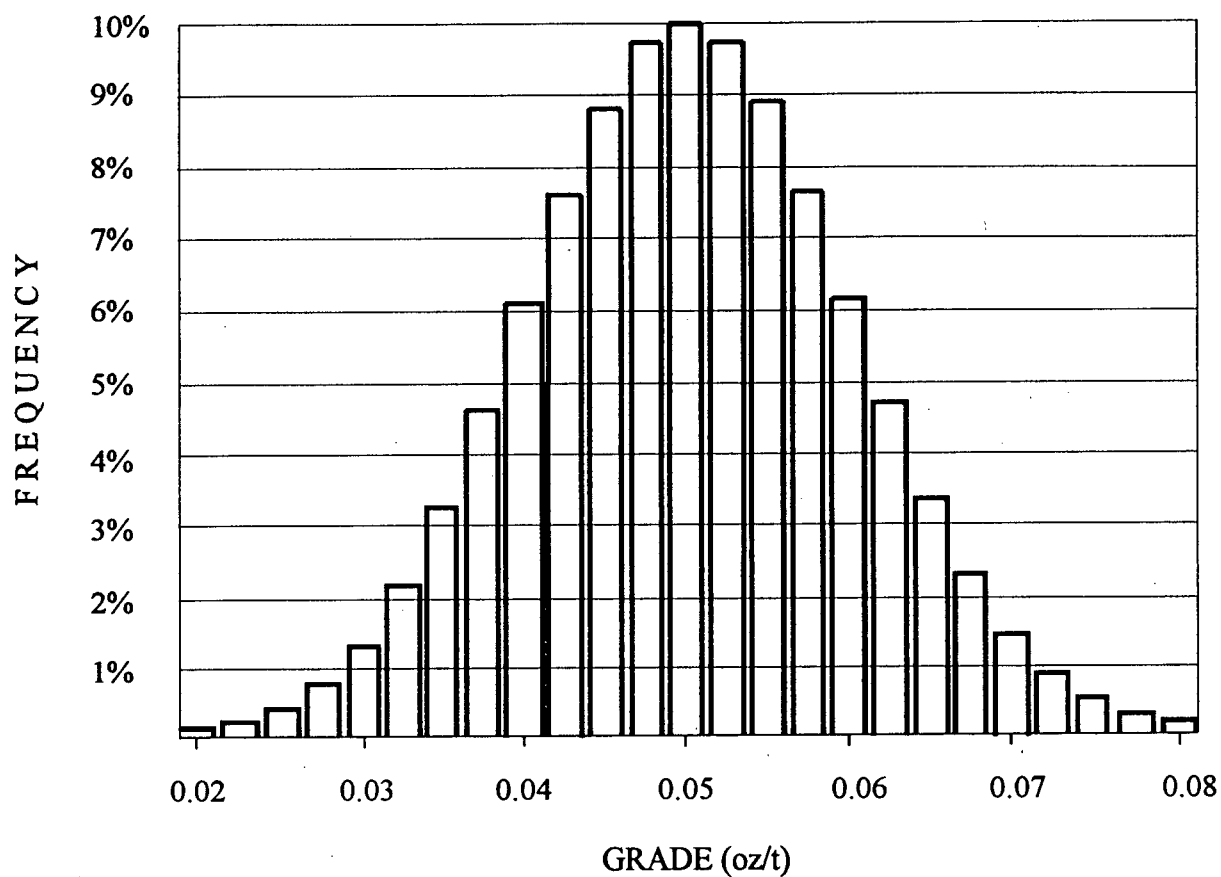


Figure 4-1: Normal estimated grade distribution with mean of 0.05 oz/t and standard deviation of 0.01 oz/t. Note that the true uniform grade is 0.05 oz/t and that dispersion of estimates arises entirely because of estimation error. After Springett (1989).

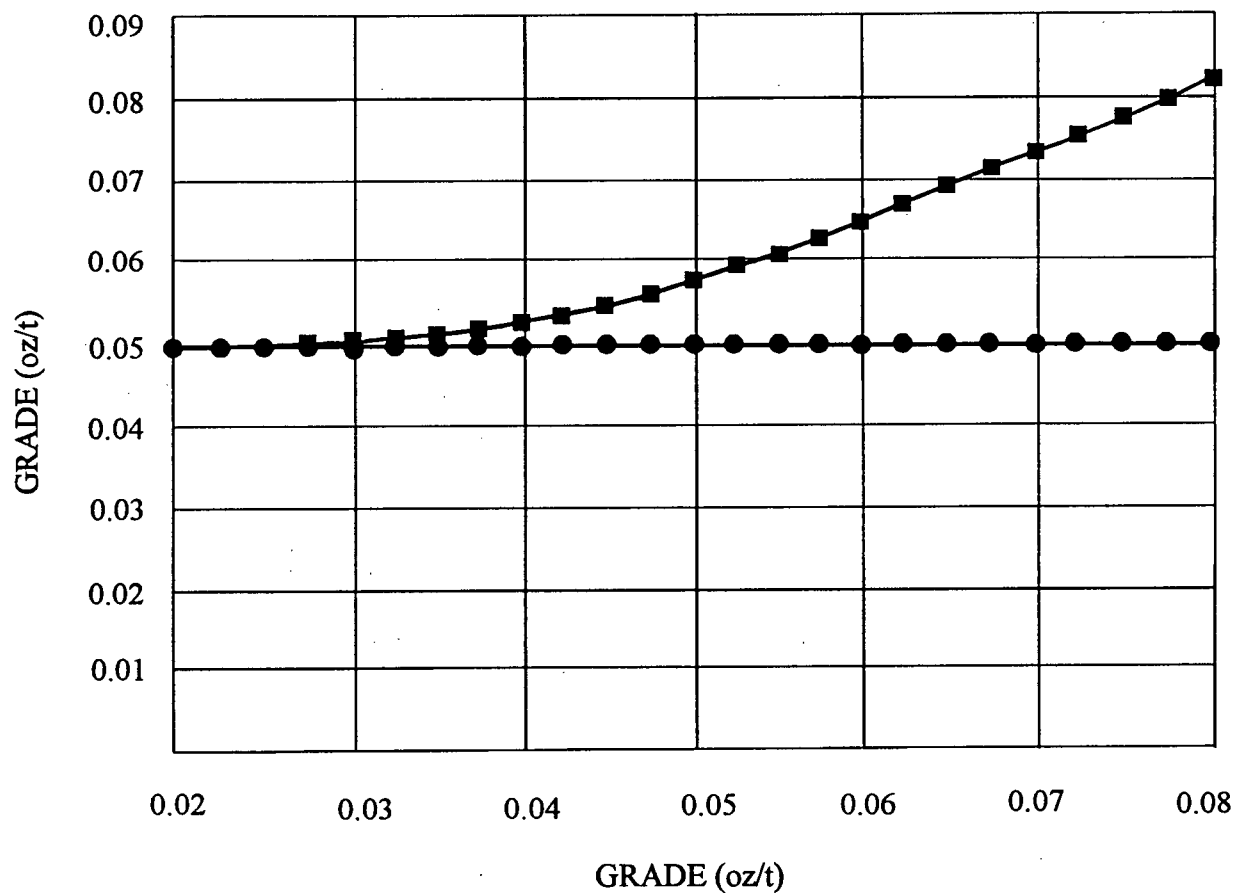


Figure 4-2: Estimated and true grades of production versus cutoff grade for the normal distribution of Figure 4-1. Squares are estimated average grade of blocks estimated due to error as having grade above the true grade. Circles indicate true grade of blocks selected as ore. Modified from Springett (1989).

A more realistic detailed example of the impact of various levels of error on the distribution of true copper grades at the Bougainville porphyry copper deposit is documented by David and Toh, 1989, and Sinclair, 1995. In general, if the cutoff grade is greater than the mean grade of the distribution, the effect of sampling and/or estimation error is to increase tonnage and to decrease average grade relative to reality; and for cutoff grades less than the average grade, to decrease tonnage and to increase average grade relative to reality. In the latter case the increase in grade is generally very slight, perhaps imperceptible.

4.2: Effect of Error of Block Estimates on Tonnage, Grade, and Metal Recovery

Sampling and/or estimation error can have a dramatic impact on metal recovery. Clearly, if some blocks of ore are inadvertently classed as waste, metal is lost; similarly if blocks of waste are included in ore, total tonnage is increased but average grade is decreased (i.e. dilution occurs). The problem is illustrated in Figure 4-3 and Figure 4-4 from David and Toh (1989) who were among the first to provide quantitative documentation of the concept of dilution due to analytical error in a case history of the Bougainville copper deposit. Their analysis will be redone here in less ambiguous fashion and extended to provide a more comprehensive example of the implications of not only error vis-a-vis dilution but also error vis-a-vis ore loss.

The likelihood of misclassification is seen to be a function of the true estimated grade and the error distribution curve. The upper half of Figure 4-3 shows two error curves centered on the cutoff grade of 0.215% Cu. This diagram demonstrates that almost equal proportion of blocks at or near the cutoff grade will be classed as ore and waste.

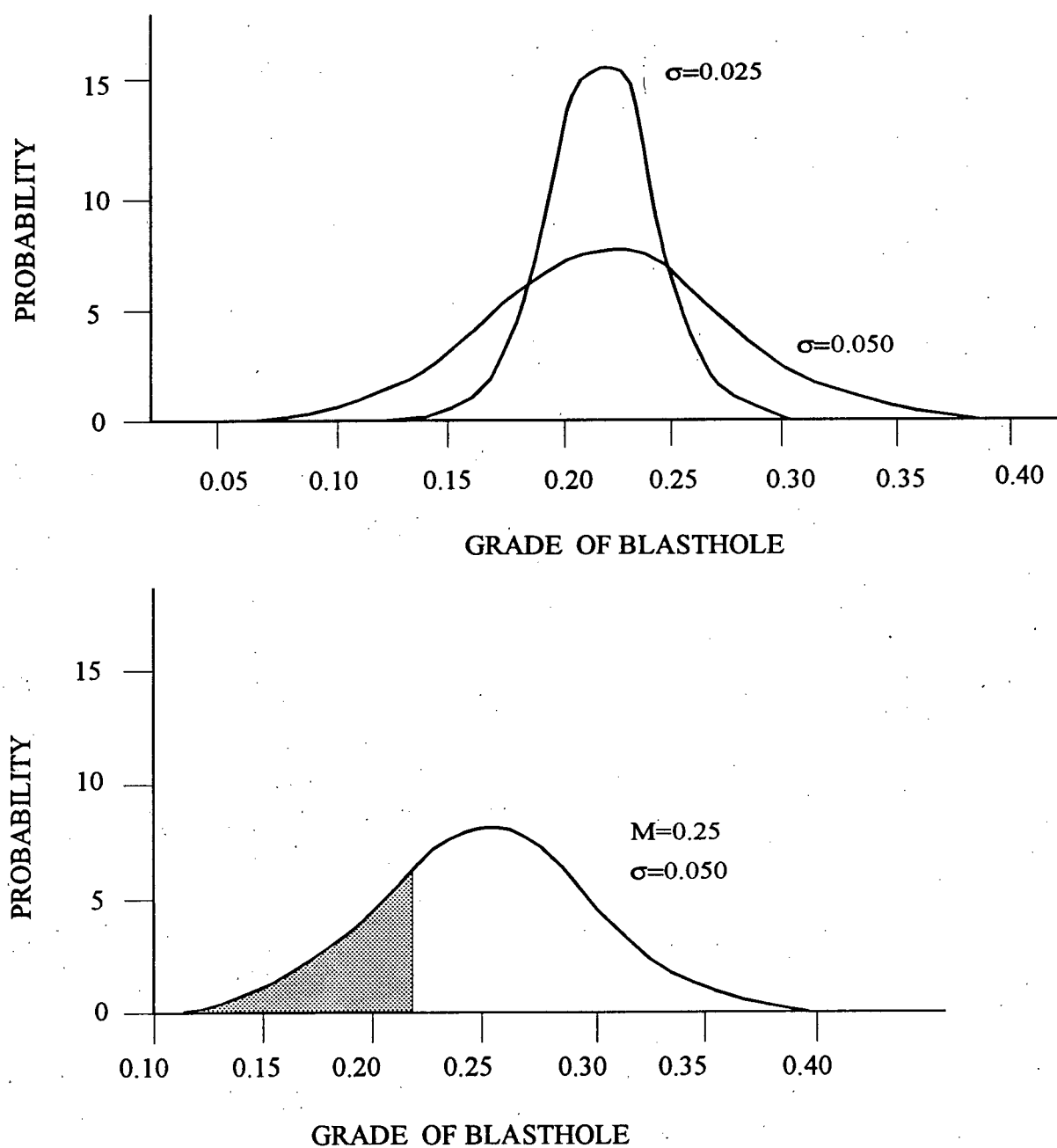


Figure 4-3: (Upper) Two examples of error curves superimposed on a blasthole grade 0.215% Cu. (Lower) An error curve centered on a true blasthole grade of 0.25% Cu showing that 24% of estimates will be below the cutoff grade (shaded area). Modified from David and Toh (1988).

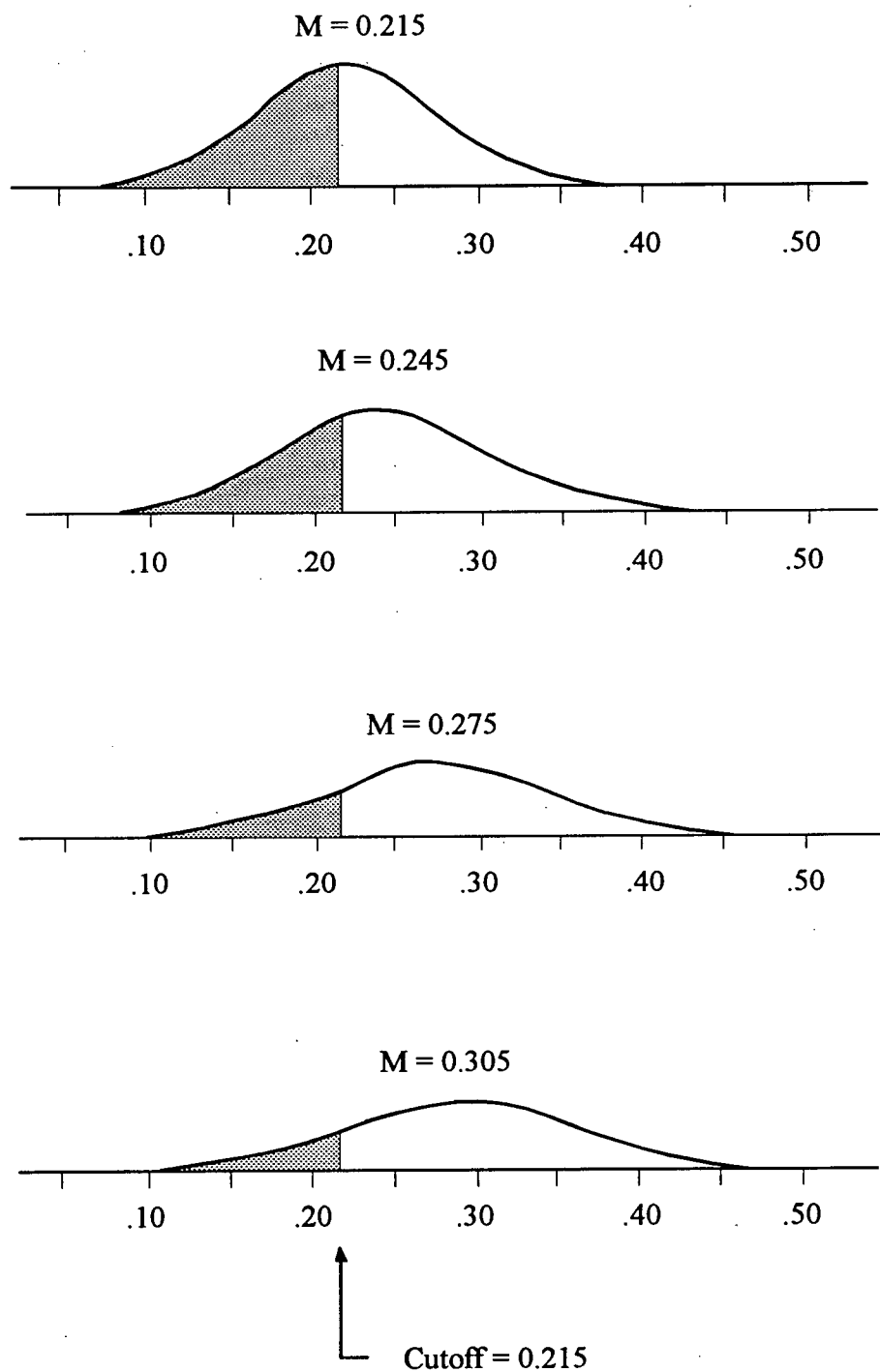


Figure 4-4: Four examples of various error curves centered on various true grades, illustrating that a significant proportion of estimates will be below the Bougainville cutoff grade of 0.215% Cu. After David and Toh (1988).

The effect is more dramatic if the error is large, as shown by the curve with the wider spread. In the example on the lower part of Figure 4-3, the mean grade is 0.25% Cu and standard deviation is 0.05, that is, a 20% error curve centered on ore blocks grading 0.25% Cu. The cutoff grade of 0.215% Cu imposed on this error curve shows that 24% of the blocks grading about 0.25% Cu will be identified as being below cutoff grade and will be sent to waste (Table 4-2). If the error dispersion were less, say 10%, then only 8% of such blocks would be classed as waste (Table 4-2). This example shows that the quality of block estimates has an impact on metal recovery and consequently on operating profit.

Figure 4-4 shows four examples of various error curves centered on various true grades (M). Consequently different proportions of ore blocks of various grades will be misclassified as waste as a function of estimation error. The same approach applies to waste blocks. Because of estimation error some waste blocks will be misclassified as ore and dilution results.

Clearly, estimation error results in both dilution of ore by waste and loss of low grade ore to waste. An estimate of the impact of error on metal loss can be made under certain conditions; in particular, it must be possible to estimate the true distribution of grades and the sampling error must be known or assumed. In the case of the Bougainville example, the distribution of blasthole grades is assumed to represent the true distribution of grades. This distribution is assumed to be lognormal with mean of raw data of blasthole grades equal to 0.45% Cu, and natural logvariance of 0.21 (natural logs mean = -0.9035, while variance of raw data of blasthole grades = 0.0473). Small departures from this assumed distribution will have negligible impact on the principal conclusions that follow. The cutoff grade is quoted as 0.215% Cu (David and Toh, *ibid*). Hence, equations A6-6,

TABLE 4-1

**NUMBER OF WASTE BLOCKS MISTAKENLY INCLUDED IN ORE DUE TO
VARIOUS LEVELS OF ERROR, BOUGAINVILLE PORPHYRY DEPOSIT,
COPPER GRADE DISTRIBUTION**

Grade intvl. centre	Freq. in 1000 blks	10% error P>c	Freq.* P>c	20% error P>c	Freq.* P>c	30% error P>c	Freq.* P>c
0.11	1.1					0.000	0.000
0.12	1.8					0.003	0.005
0.13	2.7			0.000	0.001	0.012	0.033
0.14	3.9			0.003	0.010	0.034	0.131
0.15	5.2			0.013	0.067	0.071	0.373
0.16	6.7	0.000	0.001	0.040	0.268	0.124	0.833
0.17	8.4	0.003	0.024	0.090	0.754	0.187	1.568
0.18	10.1	0.023	0.232	0.164	1.647	0.258	2.592
0.19	11.8	0.091	1.075	0.255	2.994	0.330	3.883
0.20	13.4	0.226	3.032	0.354	4.751	0.401	5.390
0.21	15.0	0.406	6.104	0.453	6.807	0.468	7.044
Sum of misclassified waste blocks:			10.468		17.298		21.854
Average true grade of misclassified waste blocks:							
			0.204		0.198		0.194

TABLE 4-2

**NUMBER OF ORE BLOCKS MISTAKENLY INCLUDED IN WASTE DUE TO
VARIOUS LEVELS OF ERROR, BOUGAINVILLE PORPHYRY DEPOSIT,
COPPER GRADE DISTRIBUTION**

Grade intvl. centre	Freq. in 1000 blks	10% error P<c	Freq.* P<c	20% error P<c	Freq.* P<c	30% error P<c	Freq.* P<c
0.22	16.6	0.410	6.787	0.455	7.527	0.470	7.776
0.23	17.9	0.256	4.602	0.372	6.676	0.414	7.427
0.24	19.2	0.147	2.819	0.301	5.776	0.364	6.989
0.25	20.3	0.078	1.580	0.241	4.896	0.320	6.499
0.26	21.3	0.039	0.821	0.192	4.084	0.282	5.984
0.27	22.1	0.018	0.400	0.152	3.361	0.248	5.467
0.28	22.7	0.008	0.185	0.121	2.738	0.219	4.962
0.29	23.2	0.004	0.082	0.095	2.212	0.193	4.481
0.30	23.6	0.002	0.036	0.075	1.777	0.171	4.029
0.31	23.8	0.001	0.015	0.060	1.420	0.152	3.612
0.32	23.9	0.000	0.006	0.047	1.132	0.135	3.229
0.33	23.9	0.000	0.003	0.038	0.900	0.120	2.881
0.34	23.8	0.000	0.001	0.030	0.715	0.108	2.567
0.35	23.7	0.000	0.000	0.024	0.568	0.097	2.285
0.36	23.4			0.019	0.451	0.087	2.032
0.37	23.1			0.016	0.358	0.078	1.807
0.38	22.7			0.013	0.285	0.071	1.606
0.39	22.2			0.010	0.228	0.064	1.428
0.40	21.7			0.008	0.182	0.058	1.270
0.41	21.2					0.053	1.129
0.42	20.6					0.049	1.005
0.43	20.0					0.045	0.895
0.44	19.4					0.041	0.797
0.45	18.8					0.038	0.711
0.46	18.2					0.035	0.634
0.47	17.6					0.032	0.566
0.48	17.0					0.030	0.506
0.49	16.3					0.028	0.452
0.50	15.7					0.026	0.405
0.51	15.1					0.024	0.363
0.52	14.5					0.022	0.325
0.53	13.9					0.021	0.292
Sum of misclassified ore blocks:			17.339		45.284		84.410
Average true grade of misclassified ore blocks:			0.233		0.261		0.298

A6-7, A6-9 and A6-10 (Appendix 6) can be used to demonstrate that 91.9% of true grades are above cutoff grade, that 97% of the contained metal is in the material above cutoff grade, and that the average grade of material above cutoff grade is 0.475% Cu.

For this example an ideal situation is assumed wherein each blasthole is considered to be centrally located within a block of ore and the average grade assigned to the blasthole will be used to classify the block as ore or waste (i.e. classical polygonal estimate). For 1000 such blocks only 919 are truly ore although classification of blocks as ore or waste will be in error to some extent if the true grades are near the cutoff grade.

A computer program GAINLOSS has been written in FORTRAN77 (cf. Reddy and Ziegler, 1989; Appendix 7 contains algorithm of the program and printout of the source code) to estimate the impact of such error on dilution and ore loss, where the distribution of block grades can be approximated by a normal or lognormal distribution.

The user must input:

1. The name of the target text file.
2. The name of variable (e.g. Copper, Gold).
3. The unit for variable - either percent or gram/tonne.
4. Mean and standard deviation of block grade distribution.
5. The cutoff grade.
6. Limits of the first and last grade intervals.
7. Estimation error.
8. Number of blocks and tonnage of individual blocks.
9. The user has to declare if the distribution of block grades is normal or lognormal.

The output from the program consists of three tabulations:

1. For grade intervals below cutoff grade the number of misclassified waste blocks both in contiguous short grade intervals and total number of all misclassified waste blocks are given as well as their average true grade (Tables 4-1, 4-4, and 4-7)).
1. For grade intervals above cutoff grade the number of misclassified ore blocks both in contiguous short grade intervals and total number of all misclassified ore blocks are given as well as their average true grade (Tables 4-2, 4-5, and 4-8)).
1. Metal accounting summary tabulation (Tables 4-3, 4-6, and 4-9) gives net cost of mining waste classed as ore and net loss of metal in ore classed as waste as well as total operating loss of metal in tonnes (if percent was declared as units) or in both grams and troy ounces (if gram/tonne option was chosen).

The likelihood of misclassification is seen to be a function of the true estimated grade and the error distribution curve (e.g. Figure 4-4). The GAINLOSS program calculates the number of misclassified blocks for contiguous short grade intervals centered on the middle point (grade) of each interval. To illustrate the procedure that the GAINLOSS program uses, consider a short grade interval of 0.195 to 0.205% Cu which is assumed to be centered on 0.20% Cu and a sampling and analytical error of 10% (i.e. error as one standard deviation is 0.020). The program uses equations A6-2 and A6-4 (cf. Appendix 6) to estimate the proportion of blocks with true grade of 0.20% Cu that will be

reported with a grade above cutoff grade; that proportion is 0.226. For the lognormal distribution (Bougainville case) the GAINLOSS program uses equations A6-6 and A6-7 (Appendix 6) to estimate the cumulative proportion of grades from infinity to each side of the grade interval: the difference in these two cumulative percentages is the frequency within the interval and is estimated to be 0.0134. Thus, for the 1000 block example, 13.4 (say 13) blocks will have true values between 0.195 and 0.205%Cu, and $13 \times 0.0226 = 2.9$ (say 3) of these waste blocks will be misclassified as ore if the error is 10%. The GAINLOSS program follows a similar procedure for many contiguous short grade intervals below cutoff grade and the number of misclassified blocks is determined in each case. The GAINLOSS program outputs the results of such a calculation to the first tabulation in the target text file. Table 4-1 is a summary of such results in the case of Bougainville copper for assumed errors of 10%, 20%, 30%. The table includes the average total number of diluting blocks (per 1000 blocks) and their true average grade for each of the three error scenarios. In the case of 10% error 10 blocks of waste, averaging 0.204% Cu are incorrectly classed as ore. In the case of 20% error 17 blocks of waste, averaging 0.198% Cu are incorrectly classed as ore. Finally in the case of 30% error 22 blocks of waste, averaging 0.194% Cu are incorrectly classed as ore. The true average grades were determined as a weighted average of the central grade of each grade interval weighted by the number of diluting blocks.

Of course, errors of misclassification also apply to blastholes above but near cutoff grade; some ore blocks are inadvertently classed as waste. In this case, for any short grade interval the GAINLOSS program determines the proportion of ore blocks that will be incorrectly classed as waste using procedure comparable to that described above. For each

short grade interval above cutoff grade the program estimates the proportion of blocks that will be incorrectly classed as waste due to any specified error.

The GAINLOSS program outputs the results of such a calculation to the second tabulation in the target text file. Calculations of this nature for the Bougainville Cu distribution are summarized in Table 4-2 for errors (as standard deviation) of 10%, 20% and 30%. In the case of the 10% error scenario an average of 17 blocks of low grade ore (averaging 0.233% Cu) are classed as waste. In the case of the 20% error scenario an average of 45 blocks of low grade ore (averaging 0.261% Cu) are classed as waste. Finally in the case of the 30% error scenario an average of 84 blocks of low grade ore are classed as waste. These blocks average 0.298% Cu, substantially above cutoff grade, and the loss of profit is evident.

Metal accounting summarizes losses and gains in terms of metal above cutoff grade (Sinclair, 1995). This is a metal operating profit that program GAINLOSS calculates according to the following equation:

$$q_i = (g_i - g_c) * T$$

where:

q_i is quantity of metal (it is equivalent to the operating profit)

g_i is an average true grade (it is equivalent to the operating revenue)

g_c is the cutoff grade (it is equivalent to the operating cost)

T is tonnage of misclassified blocks

The GAINLOSS program outputs the results of such a calculation to the third tabulation in the target text file. Calculations of this nature for the Bougainville Cu

distribution are summarized in Table 4-3 for errors (as standard deviations) of 10%, 20% and 30%. In the case of the 10% error scenario an average of 8 tonnes of copper is lost, in the case of the 20% error scenario an average of 47 tonnes of copper is lost, while in the case of the 30% error scenario an average of 150 tonnes of copper is lost. At the metal prices of approximately US \$0.80 per lb the loss at 30% error level is:

$$150 \text{ t Cu} * 2,205 \text{ lb} * 0.8 = \text{US } \$264,600 \text{ per } 1000 \text{ blocks (2000 tonnes each) mined.}$$

It is important to note, that:

1. There will always be some loss, because there is always an error involved.
2. Alternative scenarios with larger or smaller errors can be compared, the difference can be translated into dollars, and an evaluation can be made of the worth of improving the quality of estimates.

The results are of considerable significance for several reasons. In addition, the effect of dilution and ore loss on grade of production can be calculated. Return to the 1000 block and 10% error scenario; 919 blocks are truly above cutoff grade. Of these 919 blocks, 17 are inadvertently classed as waste leaving 902 blocks with average grade (g_{902}) as follows:

$$902 \times g_{902} = 919 \times 0.475 - 17 \times 0.233$$

$$g_{902} = 0.480\% \text{ Cu}$$

TABLE 4-3

**METAL ACCOUNTING SUMMARY OF OPERATING LOSS (METAL)
FOR BLOCK MISCLASSIFICATION DUE TO VARIOUS LEVELS OF
ERROR, BOUGAINVILLE PORPHYRY DEPOSIT, COPPER GRADE
DISTRIBUTION***

	10% error		20% error		30% error
Net cost of mining waste classed as ore (tonnes of metal):	-2.24		-5.83		-9.15
Net loss of metal in ore classed as waste (tonnes of metal):	-6.23		-41.63		-140.55
TOTAL OPERATING LOSS (TONNES OF METAL):	-8.47		-47.47		-149.70

* For a hypothetical scenario with 1000 blocks (2000 tonnes each)

Now add the dilution resulting from the 10 blocks of waste (cf. Table 4-1) that are incorrectly classed as ore: the resulting average grade is:

$$912 \times g_{912} = 902 \times 0.480 + 10 \times 0.204$$

to give $g_{912} = 0.477\%$ Cu. The important point to be made is that although dilution has occurred, the average grade of mined ore is slightly higher than the overall average grade above cutoff (0.477% Cu vs. 0.475% Cu) because the effect of losing 17 blocks of low grade ore slightly overshadows the diluting effects of including 10 blocks of relatively high grade waste. So a loss in tonnage has resulted in a somewhat higher grade than expected from all true ore blocks. This effect occurs in reverse if the cutoff grade is on the upper tail of the distribution of real grades, that is, if a high absolute number of waste blocks are included with ore, relative to the number of ore blocks lost as waste. In this latter case, the effect of dilution predominates over the effect of losing ore to the waste dump, and the mean grade of material classed as ore is less than the mean grade of all ore blocks.

Moreover, the tonnage of material classed as ore is greater than the tonnage of true ore.

The effects of error are likely to be overlooked if they are on the scale indicated by the 10% error case discussed above because there is a minimal improvement in grade and a relatively small loss in tonnes, although the actual metal loss is significant. As the level of error increases, however, the impact becomes more and more significant. The results for 20% and 30% errors applied to the Bougainville example summarized as metal accounting in Table 4-3 demonstrate the serious loss of metal as the level of estimation error increases. For the 30% relative error scenario the loss of metal as discussed above is very high (150 tonnes of Cu metal). The effect on grade of material classed as ore can be

calculated as done above for the 10% error scenario. For example, the effect of 84 blocks of lost ore is

$$919 \times 0.475 - 84 \times 0.298 = 835 \times g_{835}$$

from which g_{835} is found to be 0.493% Cu. Now add the 22 blocks of dilution:

$$0.493 \times 835 + 0.194 \times 22 = 857 \times g_{857}$$

from which g_{857} is found to be 0.485% Cu. Note that the average grade of material classed as ore is significantly higher than the expected average (0.485% Cu vs. 0.475% Cu); however assuming 2000 tonnes per each block, the loss of tonnes is: $(919 - 857) \times 2000 = 124,000$ tonnes per 1000 blocks mined. For distributions for which the cutoff grade is on the high grade tail (rather than the low grade tail as is the case here) the average grade would be below the expected grade because the effects of diluting with waste would be greater than relatively small losses of ore. Although idealized, these calculations provide useful insight into the need for high quality in both sampling and assaying.

4.3: Application of GAINLOSS to the Huckleberry deposit

The second example is the West domain in the East zone of Huckleberry deposit (Jackson and Illerbrun, 1995). Figure 4-5 shows a naive histogram of 8m composites of Copper values from exploration diamond drillhole data for W domain. Mean value is 0.4243% Cu and standard deviation is 0.2503% Cu. However, to estimate the impact of selection error on metal loss and dilution, the parameters of block grade distribution have to be found. A volume-variance relationship (cf. Parker, 1979) based on declustered data and semivariogram model is used to derive the parameters of a 20mx20mx8m block grade distribution.

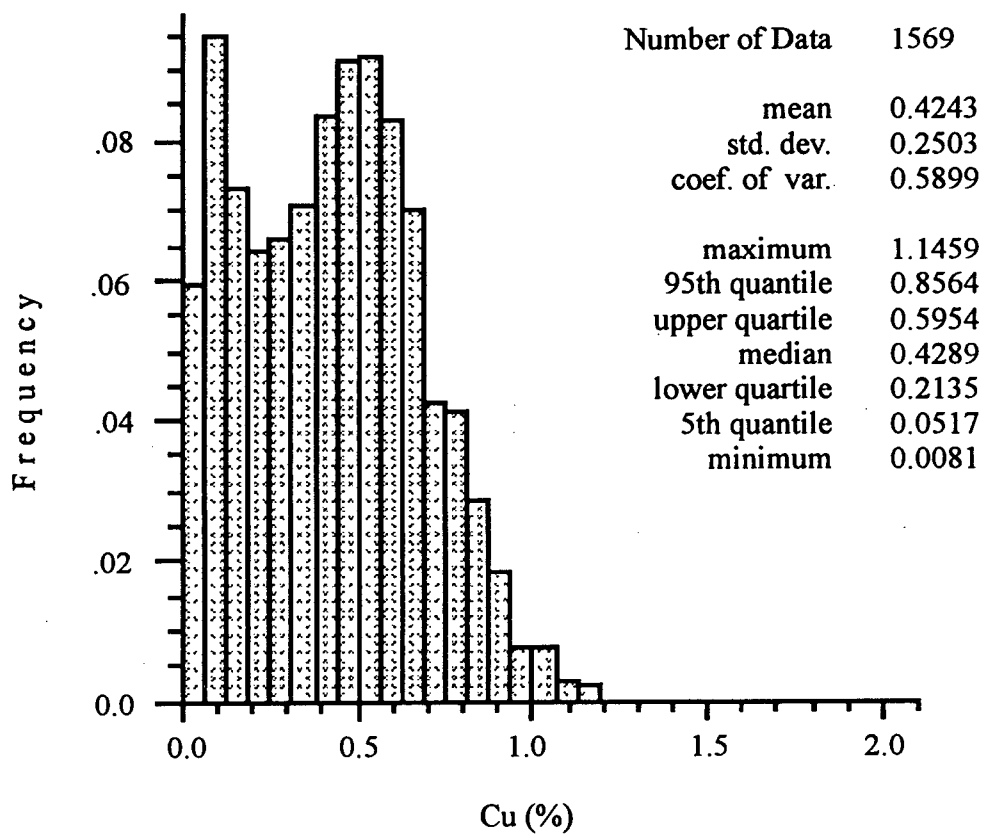


Figure 4-5: Huckleberry, East zone, West domain. Naive histogram of Cu 8 m composites.

Figure 4-6 shows a declustered histogram of Cu 8m composites from diamond drillhole data for W domain. There is a considerable decrease in mean value (0.3196% Cu) and also some decrease in dispersion (standard deviation = 0.2418% Cu). Declustering refers to methods used to minimize the effects of biased spatial distributions of sample data (cf. Giroux and Sinclair, 1986). Exploration data are commonly concentrated in zones of relatively high grade, so the histogram of raw data contains too high a proportion of high grade samples, leading to overestimates of both mean grade and dispersion of the data. This bias is offset by applying less weight to those samples that occur in clusters. Figure 4-6 shows that the cell size for assigning weights to assays is 158m. The approximate cell size for obtaining unbiased mean estimates of a deposit occurs where the mean passes through the minimum, as in the lower part of Figure 4-6, which is a plot of unbiased mean versus various sizes of blocks used for declustering.

The unbiased histogram reveals the true parameters of the W domain data distribution and, in combination with the volume-variance relationship, allows determination of parameters (mean and standard deviation) of block grade distribution. To do this, a correction has to be applied to an unbiased histogram of sample grades using the volume-variance relationship (cf. Parker, 1979) as follows:

$$D^2(b/V) = D^2(o/V) - D^2(o/b)$$

where

$D^2(b/V)$ is the dispersion variance of average grades of the blocks (b) in the deposit (V)

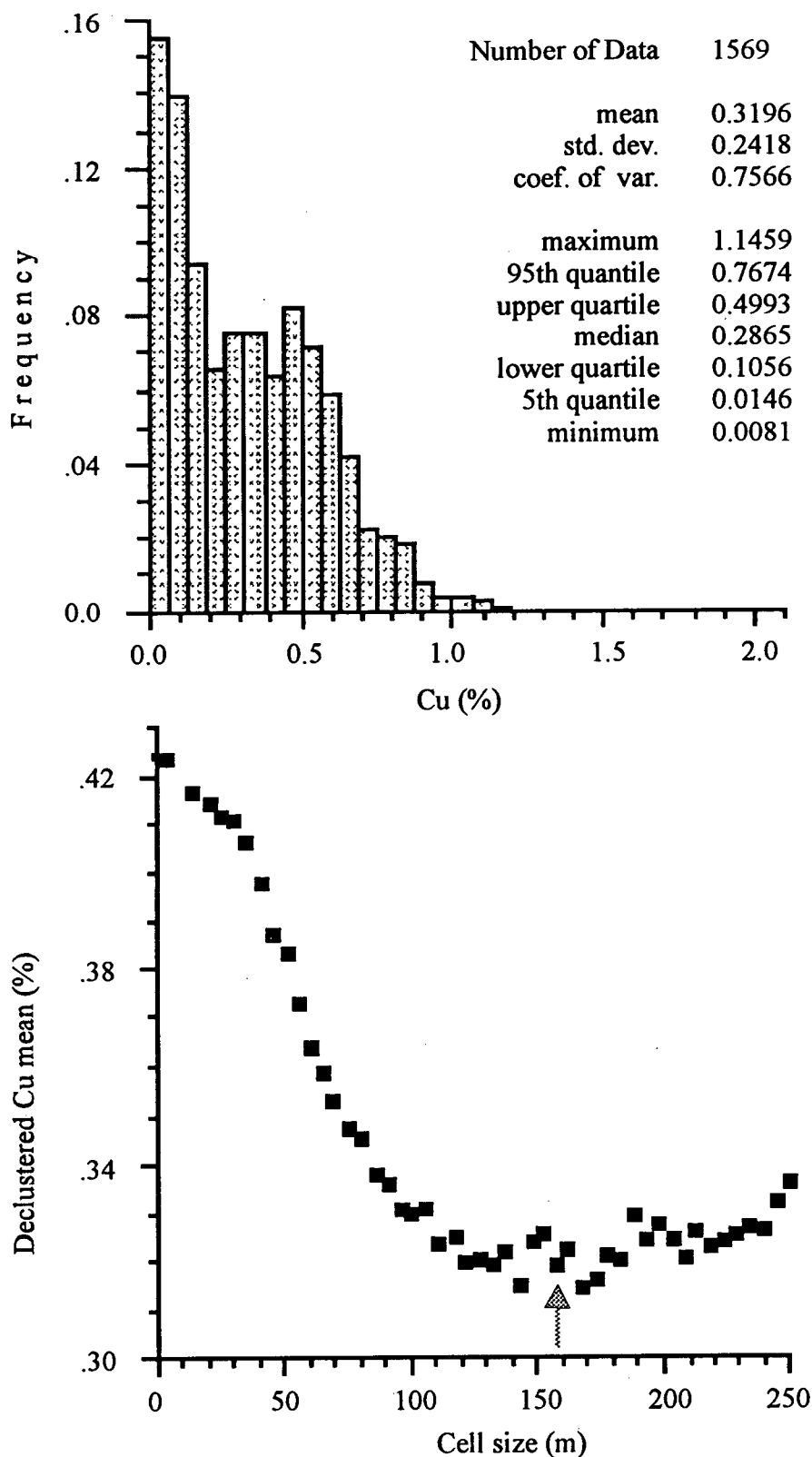


Figure 4-6: Huckleberry, East zone, West domain. (Upper) declustered histogram of Cu 8 m composites; (Lower) binary diagram of declustered mean Cu value versus block dimensions used for declustering.

$D^2(o/V)$ is the dispersion variance of sample grades (o) in the deposit (V),
and

$D^2(o/b)$ is the dispersion variance of sample grades (o) in the blocks (b)

$D^2(o/b)$ was obtained using F auxiliary function charts given in Journel and Huijbregts (1978). A good quality semivariogram is important to the determination of the F function, consequently the model of the W domain semivariogram from the East zone (cf. Appendix 4) was used to determine the F function. $D^2(o/b)$ was determined to be 0.08. $D^2(o/V) = 0.6$, was determined as the value of the sill of the semivariogram model for W domain. Consequently $D^2(b/V)$ is equal 0.52. However this value cannot be used as the dispersion variance of blocks in the deposit because the semivariogram model used is a pairwise relative semivariogram. Consequently, the sought for value 0.05 of $D^2(b/V)$ was obtained using ratio $0.52/0.6$ and the value 0.058 for $D^2(o/V)$ which is the variance from the unbiased histogram (cf. Figure 4-6). Thus, to derive a histogram of block grades the variance of the declustered sample distribution was reduced, without changing its mean, so the parameters of 20mx20mx8m block grade distribution, assumed to be lognormal, are:

mean = 0.3196 and,

standard deviation = $(0.05)^{1/2} = 0.2236$

The cutoff grade is taken as 0.4% Cu (cf. Chapter 3). Tables 4-4, 4-5, and 4-6 illustrate the situation for assumed errors equal respectively 10%, 15% and 20% for 627 blocks (8,608 tonnes per block), which represent annual production at Huckleberry.

Table 4-4 includes the average total number of diluting blocks (per 627 blocks) and their true average grade for each of the three error scenarios. In the case of 10% error

TABLE 4-4

**NUMBER OF WASTE BLOCKS MISTAKENLY INCLUDED IN ORE
DUE TO VARIOUS LEVELS OF ERROR, HUCKLEBERRY PORPHYRY
DEPOSIT, EAST ZONE, W DOMAIN, COPPER GRADE
DISTRIBUTION**

Grade intvl. centre	Freq. in 1000 blks	10% error P>c	Freq.* P>c	15% error P>c	Freq.* P>c	20% error P>c	Freq.* P>c
0.215	17.6					0.000	0.000
0.225	17.1					0.000	0.000
0.235	16.6					0.000	0.002
0.245	16.1					0.000	0.007
0.255	15.5			0.000	0.000	0.001	0.023
0.265	15.0			0.000	0.002	0.004	0.060
0.275	14.4			0.001	0.010	0.009	0.135
0.285	13.8	0.000	0.000	0.003	0.034	0.019	0.263
0.295	13.2	0.000	0.001	0.007	0.092	0.034	0.455
0.305	12.6	0.001	0.007	0.016	0.206	0.057	0.715
0.315	12.1	0.002	0.029	0.033	0.398	0.086	1.036
0.325	11.5	0.008	0.098	0.059	0.679	0.122	1.407
0.335	11.0	0.023	0.256	0.095	1.047	0.164	1.807
0.345	10.5	0.052	0.548	0.142	1.488	0.212	2.218
0.355	10.0	0.100	0.997	0.198	1.975	0.262	2.621
0.365	9.5	0.167	1.589	0.261	2.479	0.316	3.000
0.375	9.0	0.252	2.278	0.328	2.969	0.369	3.342
0.385	8.6	0.348	2.997	0.397	3.421	0.423	3.638
0.395	8.2	0.450	3.679	0.466	3.816	0.475	3.885
Sum of misclassified waste blocks:			12.480		18.617		24.615
Average true grade of misclassified waste blocks:							
			0.378		0.368		0.360

TABLE 4-5

**NUMBER OF ORE BLOCKS MISTAKENLY INCLUDED IN WASTE DUE TO
VARIOUS LEVELS OF ERROR, HUCKLEBERRY PORPHYRY DEPOSIT,
EAST ZONE, W DOMAIN, COPPER GRADE DISTRIBUTION**

Grad intv centre	Freq. in 1000 blks	10% error P<c	Freq.* P<c	15% error P<c	Freq.* P<c	20% error P<c	Freq.* P<c
0.405	7.8	0.451	3.506	0.467	3.633	0.475	3.697
0.415	7.4	0.359	2.651	0.405	2.991	0.428	3.165
0.425	7.0	0.278	1.949	0.347	2.438	0.384	2.698
0.435	6.7	0.209	1.396	0.295	1.970	0.344	2.291
0.445	6.3	0.154	0.976	0.249	1.579	0.306	1.939
0.455	6.0	0.111	0.667	0.209	1.257	0.272	1.637
0.465	5.7	0.078	0.446	0.174	0.994	0.242	1.379
0.475	5.4	0.054	0.293	0.144	0.782	0.214	1.159
0.485	5.1	0.037	0.189	0.119	0.612	0.189	0.973
0.495	4.9	0.025	0.120	0.098	0.477	0.167	0.815
0.505	4.6	0.016	0.075	0.080	0.371	0.147	0.683
0.515	4.4	0.011	0.046	0.065	0.287	0.130	0.572
0.525	4.2	0.007	0.028	0.053	0.222	0.115	0.478
0.535	4.0	0.004	0.017	0.043	0.171	0.101	0.400
0.545	3.8	0.003	0.010	0.035	0.132	0.089	0.335
0.555	3.6	0.002	0.006	0.028	0.101	0.078	0.280
0.565	3.4	0.001	0.004	0.023	0.078	0.069	0.234
0.575	3.2	0.001	0.002	0.019	0.060	0.061	0.196
0.585	3.1	0.000	0.001	0.015	0.046	0.054	0.164
0.595	2.9	0.000	0.001	0.012	0.035	0.047	0.138
0.605	2.8			0.010	0.027	0.042	0.116
0.615	2.6			0.008	0.021	0.037	0.097
0.625	2.5			0.006	0.016	0.033	0.082
0.635	2.4			0.005	0.012	0.029	0.069
0.645	2.2			0.004	0.009	0.026	0.058
0.655	2.1			0.003	0.007	0.023	0.049
0.665	2.0			0.003	0.006	0.020	0.041
0.675	1.9			0.002	0.004	0.018	0.035
0.685	1.8			0.002	0.003	0.016	0.030
0.695	1.7			0.002	0.003	0.014	0.025
0.705	1.7			0.001	0.002	0.013	0.021
0.715	1.6			0.001	0.002	0.012	0.018
0.725	1.5			0.001	0.001	0.010	0.015
0.735	1.4			0.001	0.001	0.009	0.013
0.745	1.3			0.001	0.001	0.008	0.011
0.755	1.3			0.000	0.001	0.007	0.010
0.765	1.2					0.007	0.008
0.775	1.2					0.006	0.007
0.785	1.1					0.005	0.006
0.795	1.1					0.005	0.005
0.805	1.0					0.004	0.004
0.815	1.0					0.004	0.004
0.825	0.9					0.004	0.003
0.835	0.9					0.003	0.003
0.845	0.8					0.003	0.002
0.855	0.8					0.003	0.002
0.865	0.7					0.003	0.002
0.875	0.7					0.002	0.002
0.885	0.7					0.002	0.001
Sum of misclassified ore blocks:			12.387		18.352		23.972
Average true grade of misclassified ore blocks:			0.427		0.442		0.458

TABLE 4-6

**METAL ACCOUNTING SUMMARY OF OPERATING LOSS (METAL)
FOR BLOCK MISCLASSIFICATION DUE TO VARIOUS LEVELS OF
ERROR, HUCKLEBERRY PORPHYRY DEPOSIT, EAST ZONE, W
DOMAIN, COPPER GRADE DISTRIBUTION***

	10% error		15% error		20% error
Net cost of mining waste classed as ore (tonnes of metal):	-23.95		-50.77		-85.16
Net loss of metal in ore classed as waste (tonnes of metal):	-29.01		-66.91		-119.91
TOTAL OPERATING LOSS (TONNES OF METAL):	-52.96		-117.69		-205.07

* For a hypothetical scenario with 627 blocks (8600 tonnes each)

12 blocks of waste, averaging 0.378% Cu are incorrectly classed as ore. In the case of 15% error 19 blocks of waste, averaging 0.368% Cu are incorrectly classed as ore. Finally in the case of 20% error 25 blocks of waste, averaging 0.360% Cu are incorrectly classed as ore.

Table 4-5 shows the average total number of ore blocks mistakenly included in waste (per 627 blocks) and their average grade for each of the three error scenarios. In the case of the 10% error an average of 12 blocks of low grade ore are classed as waste, averaging 0.427% Cu. In the case of the 15% error scenario an average of 18 blocks of low grade ore are classed as waste, averaging 0.442% Cu. Finally in the case of the 20% error scenario an average of 24 blocks of low grade ore are classed as waste. These blocks average 0.458% Cu, substantially above cutoff grade, and the loss of profit is evident.

Table 4-6 reveals the metal accounting summary. In the case of 10% error, the annual operating loss equals 53 tonnes of copper or roughly US \$90,000 (at metal prices of approximately US \$0.80 per lb.), when the error is 15% the annual operating loss is increased to 118 tonnes of metal and finally for 20% error the annual operating loss is 205 tonnes of copper or US \$360,000. Thus, when error doubles, the operating loss quadruples.

These results are of considerable significance. In addition, the effect of dilution and ore loss on grade of production was also calculated. For 627 blocks equations A6-6, A6-7, A6-9 and A6-10 (cf. Appendix 6) were used to demonstrate that 25.0% of true grades (157 blocks out of 627) are above cutoff grade, that 48% of the contained metal is in the material above cutoff grade, and that the average grade of material above cutoff grade is

0.618% Cu. For 20% error scenario 24 of these 157 blocks are inadvertently classed as waste leaving 133 blocks with average grade (g_{133}) as follows:

$$133 \times g_{133} = 157 \times 0.618 - 24 \times 0.458$$

$$g_{133} = 0.647\% \text{ Cu}$$

Now add the dilution resulting from the 24.5 blocks of waste (cf. Table 4-4) that are incorrectly classed as ore; the resulting average grade is:

$$157.5 \times g_{157.5} = 133 \times 0.647 + 24.5 \times 0.360$$

to give $g_{157.5} = 0.602\% \text{ Cu}$.

In this case, the cutoff grade is on the higher tail of the grade distribution, so the effect of dilution slightly predominates over the effect of losing ore to the waste dump. The tonnage of material classed as ore is slightly greater than the tonnage of true ore. In this case the increase in tonnage is $(157.5 - 157) \times 8,608 \text{ tonnes} = 4,304 \text{ tonnes per } 627 \text{ blocks}$. Moreover, the mean grade of material classed as ore (0.602% Cu) is less than the mean grade of all ore blocks (0.618% Cu).

The important point to be made is that the effects of error are likely to be overlooked if they are on the scale indicated by the 20% error case discussed above because there is a small decrease in grade and almost negligible increase in tonnes, although the actual metal loss is significant (205 tonnes of copper).

4.4: Application of GAINLOSS to the Oritz gold deposit, New Mexico

The last example is illustrated by Oritz gold deposit in New Mexico (Springett, 1983). The parameters of block grade distribution, assumed to be lognormal, are:

mean = 0.051 oz/st or 1.75 g/t and,

standard deviation = 0.036 oz/st or 1.23 g/t

The cutoff grade is assumed to be 0.025 oz/st or 0.85 g/t. Tables 4-7, 4-8, and 4-9 illustrate the situation for assumed errors equal respectively 10%, 20% and 30% for 100,000 blocks (30 shortton or 27.2 metric tonnes per block), which roughly represent semi-annual production.

Table 4-7 includes the average total number of diluting blocks (per 100,000 blocks) and their true average grade for each of the three error scenarios. In the case of 10% error 1451 blocks of waste, averaging 0.79 g/t Au are incorrectly classed as ore. In the case of 20% error 2709 blocks of waste, averaging 0.77 g/t Au are incorrectly classed as ore. Finally in the case of 30% error 3672 blocks of waste, averaging 0.75 g/t Au are incorrectly classed as ore

Table 4-8 shows the average total number of ore blocks mistakenly included in waste (per 100,000 blocks) and their average grade for each of the three error scenarios. In the case of the 10% error an average of 1957 blocks of low grade ore are classed as waste, averaging 0.92 g/t Au. In the case of the 20% error scenario an average of 4744 blocks of low grade ore are classed as waste, averaging 1.02 g/t Au. Finally in the case of the 30% error scenario an average of 8176 blocks of low grade ore are classed as waste. These blocks average 1.17 g/t Au, substantially above cutoff grade, and the loss of profit is evident.

TABLE 4-7

**NUMBER OF WASTE BLOCKS MISTAKENLY INCLUDED IN ORE
DUE TO VARIOUS LEVELS OF ERROR, ORITZ GOLD DEPOSIT, NEW
MEXICO, GOLD GRADE DISTRIBUTION**

Grade intvl. centre	Freq. in 1000 blks	10% error P>c	Freq.* P>c	20% error P>c	Freq.* P>c	30% error P>c	Freq.* P>c
0.3	886.4					0.000	0.000
0.4	1996.8			0.000	0.000	0.000	0.065
0.5	3162.5	0.000	0.000	0.000	0.324	0.008	24.895
0.6	4131.3	0.000	0.016	0.016	66.228	0.080	328.617
0.7	4814.3	0.014	65.595	0.140	673.861	0.237	1139.483
0.8	5219.4	0.265	1385.163	0.377	1968.978	0.417	2178.874
Sum of misclassified waste blocks:			1450.774		2709.391		3671.934
Average true grade of misclassified waste blocks:			0.795		0.770		0.749

TABLE 4-8

**NUMBER OF ORE BLOCKS MISTAKENLY INCLUDED IN WASTE DUE TO
VARIOUS LEVELS OF ERROR, ORITZ GOLD DEPOSIT, NEW MEXICO,
GOLD GRADE DISTRIBUTION**

Grade intvl. centre	Freq. in 1000 blks	10% error P<c	Freq.* P<c	20% error P<c	Freq.* P<c	30% error P<c	Freq.* P<c
0.9	5393.6	0.289	1557.788	0.391	2106.382	0.427	2300.512
1.0	5392.2	0.064	343.742	0.226	1216.937	0.308	1661.934
1.1	5265.2	0.009	49.587	0.126	661.691	0.223	1176.183
1.2	5053.5	0.001	5.624	0.069	350.555	0.164	827.727
1.3	4788.7	0.000	0.583	0.039	184.949	0.122	584.210
1.4	4494.2	0.000	0.061	0.022	98.500	0.092	415.529
1.5	4186.7	0.000	0.007	0.013	53.390	0.071	298.602
1.6	3878.1	0.000	0.001	0.008	29.589	0.056	217.056
1.7	3576.4			0.005	16.805	0.045	159.669
1.8	3286.8			0.003	9.787	0.036	118.851
1.9	3012.5			0.002	5.845	0.030	89.490
2.0	2755.4			0.001	3.576	0.025	68.126
2.1	2516.1			0.001	2.239	0.021	52.404
2.2	2294.6			0.001	1.433	0.018	40.707
2.3	2090.7			0.000	0.936	0.015	31.912
2.4	1903.6			0.000	0.623	0.013	25.233
2.5	1732.3			0.000	0.423	0.012	20.113
2.6	1575.9			0.000	0.291	0.010	16.152
2.7	1433.4			0.000	0.204	0.009	13.063
2.8	1303.6			0.000	0.145	0.008	10.633
2.9	1185.5			0.000	0.104	0.007	8.709
3.0	1078.3					0.007	7.174
3.1	980.8					0.006	5.941
3.2	892.4					0.006	4.945
3.3	812.1					0.005	4.135
3.4	739.3					0.005	3.474
3.5	673.2					0.004	2.930
3.6	613.2					0.004	2.482
3.7	558.8					0.004	2.109
3.8	509.4					0.004	1.799
3.9	464.5					0.003	1.540
4.0	423.8					0.003	1.322
4.1	386.8					0.003	1.139
Sum of misclassified ore blocks:			1957.393		4744.402		8175.791
Average true grade of misclassified ore blocks:			0.924		1.021		1.174

TABLE 4-9

**METAL ACCOUNTING SUMMARY OF OPERATING LOSS (METAL)
FOR BLOCK MISCLASSIFICATION DUE TO VARIOUS LEVELS OF
ERROR, ORITZ GOLD DEPOSIT, NEW MEXICO, GOLD GRADE
DISTRIBUTION***

	10% error		20% error		30% error
Net cost of mining waste classed as ore (grams of metal):	-2152		-5881		-10085
<i>(troy ounces of metal):</i>	<i>-69.2</i>		<i>-189.0</i>		<i>-324.2</i>
Net loss of metal in ore classed as waste (grams of metal):	-3920		-22120		-71951
<i>(troy ounces of metal):</i>	<i>-126.0</i>		<i>-711.1</i>		<i>-2313.1</i>
TOTAL OPERATING LOSS (GRAMS OF METAL):	-6072		-28001		-82035
<i>(TROY OUNCES OF METAL):</i>	<i>-195.2</i>		<i>-900.2</i>		<i>-2627.3</i>

* For a hypothetical scenario with 100,000 blocks (27 tonnes each)

Table 4-9 reveals the metal accounting summary. In the case of 10% error, the operating loss equals 195 troy ounces (6,072 grams) of gold or roughly US \$58, 500 (at metal prices of approximately US \$300 per oz.), when the error is 20% the operating loss is increased to 900 troy ounces (28,000 gram) of metal or roughly US \$270,000 and finally for 30% error the operating loss is 2,637 troy ounces (82,035 grams) of gold or US \$791,000. Thus, when error doubles, the operating loss increases form threefold to more than quadruples.

These results are of considerable significance. In addition, the effect of dilution and ore loss on grade of production was also calculated. For 100,000 blocks equations A6-6, A6-7, A6-9 and A6-10 (cf. Appendix 6) were used to demonstrate that 79.569% of true grades (79,569 blocks out of 100,000) are above cutoff grade, that 93% of the contained metal is in the material above cutoff grade, and that the average grade of material above cutoff grade is 2.05 g/t Au. For 10% error scenario 1957 of these 79,569 blocks are inadvertently classed as waste leaving 77,612 blocks with average grade ($g_{77,612}$) as follows:

$$77,612 \times g_{77,612} = 79,569 \times 2.05 - 1,957 \times 0.92$$

$$g_{77,612} = 2.08 \text{ g/t Au}$$

Now add the dilution resulting from the 1,451 blocks of waste (cf. Table 4-7) that are incorrectly classed as ore: the resulting average grade is:

$$79,063 \times g_{79,063} = 77,612 \times 2.08 + 1,451 \times 0.79$$

to give $g_{79,063} = 2.06 \text{ g/t Au.}$

Although dilution has occurred, the average grade of mined ore is almost identical to the overall average grade above cutoff grade (2.06 g/t Au vs. 2.05 g/t Au). The loss of

tonnes is also small and equals $(79,569 - 79,063) \cdot 27.2 = 13,760$ tonnes of a total of 2,160,000 tonnes.

The important point to be made is that the effects of error are likely to be overlooked if they are on the scale indicated by the 10% error case discussed above.

In the case of 30% error 8,176 of the 79,569 blocks are inadvertently classed as waste leaving 71,393 blocks with average grade ($g_{71,393}$) as follows:

$$71,393 \times g_{71,393} = 79,569 \times 2.05 - 8,176 \times 1.17$$

$$g_{71,393} = 2.15 \text{ g/t Au}$$

Now add the dilution resulting from the 3,672 blocks of waste (cf. Table 4-7) that are incorrectly classed as ore: the resulting average grade is:

$$75,065 \times g_{75,065} = 71,393 \times 2.15 + 3,672 \times 0.75$$

to give $g_{75,065} = 2.08 \text{ g/t Au}.$

Although dilution has occurred, the average grade of mined ore is slightly higher than the overall average grade above cutoff grade (2.08 g/t Au vs. 2.05 g/t Au). The loss of tonnes however, equals $(79,569 - 75,065) \cdot 27.2 = 122,500$ tonnes of a total of 2,160,000 tonnes.

4.5: Conclusions

These examples show the impact of various levels of sampling, analytical and block estimation errors on grade and tonnes of ore. The results are deposit-specific because they depend on the particular data distribution and the cutoff grade. However, results are fairly

robust and small changes in the distribution of real metal grades would not have a large impact on the results. The procedure is worth repeating for any particular situation to estimate whether or not the effort of improving low quality estimates is affordable. The GAINLOSS program provides a basis for determining the worth of improving block estimation errors.

Acknowledgements

Special thanks are extended to Dr. A.J. Sinclair for supervising the research work on this paper, assisting with problems and providing constructive criticism throughout the study. The author is also very grateful to Dr. Richard Poulin for insight into aspects of mineral economics.

References

David, M., 1977, Geostatistical ore reserve estimation; Elsevier Sc. Pub. Co., Amsterdam, 364 p.

David, M., and Toh E., 1989, Grade control problems, dilution and geostatistics: choosing the required quality and number of samples for grade control; CIM Bull., v. 82, no. 931, p. 53-60

Giroux, G.H., and Sinclair, A.J., 1986, Geostatistics at Equity Silver Mines Ltd.: Global reserves of the South Tail zone by volume-variance relations; in David, M., et al, (eds.) Proc. Symp. on "Ore reserve estimation: methods, models and reality", Montreal, Que., May 10-11, 1986, Can. Inst. Min. Metall., p. 218-237

Jackson, A., and K. Illerbrun, 1995, Huckleberry porphyry copper deposit, Tahtsa Lake ditrict, west-central British Columbia; in Porphyry deposits of the Northwestern Cordillera of North America, Spec. Vol. 46, Can. Inst. Min. Metall., p. 313-321.

Journel, A.G., and Huijbregts, C., 1978, Mining geostatistics; Academic Press, New York, 599 p.

Parker, H., 1979, The volume-variance relationship: a useful tool for mine planning; Engineering and Mining Journal, v.180, no. 10, p. 106 -123

Reddy, R.N., and Ziegler, C.A., 1989, FORTRAN77 with applications for scientists and engineers; West Publishing Company, New York, 565 p.

Sinclair, A.J., 1995, Selected topics in mineral inventory estimation; short course notes for a lecture series sponsored by the British Columbia and Yukon Chamber of Mines, Vancouver, B.C.

Springett, M., 1989, Biasing unbiased data: mine versus mill; 21st APCOM Application of Computers and Operations Research in the Mineral Industry (ed. A. Weiss), p. 286-296.

Springett, M., 1983, Sampling and ore reserve estimation for the Ortiz gold deposit, New Mexico; Nevada Bur. Mines and Geol., Rpt. 36, p. 152-164

CHAPTER 5

CONCLUSIONS

Mineral inventory estimation in porphyry-type deposits can be highly enhanced by adding geological information at early stages of resource/reserve estimation. The importance of geological control before application of any estimation procedure cannot be overstated. Detailed geology provides information for a geometric model of a deposit. Substantial effort is required to characterize the geometric margins of a deposit and the relation of these margins to the simplistic geometric form that normally emerges as an interpretation. Models of variations in zoning patterns of mineralization, alteration, and sulphide occurrence in porphyry-type deposits are very important, because they contribute substantially to confidence in developing a 3-dimensional geometric model of a deposit for mine planning. Several widely accepted models were discussed to illustrate the range of geological features that require special attention in establishing mineral inventory in porphyry-type deposits. Examples from the literature illustrate that the recognition of the different styles of mineralization allows the separation of the deposit into different mineralization domains having different geological and value continuities. It is important to distinguish geological continuity and value continuity. A wide range of classical geological methods are useful in examining geological continuity; value continuity is best viewed as a statistical characteristic that is quantified by any of several measures of

autocorrelation (e.g. semivariogram model). Continuity is dependent on mineralization style and may be controlled structurally and/or lithologically.

Mineralogical studies also relate to many aspects of deposit evaluation including abundances of ore and deleterious minerals, spatial distribution of ore, grain size characteristics of important minerals and liberation properties of ores.

Three separate mineralized zones (Main and East zones of Huckleberry deposit and the Virginia zone of the Copper Mountain porphyry system) illustrate the impact of close geological control on semivariogram modeling and consequently the economic impact on geostatistical resource/reserve estimation. Analyses were done using a variety of procedures. First the general (less accurate) semivariogram model was developed for an entire mineralized zone without taking geology into consideration in each of the mineralized zones. Then geological information and contour maps were examined in order to separate the entire mineralized zone into different domains. Consequently, semivariogram models were developed independently for each domain. Then cross-validation was applied followed by ordinary kriging, which was used to estimate a 3-dimensional block array. Finally the two estimation approaches were compared using metal accounting.

In the Main zone of the Huckleberry deposit the copper mineralization is centered in volcanic rocks on the eastern margin of a granodiorite stock. Copper grade contour maps show significant variations in trend directions, that coincide (as geological information reveals) with the dominant direction of stockwork development. It is shown that these directions of dominant mineralization control effectively separate the Main zone

into three domains. The three semivariogram models, that were developed independently for each domain differ significantly one from each other. Metal accounting calculations show that the application of a general (less accurate) semivariogram model produces an annual loss of 300 tonnes of metal in operating profit. The identical procedure applied to the East zone of Huckleberry deposit reveals that the application of the general semivariogram model produces an annual loss of 700 tonnes of metal in operating profit.

In the case of Virginia zone the principal control on mineralization is a set of easterly striking, vertically dipping veins. Contour maps of Cu and Au grades for all levels showed remarkable similarity and reflected the direction of strongest geological continuity (east striking vertical plane). The widely spaced exploration data are barely adequate to demonstrate the existing anisotropy. The geology thus provided insight into principal directions controlling the semivariogram model for the deposit.

Based on the work done in this study it is evident that geology exerts a significant control on continuity, and clearly, geology is the basis for defining domains and preferred directions of continuity for mineral inventory estimation in porphyry-type deposits.

A novel approach to errors of block grade estimates was developed during the course of this work. It was shown that where block (smu) grade distribution can be approximated by normal or lognormal distribution, the effect of average errors of block grades can be evaluated quantitatively. The author has developed a computer program called GAINLOSS for this purpose. For a given estimation error and cutoff grade, the GAINLOSS program calculates both the quantity of metal that is lost as a result of misclassifying ore blocks as waste and the dilution that results from misclassifying waste

blocks as ore. Calculations were made using realistic block grade distribution parameters for both porphyry-type deposits and a gold deposit. In addition, the effect of dilution and ore loss on grade of production was calculated. As a result the following fundamental relations were revealed:

1. Where the cutoff grade is on the lower tail of the grade distribution, metal arising from dilution can be much less than metal lost through misclassifying ore as waste. Hence, the average grade of milled material could possibly be higher than expected (estimated) and tonnes milled will be smaller than estimated.
2. Where the cutoff grade is on the higher tail of the grade distribution, tonnes arising from dilution will be greater than tonnes lost by misclassifying ore as waste. Hence, a possibility exists that the average grade of milled material will be less than estimated and tonnes milled will be larger than expected.

The GAINLOSS software permits rapid comparison of the tonnes and average grade for all waste blocks misclassified as ore, and for all ore blocks misclassified as waste. It compares losses and gains in terms of metal above cutoff grade (metal operating profit). Such comparisons were done for variety of levels of block estimation errors. Consequently, these comparisons can be incorporated in a financial analysis to evaluate whether or not it is worthwhile to improve usually high average block estimation errors to some lower values. Clearly, quality of block estimates has an impact on both metal recovery and operating profit.

REFERENCES

- Beane, R.E. and Titley, S.R., 1981, Porphyry copper deposits, Part II. Hydrothermal alteration and mineralization; *Economic Geology*, 75th Anniversary Volume, p. 235-269
- Bentzen A., and Sinclair A. J., 1994, P-RES a computer program to aid in the investigation of polymetallic ore reserves; Tech. Rept. MT-9, Mineral Deposit Research Unit, Dept. of Geological Sciences, Univ. of B.C., Vancouver, Canada, includes diskette
- Bysouth, G.D. and Wong, G.Y., 1995, The Endako molybdenum mine, central British Columbia: An update; in Schroeter, T.G., ed., *Porphyry Deposits of the Northwestern Cordillera of North America*; Canadian Institute of Mining Metallurgy, Special Volume 46, p. 697-703
- Carr, J.M. and Reed, A.J., 1976 Afton: A supergene copper deposit; in Sutherland Brown, A., ed., *Porphyry Deposits of the Canadian Cordillera*; Canadian Institute of Mining and Metallurgy, Special Volume 15, p. 376-387
- Cuddy, A.S. and Kesler, S.E., 1982, Gold in the Gransile and Bell Copper porphyry copper deposits, British Columbia; in Levison, A.A., ed., *Precious Metals in the Northern Cordillera*; The Association of Exploration Geochemists p. 139-155
- Craig, J.R. and Vaughan, D.J., 1981, *Ore microscopy and ore petrography*; John Wiley and Sons, New York, 406 p.
- David M., 1988, *Handbook of applied advanced geostatistical ore reserve estimation*; Developments in geomathematics 6, Elsevier, Amsterdam, 216p.
- David, M., 1977, *Geostatistical ore reserve estimation*; Elsevier Sc. Pub. Co., Amsterdam, 364 p.
- David, M., and Toh E., 1989, Grade control problems, dilution and geostatistics: choosing the required quality and number of samples for grade control; *CIM Bull.*, v. 82, no. 931, p. 53-60
- Deutsch, C. V., Journel, A. G., 1992, *GSLIB Geostatistical Software Library and User's Guide*; Oxford University Press, New York, 340 p. plus diskette
- Drummond, A.D. and Godwin, C.I., 1976, Hypogene mineralization - an empirical evaluation of alteration zoning; in Sutherland Brown, A., ed., *Porphyry Deposits of the Canadian Cordillera*; Canadian Institute of Mining and Metallurgy, Special Volume 15, p. 52-63

Drummond, A.D., Sutherland Brown, A., Young, R.J. and Tennant, S.J., 1976, Gibraltar - regional metamorphism, mineralization, hydrothermal alteration and structural development; in Sutherland Brown, A., ed., *Porphyry Deposits of the Canadian Cordillera*; Canadian Institute of Mining and Metallurgy, Special Volume 15, p. 195-205

Fairweather, M. J., 1997, Values and impurities in base metal concentrates; *CIM Bull.*, v. 90, no. 1014, p.91-94

Giroux, G.H., and Sinclair, A.J., 1986, Geostatistics at Equity Silver Mines Ltd.: Global reserves of the South Tail zone by volume-variance relations; in David, M., et al, (eds.) *Proc. Symp. on "Ore reserve estimation: methods, models and reality"*, Montreal, Que., May 10-11, 1986, *Can. Inst. Min. Metall.*, p. 218-237

Guilbert, J.M. and Lowell, J.D., 1974, Variations in zoning patterns in porphyry ore deposits; *Canadian Institute of Mining and Metallurgy, Bulletin*, v.67, no. 742, p. 99-109

Gustafson, L.B., 1978 Some major factors of porphyry copper genesis; *Economic Geology*, v.73, p.600-607

Heberlein, D.R. and Godwin, C.I., 1984, Hypogene alteration at the Berg porphyry copper-molybdenum property, North-Central British Columbia; *Economic Geology*, v. 79, p. 902-918

Hollister, V.F., 1991, Chapter 1: Porphyry copper and related skarn deposits; in Hollister, V.F., ed., *Porphyry copper, molybdenum and gold deposits, volcanogenic deposits (massive sulphides), and deposits in layered rocks*, AIME, Case histories of mineral discoveries, Volume 3; Society for Mining, Metallurgy and Exploration Inc., p. 1-43

Hollister, V.F., 1978, *Geology of the porphyry copper deposits of the western hemisphere*; Society of Mining Engineers of AIME, New York, 219 p.

Isaaks, E.H. and Srivastava, R.M., 1989, *An introduction to applied geostatistics*; Oxford University Press, New York, 561 p.

Jackson, A., and Illerbrun K., 1995, Huckleberry porphyry copper deposit, Tahtsa Lake district, west-central British Columbia; in *Porphyry deposits of the Northwestern Cordillera of North America*, Spec. Vol. 46, *Can. Inst. Min. Metall.*, p.313-321

James, A.H., 1971, Hypothetical diagrams of several porphyry copper deposits; *Economic Geology*, v. 66, p. 43-47

Journel A.G. and Huijbregts, 1978, *Mining geostatistics*; Academic Press, New York, 599 p.

Kimura, E.T., Bysouth, G.D. and Drummond, A.D., 1976, Endako; in Sutherland Brown, A., ed., *Porphyry Deposits of the Canadian Cordillera*; Canadian Institute of Mining and Metallurgy, Special Volume 15, p. 444-454

King, H.F., McMahon, D.W., Bujtor, G.J. and Scott, A.K., 1985, *Geology in the understanding of ore reserve estimation: an australian viewpoint*; Society of Mining Engineers of AIME, preprint no. 85-355, 13 p.

Kingston, G. A., 1992, Mineralogy in the evaluation of ore deposits; in Annels, A. E. (ed.), *Case Histories and Methods in Mineral Resource Evaluation*: Geol. Soc. Spec. Pub. No. 63, p. 47-59.

Kirkham, R.V. and Sinclair, W.D., 1995, Chapter 19: Porphyry copper, gold, molybdenum, tungsten, tin, silver; in Eckstrand, O.R., Sinclair, W.D and Thrope, R.I., eds., *Geology of Canadian mineral type deposits*, Geology of Canada, no. 8; Geological Survey of Canada, p.420-446

Krige, D.G. and Dunn, P.G., 1995, Some practical aspects of ore reserve estimation at Chuquibambilla Copper Mine, Chile; Proc. APCOM XXV Conference, 9-14 July, 1995, Brisbane, Australia, p. 125-133

Lowell, J.D., 1989, Gold mineralization in porphyry copper deposits discussed; *Mining Engineering*, v. 41, no. 4, p.227-231

Lowell, J.D. and Guilbert, J.M., 1970, Lateral and vertical alteration-mineralization zoning in porphyry ore deposits; *Economic Geology*, v. 65, p. 373-408

Matheron, G., 1971, The theory of regionalized variables and its applications; Centre de Morphologie Mathematique de Fontainebleau, France, Cahiers No. 5, 211 p.

McMillan, W.J., 1991, Porphyry deposits in the Canadian Cordillera; in *Ore deposits, tectonics and metallogeny in the Canadian Cordillera*; British Columbia Ministry of Energy, Mines and Petroleum resources, paper 1991-4, 253-276

Mueller, W., 1981, The role of the process mineralogist in the operation of Magma Copper Company's mine and plant, San Manuel, Arizona; in Hausen, D. M., and W. C. Park (eds.), *Process mineralogy*, The Metallurgical Soc. Of A.I.M.E., Warrendale, Pa., p. 397-406.

Newell, J.M and Peatfield, G.R., 1995, The Red-Chris porphyry copper-gold deposit, northwestern British Columbia, in Schroeter, T.G., ed., *Porphyry Deposits of the Northwestern Cordillera of North America*; Canadian Institute of Mining Metallurgy, Special Volume 46, p. 674-688

Ney, C.S., Cathro, R.J., Panteleyev, A. and Rotherham, D.C., 1976, Supergene copper mineralization; in Sutherland Brown, A., ed., *Porphyry Deposits of the Canadian Cordillera*; Canadian Institute of Mining and Metallurgy, Special Volume 15, p. 72-78

Nielsen, R.L., 1984, Evolution of porphyry copper ore deposit models; *Mining Engineering*, v. 36, no. 12, p. 1637-1641

Noble, A.C. and Ranta, D.E., 1984, Zoned kriging - a successful union of geology and geostatistics; in Erickson, A.J., Jr., ed., *Applied mining geology*; Society of Mining Engineers of AIME, p. 115-128

Oriel, W.M., 1972, Detailed bedrock geology of the Brenda copper-molybdenum mine, Peachland, British Columbia; unpublished MSc thesis, UBC

Parker, H., 1979, The volume-variance relationship: a useful tool for mine planning; *Engineering and Mining Journal*, v.180, no. 10, p. 106 -123

Postolski, T.A., and Sinclair, A.J., 1998, Geology as a basis for refining semivariogram models for porphyry-type deposits; In Press (Paper presented at CIM 100th Annual General Meeting, Quality Control of Resource Estimation: An ISO Perspective Session, Montreal, Quebec, 03 – 07 May, 1998)

Postolski, T. A., and Sinclair, A. J., 1994, Mineralogy and Paragenesis of nine sulphide-bearing specimens from the Huckleberry deposit; unpublished report submitted to New Canamin resources Ltd., Vancouver, B.C.

Ranjbar, H., 1997, Litogeochemical patterns associated with the Darrehzar porphyry copper deposit, Pariz area, Iran, *Canadian Institute of Mining and Metallurgy, Bulletin*, v.90, no. 1014, p. 85-90

Ranta, D.E., Ward, A.D. and Ganster, M.W., 1984, Ore zoning applied to geologic reserve estimation of molybdenum deposits; in Erickson, A.J., Jr., ed., *Applied mining geology*; Society of Mining Engineers of AIME, p. 83-114

Raymond, G.F. and Armstrong, W.P., 1988, Sample bias and conditional probability ore reserve estimation at Valley; *Canadian Institute of Mining and Metallurgy, Bulletin*, v.81, no. 911, p.128-136

Reddy, R.N., and Ziegler, C.A., 1989, *FORTTRAN77 with applications for scientists and engineers*; West Publishing Company, New York, 565 p.

Reed, A., 1983, Structural geology and geostatistical parameters of the Afton copper-gold mine, Kamloops, B.C.; *Canadian Institute of Mining and Metallurgy, Bulletin*, v.76, no. 856 p. 45-55

Rendu, J.M., 1986, How the geologist can prevent a geostatistical study from running out of control: some suggestions; in Ranta, D.E., ed., *Applied mining geology: ore reserve estimation*; Society of Mining Engineers of AIME, p. 11-17

Rendu, J.M., 1984, Geostatistical modelling and geological controls; *Trans. Inst. Min. Metall*, Sect. B., v. 93, p. B166-B172

Rendu, J.M. and Readdy L., 1982, Geology and the semivariogram - a critical relationship; 17th APCOM Application of Computers and Operations Research in the Mineral Industry (ed. Readdy, L.), p. 771-783

Robertson, R., 1998, Imperial hopes to stave off closure of Mount Polley mine; *The Northern Miner*, June 29, p. 1.

Seraphim, R.H. and Hollister, V.F., 1976, Structural settings; in Sutherland Brown, A., ed., *Porphyry Deposits of the Canadian Cordillera*; Canadian Institute of Mining and Metallurgy, Special Volume 15, p. 30-43

Sillitoe, R.H., 1993, Gold-rich porphyry copper deposits: Geological model and exploration implications; in Kirkham, R.V., Sinclair, W.D., Thrope, R.I. and Duke, J.M., eds., *Mineral deposit modeling*; Geological Association of Canada, Special Paper 40, p. 465-478

Sides, E.J., 1994, Quantifying differences between computer models of orebody shapes; in Whateley, M.K.G., and Harvey, P.K. (eds.), *Mineral resource evaluation II: methods and case histories*; Geological Society Spec. Pub. No. 79, p. 109-121

Sillitoe, R.H., 1979, Some thoughts on gold-rich porphyry copper deposits; *Mineralium Deposita* (Berl.), v. 14, p. 161-174

Sillitoe, R.H. and Gappe, I.M., Jr., 1984, Philippine porphyry copper deposits: Geologic setting and characteristics; United Nations ESCAP, CCOP Technical Publication 14, 89 p.

Sinclair, A.J., 1998, A new look at geological controls in resource/reserve estimation; In Press (Paper presented at CIM 100th Annual General Meeting, Quality Control of Resource Estimation: An ISO Perspective Session, Montreal, Quebec, 03 - 07 May, 1998)

Sinclair, A.J., 1995, Selected topics in mineral inventory estimation; short course notes for a lecture series sponsored by the British Columbia and Yukon Chamber of Mines, Vancouver, B.C.

Sinclair, A.J. and Giroux, G.H., 1984, Geological controls of semi-variograms in precious metal deposits; in Verley, G., et al., eds., *Geostatistics for Natural Resources Characterization*, Part 2, p. 965-978, D. Reidel Pub. Co., Dordrecht, Netherlands.

Sinclair, A.J. and Vallee, M., 1994a, Improved sampling control and data gathering for improved mineral inventories and production control; in Dimitrakopoulos, R., ed., *Geostatistics for the next century*; Kulwer Academic publishers, The Netherlands, p.323-329

Sinclair, A.J. and Vallee, M., 1994b, Reviewing continuity: an essential element of quality control for deposit and reserve estimation; *Exploration and Mining Geology*, v. 3, no. 2, p. 95-108

Sketchley, D.A., Rebagliati, C.M. and DeLong, C., 1995, Geology, alteration and zoning patterns of the Mt. Milligan copper-gold deposits; in Schroeter, T.G., ed., *Porphyry Deposits of the Northwestern Cordillera of North America*; Canadian Institute of Mining Metallurgy, Special Volume 46, p. 650-665

Soregaroli, A.E. and Nelson, W.I., 1976, Boss Mountain; in Sutherland Brown, A., ed., *Porphyry Deposits of the Canadian Cordillera*; Canadian Institute of Mining and Metallurgy, Special Volume 15, p. 432-443

Springett, M., 1989, Biasing unbiased data: mine versus mill; 21st APCOM Application of Computers and Operations Research in the Mineral Industry (ed. A. Weiss), p. 286-296.

Springett, M., 1983, Sampling and ore reserve estimation for the Oritz gold deposit, New Mexico; *Nevada Bur. Mines and Geol., Rpt. 36*, p. 152-164

Srivastava, R.M., 1987, Minimum variance or maximum profitability; *Canadian Institute of Mining and Metallurgy, bulletin*, v. 80, no. 901, p.63-68

Stanley, C. R., Holbek, P. M., Huyck, H. L. O., Lang, J. R., Preto, V. A. G., Blower S. J., and Bottaro, J. C., 1995, Geology of the Copper Mountain alcalic copper-gold porphyry deposit, Princeton, British Columbia; in *Porphyry deposits of the Northwestern Cordillera of North America*, Spec. Vol. 46, Can. Inst. Min. Metall., p. 537-564

Stoiser, L.R., 1986, Exploration and geologic evaluation of the Los Bronces copper-molybdenum deposit, Chile; *Mining Engineering*, v. 38, no.3, p. 187-194

Tobar, A., Lyall, G. and Betzhold J., 1997, Quellaveco, Peru: Evaluating resources of a porphyry copper; in Baafi, E.Y. and Schofield, N.A., (eds.), *Geostatistics Wollongong'96*, Volume 2, p. 882-894, Kulwer Academic Publishers.

Van Nort, S.D., Atwood, G.W., Collinson, T.B., Flint, D.C. and Potter, D.R., 1991, Geology and mineralization of the Grasberg porphyry copper-gold deposit, Irian Jaya, Indonesia; *Mining Engineering*, v. 43, no. 3, p.300-304

Vila, T. and Sillitoe, R.H., 1991, Gold-rich porphyry systems in the Maricunga Belt, Northern Chile; *Economic Geology*, v. 86, p.1238-1260

Wallace, S.R., 1991, Model development: porphyry molybdenum deposits; in Hutchinson, R.W. and Grauch, R.I eds., *Economic Geology monograph 8 - Historical perspectives of genetic concepts and case histories*, p. 207-224

Wallace, S.R., 1974, The Henderson ore body - elements of discovery, reflections; *Am. Inst. Mining Metall. Petroleum Engineers Transactions*, v.256, p. 216-256

Wallace, S.R., Muncaster, N.K., Jonson, D.C., MacKenzie, W. B., Bookstrom, A.A. and Surface, V.E., 1968, Multiple intrusion and mineralization at Climax, Colorado, in Ridge, J.D., ed., *Ore deposits of the United States, 1933-1967 (Graton-Sales Vol.)*; New York, Am. Inst. Mining Metall. Petroleum Engineers, p.605-640

White, W.H., Bookstrom, A.A., Kamilli, R.J., Ganster, M.W., Smith, R.P., Ranta, D.E. and Steininger, R.C., 1981, Character and origin of Climax-type molybdenum deposits; *Economic Geology*, 75th Anniversary Volume, p.270-316

APPENDIX 1

HUCKLEBERRY MAIN ZONE, GENERAL SEMIVARIOGRAM MODEL

This appendix contains figures of experimental pairwise relative semivariograms and their models for the entire Main zone (general semivariogram) developed in vertical direction as well as in eight different horizontal directions. There is also included a structural ellipse of ranges in the eight horizontal directions.

Parameters of the resulting 3-dimensional model are as follows:

nugget effect: $C_0 = 0.045$

first structure: $C_1 = 0.16$, $A_m = 75$ m, $A_p = 47$ m, $A_v = 47$ m

direction of major continuity: azimuth = 22°

where:

C_1 - contribution of the first structure

A_m - range in the direction of major continuity

A_p - range in the perpendicular direction in horizontal plane

A_v - range in the vertical direction

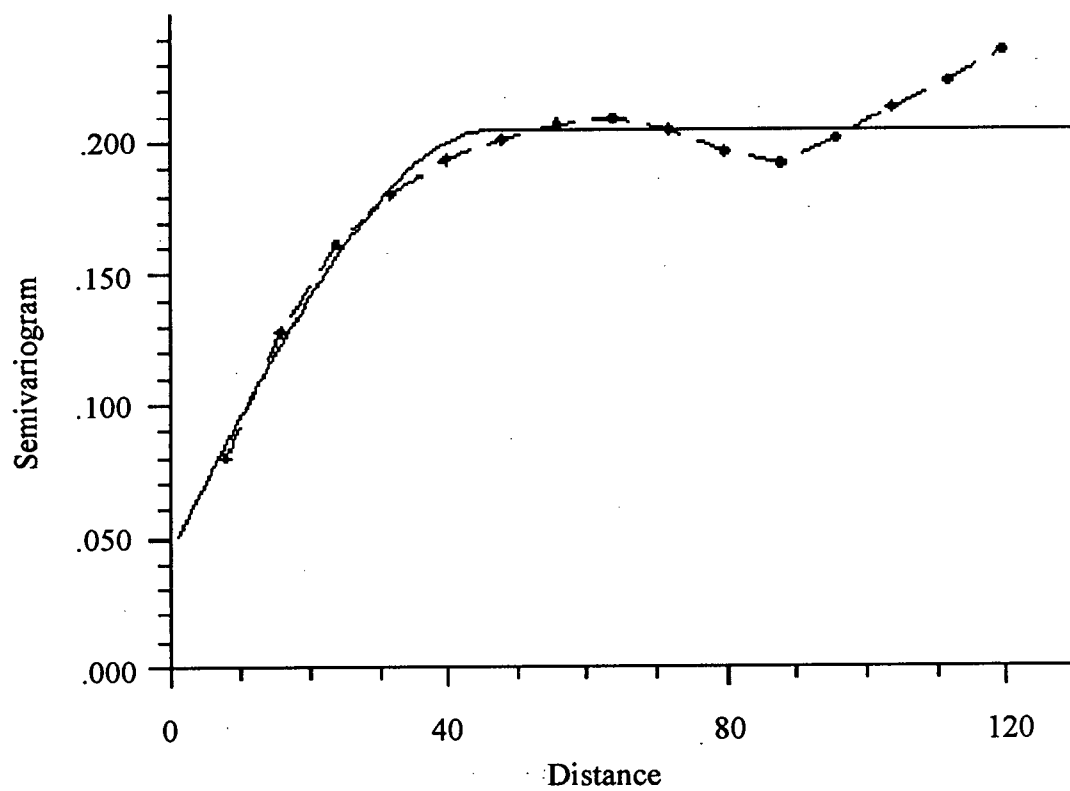


Figure A1-1: Cu semivariogram model in vertical direction;
 $C_0=0.045$, $C_1=0.16$, $A = 47$

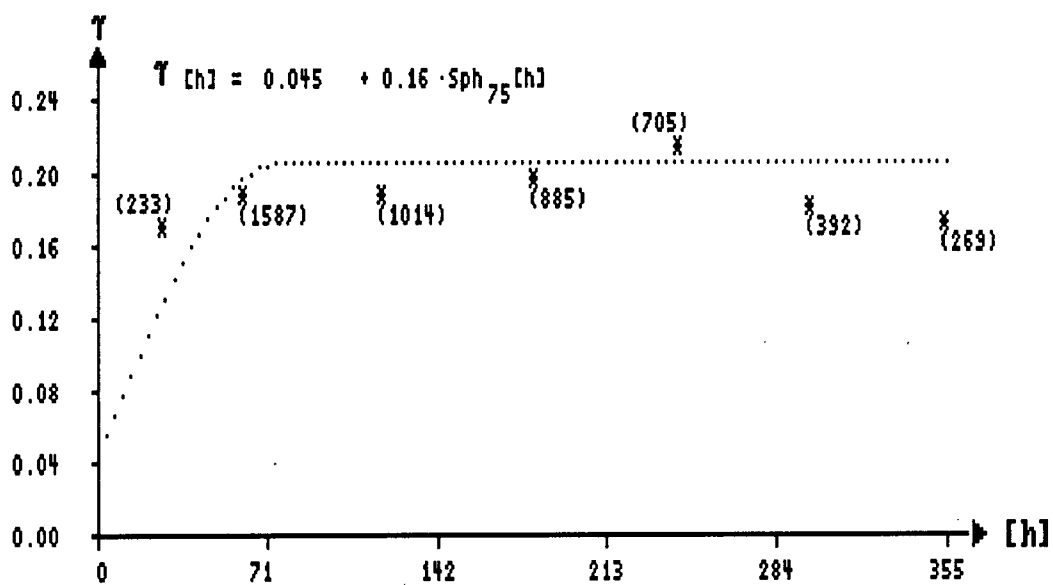
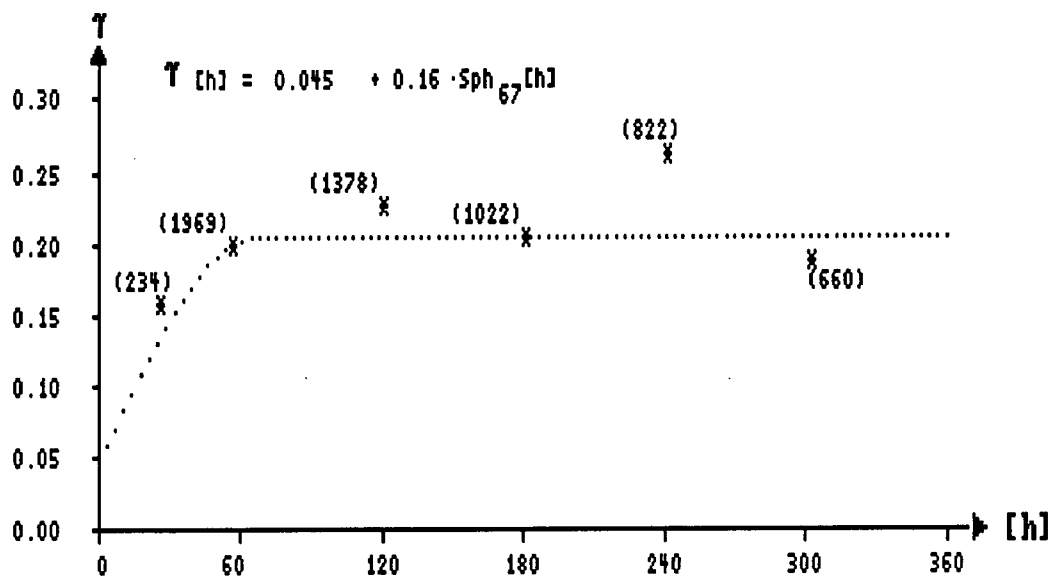


Figure A1-2: Cu semivariogram models in horizontal directions;
azimuth 0 (top) and 22 (bottom)

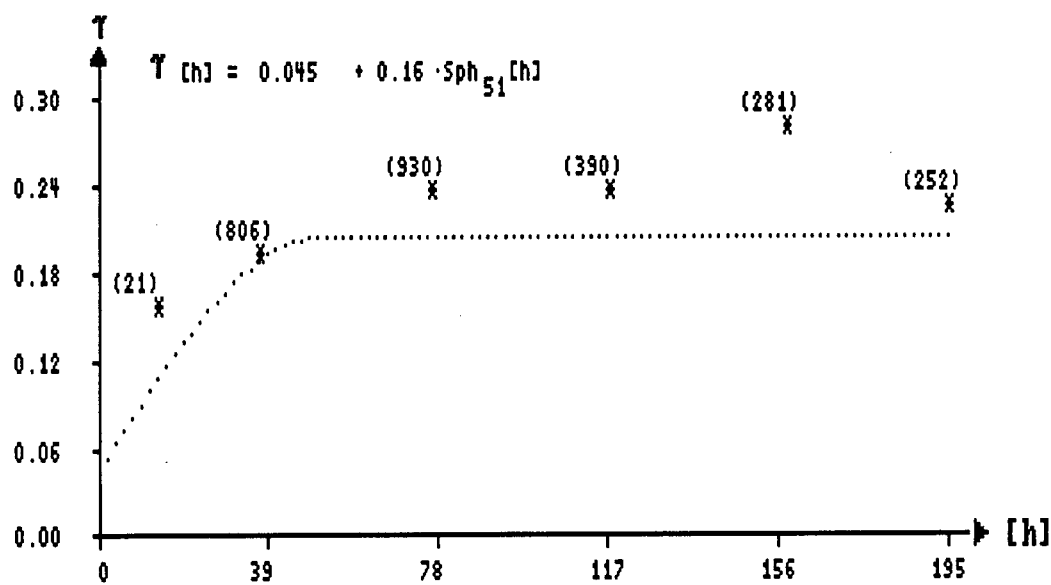
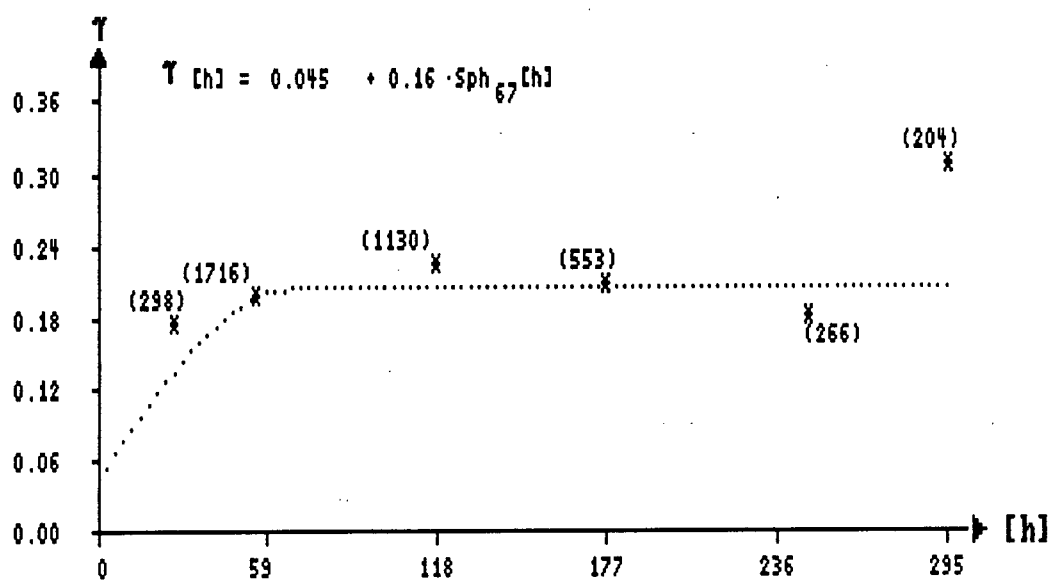


Figure A1-3: Cu semivariogram models in horizontal directions;
azimuth 45 (top) and 67 (bottom)

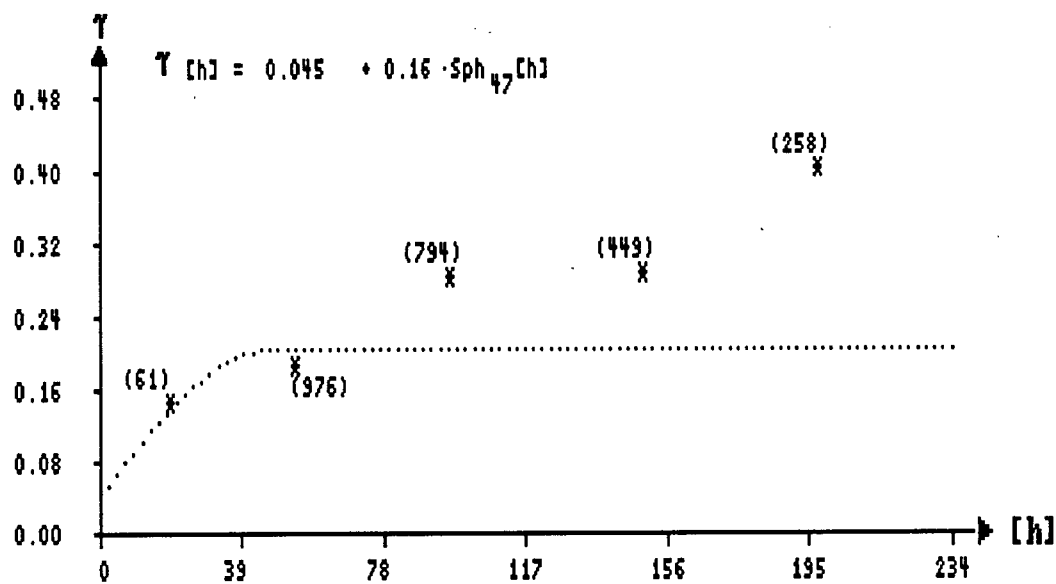
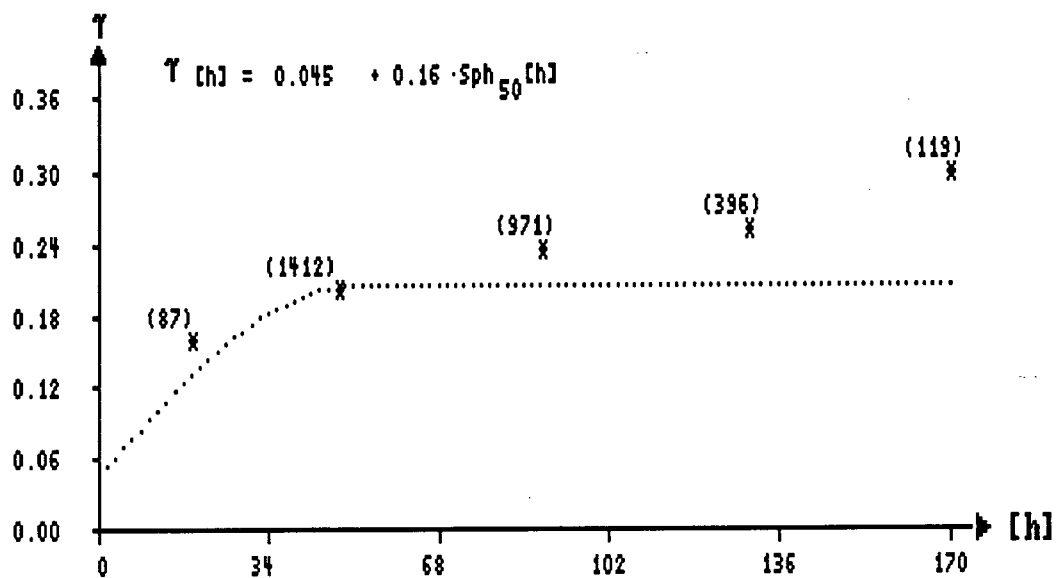


Figure A1-4: Cu semivariogram models in horizontal directions;
azimuth 90 (top) and 112 (bottom)

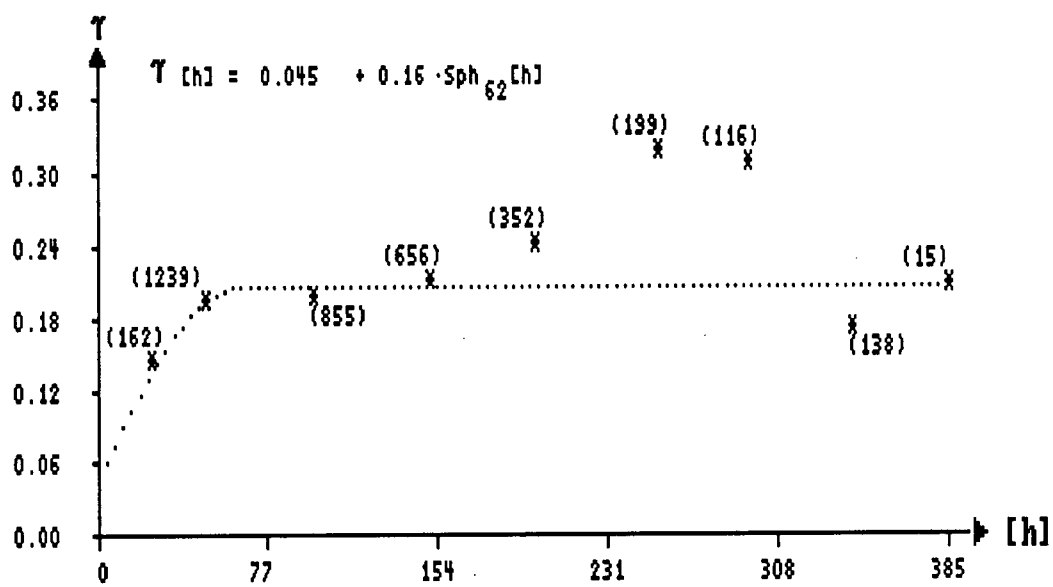
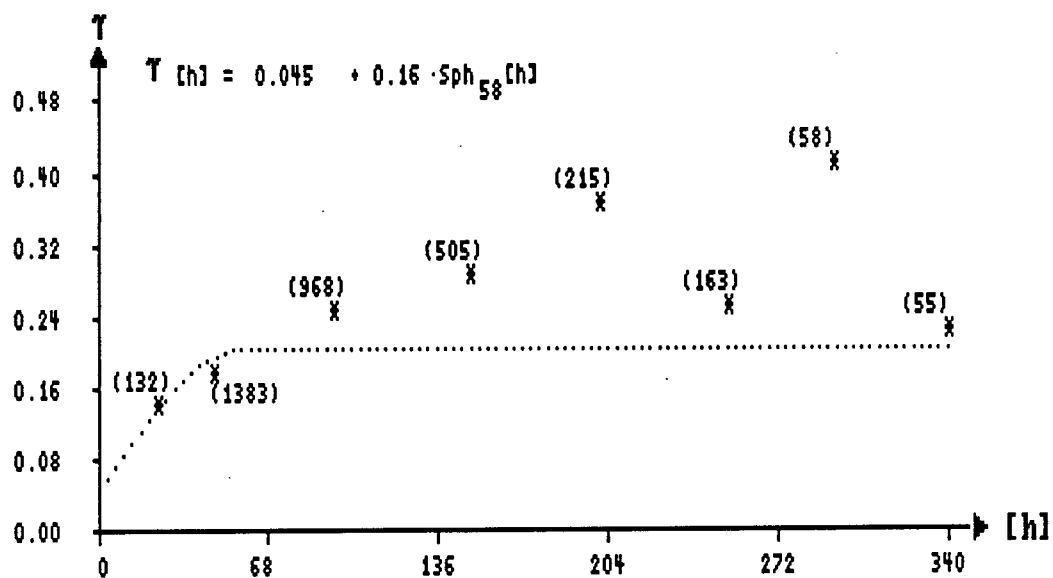


Figure A1-5: Cu semivariogram models in horizontal directions;
azimuth 135 (top) and 157 (bottom)

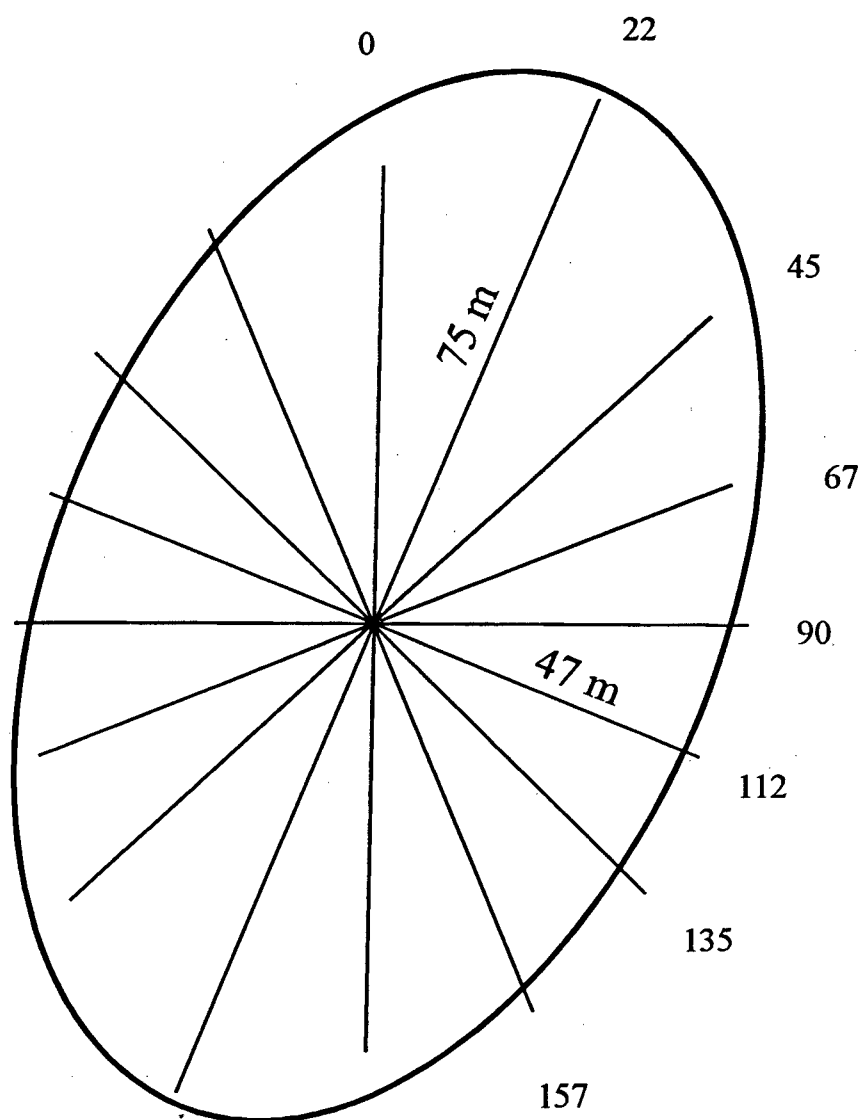


Figure A1-6: Structural ellipse of ranges in the eight directions showing directions of maximum (azimuth 22) and minimum (azimuth 112) continuity of Cu semivariogram model

APPENDIX 2

HUCKLEBERRY MAIN ZONE, DOMAIN SEMIVARIOGRAM MODELS

This appendix contains figures of experimental pairwise relative semivariograms and their models for NE domain, SE domain, and SW domain of the Main zone developed for each domain in vertical direction as well as in four different horizontal directions. There are also included structural ellipses of ranges in the four horizontal directions for each domain.

Parameters of the resulting 3-dimensional model for NE domain are as follows:

nugget effect: $C_0 = 0.03$

first structure: $C_1 = 0.175$, $A_m = 73$ m, $A_p = 51$ m, $A_v = 38$ m

direction of major continuity: azimuth = 145°

Parameters of the resulting 3-dimensional model for SE domain are as follows:

nugget effect: $C_0 = 0.06$

first structure: $C_1 = 0.15$, $A_m = 65$ m, $A_p = 65$ m, $A_v = 65$ m

direction of major continuity: model is isotropic

Parameters of the resulting 3-dimensional model for SW domain are as follows:

nugget effect: $C_0 = 0.03$

first structure: $C_1 = 0.16$, $A_m = 120$ m, $A_p = 41$ m, $A_v = 41$ m

direction of major continuity: azimuth = 80°

where:

C_1 - contribution of the first structure

A_m - range in the direction of major continuity

A_p - range in the perpendicular direction in horizontal plane

A_v - range in the vertical direction

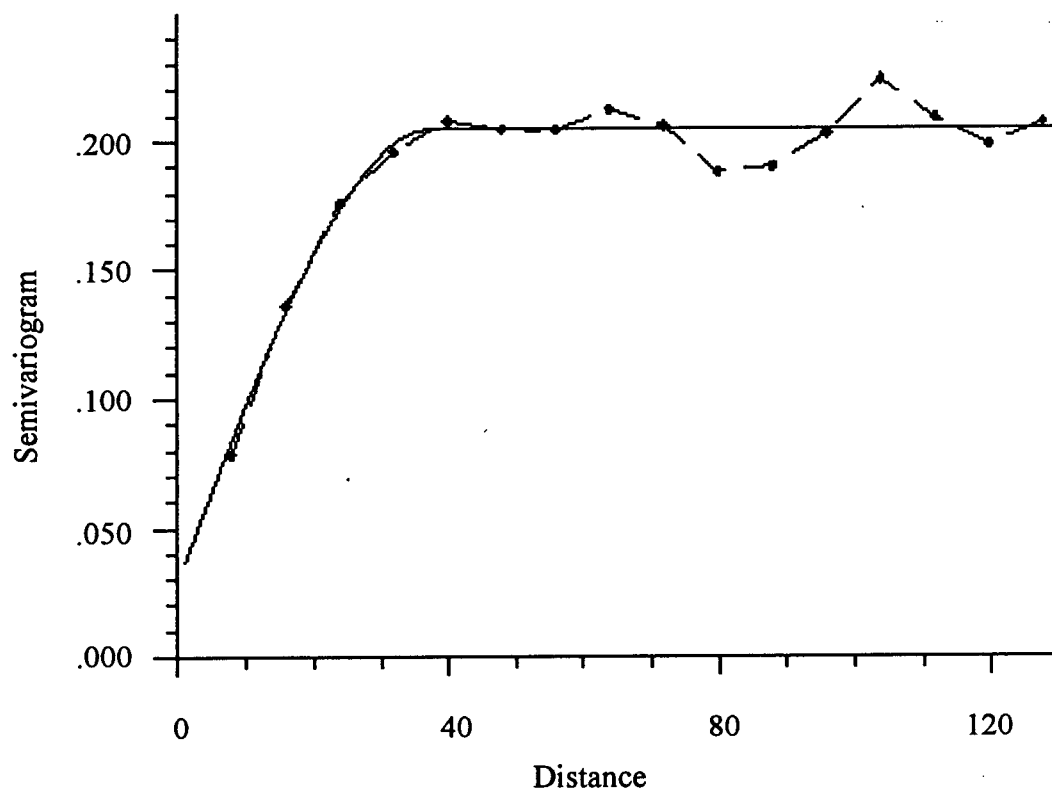


Figure A2-1: Cu semivariogram model in vertical direction, NE domain;
 $C0 = 0.03$, $C1 = 0.175$, $A = 38$

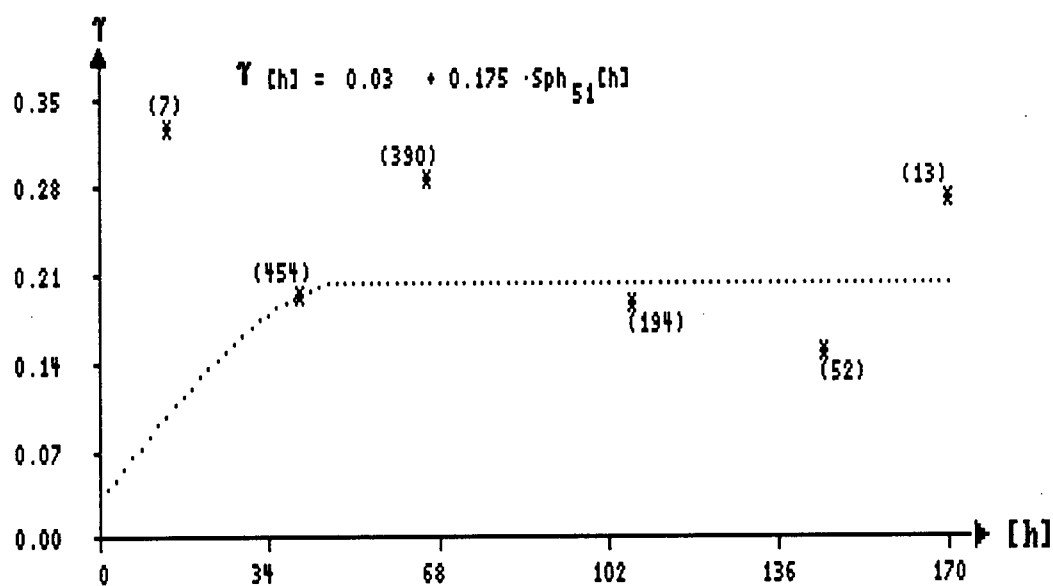
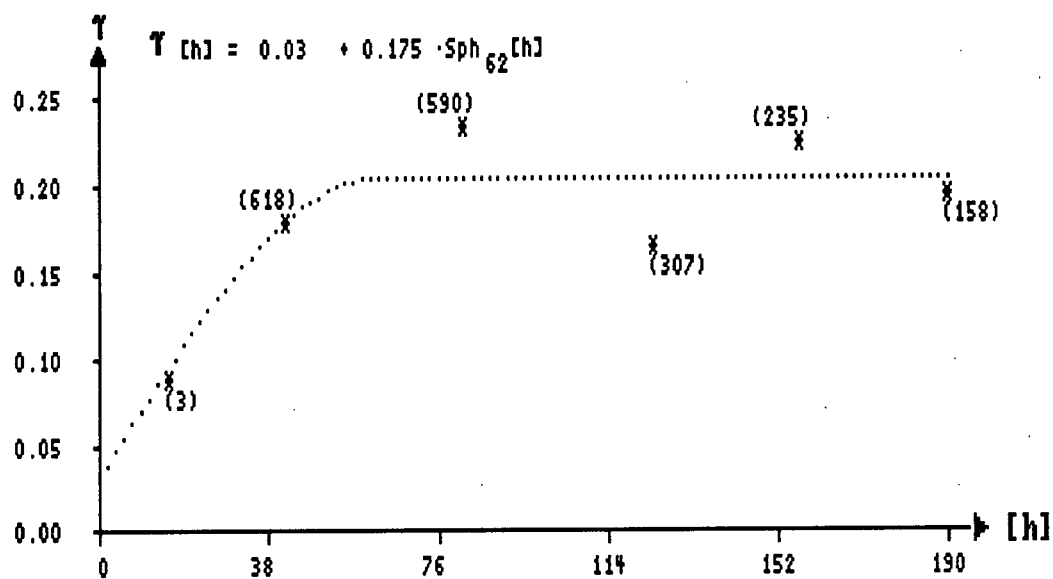


Figure A2-2: Cu semivariogram models in horizontal directions,
NE domain; azimuth 0 (top) and 55 (bottom)

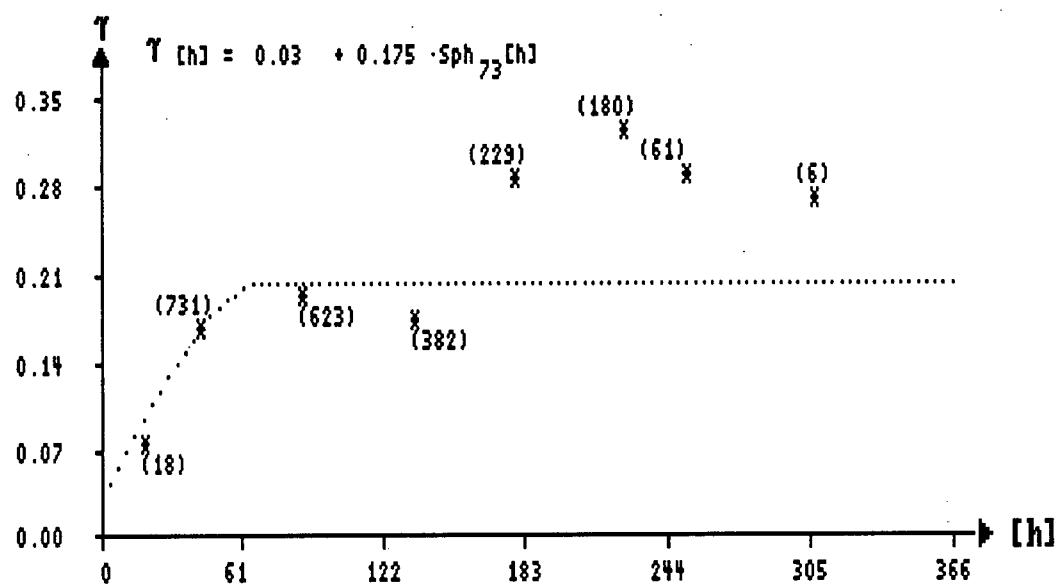
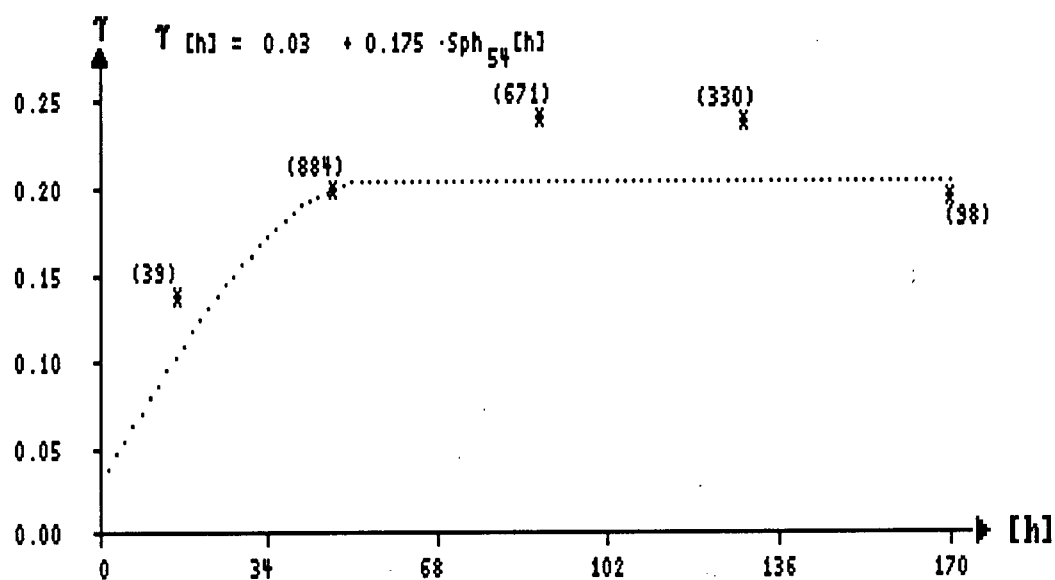


Figure A2-3: Cu semivariogram models in horizontal directions,
NE domain; azimuth 90 (top) and 145 (bottom)

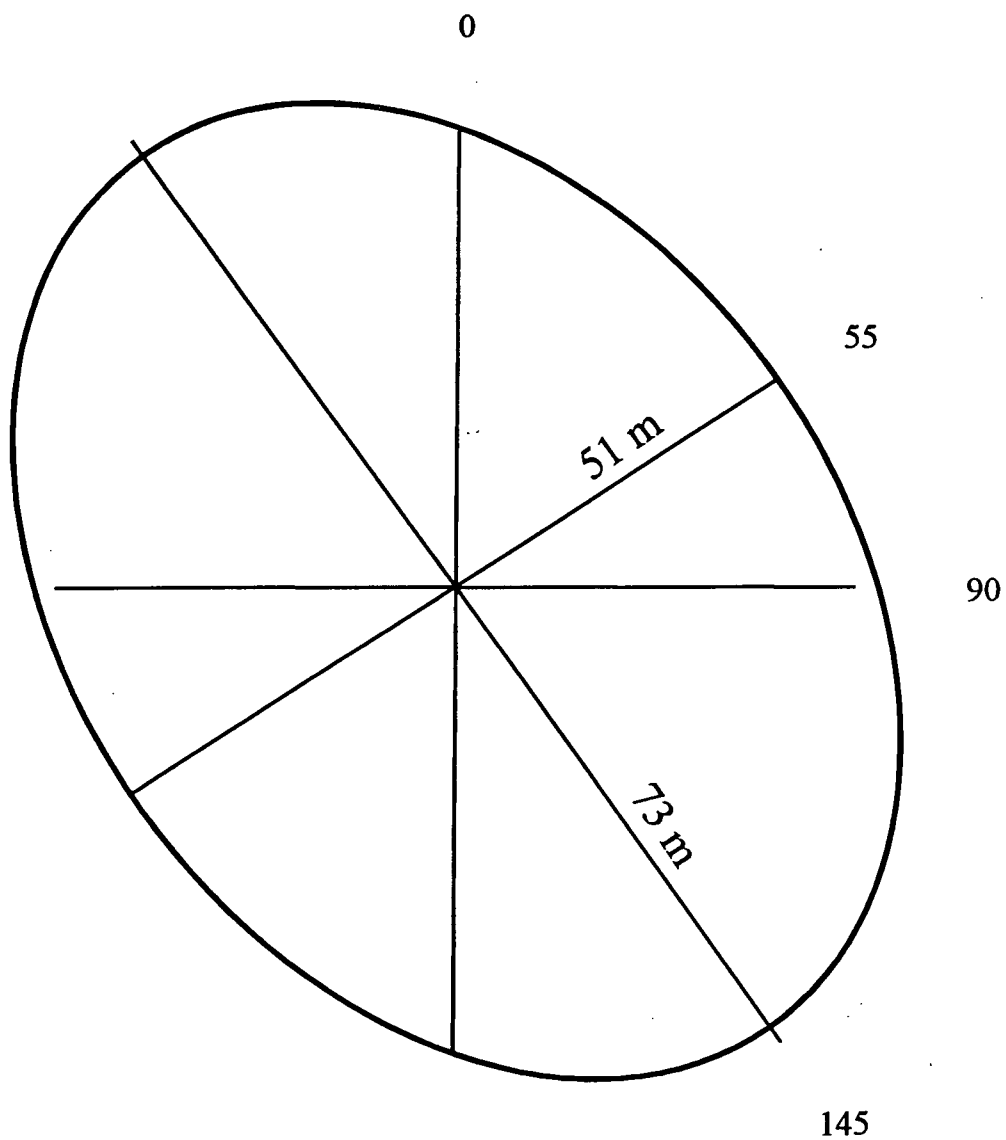


Figure A2-4: Structural ellipse of ranges in the four directions showing directions of maximum (azimuth 145) and minimum (azimuth 55) continuity of Cu semivariogram model, NE domain

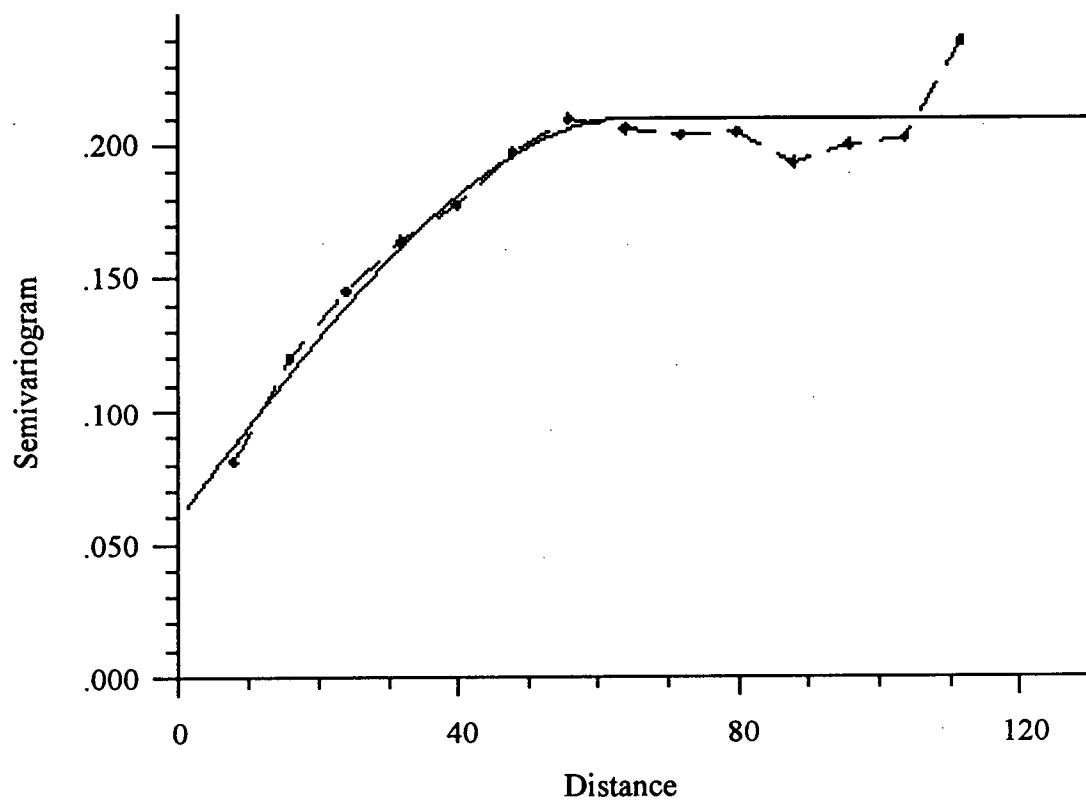


Figure A2-5: Cu semivariogram model in vertical direction, SE domain;
 $C0=0.06$, $C1=0.15$, $A = 65$

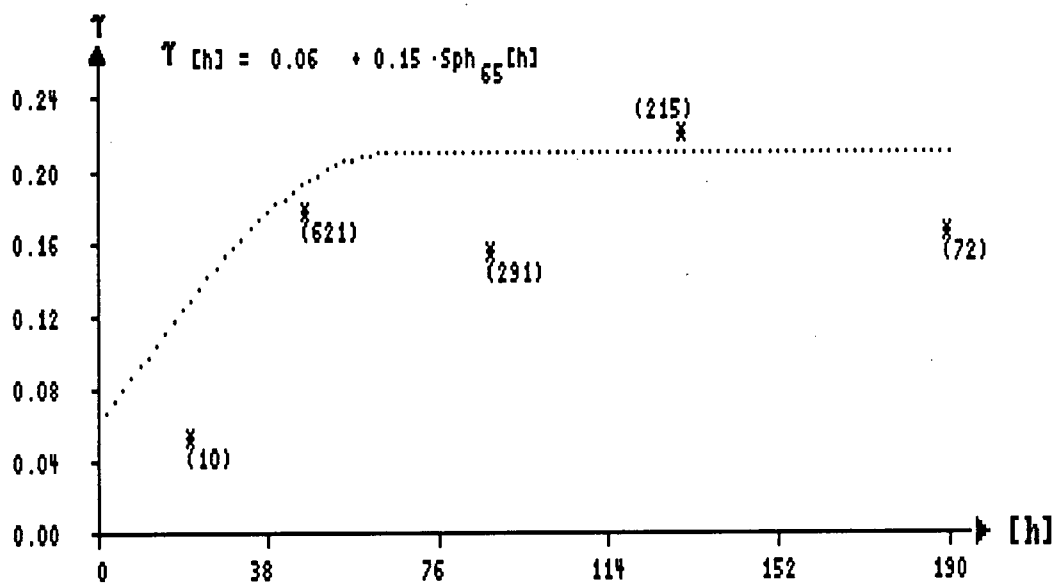
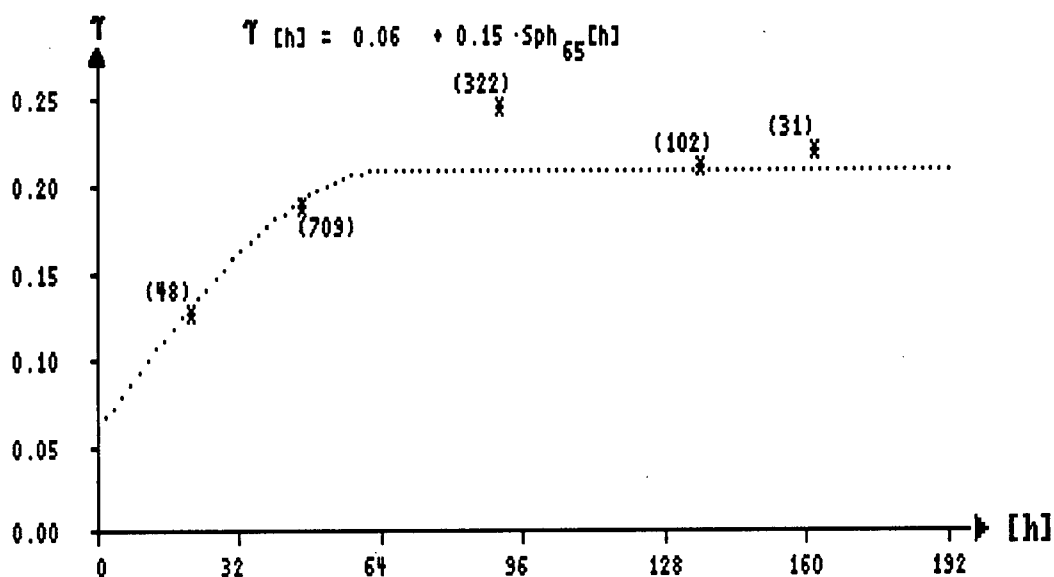


Figure A2-6: Cu semivariogram models in horizontal directions,
SE domain; azimuth 0 (top) and 30 (bottom)

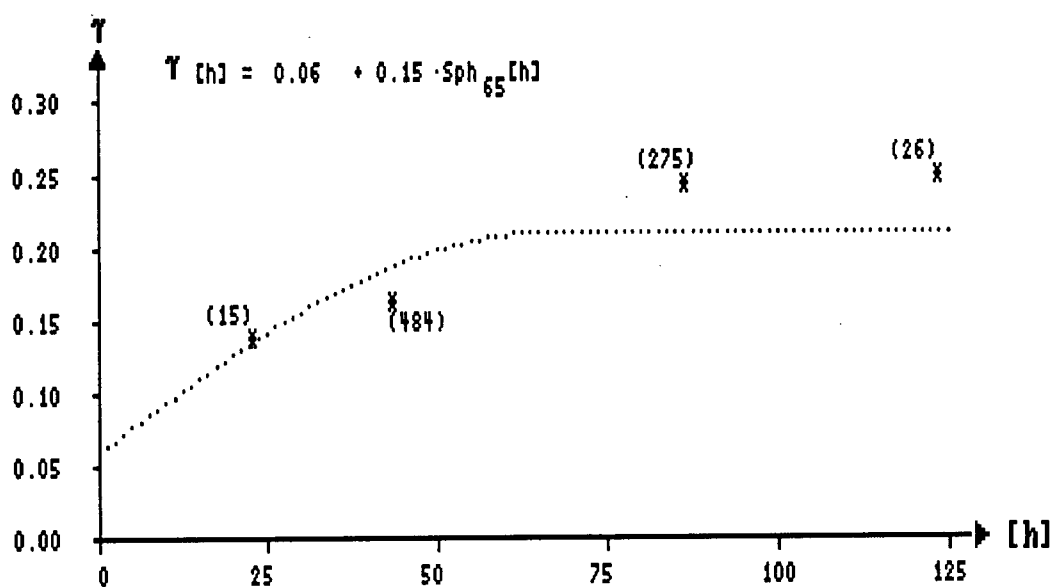
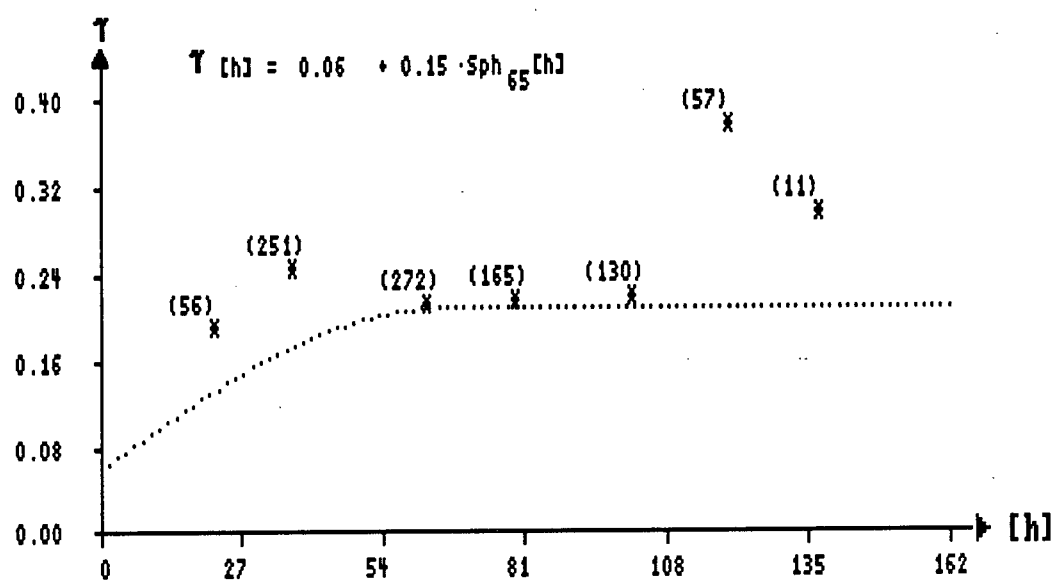


Figure A2-7: Cu semivariogram models in horizontal directions, SE domain; azimuth 90 (top) and 120 (bottom)

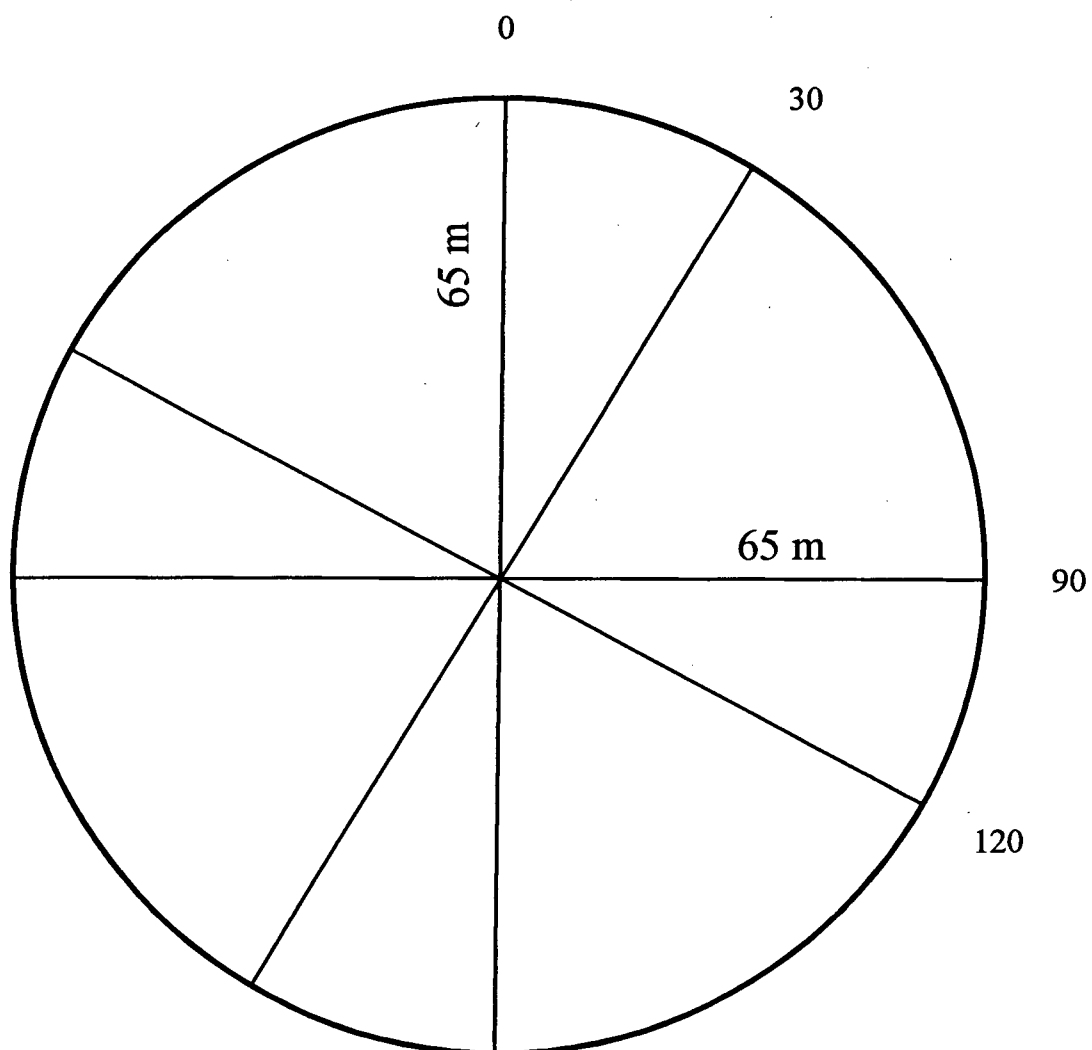


Figure A2-8: Structural ellipse of ranges in the four directions showing an isotropic Cu semivariogram model, SE domain

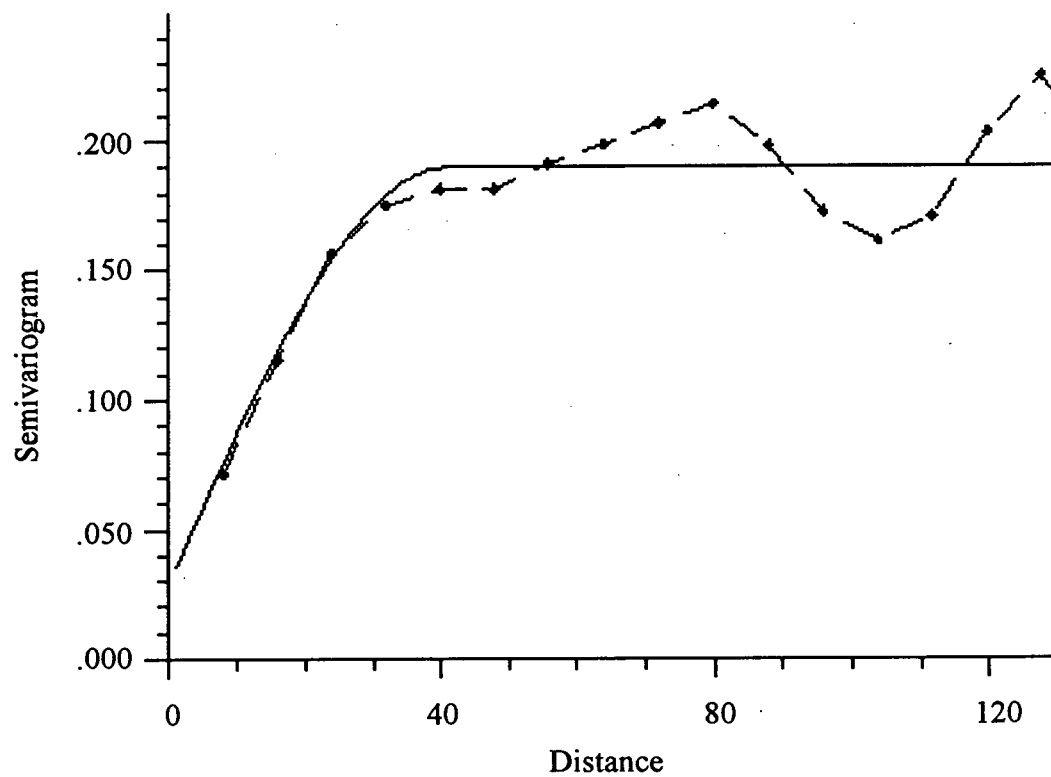


Figure A2-9: Cu semivariogram model in vertical direction, SW domain;
 $C_0=0.03$, $C_1=0.16$, $A=41$

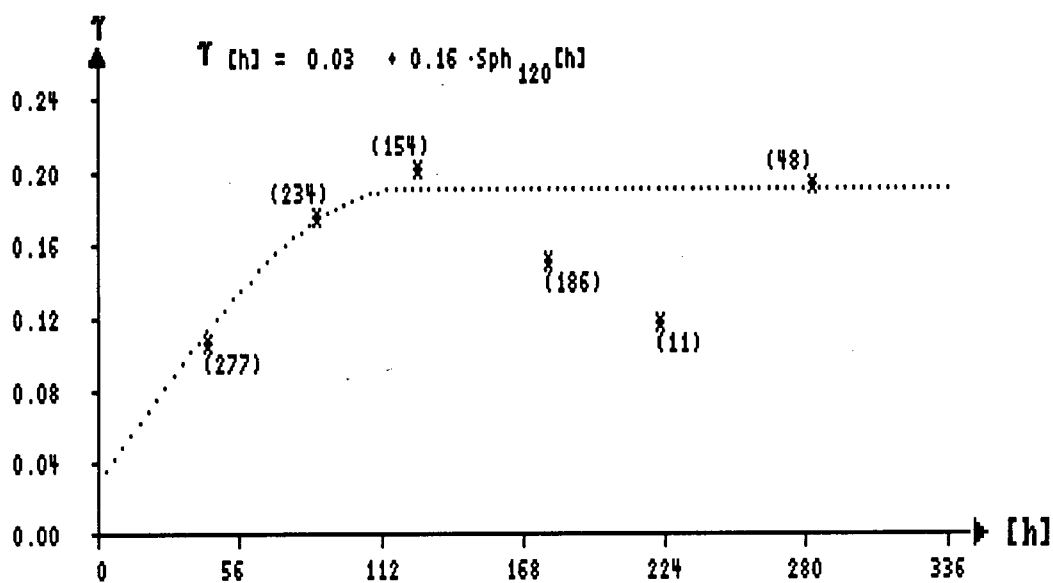
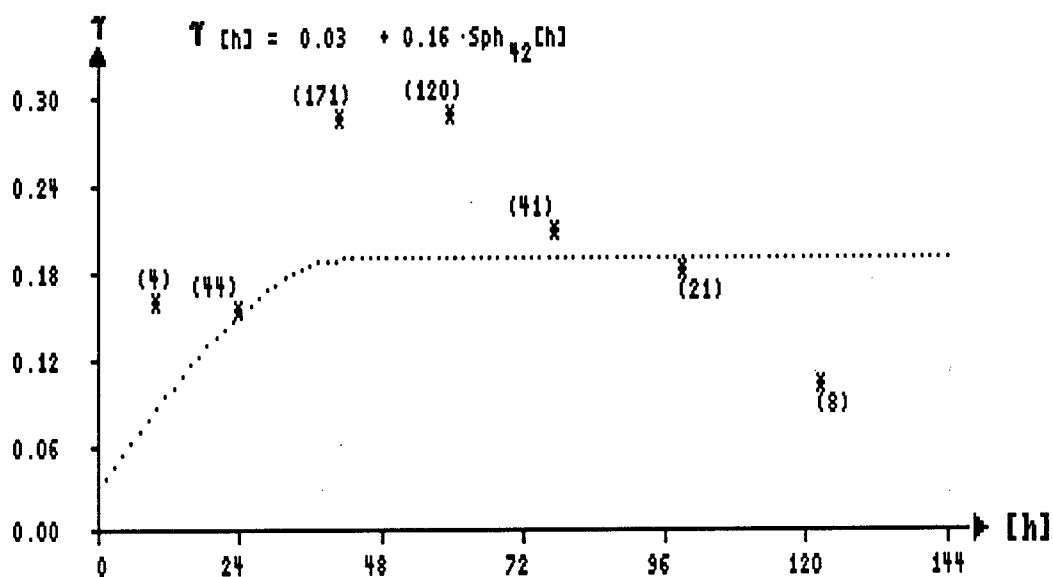


Figure A2-10: Cu semivariogram models in horizontal directions,
SW domain; azimuth 0 (top) and 80 (bottom)

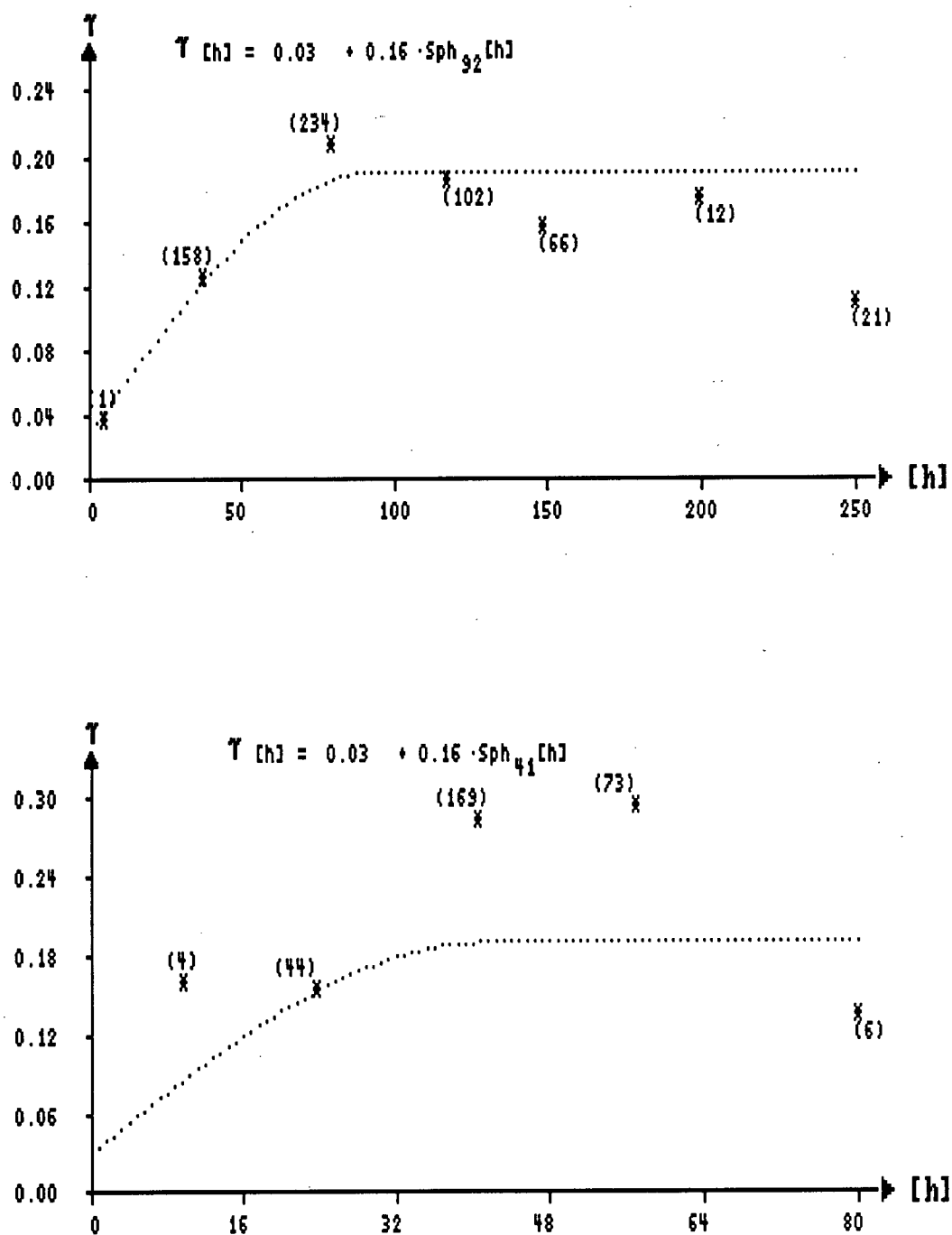


Figure A2-11: Cu semivariogram models in horizontal directions,
SW domain; azimuth 90 (top) and 170 (bottom)

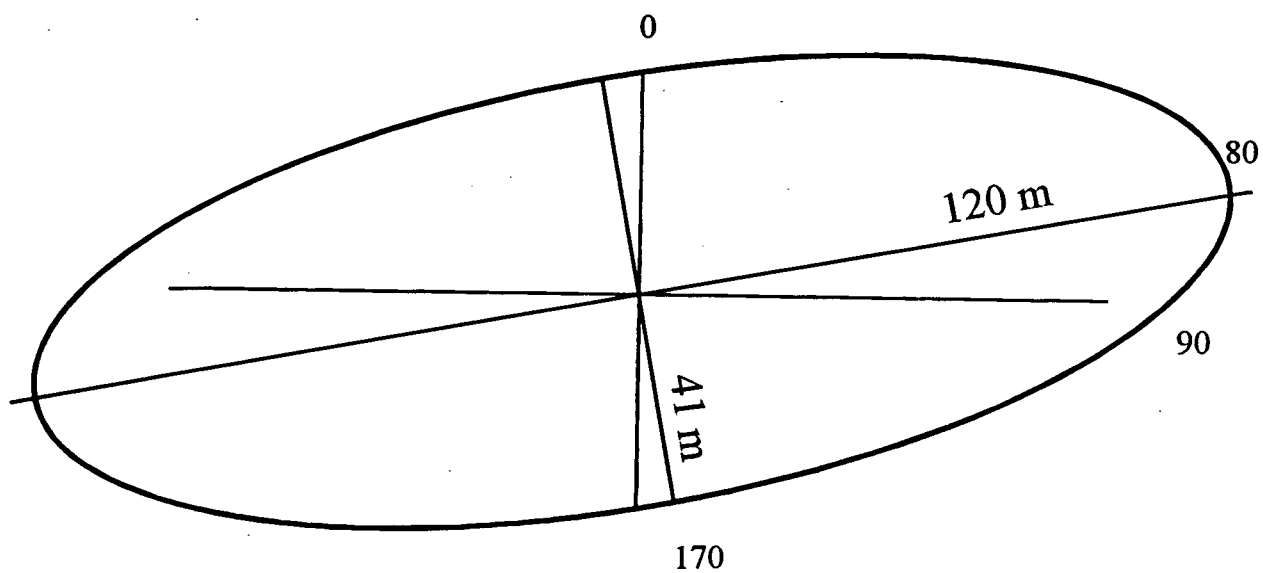


Figure A2-12: Structural ellipse of ranges in the four directions showing directions of maximum (azimuth 80) and minimum (azimuth 170) continuity of Cu semivariogram model, SW domain

APPENDIX 3

HUCKLEBERRY EAST ZONE, GENERAL SEMIVARIOGRAM MODEL

This appendix contains figures of experimental pairwise relative semivariograms and their models for the entire East zone (general semivariogram) developed in vertical direction as well as in eight different horizontal directions. There is also included a structural ellipse of ranges in the eight horizontal directions.

Parameters of the resulting 3-dimensional model are as follows:

nugget effect: $C_0 = 0.045$

first structure: $C_1 = 0.05$, $A_m = 36$ m, $A_p = 36$ m, $A_v = 36$ m

second structure: $C_2 = 0.5$, $A_m = 650$ m, $A_p = 220$ m, $A_v = 780$ m

direction of major continuity: azimuth = 67°

where:

C_1 - contribution of the first structure

C_2 - contribution of the second structure

A_m - range in the direction of major continuity

A_p - range in the perpendicular direction in horizontal plane

A_v - range in the vertical direction

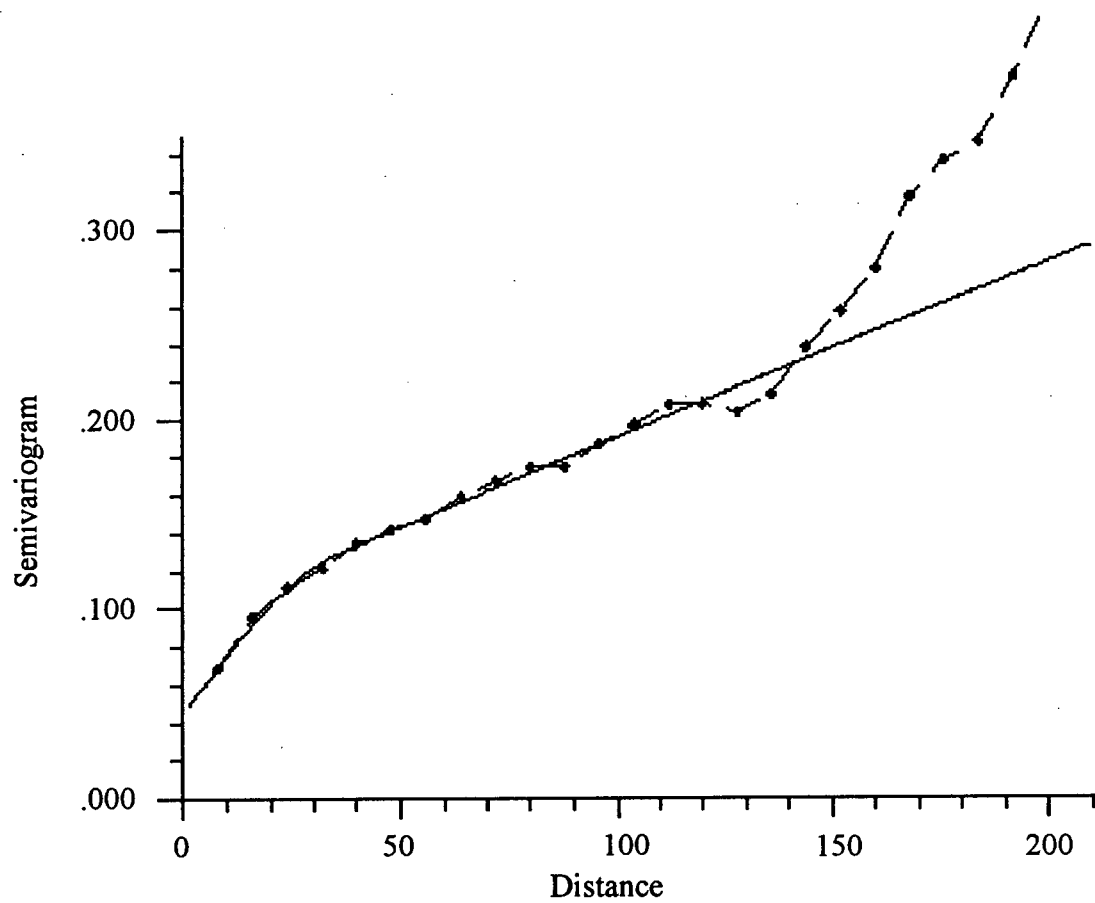


Figure A3-1: Cu semivariogram model in vertical direction;
 $C0=0.045$, $C1=0.05$, $A1=36$, $C2=0.5$, $A2=780$

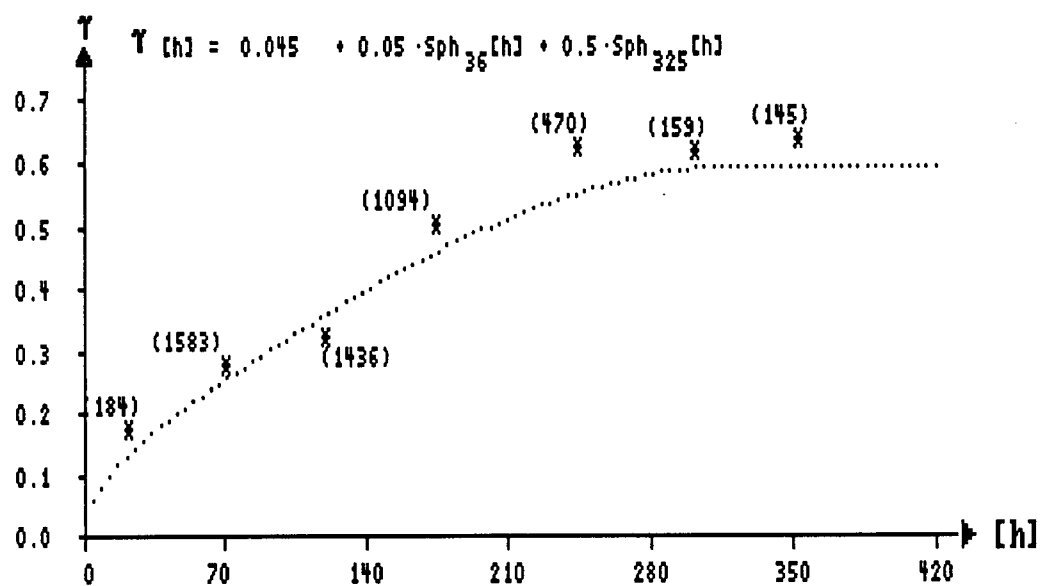
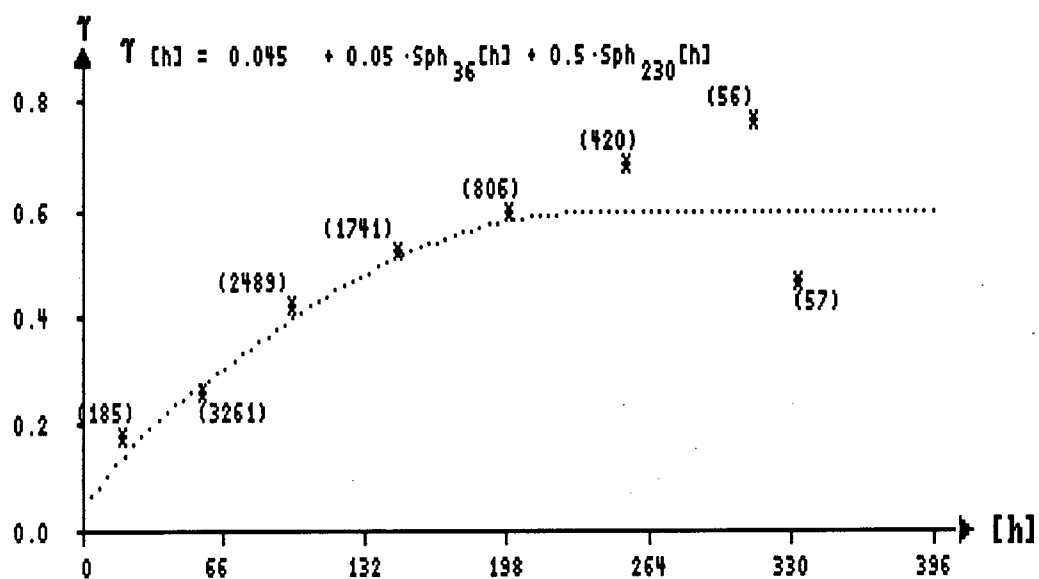


Figure A3-2: Cu semivariogram models in horizontal directions;
azimuth 0 (top) and 22 (bottom)

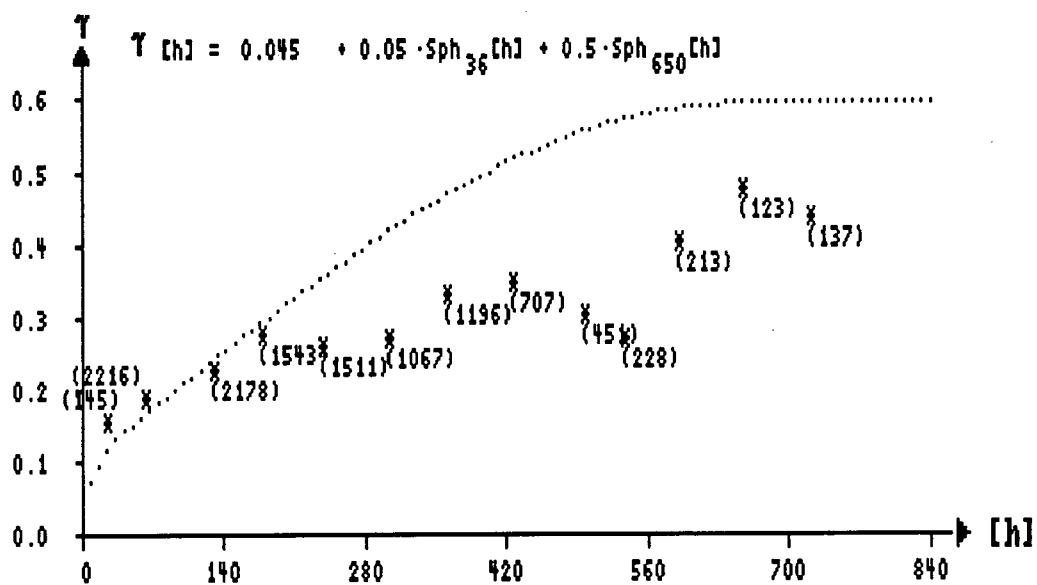
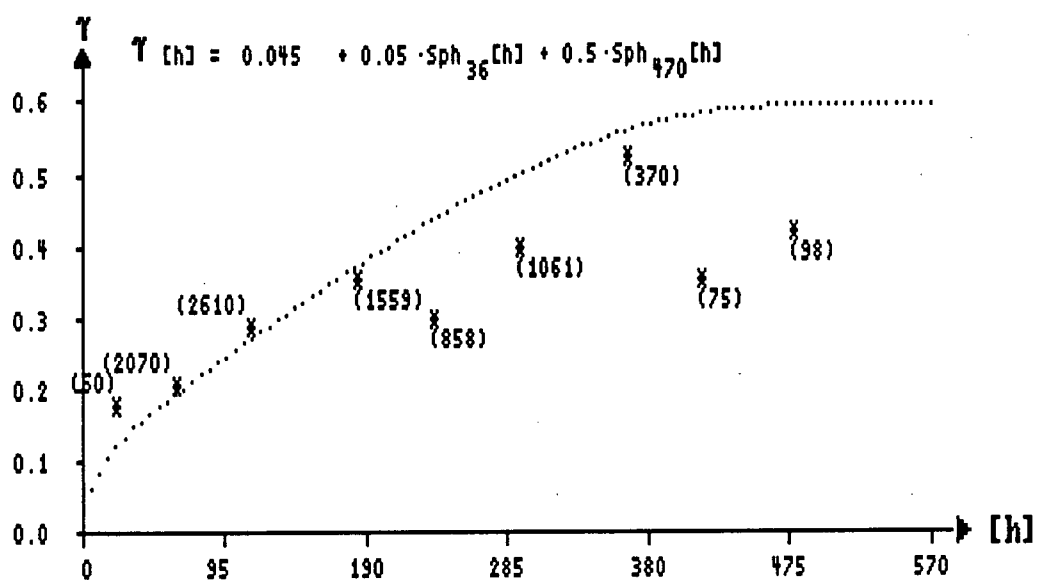


Figure A3-3: Cu semivariogram models in horizontal directions;
azimuth 45 (top) and 67 (bottom)

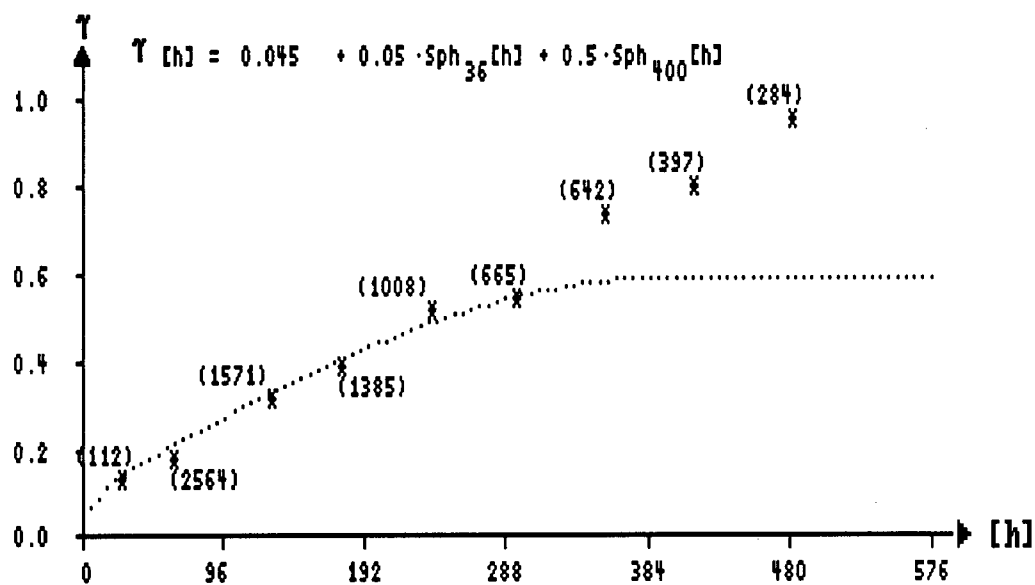
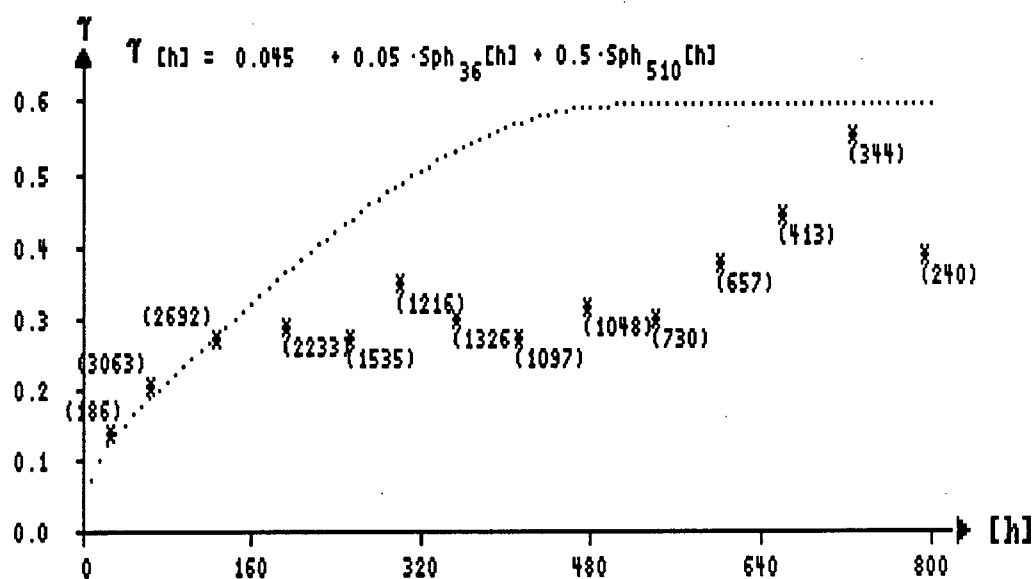


Figure A3-4: Cu semivariogram models in horizontal directions;
azimuth 90 (top) and 112 (bottom)

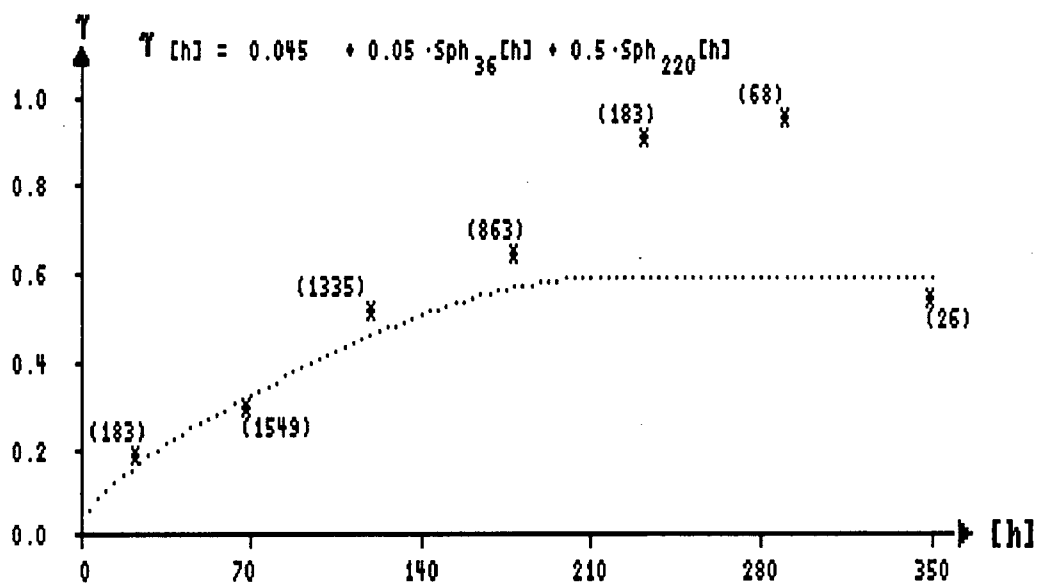
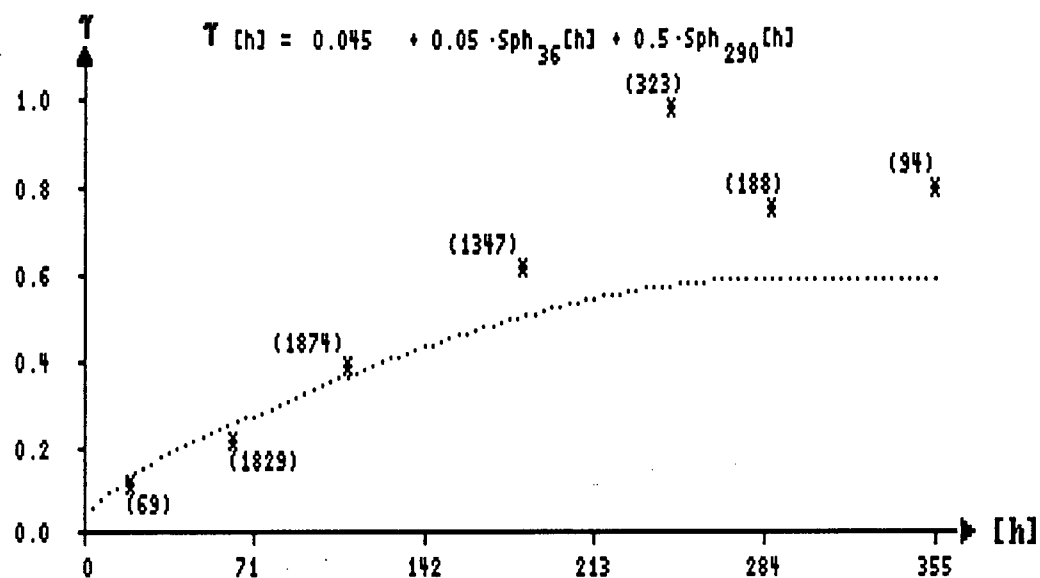


Figure A3-5: Cu semivariogram models in horizontal directions;
azimuth 135 (top) and 157 (bottom)

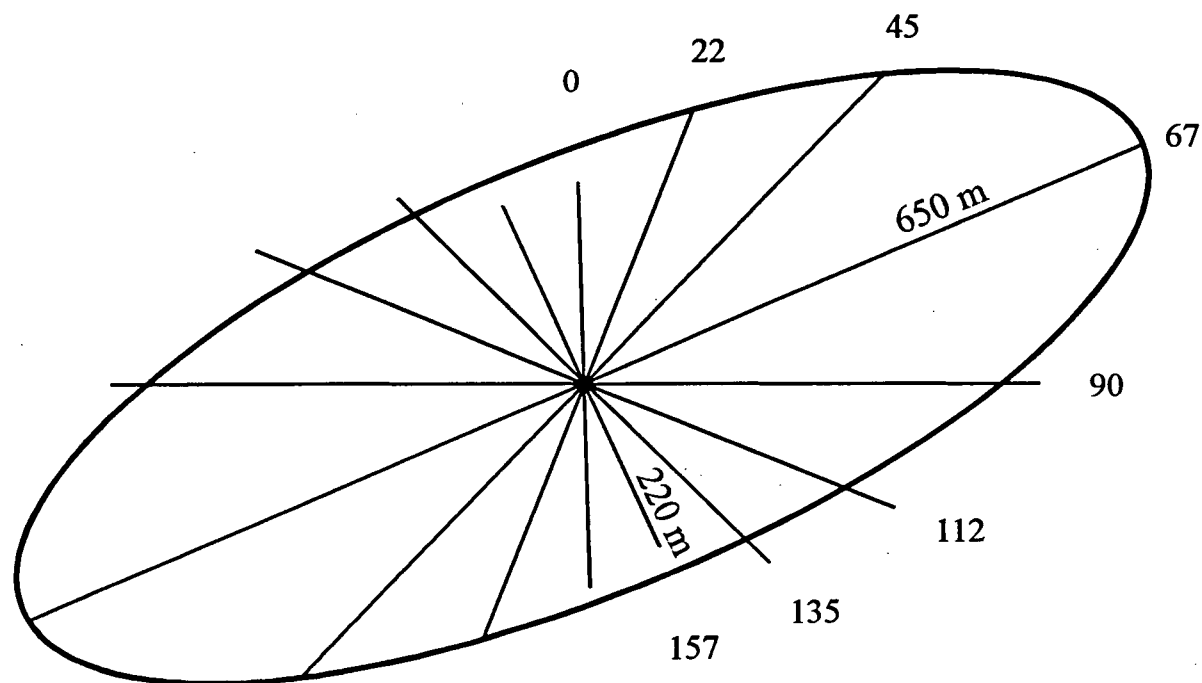


Figure A3-6: Structural ellipse of ranges in the eight directions showing directions of maximum (azimuth 67) and minimum (azimuth 157) continuity of Cu semivariogram model

APPENDIX 4

HUCKLEBERRY EAST ZONE, DOMAIN SEMIVARIOGRAM MODELS

This appendix contains figures of experimental pairwise relative semivariograms and their models for E domain, and W domain of the East zone developed for each domain in vertical direction as well as in eight different horizontal directions. There are also included structural ellipses of ranges in the eight horizontal directions for each domain.

Parameters of the resulting 3-dimensional model for E domain are as follows:

nugget effect: $C_0 = 0.01$

first structure: $C_1 = 0.048$, $A_m = 20$ m, $A_p = 20$ m, $A_v = 20$ m

second structure: $C_2 = 0.412$, $A_m = 340$ m, $A_p = 190$ m, $A_v = 380$ m

direction of major continuity: azimuth = 112°

Parameters of the resulting 3-dimensional model for W domain are as follows:

nugget effect: $C_0 = 0.055$

first structure: $C_1 = 0.045$, $A_m = 32$ m, $A_p = 32$ m, $A_v = 32$ m

second structure: $C_2 = 0.5$, $A_m = 670$ m, $A_p = 240$ m, $A_v = 850$ m

direction of major continuity: azimuth = 67°

where:

C1 - contribution of the first structure

C2 - contribution of the second structure

A_m - range in the direction of major continuity

A_p - range in the perpendicular direction in horizontal plane

A_v - range in the vertical direction

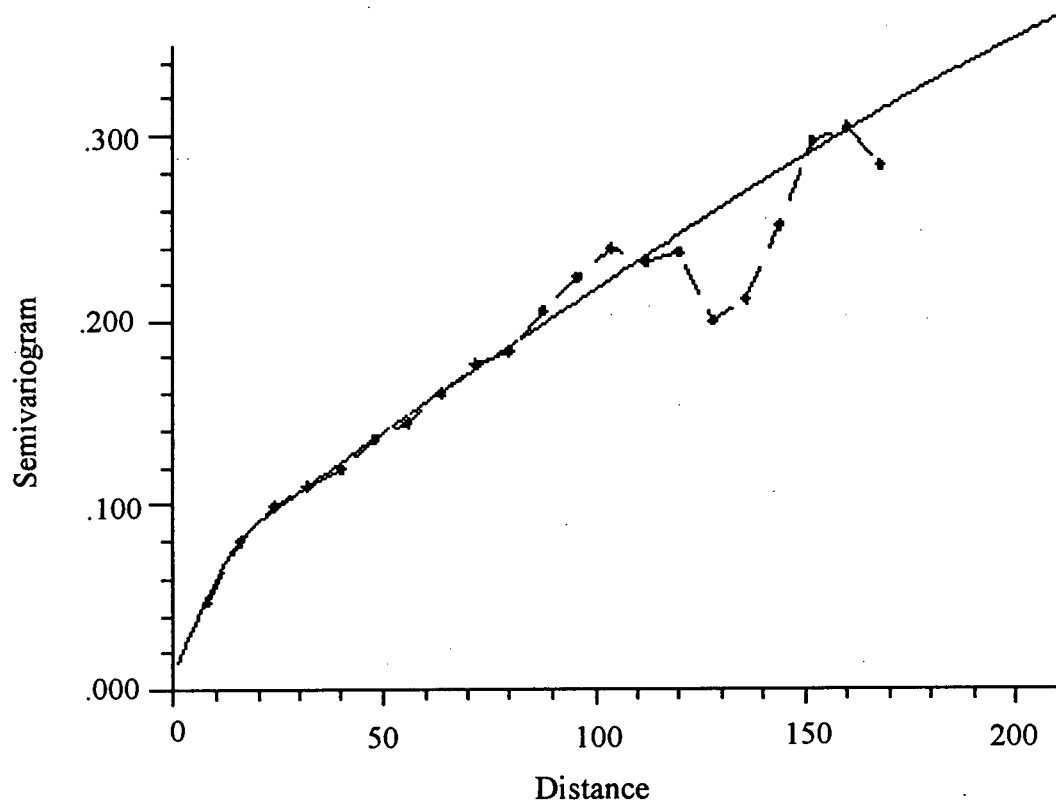


Figure A4-1: Cu semivariogram model in vertical direction, E domain;
 $C0 = 0.01$, $C1 = 0.048$, $A1 = 20$, $C2 = 0.412$, $A2 = 380$

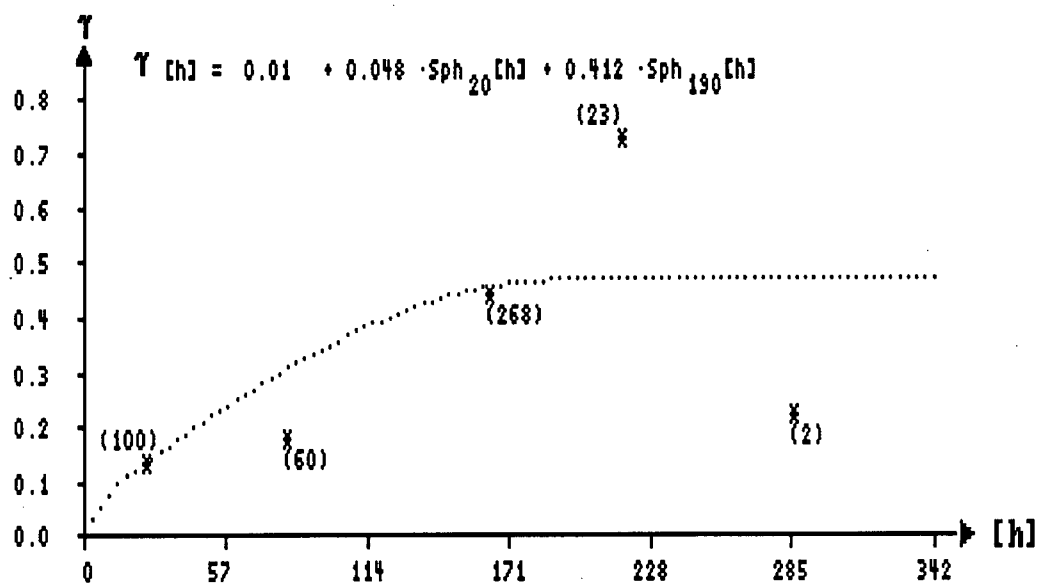
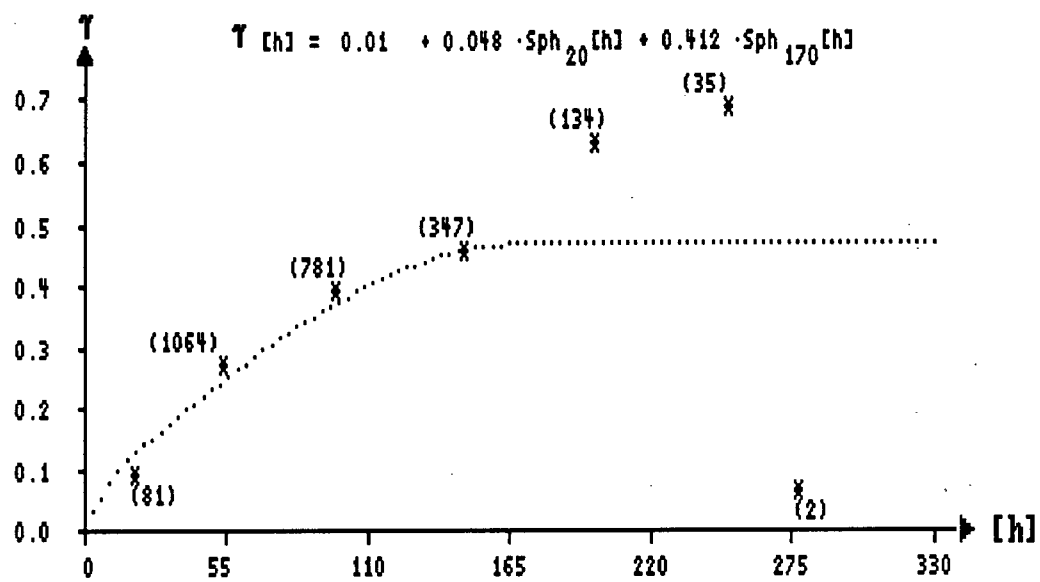


Figure A4-2: Cu semivariogram models in horizontal directions,
E domain; azimuth 0 (top) and 22 (bottom)

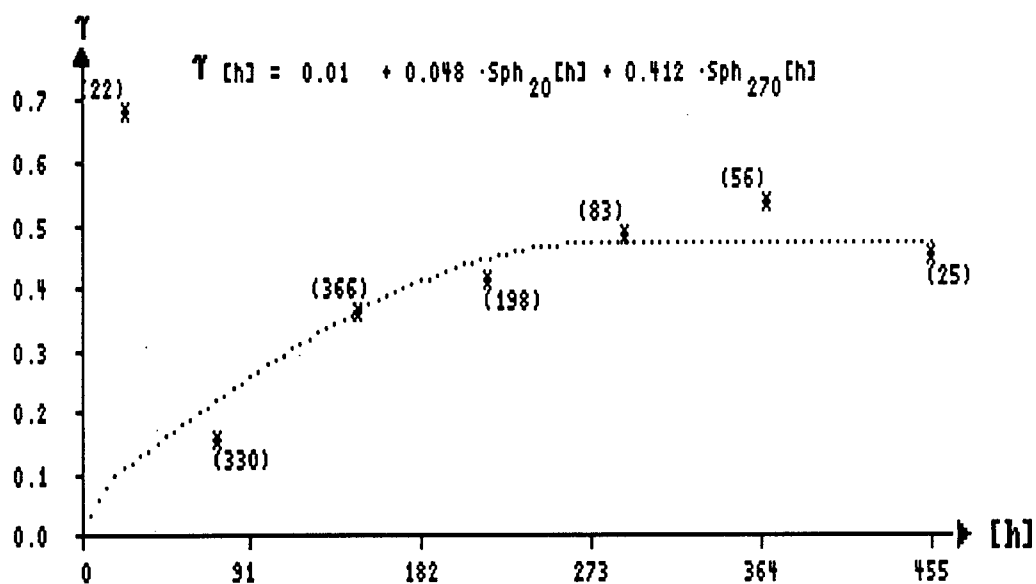
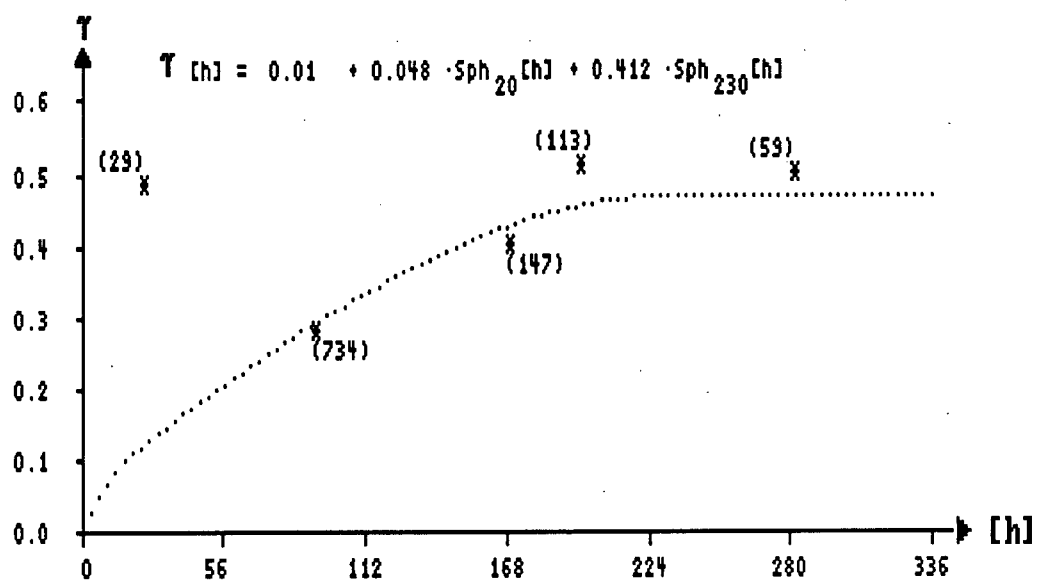


Figure A4-3: Cu semivariogram models in horizontal directions,
E domain; azimuth 45 (top) and 67 (bottom)

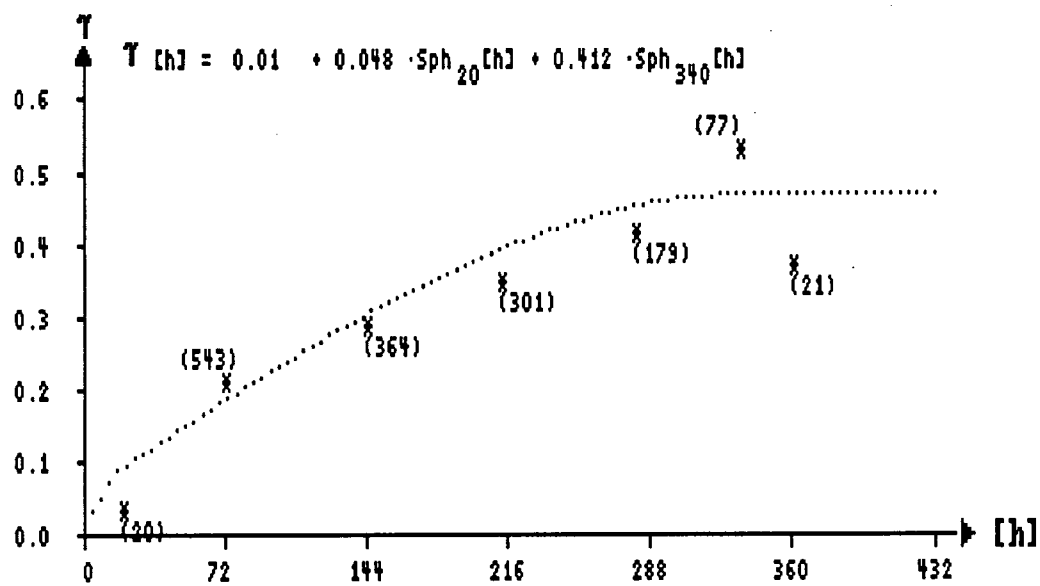
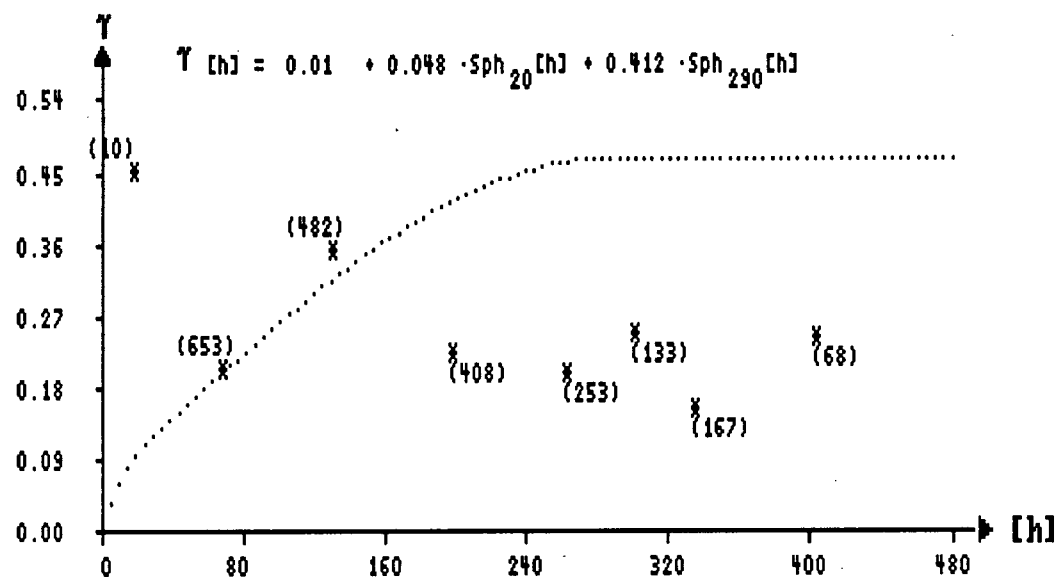


Figure A4-4: Cu semivariogram models in horizontal directions,
E domain; azimuth 90 (top) and 112 (bottom)

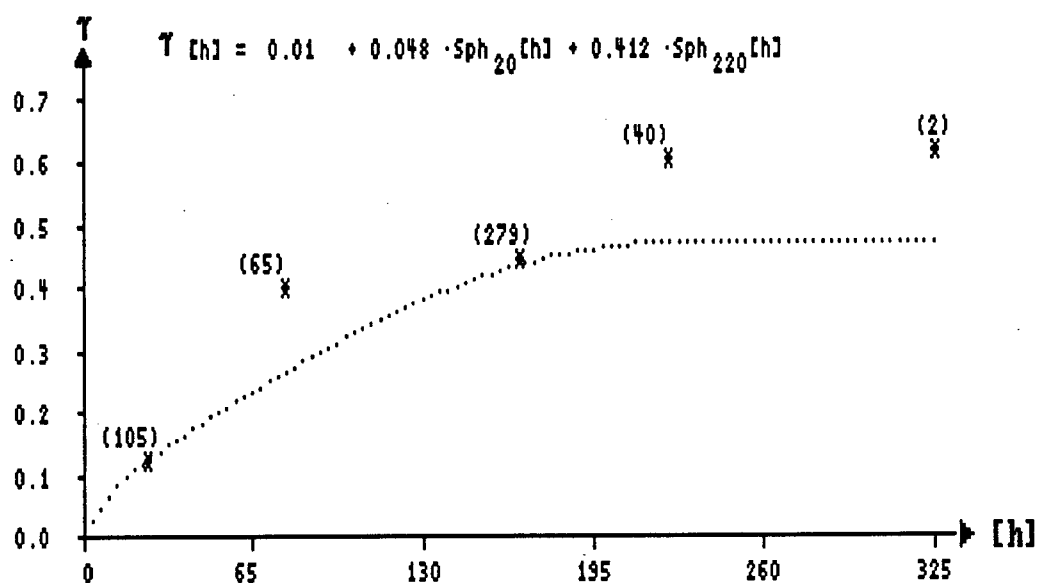
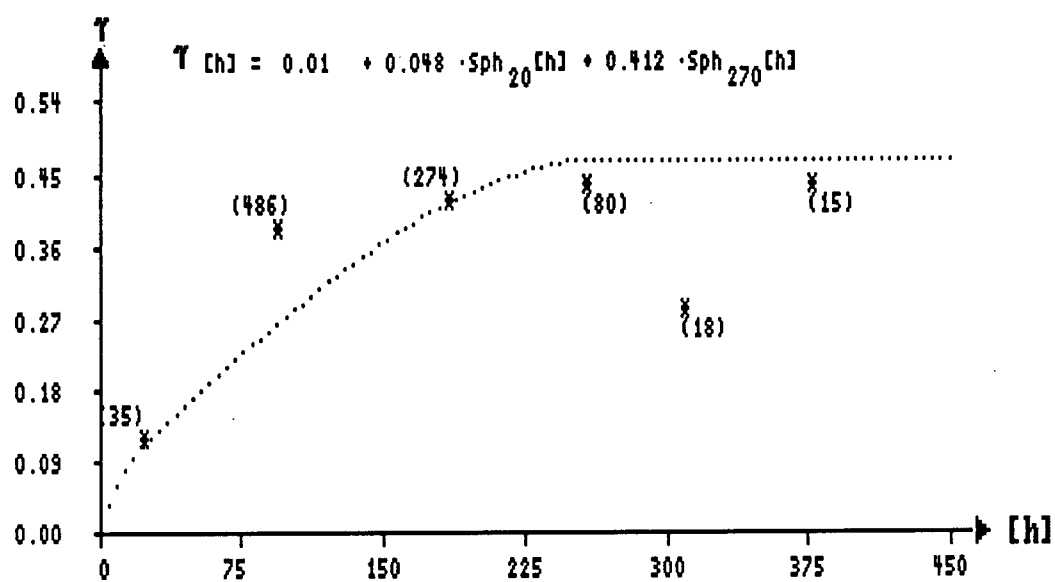


Figure A4-5: Cu semivariogram models in horizontal directions,
E domain; azimuth 135 (top) and 157 (bottom)

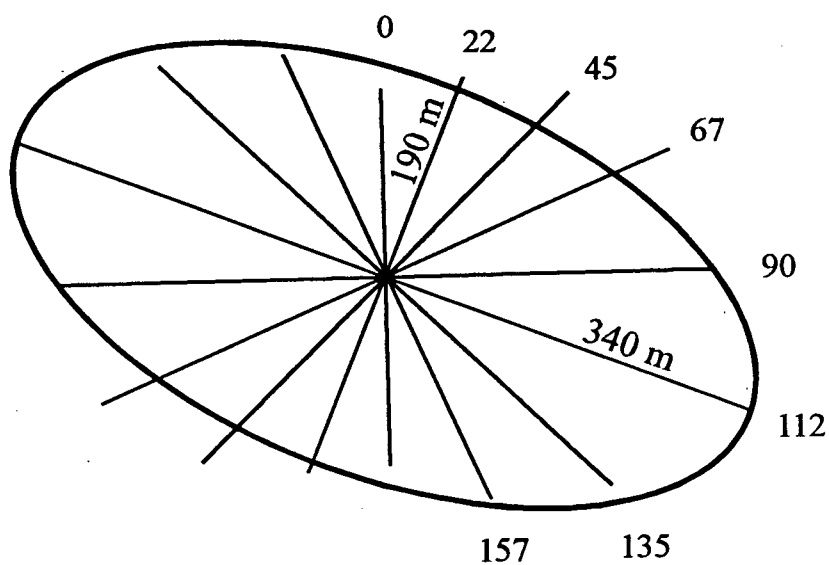


Figure A4-6: Structural ellipse of ranges in the eight directions showing directions of maximum (azimuth 112) and minimum (azimuth 22) continuity of Cu semivariogram model, E domain

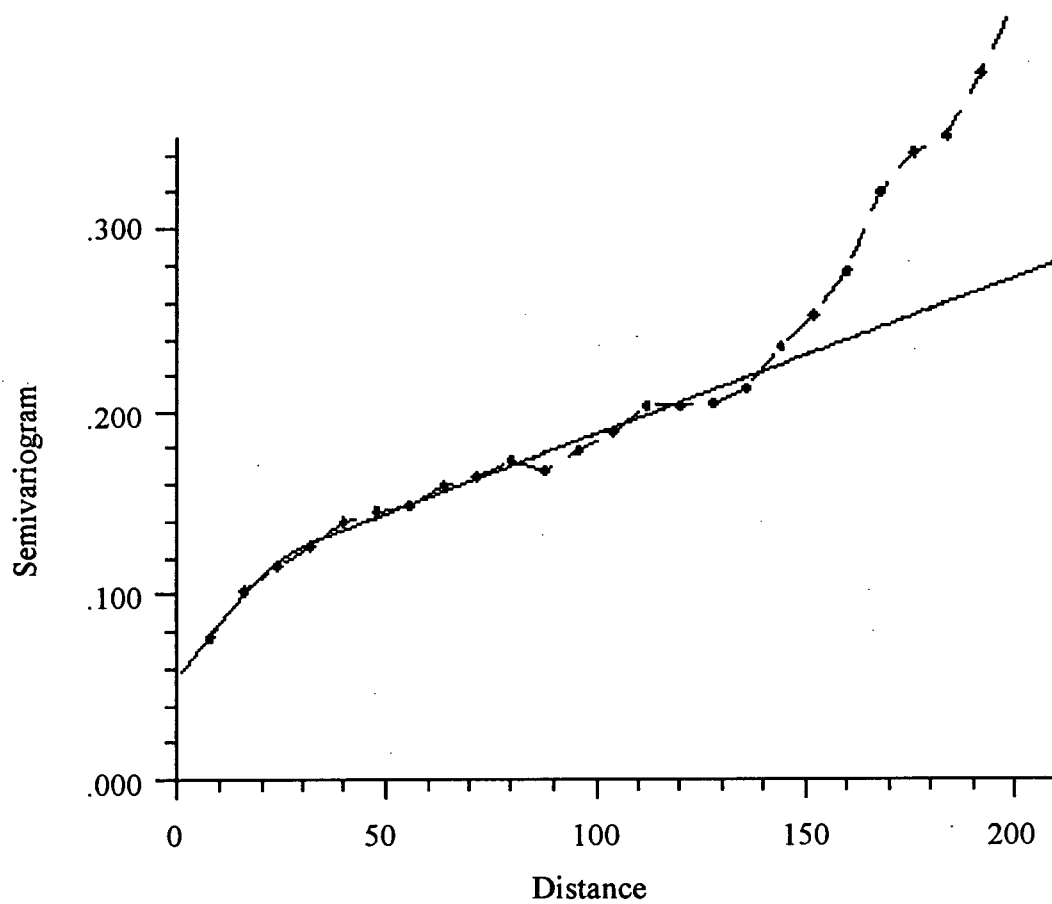


Figure A4-7: Cu semivariogram model in vertical direction, W domain;
 $C_0 = 0.055$, $C_1 = 0.045$, $A_1 = 32$, $C_2 = 0.5$, $A_2 = 850$

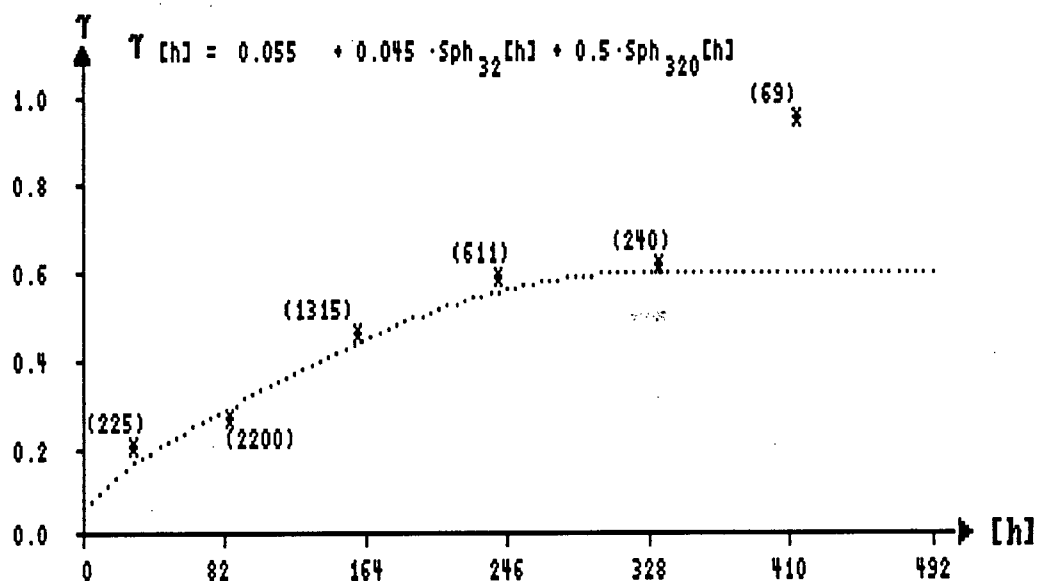
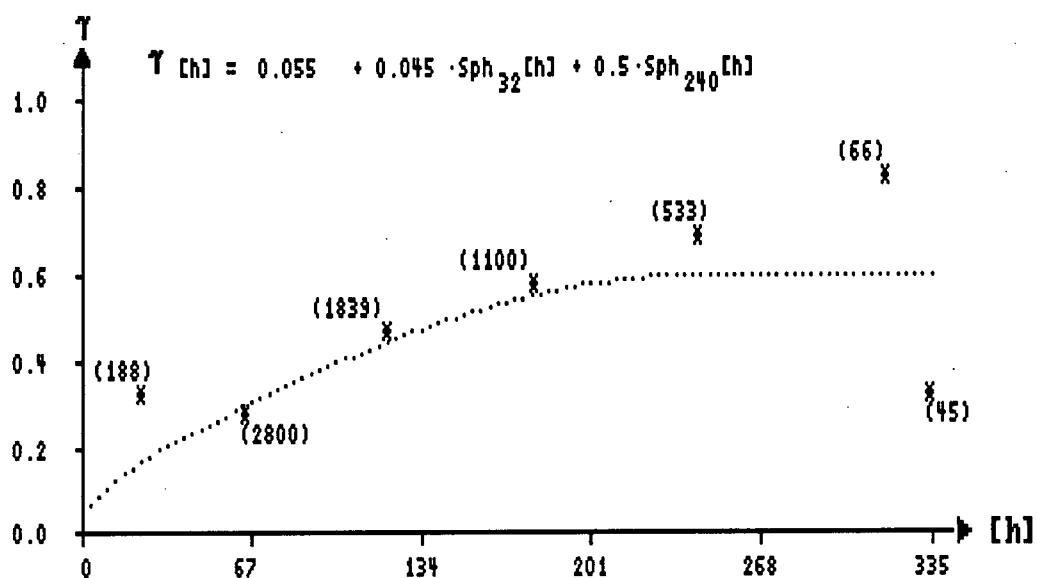


Figure A4-8: Cu semivariogram models in horizontal directions,
W domain; azimuth 0 (top) and 22 (bottom)

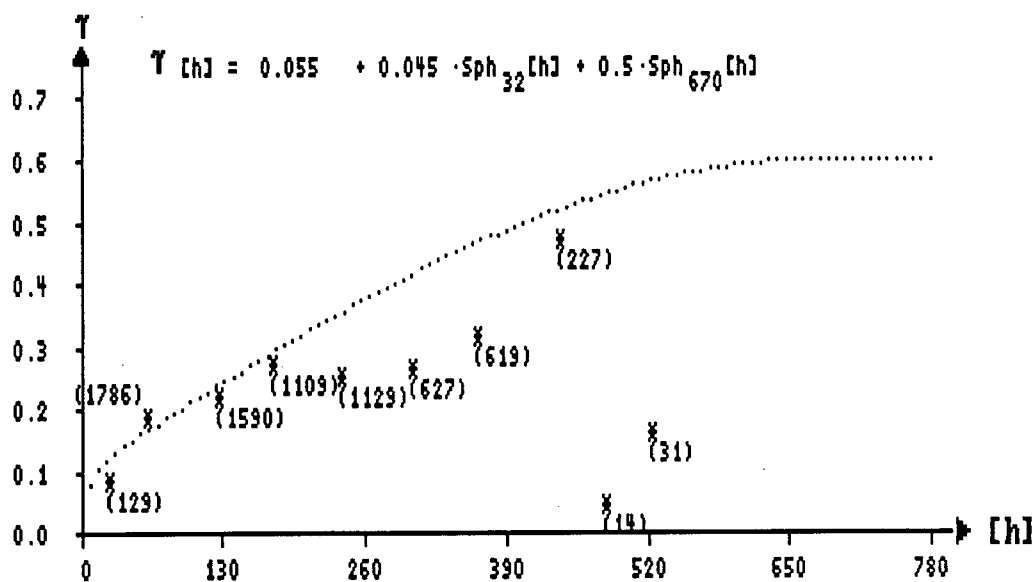
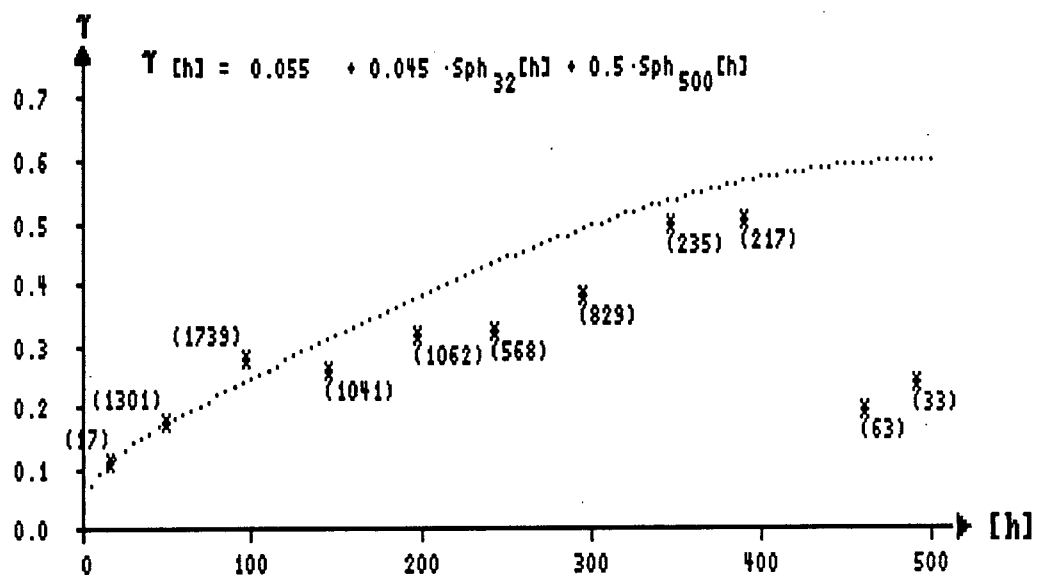


Figure A4-9: Cu semivariogram models in horizontal directions,
W domain; azimuth 45 (top) and 67 (bottom)

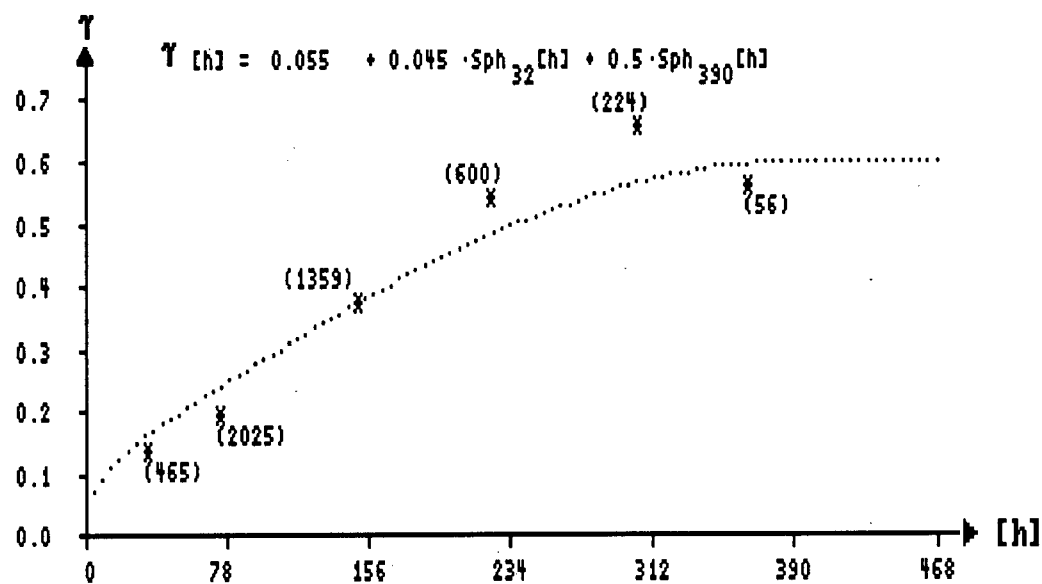
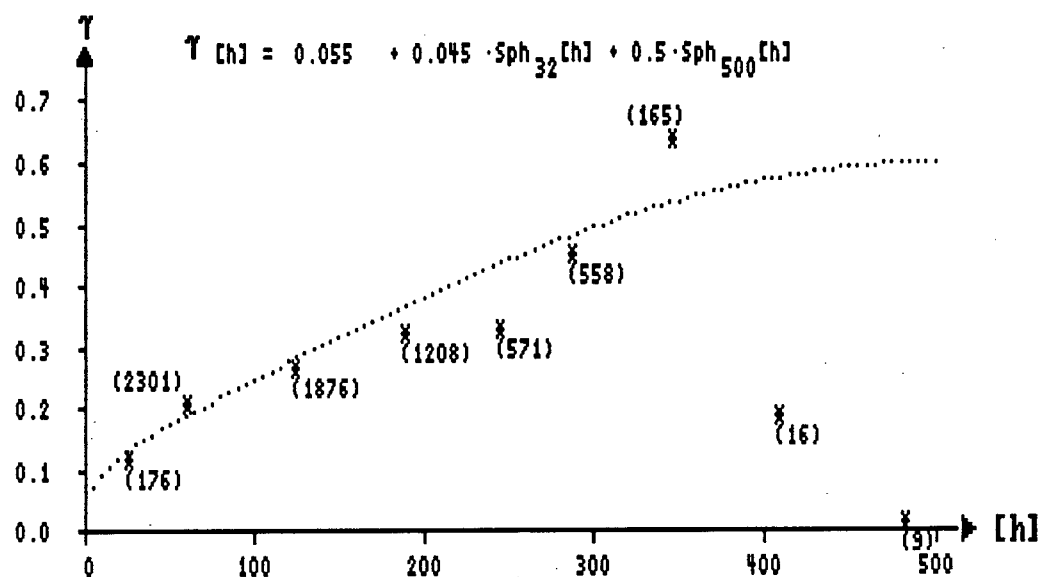


Figure A4-10: Cu semivariogram models in horizontal directions,
W domain; azimuth 90 (top) and 112 (bottom)

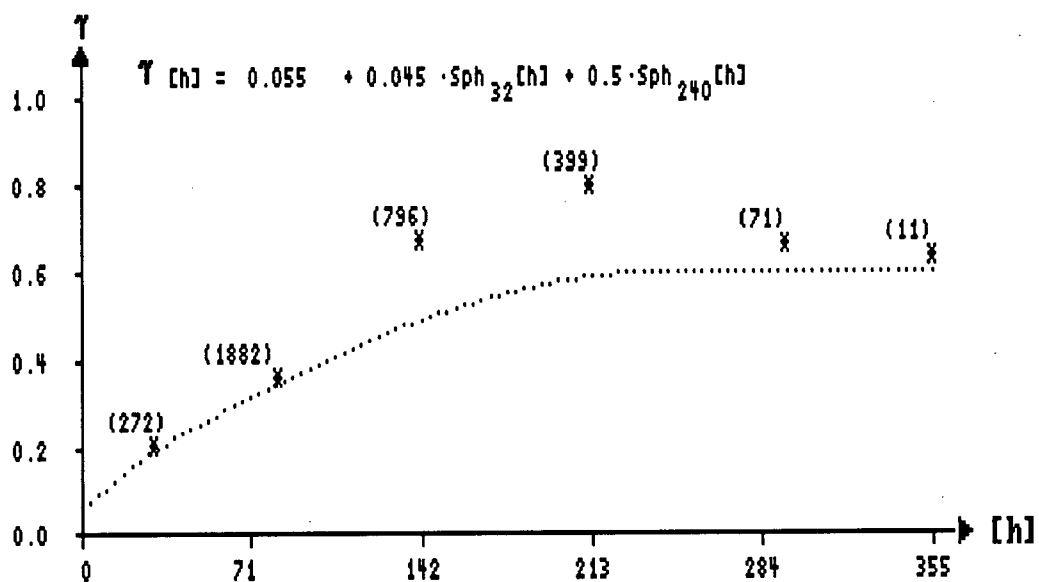
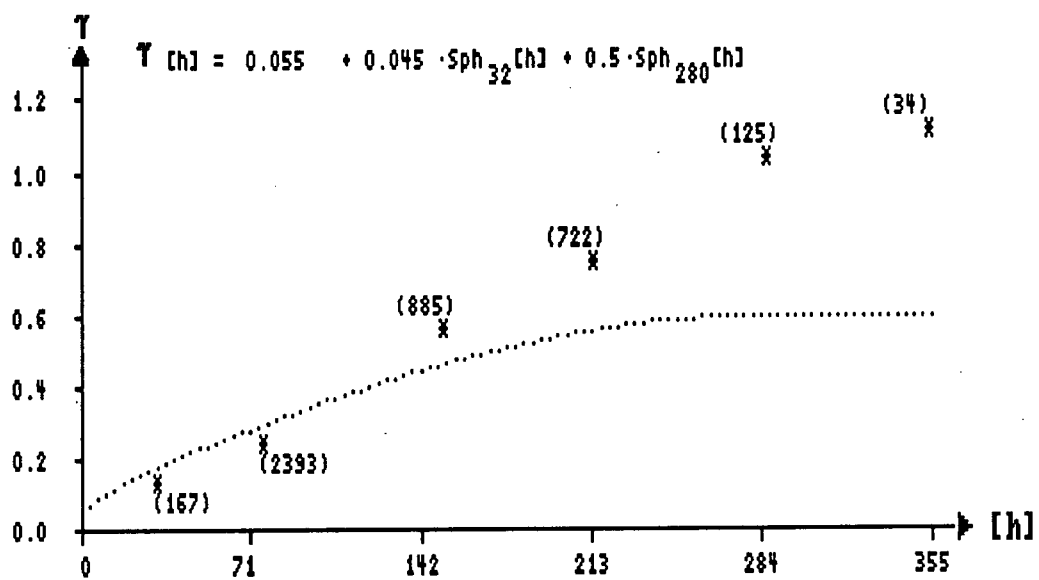


Figure A4-11: Cu semivariogram models in horizontal directions,
W domain; azimuth 135 (top) and 157 (bottom)

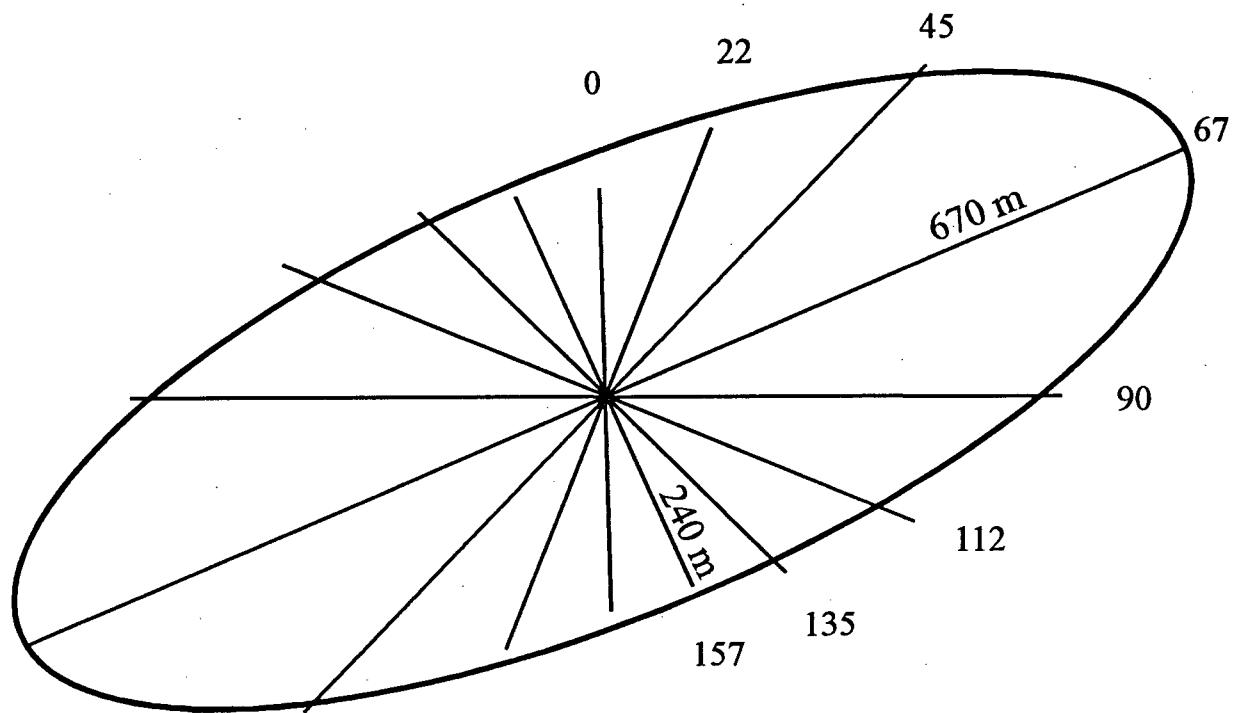


Figure A4-12: Structural ellipse of ranges in the eight directions showing directions of maximum (azimuth 67) and minimum (azimuth 157) continuity of Cu semivariogram model, W domain

APPENDIX 5

VIRGINIA ZONE, SEMIVARIOGRAM MODELS

This appendix contains figures of experimental pairwise relative semivariograms and their models for Cu and Au developed for several directions within the vertical East-West trending plane (horizontal direction, -10° dip direction, -20° dip direction, -30° dip direction), as well as in the cross-vein direction (azimuth 0°). There are also included Cu and Au vertical semivariograms both for entire mineralized zone and for different parts of Virginia zone as well as structural ellipses of ranges in the two horizontal directions for each metal.

Parameters of the resulting 3-dimensional model for Cu are as follows:

nugget effect: $C_0 = 0.22$

first structure: $C_1 = 0.17$, $A_m = 50$ ft, $A_p = 50$ ft, $A_v = 50$ ft

second structure: $C_2 = 0.15$, $A_m = 220$ ft, $A_p = 130$ ft, $A_v = 310$ ft

direction of major continuity: azimuth = 90°

Parameters of the resulting 3-dimensional model for Au are as follows:

nugget effect: $C_0 = 0.28$

first structure: $C_1 = 0.16$, $A_m = 55$ ft, $A_p = 55$ ft, $A_v = 55$ ft

second structure: $C_2 = 0.12$, $A_m = 300$ ft, $A_p = 120$ ft, $A_v = 360$ ft

direction of major continuity: azimuth = 90°

where:

C1 - contribution of the first structure

C2 - contribution of the second structure

A_m - range in the direction of major continuity

A_p - range in the perpendicular direction in horizontal plane

A_v - range in the vertical direction

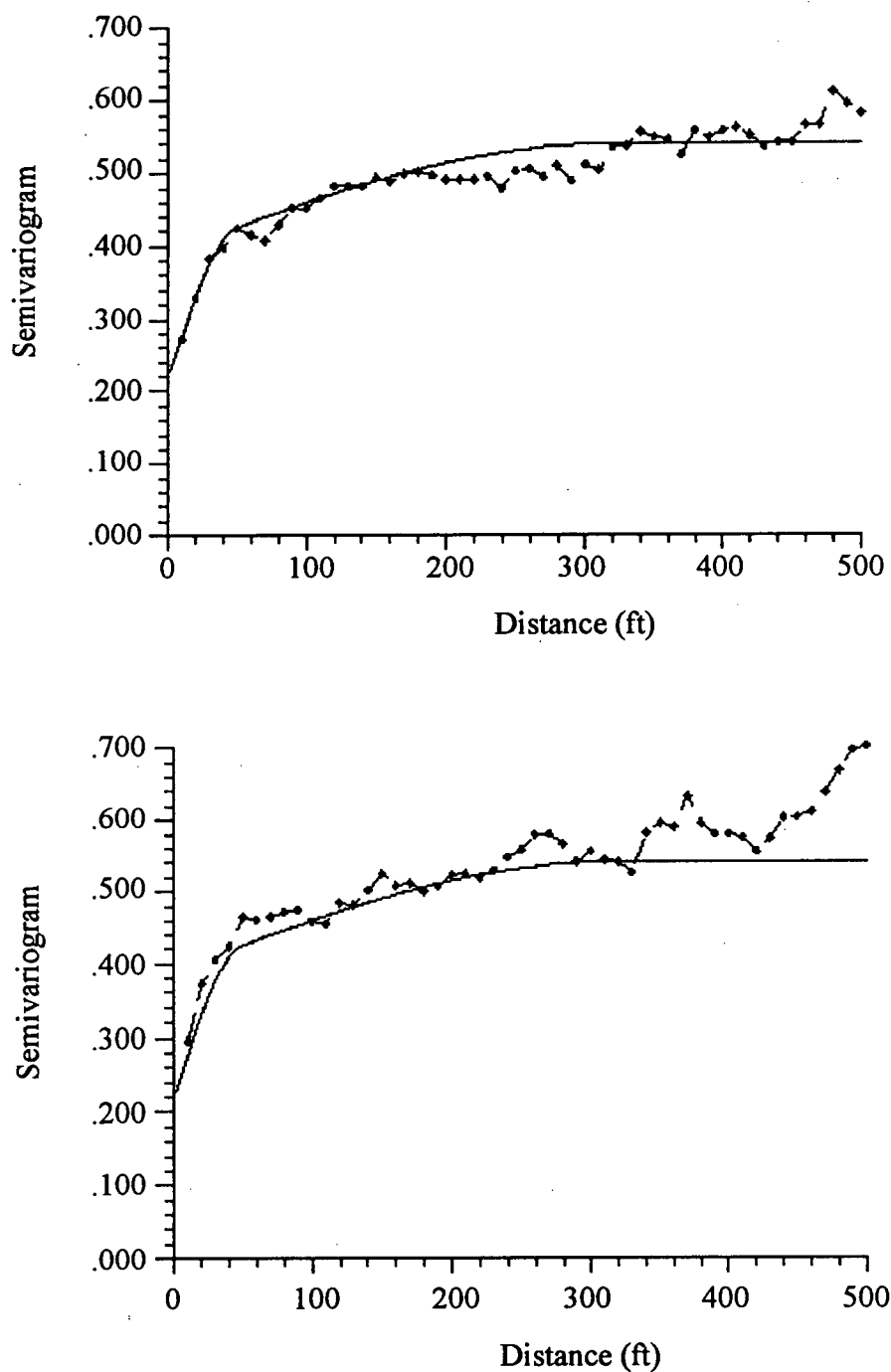


Figure A5-1: Cu experimental semivariograms in vertical direction, East part (top), middle part (bottom), with superimposed model for the entire zone; $C0 = 0.22$, $C1 = 0.17$, $A1 = 50$, $C2 = 0.15$, $A2 = 310$

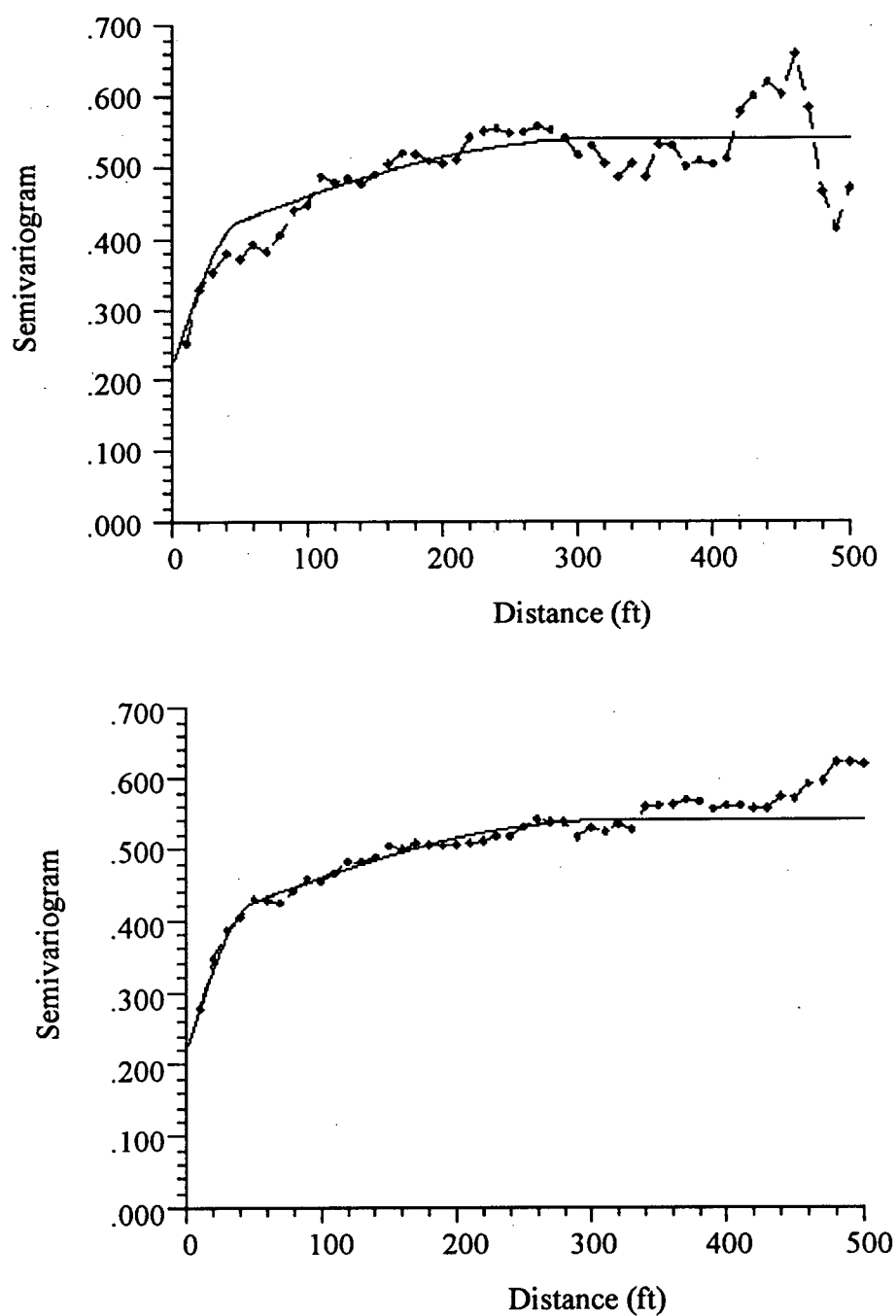


Figure A5-2: Cu experimental semivariograms in vertical direction, West part (top), entire zone (bottom), with superimposed model for the entire zone; $C_0 = 0.22$, $C_1 = 0.17$, $A_1 = 50$, $C_2 = 0.15$, $A_2 = 310$

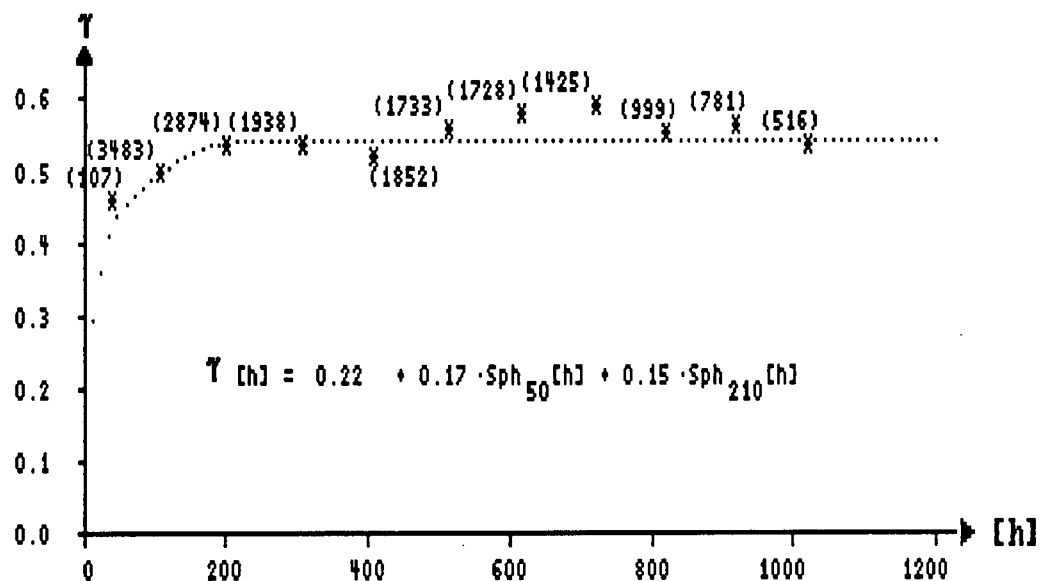
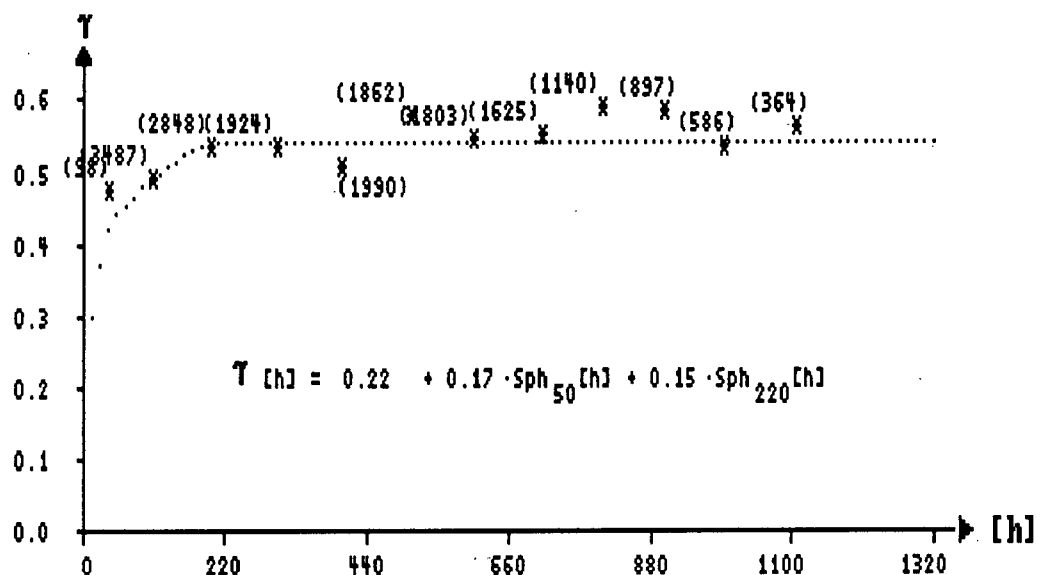


Figure A5-3: Cu semivariogram models in horizontal directions,
azimuth 90; dip 0 (top) and dip -10 (bottom)

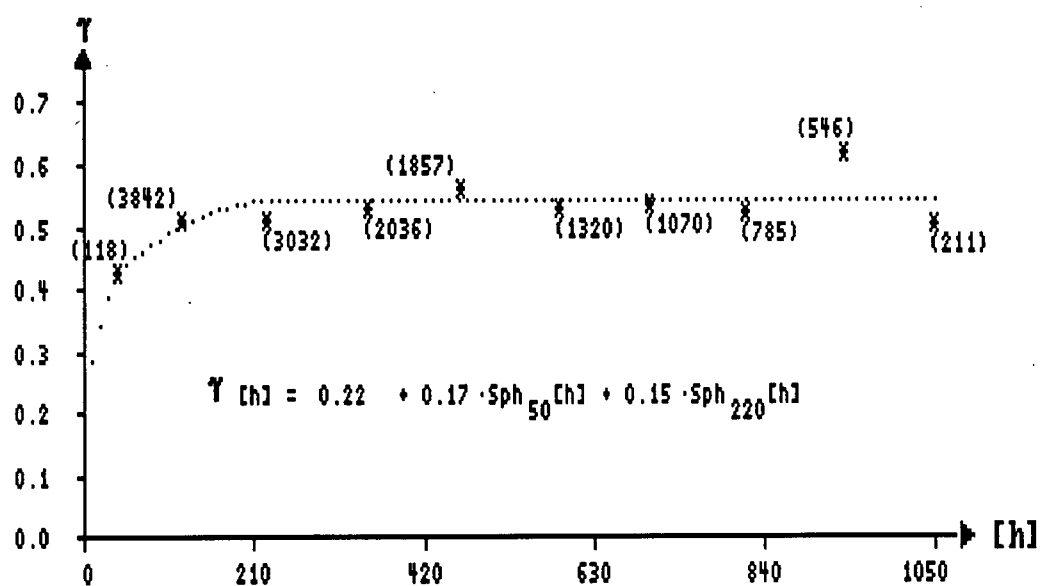
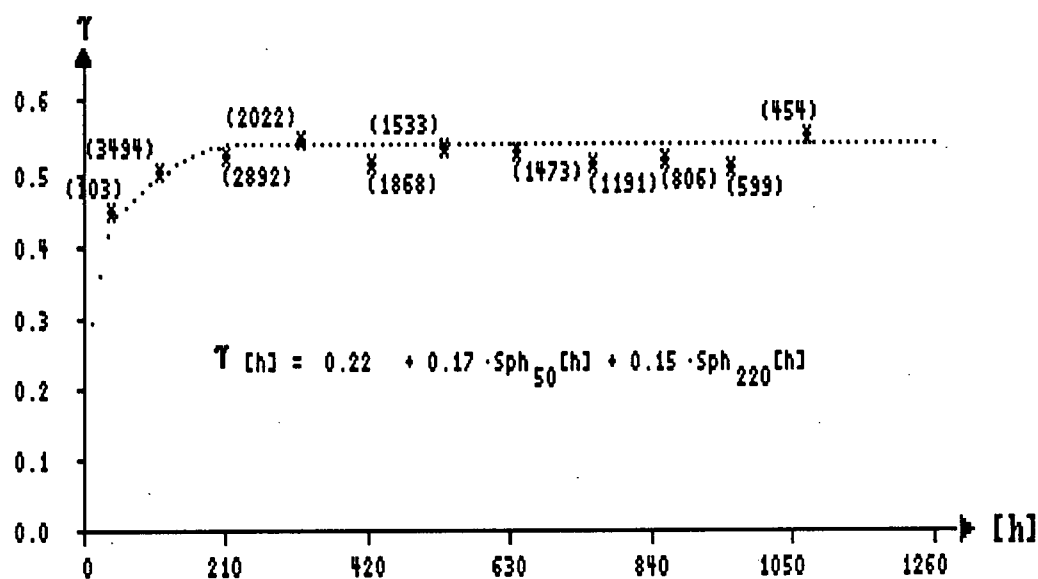


Figure A5-4: Cu semivariogram models in horizontal directions, azimuth 90; dip -20 (top) and dip -30 (bottom)

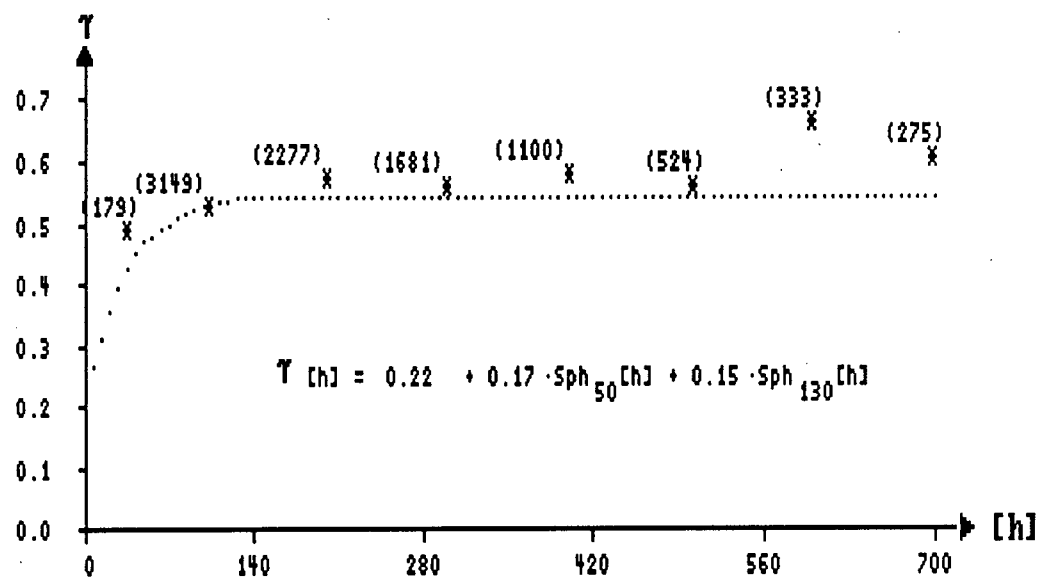


Figure A5-5: Cu semivariogram model in horizontal direction,
azimuth 0, dip 0

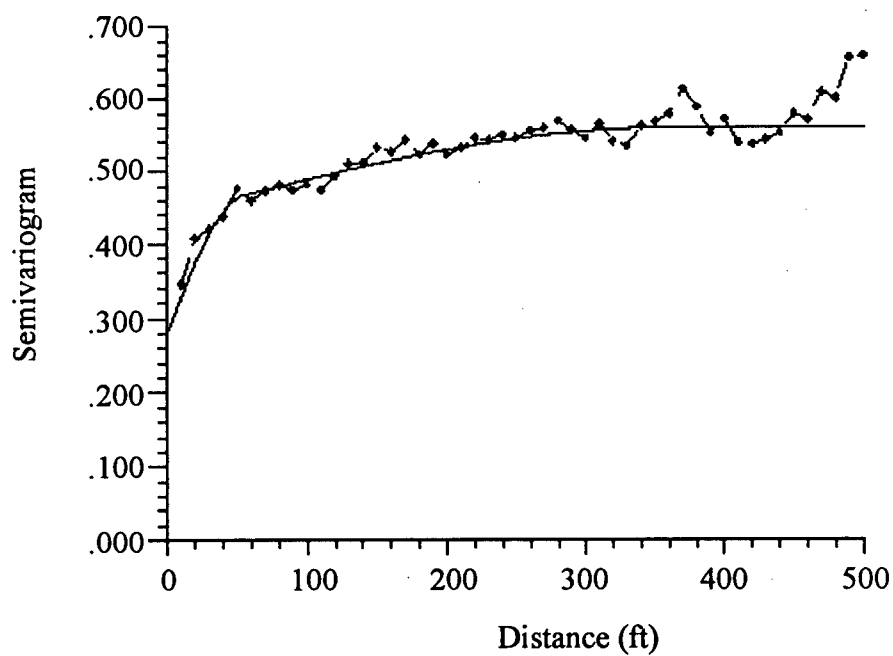
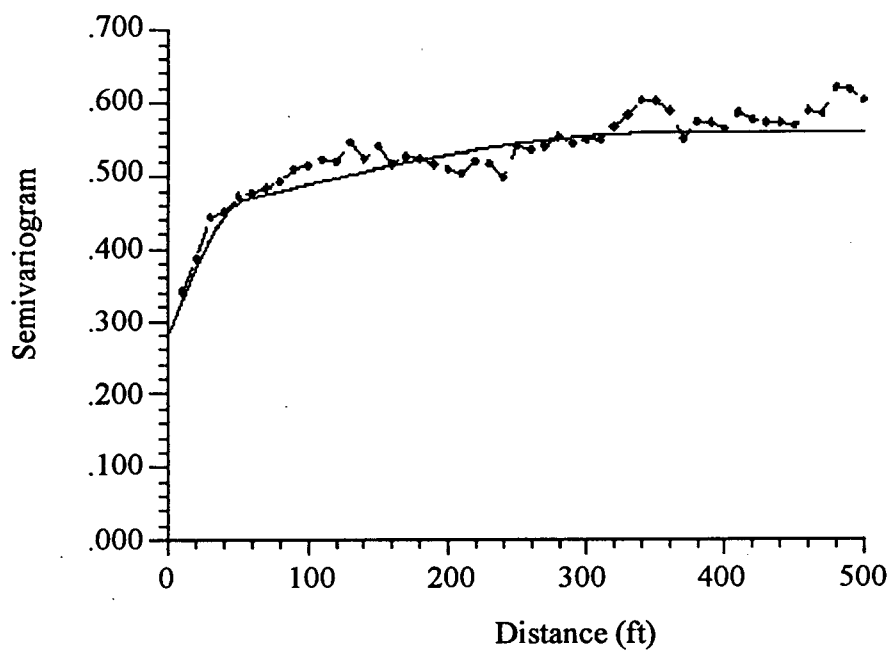


Figure A5-6: Au experimental semivariograms in vertical direction, East part (top), middle part (bottom), with superimposed model for the entire zone; $C_0 = 0.28$, $C_1 = 0.16$, $A_1 = 55$, $C_2 = 0.12$, $A_2 = 360$

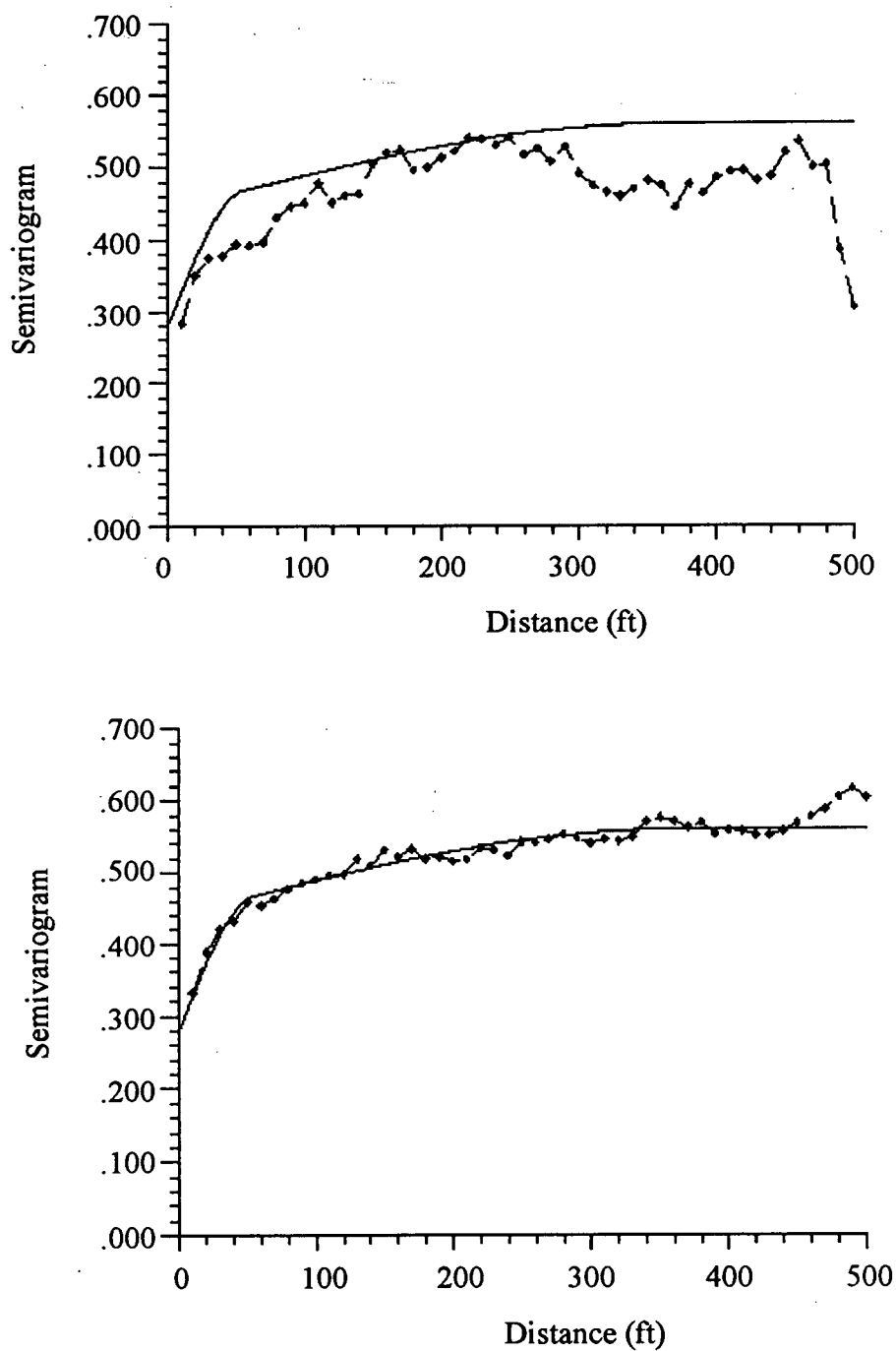


Figure A5-7: Au experimental semivariograms in vertical direction, West part (top), entire zone (bottom), with superimposed model for the entire zone; $C_0 = 0.28$, $C_1 = 0.16$, $A_1 = 55$, $C_2 = 0.12$, $A_2 = 360$

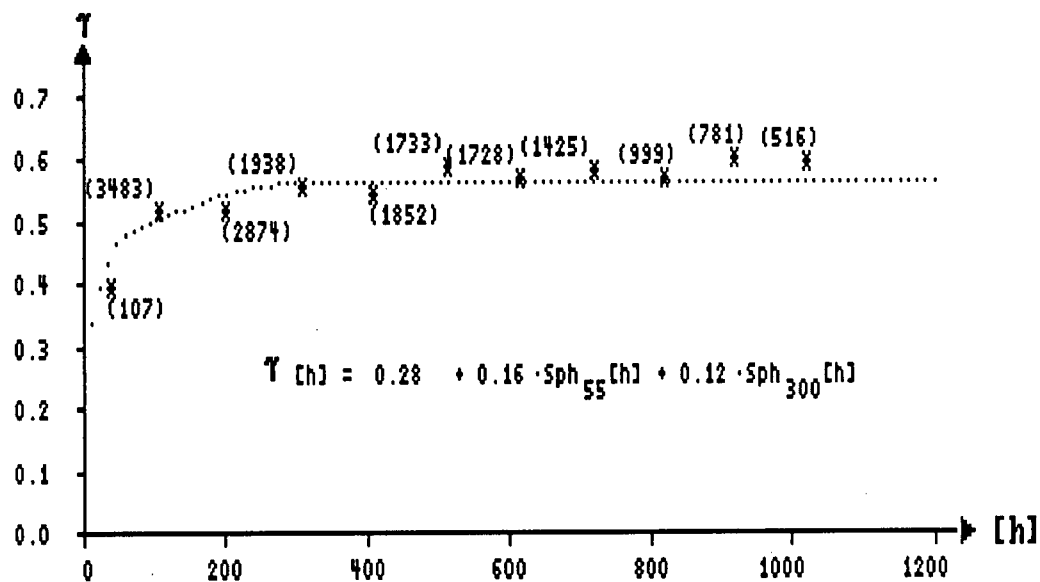
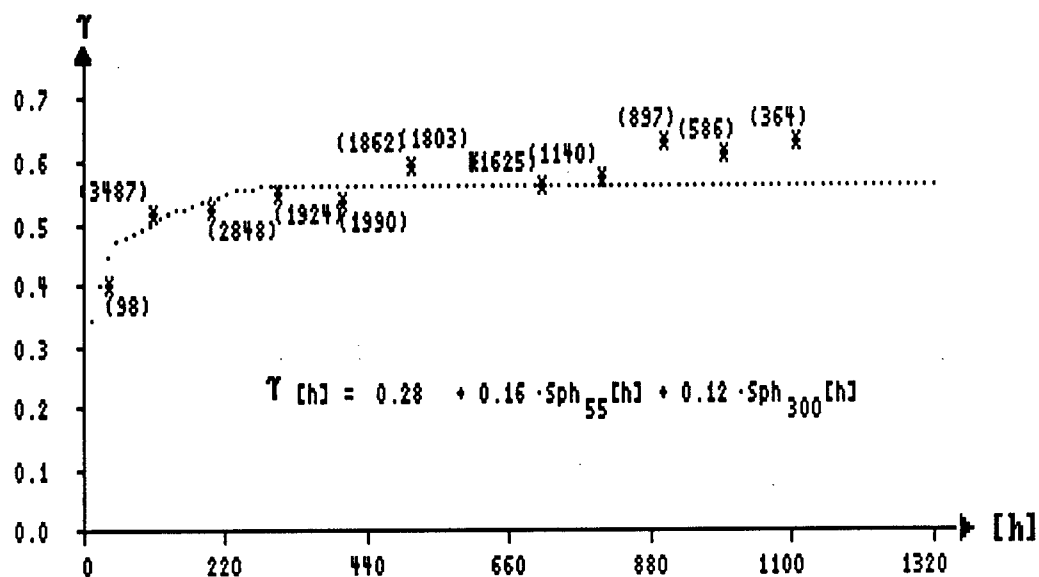


Figure A5-8: Au semivariogram models in horizontal directions, azimuth 90; dip 0 (top) and dip -10 (bottom)

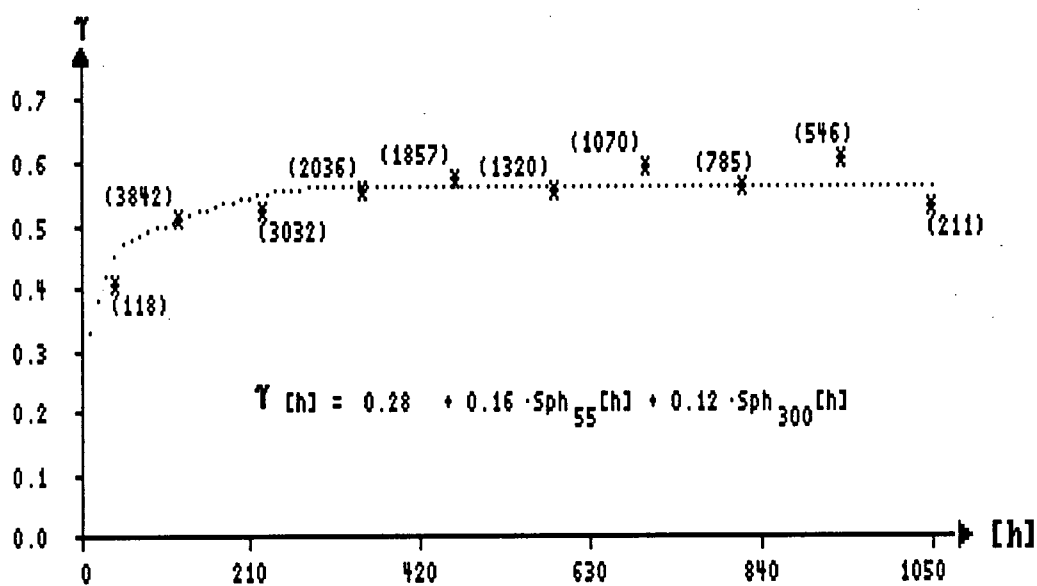
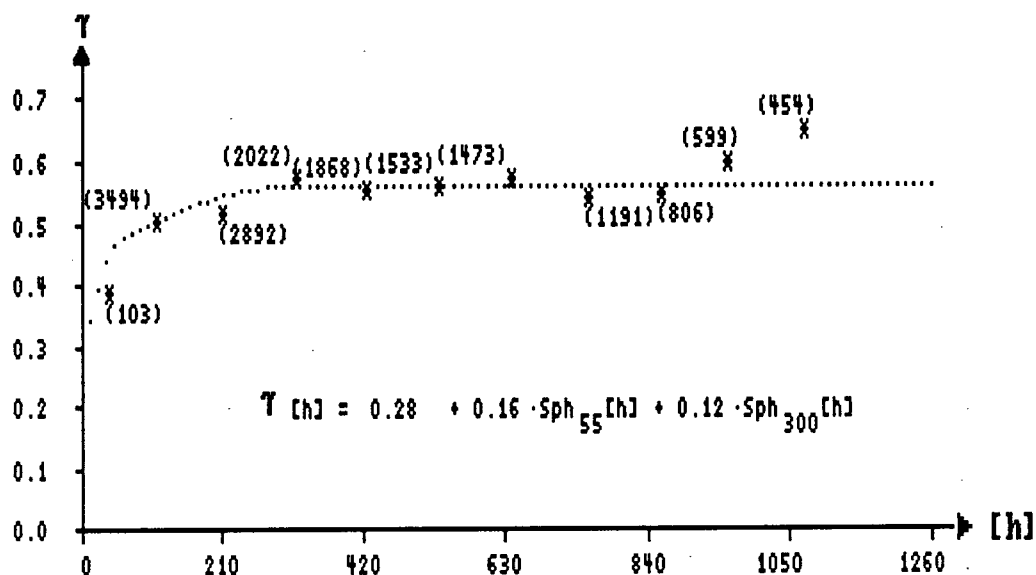


Figure A5-9: Au semivariogram models in horizontal directions, azimuth 90; dip -20 (top) and dip -30 (bottom)

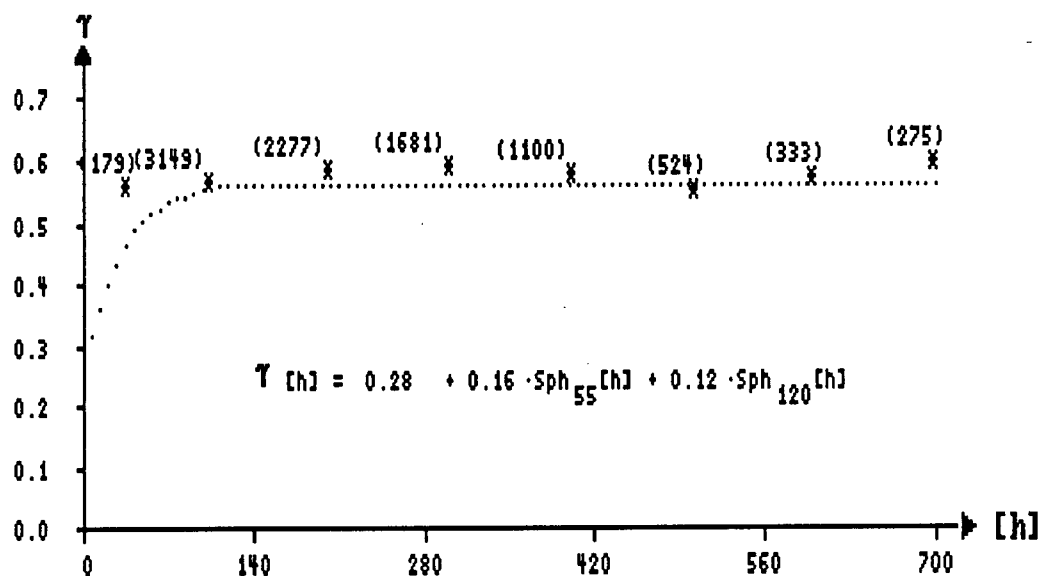


Figure A5-10: Au semivariogram model in horizontal direction,
azimuth 0, dip 0

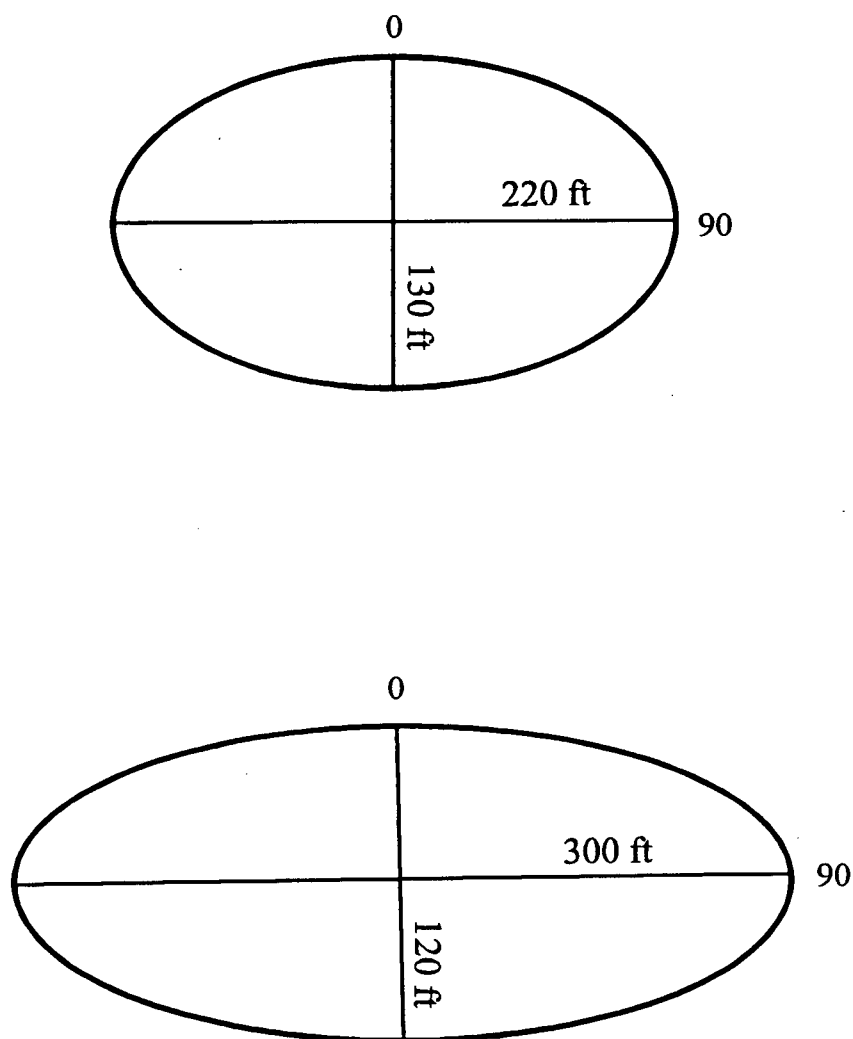


Figure A5-11: Structural ellipses of ranges in the two directions showing directions of maximum (azimuth 90) and minimum (azimuth 0) continuity of Cu semivariogram model (top) and Au semivariogram model (bottom)

APPENDIX 6

EQUATIONS USED IN THE GAINLOSS PROGRAM

A summary of the most important equations for normal and lognormal distributions is included here.

Normal distribution

The normal or Gaussian density function is a bell-shaped curve, symmetric about the mean value. It is defined by equation A6-1:

$$y = [(2 \cdot \pi)^{-1/2} \cdot s^{-1}] \cdot \exp[-(x - x_m)^2 / 2 \cdot s^2] \quad (\text{A6-1})$$

where x_m is the estimate of the arithmetic mean, x is any measurement, s^2 is the estimate of variance of the population and s is the standard deviation.

All measurements of any normal distribution can be transformed to the standard normal distribution as shown by the following equation:

$$z_i = (x_i - x_m) / s \quad (\text{A6-2})$$

which means that each measurement is transferred to its "z score". A "z score" is the number of standard deviations away from the mean, that particular measurement is located. This transformation produces a standard normal distribution with a mean of zero

and a standard deviation of one, and leads to a formula for the standard normal distribution as follows:

$$y=(2\cdot\pi)^{-1/2}\cdot\exp(-z_i^2/2) \quad (\text{A6-3})$$

Commonly used statistical tables are based on the standard normal distribution. Thus any normal distribution, regardless of mean and standard deviation can be related to standardized statistical tables through the transform of equation A6-2.

The likelihood that a randomly drawn sample from the normal distribution will be less than a specified value, x , is given by the proportion of area under the normal curve from minus infinity to x . This area or probability can be found by transforming x to a corresponding z value (equation A6-2) and searching a set of tables of cumulative area from minus infinity to any z score. The difference between such cumulative areas for any two z values gives the probability that a randomly drawn sample will lie between these two z values. Because the probabilities are in the range 0 to 1.0, and if the probability that a randomly drawn sample is less than z , is given by $P_{<z}$, then the probability that the random draw will be greater than z is given by $P_{>z}=1-P_{<z}$.

The use of tables would be awkward, so instead of tables, the computer program GAINLOSS utilizes formulas recommended by David (1977). These formulas approximate the proportion under the standard normal curve, and for positive values of z are as follows:

$$P_{<z}=0.5\cdot[1+\{1-\exp(-2\cdot z^2/\pi)\}^{1/2}] \quad (\text{A6-4})$$

or

$$P_{>z} = 1 - P_{<z} \quad (\text{A6-5})$$

where $P_{<z}$ is the proportion of the population (under the curve) below the selected positive z-score and $P_{>z}$ is the proportion of the population (under the curve) above the selected positive z-score. When z-score is negative the formula A6-4 directly calculates the proportion of the population that is greater than z (from z to plus infinity).

Formulas A6-4 and A6-5 can be applied to lognormal populations if data are transformed to logarithms, which are normally distributed.

Lognormal distribution

The variable x is said to have a lognormal distribution if after transforming it to natural logarithms (i.e. $t = \ln(x)$), these log values have a normal distribution. The raw data (untransformed values) of a lognormal distribution are positively skewed, but not all positively skewed distributions are lognormal.

As with the normal distribution, for a lognormal distribution of grades it is also possible to estimate the proportion of area under the curve (tonnage) above the particular cut-off grade ($P_{>c}$, from cut-off grade x_c to plus infinity) using the following formula:

$$P_{>c} = 1 - \Phi(z_{\log}) \quad (\text{A6-6})$$

where

$$z_{\log} = \{[\ln(x_c/x_m)]/s_n + s_n/2\} \quad (\text{A6-7})$$

where s_n is the standard deviation of natural logarithms of raw data, and is related to parameters of raw data distribution by formula A6-8:

$$s_n = [\text{Ln}(s^2/x_m^2 + 1)]^{1/2} \quad (\text{A6-8})$$

In equation A6-6 the expression $\phi(z_{\log})$ is the cumulative distribution function (area under the standard normal curve) of a standard normal variable from minus infinity to z_{\log} , and as such can be found in the tables of standard normal distribution. In the case of the computer program GAINLOSS value z_{\log} is calculated in the equation A6-7 and is substituted for z in equation A6-4.

The recoverable metal, $R_{>c}$, that is, the proportion of total metal that is contained in the tonnage above cutoff grade, is given by

$$R_{>c} = 1 - \phi\{[\text{Ln}(x_c/x_m)]/s_n - s_n/2\} \quad (\text{A6-9})$$

The average grade $x_{>c}$ of that proportion of material above cutoff grade x_c is given by

$$x_{>c} = x_m \cdot R_{>c} / P_{>c} \quad (\text{A6-10})$$

Value $R_{>c}$ can be estimated using equation A6-4 (and A6-5), the same way $P_{>c}$ was estimated.

APPENDIX 7

ALGORITHM OF THE GAINLOSS PROGRAM AND THE PROGRAM PRINTOUT

The GAINLOSS program calculates the effect of misclassification on recovery due to estimation error and a summary of metal accounting. This is an interactive program, that consists of four parts. The results are summarized in the output file, which name is interactively input by the user.

First part is an introductory, interactive part in which user is asked by the program to input information as described in Chapter 4.

Second part of the program (lines 2000's) starts with calculation of waste blocks that are mistakenly included in the ore due to estimation error. First s_n value is calculated using equation A6-8. Next grade interval center and grade interval range are calculated based on lower and upper limits of the first grade interval input by the user.

Then program enters a loop that is performed until upper limit of grade interval equals cut-off grade (e.g. 0.215% Cu). Each loop is calculated separately for each single grade interval (e.g. 0.195 to 0.205% Cu), which is assumed to be centered on it's middle point (e.g. 0.20% Cu). Then estimation error is calculated (error as one standard deviation), by multiplying error value (input by the user) by grade interval center and showing it in percent (divide by 100). In the example of 10% error centered on 0.20% Cu the error as one standard deviation is equal 0.02.

Because errors are assumed to have normal distribution the next step is to calculate z-score using equation A6-2, where x_i =cutoff, x_m =grade interval center, and s =error calculated in the previous step.

Next $P_{>z}$ is calculated using either equation A6-4 or A6-5. This step estimates the proportion of blocks with true grade, e.g. 0.2% Cu, that will be reported as above cut-off grade. In our example this proportion is equal 0.226. In the output file symbol $P_{>c}$ is used instead of symbol $P_{>z}$.

Next step is to estimate the cumulative proportion of grades from infinity to each side of the grade interval. This has been done using equations A6-6 and A6-7 to calculate z-scores for lognormally distributed data of block grades, where x_c is equal respectively to upper and lower limits of each single interval. Then these z-scores are substituted to equations A6-4 and A6-5 to finish calculation of this step.

In the next step cumulative proportion of grades from infinity to the upper limit of the grade interval is subtracted from cumulative proportion of grades from infinity to the lower limit of the grade interval and multiplied by number of blocks (e.g. 1000) to give the frequency (F) in blocks within the interval(e.g. 13). Thus, for the 1000 block example, 13 blocks will have true values between 0.195 and 0.205% Cu.

Then frequency (F) in blocks (e.g. 13) is multiplied by $P_{>c}$ (e.g. 0.226) to calculate number of waste blocks (e.g. 2.9) that will be misclassified as ore, in particular grade interval.

All the above procedures are followed in each loop for many contiguous short grade intervals until cut-off grade is reached.

In the next step all misclassified waste blocks are added together, and their true average grade is calculated as a weighted average of the central grade of each grade interval, weighted by the number of diluting blocks.

Second half of part two of the program, the half with lines 3000's, contains almost identical steps that lead to calculation of ore blocks, that are mistakenly included in waste due to estimation error. Here only the differences, from the first half of part two of the program will be explained.

After entering the initial loop, the loop is performed until the upper limit of grade interval equals mean plus user declared number multiplied by standard deviation.

Next difference is that, because cutoff grade now is considered as not the highest, but the lowest grade, that we are interested in, so not $P_{>z}$, but $P_{<z}$ is calculated using equations A6-4 or A6-5. This step estimates the proportion of blocks with true grades above cut-off grade, that will be reported due to estimation error as being below cutoff grade.

One more difference is that frequency (F) given in blocks is multiplied by $P_{<z}$ (the same as $P_{<z}$ as explained above), to calculate the number of blocks that will be misclassified as waste, in particular grade interval. As a result, after leaving the loop the program calculates the sum of misclassified ore (not waste) blocks and their average true grade.

The third part of the program, starting with lines 5000's, is structurally identical to the second part of the program. The only difference is that it is executed if normal distribution of true grades is declared by the user.

The difference between the third part and second part of the program is only in applying equation A6-2 instead of equation A6-7, while calculating cumulative proportions of grades from infinity to each side of the grade interval. Equation A6-2 is used to calculate z-scores for normally distributed data of true values. While applying this equation, x_i is equal respectively to the upper and lower limits of each single grade interval.

The fourth part of the program (lines 9000's) is the final part, that calculates metal accounting summary. Total operating loss of metal is a sum of net cost of mining waste classed as ore and net loss of metal in ore classed as waste, given in tonnes of metal in the case when percent was declared as variable unit, and in grams and troy ounces when grams/tonne was chosen as variable units.

Net cost of mining waste is calculated as a result of multiplying the number of misclassified waste blocks by user declared size of single block (in tonnes) and by difference between calculated in part two or three average true grade of misclassified waste blocks and cutoff grade.

Net loss of metal in ore classed as waste is calculated by multiplying number of misclassified ore blocks by user defined size of single block (in tonnes) and by difference between cut-off grade and calculated in part two or three average true grade of misclassified ore blocks.

```

c                               GAINLOSS  PROGRAM
c
c MEAN - mean of raw data
c STDEV - stand. deviat. of raw data
c STDEV1 - stand. deviat. of natural logarithms of raw data
c CUTOFF - cutoff grade
c LWLMT - lower limit of the first grade interval and all other intervals
c UPLMT - upper limit of the first grade interval and all other intervals
c ERROR - sampling and analitical error
c BLKS - number of blocks used to calculate frequency
c NUMBER - last grade interval limit, as number of STDEVs above MEAN
c CLRANG - range of grade interval
c CLMID - centre of grade interval
c ERSTDV - error as one stand. deviat.
c Z - 'z' value of normal standard distribution; equation A-2
c PMNZ -  $P < z$ , proportion of area under the curve from minus infinity to
c        'z'; equation A-4 for  $Z > 0$ , 0.5 for  $Z = 0$ , A-5 for  $Z < 0$ 
c PWIZ -  $P > z$ , proportion of area under the curve from 'z' to plus
c        infinity; equat. A-5 for  $Z > 0$ , 0.5 for  $Z = 0$ , A-4 for  $Z < 0$ 
c ZU - 'z' value corresponding to upper limits of grade intervals, for
c        lognormal distribution equat. A-15, for normal distrib. equat. A-2
c ZL - 'z' value corresponding to lower limits of grade intervals, for
c        lognormal distribution equat. A-15, for normal distrib. equat. A-2
c PMNCU - proportion of area under the curve from minus infinity to Upper
c        limit of grade range, equation A-4 for  $ZU > 0$ , 0.5 for  $ZU = 0$ , A5
c        for  $ZU < 0$ 
c PWICU - proportion of area under the curve from Upper limit of grade
c        range to plus infinity, equation A-5 for  $ZU > 0$ , 0.5 for  $ZU = 0$ , A-4
c        for  $ZU < 0$ 
c PMNCL - proportion of area under the curve from minus infinity to Lower
c        limit of grade range, equation A-4 for  $ZL > 0$ , 0.5 for  $ZL = 0$ , A5
c        for  $ZL < 0$ 
c PWICL - proportion of area under the curve from Lower limit of grade
c        range to plus infinity, equation A-5 for  $ZL > 0$ , 0.5 for  $ZL = 0$ , A-4
c        for  $ZL < 0$ 
c CLFRQ - grade range frequency (F), frequency in BLKS (e.g. 1000) blocks
c FXPWIZ - column 4 in output file; equal column 2 (CLFRQ, frequency F)
c        times column 3 (PWIZ)
c SUM - sum of all values (misclassified blocks) from column 4 (FXPWIZ)
c COL1X4 - column 1 (CLMID) times column 4 (FXPWIZ)
c C1X4 - sum of all values of COL1X4
c TRUEG - average true grade of misclassified blocks
c TWOSTDEV - the last grade interval limit as number of STDEV above MEAN
c WSUM - sum of all misclassified WASTE blocks
c OSUM - sum of all misclassified ORE blocks
c WTRUEG - average true grade of misclassified WASTE blocks
c OTRUEG - average true grade of misclassified ORE blocks
c BLKTONNE - block size in tonnes
c COSTW - cost (in tonnes) of mining waste classed as ore (table 5-5)
c LOSSORE - net loss (in tonnes) of metal contained in blocks classed
c        as waste (table 5-5)
c TOTAL - total operating loss of metal (in tonnes); COSTW+LOSSORE
c OZCOSTW - the same as COSTW, but given in troy ounces
c OZLOSSOR - the same as LOSSORE, but given in troy ounces
c OZTOTAL - the same as TOTAL, but given in troy ounces

```

```

PARAMETER(PI=3.14159,EP SL=1.0e-6,OZTROY=0.032148)
CHARACTER str1*40,str2*40,variable*40,str3*20
real STDEV1,CUTOFF,LW LMT,UPLMT,MEAN,NUMBER,BLKTONNE
REAL STDEV,CLRANG,CLMID,ERSTDV,PMNZ,PWIZ,Z,ZU,TOTAL,LOSSORE,COSTW
REAL PMNCU,PWICU,PMNCL,PWICL,FXPWIZ,SUM,COL1X4,WSUM,OSUM,WTRUEG
REAL TRUEG,C1X4,ERROR,CLFRQ,ZL,TWOSTDEV,FXPMNZ,OTRUEG
REAL OZCOSTW,OZLOSSOR,OZTOTAL
INTEGER BLKS

```

c Variables entry block

```

WRITE(*,970)
970 FORMAT(//)
write(*,*) ' THIS PROGRAM CALCULATES THE EFFECT OF MISCLASSIFICAT
+ION'
WRITE(*,*)
WRITE(*,*) ' ON RECOVERY DUE TO SAMPLING ERROR,'
WRITE(*,*)
WRITE(*,*) ' AND SUMMARY OF METAL ACCOUNTING'
WRITE(*,*)
WRITE(*,1000)
1000 FORMAT(//)
WRITE(*,*) 'INPUT NAME OF TARGET FILE, SUMMARIZING THE RESULTS:'
READ(*,'(a20)')str1(1:20)
OPEN(UNIT=6,FILE=str1(1:20),STATUS='NEW')
WRITE(*,*)
WRITE(*,*)

WRITE(*,*) 'Input the name of VARIABLE of true grades (e.g. COPPER
+, GOLD):'
READ(*,'(a20)')variable(1:20)

WRITE(*,*)
WRITE(*,*) 'If VARIABLE is in g/t then type: G'
WRITE(*,*) 'If VARIABLE is in % then type: P'
READ(*,'(a20)')str3(1:20)

if(str3(1:1).eq.'G'.or.str3(1:1).eq.'g'.or.str3(1:1).eq.'P'.or.str
+3(1:1).eq.'p') then
goto 1500

else

WRITE(*,*)
WRITE(*,*) 'ERROR - you must type either G or P TRY AGAIN'
WRITE(*,*)

stop
endif

WRITE(*,*)

```

```

1500 WRITE(*,*)'Input MEAN of raw data ( e.g. 0.45):'
      Read(*,*)MEAN
      WRITE(*,*)'Input STD. DEVIAT. of raw data ( e.g. 0.218):'
      Read(*,*)STDEV

      Write(*,*)

      Write(*,*)'Input CUT-OFF grade ( e.g. 0.215):'
      Read(*,*)CUTOFF

      Write(*,*)

      Write(*,*)'Input LOWER LIMIT of the first grade interval (MUST BE
+< CUT-OFF):'
      READ(*,*)LWLMT
      Write(*,*)'Input UPPER LIMIT of the first grade interval (MUST BE
+< CUT-OFF):'
      READ(*,*)UPLMT

      WRITE(*,*)

      WRITE(*,*)'Input the last grade interval limit as number of STD. D
+EVIAT.'
      WRITE(*,*)'ABOVE the MEAN (e.g. 2 or -0.5 ):'
      Read(*,*)NUMBER

      Write(*,*)

      Write(*,*)'Input sampling ERROR value in percent(e.g. 10 ):'
      READ(*,*)ERROR

      WRITE(*,*)
      WRITE(*,*)'Input the number of BLOCKS (e.g. 1000):'
      READ(*,*)BLKS
      WRITE(*,*)'Input the BLOCK size in TONNES (e.g. 2000):'
      READ(*,*)BLKTONNE
      write(*,*)

      WRITE(*,*)'Is this distribution of true grades NORMAL or LOGNORMAL
+?:'
      WRITE(*,*)'                                LOGNORMAL is default, otherwise type N'
      READ(*, '(a20)')str2(1:20)

      if(str2(1:1).eq.' '.or.str2(1:1).eq.'L'.or.str2(1:1).eq.'l') then
        goto 2000
      elseif(str2(1:1).eq.'N'.or.str2(1:1).eq.'n') then
        goto 5000
      else

      WRITE(*,*)
      WRITE(*,*)'ERROR - type ENTER or L for lognormal distribution '
      WRITE(*,*)'          type N for normal distribution,      TRY AGAIN'
      WRITE(*,*)
      STOP
      ENDIF

```

```

2000 write(6,*)'                                LOGNORMAL distribution of true grades'
      WRITE(6,*)
      WRITE(6,*)

```

C WASTE BLOCKS MISTAKENLY INCLUDED IN ORE DUE TO SAMPLING AND ANALITICAL
C ERROR. LOGNORMAL DISTRIBUTION OF TRUE GRADES.

```

      WRITE(6,2020)'NUMBER OF WASTE BLOCKS MISTAKENLY INCLUDED IN ORE DU
+E TO',ERROR,'% ERROR'
2020 FORMAT(A56,1X,F4.1,A7)

```

```

      if(str3(1:1).eq.'G'.or.str3(1:1).eq.'g') then

        WRITE(6,2024)variable,'GRADE DISTRIBUTION',CUTOFF,'g/t CUT-OFF GR
+ADE'
2024 format(A8,A19,16X,F8.4,A17)
      write(6,*)

      else

2028 WRITE(6,2030)variable,'GRADE DISTRIBUTION',CUTOFF,'% CUT-OFF GRAD
+E'
2030 format(A8,A19,18X,F8.4,A15)
      write(6,*)

      endif

```

```

      WRITE(6,2040)'Grade intvl centre','Freq. in',BLKS,'blks',ERROR,'%e
+rror, P>c','Freq.* P>c'
2040 FORMAT(A18,4X,A8,I7,1X,A4,3X,F4.1,A11,3X,A10)

```

```

      STDEV1=SQRT(LOG((STDEV**2/MEAN**2)+1))

```

```

      CLRANG=UPLMT-LWLMT
      CLMID=(LWLMT+UPLMT)/2

```

```

      SUM=0
      C1X4=0

```

```

c      DO WHILE(UPLMT.LE.(CUTOFF+EPSL))

2050 If(UPLMT.LE.(CUTOFF+EPSL)) then
      ERSTDV=(ERROR*CLMID)/100

```

```

Z=(CUTOFF-CLMID)/ERSTDV
  IF(Z.GT.0) THEN
    PMNZ=0.5*(1+SQRT(1-EXP(-2*Z**2/PI)))
    PWIZ=1-PMNZ
  ELSEIF(Z.EQ.0) THEN
    PMNZ=0.5
    PWIZ=1-PMNZ
  ELSE
    PWIZ=0.5*(1+SQRT(1-EXP(-2*Z**2/PI)))
  ENDIF

ZU=(LOG(UPLMT/MEAN))/STDEV1+((STDEV1)/2)
  IF(ZU.GT.0) THEN
    PMNCU=0.5*(1+SQRT(1-EXP(-2*ZU**2/PI)))
    PWICU=1-PMNCU
  ELSEIF(ZU.EQ.0) THEN
    PMNCU=0.5
    PWICU=1-PMNCU
  ELSE
    PWICU=0.5*(1+SQRT(1-EXP(-2*ZU**2/PI)))
  ENDIF

ZL=(LOG(LWLMT/MEAN))/STDEV1+((STDEV1)/2)
  IF(ZL.GT.0) THEN
    PMNCL=0.5*(1+SQRT(1-EXP(-2*ZL**2/PI)))
    PWICL=1-PMNCL
  ELSEIF(ZL.EQ.0) THEN
    PMNCL=0.5
    PWICL=1-PMNCL
  ELSE
    PWICL=0.5*(1+SQRT(1-EXP(-2*ZL**2/PI)))
  ENDIF

CLFRQ=(PWICL-PWICU)*BLKS

FXPWIZ=CLFRQ*PWIZ

WRITE(6,2060)CLMID,CLFRQ,PWIZ,FXPWIZ
2060  FORMAT(5X,F8.4,17X,F6.1,12X,F5.3,10X,F7.3)

SUM=SUM+FXPWIZ

COL1X4=CLMID*FXPWIZ
C1X4=C1X4+COL1X4

LWLMT=LWLMT+CLRANG
CLMID=CLMID+CLRANG
UPLMT=UPLMT+CLRANG

goto 2050
endif

c      ENDDO

```

```

WRITE(6,*)
WRITE(6,*)
WRITE(6,2100)'SUM OF MISCLASSIFIED WASTE BLOCKS:',SUM
2100 FORMAT(A34,27X,F9.3)

```

```

TRUEG=(C1X4/SUM)
WRITE(6,*)
WRITE(6,2140)'AVERAGE TRUE GRADE OF MISCLASSIFIED WASTE BLOCKS:',T
+RUEG
2140 FORMAT(A49,10X,F11.6)

```

```

WSUM=SUM
WTRUEG=TRUEG

```

C ORE BLOCKS MISTAKENLY INCLUDED IN WASTE DUE TO SAMPLING AND ANALITICAL
C ERROR. LOGNORMAL DISTRIBUTION OF TRUE GRADES.

```

WRITE(6,3010)
3010 FORMAT(///)

```

```

WRITE(6,3020)'NUMBER OF ORE BLOCKS MISTAKENLY INCLUDED IN WASTE DU
+E TO',ERROR,'% ERROR'
3020 FORMAT(A56,1X,F4.1,A7)

```

```

if(str3(1:1).eq.'G'.or.str3(1:1).eq.'g') then

```

```

WRITE(6,3024)variable,'GRADE DISTRIBUTION',CUTOFF,'g/t CUT-OFF GR
+ADE'
3024 format(A8,A19,16X,F8.4,A17)
write(6,*)

```

```

else

```

```

3028 WRITE(6,3030)variable,'GRADE DISTRIBUTION',CUTOFF,'% CUT-OFF GRAD
+E'
3030 format(A8,A19,18X,F8.4,A15)
write(6,*)

```

```

endif

```

```

WRITE(6,3040)'Grade intvl centre','Freq. in',BLKS,'blks',ERROR,'%e
+rror, P<c','Freq.* P<c'
3040 FORMAT(A18,4X,A8,I7,1X,A4,3X,F4.1,A11,3X,A10)

```

```

SUM=0
CLX4=0

LWLMT=CUTOFF
CLMID=LWLMT+(CLRANG/2)
UPLMT=LWLMT+CLRANG

TWOSTDEV=MEAN+NUMBER*STDEV

c      DO WHILE (UPLMT.LT.TWOSTDEV)

3050  if(UPLMT.LT.TWOSTDEV) then
      ERSTDV=(ERROR*CLMID)/100

      Z=(CUTOFF-CLMID)/ERSTDV
      IF(Z.GT.0) THEN
        PMNZ=0.5*(1+SQRT(1-EXP(-2*Z**2/PI)))
      ELSEIF(Z.EQ.0) THEN
        PMNZ=0.5
      ELSE
        PWIZ=0.5*(1+SQRT(1-EXP(-2*Z**2/PI)))
        PMNZ=1-PWIZ
      ENDIF

      ZU=(LOG(UPLMT/MEAN))/STDEV1+((STDEV1)/2)
      IF(ZU.GT.0) THEN
        PMNCU=0.5*(1+SQRT(1-EXP(-2*ZU**2/PI)))
        PWICU=1-PMNCU
      ELSEIF(ZU.EQ.0) THEN
        PMNCU=0.5
        PWICU=1-PMNCU
      ELSE
        PWICU=0.5*(1+SQRT(1-EXP(-2*ZU**2/PI)))
      ENDIF

      ZL=(LOG(LWLMT/MEAN))/STDEV1+((STDEV1)/2)
      IF(ZL.GT.0) THEN
        PMNCL=0.5*(1+SQRT(1-EXP(-2*ZL**2/PI)))
        PWICL=1-PMNCL
      ELSEIF(ZL.EQ.0) THEN
        PMNCL=0.5
        PWICL=1-PMNCL
      ELSE
        PWICL=0.5*(1+SQRT(1-EXP(-2*ZL**2/PI)))
      ENDIF

      CLFRQ=(PWICL-PWICU)*BLKS

```



```

      FXPMNZ=CLFRQ*PMNZ

      WRITE(6,3060)CLMID,CLFRQ,PMNZ,FXPMNZ
3060  FORMAT(5X,F8.4,17X,F6.1,12X,F5.3,10X,F7.3)

      SUM=SUM+FXPMNZ

      COL1X4=CLMID*FXPMNZ
      C1X4=C1X4+COL1X4

      LWLMT=LWLMT+CLRANG
      CLMID=CLMID+CLRANG
      UPLMT=UPLMT+CLRANG

      goto 3050
    endif
c      ENDDO

      WRITE(6,*)
      WRITE(6,*)
      WRITE(6,3100)'SUM OF MISCLASSIFIED ORE BLOCKS:',SUM
3100  FORMAT(A32,29X,F9.3)

      TRUEG=(C1X4/SUM)
      WRITE(6,*)

      WRITE(6,3140)'AVERAGE TRUE GRADE OF MISCLASSIFIED ORE BLOCKS:',T
      +RUEG
3140  FORMAT(A47,12X,F11.6)

      OSUM=SUM
      OTRUEG=TRUEG

      goto 9000

5000  write(6,*)'          NORMAL distribution of true grades'
      WRITE(6,*)
      WRITE(6,*)

C WASTE BLOCKS MISTAKENLY INCLUDED IN ORE DUE TO SAMPLING AND ANALITICAL
C ERROR. NORMAL DISTRIBUTION OF TRUE GRADES.

```

```

WRITE(6,5020)'NUMBER OF WASTE BLOCKS MISTAKENLY INCLUDED IN ORE DU
+E TO',ERROR,'% ERROR'
5020 FORMAT(A56,1X,F4.1,A7)

```

```

if(str3(1:1).eq.'G'.or.str3(1:1).eq.'g') then

```

```

WRITE(6,5024)variable,'GRADE DISTRIBUTION',CUTOFF,'g/t CUT-OFF GR
+ADE'
5024 format(A8,A19,16X,F8.4,A17)
write(6,*)

```

```

else

```

```

5028 WRITE(6,5030)variable,'GRADE DISTRIBUTION',CUTOFF,'% CUT-OFF GRAD
+E'
5030 format(A8,A19,18X,F8.4,A15)
write(6,*)

```

```

endif

```

```

WRITE(6,5040)'Grade intvl centre','Freq. in',BLKS,'blks',ERROR,'%e
+rror, P>c','Freq.* P>c'
5040 FORMAT(A18,4X,A8,I7,1X,A4,3X,F4.1,A11,3X,A10)

```

```

CLRANG=UPLMT-LWLMT
CLMID=(LWLMT+UPLMT)/2

```

```

SUM=0
CLX4=0

```

```

c DO WHILE(UPLMT.LE.(CUTOFF+EPSL))

```

```

5050 if(UPLMT.LE.(CUTOFF+EPSL)) then
ERSTDV=(ERROR*CLMID)/100

```

```

Z=(CUTOFF-CLMID)/ERSTDV
IF(Z.GT.0) THEN
PMNZ=0.5*(1+SQRT(1-EXP(-2*Z**2/PI)))
PWIZ=1-PMNZ
ELSEIF(Z.EQ.0) THEN
PMNZ=0.5
PWIZ=1-PMNZ
ELSE
PWIZ=0.5*(1+SQRT(1-EXP(-2*Z**2/PI)))
ENDIF

```

```

ZU=(UPLMT-MEAN)/STDEV
  IF(ZU.GT.0) THEN
    PMNCU=0.5*(1+SQRT(1-EXP(-2*ZU**2/PI)))
    PWICU=1-PMNCU
  ELSEIF(ZU.EQ.0) THEN
    PMNCU=0.5
    PWICU=1-PMNCU
  ELSE
    PWICU=0.5*(1+SQRT(1-EXP(-2*ZU**2/PI)))
  ENDIF

ZL=(LWLMT-MEAN)/STDEV
  IF(ZL.GT.0) THEN
    PMNCL=0.5*(1+SQRT(1-EXP(-2*ZL**2/PI)))
    PWICL=1-PMNCL
  ELSEIF(ZL.EQ.0) THEN
    PMNCL=0.5
    PWICL=1-PMNCL
  ELSE
    PWICL=0.5*(1+SQRT(1-EXP(-2*ZL**2/PI)))
  ENDIF

CLFRQ=(PWICL-PWICU)*BLKS

FXPWIZ=CLFRQ*PWIZ

WRITE(6,5060) CLMID,CLFRQ,PWIZ,FXPWIZ
5060  FORMAT(5X,F8.4,17X,F6.1,12X,F5.3,10X,F7.3)

SUM=SUM+FXPWIZ

COL1X4=CLMID*FXPWIZ
C1X4=C1X4+COL1X4

LWLMT=LWLMT+CLRANG
CLMID=CLMID+CLRANG
UPLMT=UPLMT+CLRANG

goto 5050
endif

c      ENDDO

WRITE(6,*)
WRITE(6,*)
WRITE(6,5100) 'SUM OF MISCLASSIFIED WASTE BLOCKS:',SUM
5100  FORMAT(A34,27X,F9.3)

TRUEG=(C1X4/SUM)
WRITE(6,*)

```

```

      WRITE(6,5140)'AVERAGE TRUE GRADE OF MISCLASSIFIED WASTE BLOCKS:',T
      +RUEG
5140 FORMAT(A49,10X,F11.6)

```

```

      WSUM=SUM
      WTRUEG=TRUEG

```

C ORE BLOCKS MISTAKENLY INCLUDED IN WASTE DUE TO SAMPLING AND ANALITICAL
C ERROR. NORMAL DISTRIBUTION OF TRUE GRADES.

```

      WRITE(6,6010)
6010 FORMAT(///)

```

```

      WRITE(6,6020)'NUMBER OF ORE BLOCKS MISTAKENLY INCLUDED IN WASTE DU
      +E TO',ERROR,'% ERROR'
6020 FORMAT(A56,1X,F4.1,A7)

```

```

      if(str3(1:1).eq.'G'.or.str3(1:1).eq.'g') then

```

```

      WRITE(6,6024)variable,'GRADE DISTRIBUTION',CUTOFF,'g/t CUT-OFF GR
      +ADE'
6024 format(A8,A19,16X,F8.4,A17)
      write(6,*)

```

```

      else

```

```

6028 WRITE(6,6030)variable,'GRADE DISTRIBUTION',CUTOFF,'% CUT-OFF GRAD
      +E'
6030 format(A8,A19,18X,F8.4,A15)
      write(6,*)

```

```

      endif

```

```

      WRITE(6,6040)'Grade intvl centre','Freq. in',BLKS,'blks',ERROR,'%e
      +rror, P<c','Freq.* P<c'
6040 FORMAT(A18,4X,A8,I7,1X,A4,3X,F4.1,A11,3X,A10)

```

```

      SUM=0
      CLX4=0

```

```

      LWLMT=CUTOFF
      CLMID=LWLMT+(CLRANG/2)
      UPLMT=LWLMT+CLRANG

```

TWOSTDEV=MEAN+NUMBER*STDEV

c DO WHILE (UPLMT.LT.TWOSTDEV)

6050 if(UPLMT.LT.TWOSTDEV) then
ERSTDV=(ERROR*CLMID)/100

Z=(CUTOFF-CLMID)/ERSTDV
IF(Z.GT.0) THEN
PMNZ=0.5*(1+SQRT(1-EXP(-2*Z**2/PI)))
ELSEIF(Z.EQ.0) THEN
PMNZ=0.5
ELSE
PWIZ=0.5*(1+SQRT(1-EXP(-2*Z**2/PI)))
PMNZ=1-PWIZ
ENDIF

ZU=(UPLMT-MEAN)/STDEV
IF(ZU.GT.0) THEN
PMNCU=0.5*(1+SQRT(1-EXP(-2*ZU**2/PI)))
PWICU=1-PMNCU
ELSEIF(ZU.EQ.0) THEN
PMNCU=0.5
PWICU=1-PMNCU
ELSE
PWICU=0.5*(1+SQRT(1-EXP(-2*ZU**2/PI)))
ENDIF

ZL=(LWLMT-MEAN)/STDEV
IF(ZL.GT.0) THEN
PMNCL=0.5*(1+SQRT(1-EXP(-2*ZL**2/PI)))
PWICL=1-PMNCL
ELSEIF(ZL.EQ.0) THEN
PMNCL=0.5
PWICL=1-PMNCL
ELSE
PWICL=0.5*(1+SQRT(1-EXP(-2*ZL**2/PI)))
ENDIF

CLFRQ=(PWICL-PWICU)*BLKS

FXPMNZ=CLFRQ*PMNZ

WRITE(6,6060)CLMID,CLFRQ,PMNZ,FXPMNZ
6060 FORMAT(5X,F8.4,17X,F6.1,12X,F5.3,10X,F7.3)

SUM=SUM+FXPMNZ

COL1X4=CLMID*FXPMNZ

```

      C1X4=C1X4+COL1X4

      LWLMT=LWLMT+CLRANG
      CLMID=CLMID+CLRANG
      UPLMT=UPLMT+CLRANG

      goto 6050
    endif

c      ENDDO

      WRITE(6,*)
      WRITE(6,*)
      WRITE(6,6100) 'SUM OF MISCLASSIFIED ORE BLOCKS:',SUM
6100  FORMAT(A32,29X,F9.3)

      TRUEG=(C1X4/SUM)
      WRITE(6,*)

      WRITE(6,6140) 'AVERAGE TRUE GRADE OF MISCLASSIFIED ORE BLOCKS:',T
+RUEG
6140  FORMAT(A47,12X,F11.6)

      OSUM=SUM
      OTRUEG=TRUEG

9000  WRITE(6,9050)
9050  FORMAT(//)

      if(str3(1:1).eq.'G'.or.str3(1:1).eq.'g') then

      goto 9200
    endif

      COSTW=WSUM*BLKTONNE*(WTRUEG/100-CUTOFF/100)
      LOSSORE=OSUM*BLKTONNE*(CUTOFF/100-OTRUEG/100)
      TOTAL=COSTW+LOSSORE

      WRITE(6,*) '
      WRITE(6,*) '
      WRITE(6,9100) 'NET COST OF MINING WASTE CLASSED AS ORE (TONNES):',
+COSTW
9100  FORMAT(A50,6X,F13.2)

      WRITE(6,9140) 'NET LOSS OF METAL IN ORE CLASSED AS WASTE (TONNES):
+',LOSSORE
9140  FORMAT(A52,4X,F13.2)

```

```

WRITE(6,*)

WRITE(6,9180)'TOTAL OPERATING LOSS (TONNES OF METAL):',TOTAL
9180 FORMAT(A40,16X,F13.2)

goto 9500

9200 COSTW=WSUM*BLKTONNE*(WTRUEG-CUTOFF)
LOSSORE=OSUM*BLKTONNE*(CUTOFF-OTRUEG)
TOTAL=COSTW+LOSSORE

OZCOSTW=COSTW*OZTROY
OZLOSSOR=LOSSORE*OZTROY
OZTOTAL=TOTAL*OZTROY

WRITE(6,*)' METAL ACCOUNTING SUMMARY'
WRITE(6,*)

WRITE(6,9300)'NET COST OF MINING WASTE CLASSED AS ORE (GRAMS):',
+COSTW
9300 FORMAT(A49,5X,F14.1)
WRITE(6,9310)'(TROY OUNCES):',OZCOSTW
9310 FORMAT(A49,5X,F14.1)
WRITE(6,*)

WRITE(6,9340)'NET LOSS OF METAL IN ORE CLASSED AS WASTE (GRAMS):
+',LOSSORE
9340 FORMAT(A52,2X,F14.1)
WRITE(6,9350)'(TROY OUNCES):',OZLOSSOR
9350 FORMAT(A51,3X,F14.1)
WRITE(6,*)

WRITE(6,*)
WRITE(6,*)

WRITE(6,9380)'TOTAL OPERATING LOSS (GRAMS OF METAL):',TOTAL
9380 FORMAT(A39,15X,F14.1)
WRITE(6,9390)'(TROY OUNCES OF METAL):',OZTOTAL
9390 FORMAT(A39,15X,F14.1)
c WRITE(6,*)

9500 WRITE(6,*)
close(unit=6,Status='KEEP')

WRITE(*,*)
WRITE(*,*)
WRITE(*,*)'OUTPUT WRITTEN TO THE FILE'
WRITE(*,*)

STOP
END

```